

Ruprecht-Karls-Universität Heidelberg
Fakultät der Chemie und Geowissenschaften

Synthesis of a library of small molecule
inhibitors preventing the physical interaction
between Tec Kinase and Fibroblast Growth
Factor 2, a tumor cell survival factor

Dissertation

Vorgelegt von
Alina Isabella Muschko

Inaugural Dissertation

zur

Erlangung der Doktorwürde

der

Naturwissenschaftlich-Mathematischen Gesamtfakultät

der Universität Heidelberg

vorgelegt von

Diplom-Chemikerin Alina Isabella Muschko

geboren am 05. September 1986 in Sindelfingen

Verteidigung am 30. April 2021

Verfasst unter der Anleitung von

Prof. Dr Roland Krämer (Universität Heidelberg, Chemistry Department)

Prof. Dr. Walter Nickel (Universität Heidelberg, Biochemistry Center)

Eidesstattliche Erklärung gemäß § 8 der Promotionsordnung der
Naturwissenschaftliche-Mathematischen Gesamtfakultät der Universität Heidelberg

1. Bei der eingereichten Dissertation zu dem Thema „Synthesis of a library of small molecule inhibitors preventing the physical interaction between Tec Kinase and Fibroblast Growth Factor 2, a tumor cell survival factor“ handelt es sich um meine eigenständig erbrachte Leistung.
2. Ich habe nur die angegebenen Quellen und Hilfsmittel benutzt und mich keiner unzulässigen Hilfe Dritter bedient. Insbesondere habe ich wörtlich und sinngemäß aus anderen Werken übernommene Inhalte als solche kenntlich gemacht.
3. Die Arbeit oder Teile habe ich bislang nicht an einer Hochschule des In- und Auslands als Bestandteil einer Prüfungs- oder Qualifikationsleistung vorgelegt.
4. Die Richtigkeit der vorstehenden Erklärung bestätige ich.
5. Die Bedeutung der eidesstattlichen Versicherung und die strafrechtlichen Folgen einer unrichtigen oder unvollständigen Versicherung sind mir bekannt.

Ich versichere an Eides statt, dass ich nach dem besten Wissen die reine Wahrheit erklärt und nichts verschwiegen habe.

Ort und Datum

Unterschrift

Summary

The overexpression of Fibroblast Growth Factor 2 (FGF2) is a well-known phenotype in a number of different cancer types. It acts as a very potent pro-angiogenic mitogen promoting tumour angiogenesis as well as plays a major role in tumour cell survival promoting chemoresistance. An usual feature of FGF2 is the pathway by which it is exported from cells. Instead of being secreted through the classical ER/Golgi-dependent pathway, FGF2 is transported into the extracellular space by direct translocation across the plasma membrane. The underlying mechanism is based on the formation of lipidic membrane pores, a pathway that has been classified as type I unconventional protein secretion (UPS Type I). While a number of therapeutics have been developed targeting FGF2 signaling in cancer cells, the elucidation of the molecular mechanism of FGF2 secretion in the last two decades opened up unique opportunities to block the biological function of FGF2 under pathophysiological conditions.

A number of cis- and trans-acting factors driving FGF2 secretion have been identified with (i) the Na/K-ATPase that recruits FGF2 at the inner plasma membrane leaflet, (ii) Tec Kinase that directly binds and phosphorylates FGF2, (iii) the membrane lipid phosphatidylinositol-4,5-bisphosphate [PI(4,5)P₂] that triggers FGF2 oligomerization and pore formation and (iv) cell surface heparan sulfate proteoglycans that capture and disassemble FGF2 oligomers at the outer plasma membrane leaflet as the final step of this secretory process.

While the specific role of Tec Kinase remains to be established, it has been demonstrated that RNAi-mediated down-regulation of Tec Kinase inhibits unconventional secretion of FGF2. Recently, small molecule inhibitors have been identified that block both physical interactions between FGF2 and Tec Kinase and FGF2 secretion from cells. They are of special interest for treating cancer types that develop FGF2-dependent chemoresistance towards otherwise effective drugs such as FLT3 inhibitors in acute myeloid leukemia (AML).

The goal of this thesis was to improve the potency of FGF2/Tec inhibitors using a medicinal chemistry approach. Starting from the most potent compound, more than 130 analogues were synthesised. All compounds were tested in FGF2/Tec protein-protein interaction assays to determine their inhibitory potential. In total, thirteen compounds were identified with improved IC₅₀ values compared to the original

FGF2/Tec inhibitor. These compounds were further evaluated in cell-based assays determining their influence on FGF2 secretion. Amongst this set of compounds, two compounds were identified exerting a stronger secretion phenotype compared to the original FGF2/Tec inhibitor. Furthermore, through the structural design of the newly synthesised compounds, valuable insight was obtained into the structure-activity relationship (SAR) of the small molecule inhibitors described here. This information will be of high value in future studies aiming at the optimization of this class of FGF2/Tec inhibitors with the final goal of developing a potent drug candidate blocking the biological function of FGF2 under pathophysiological conditions.

Zusammenfassung

Die Überexpression von Fibroblast Growth Factor 2 (FGF2) ist ein in der Literatur gut bekannter Phenotyp, den man in einer großen Anzahl von verschiedenen Krebsarten findet. Neben seiner Wirkung als sehr starker Promoter der Angiogenese in Tumoren, spielt FGF2 auch eine große Rolle in der Entwicklung von Resistenzen gegen Medikamente und trägt maßgeblich zum Überleben von Krebszellen bei. Das Besondere an FGF2 ist der Transportmechanismus, mit dem es aus der Zelle sekretiert wird. Während die meisten Proteine durch den konventionellen Weg über den ER/Golgi Apparat aus der Zelle transportiert werden, wird FGF2 direkt über die Zellmembran in die Extrazelluläre Matrix transportiert. FGF2 bildet toroidale Membranporen, durch die der direkte Transport aus der Zelle ohne Signalpeptid stattfindet. Diese Art des Transportmechanismus wird weiterhin als unkonventionelle Sekretion Typ I bezeichnet (UPS Type I). Die gängige Methode, um die Signalwirkung von FGF2 in Krebszellen zu unterdrücken, ist die Hemmung der Rezeptor-FGF2 Interaktionen. Durch die Aufklärung des genauen Sekretionsmechanismus von FGF2 in den letzten 20 Jahren, kann damit nun auch der einzigartige Transportweg als möglichen Therapieansatz verfolgt werden.

Einige cis- und trans-Faktoren, die die Sekretion von FGF2 aus der Zelle vorantreiben sind identifiziert worden: (i) die Na/K-ATPase, die FGF2 an die innere Plasmamembran rekrutiert, (ii) Tec Kinase die direkt mit FGF2 interagiert und dieses phosphoryliert, (iii) das Membranlipid Phosphatidylinositol-4,5-bisphosphat [PI(4,5)P₂], das die Oligomerisierung und Porenbildung auslöst, (iv) Heparan sulfat proteoglykane an der Zelloberfläche, die FGF2 an der äußeren Plasmamembran einfangen und die gebildeten Oligomere abbauen.

Während die genaue Rolle von Tec Kinase noch näher untersucht werden muss, konnte eine Korrelation zwischen der RNAi abhängigen Reduktion von Tec Kinase und einer verminderten FGF2 Sekretion beobachtet werden. Vor kurzem wurden Inhibitoren identifiziert, die sowohl die direkte Interaktion zwischen FGF2 und Tec Kinase verhindern als auch die Sekretion von FGF2 aus der Zelle reduzieren. Diese Art von Inhibitoren ist von besonderem Interesse für die Behandlungen von Krebsarten, die eine FGF2-abhängige Resistenz entwickelt haben gegen normalerweise sehr potente Medikamente wie zum Beispiel FLT3 Inhibitoren für die Behandlungen von akuter myeloische Leukämie (AML).

Das Ziel dieser Arbeit war es, die Wirkung der FGF2/Tec Inhibitoren durch einen medizinisch chemischen Ansatz zu verbessern. Basierend auf der Struktur des potentesten Inhibitors wurden mehr als 130 analoge Verbindungen synthetisiert. Alle Verbindungen wurden auf ihre hemmende Wirkung in einem FGF2/Tec Kinase Interaktions-Assay getestet. Von den 130 Verbindungen wurden dreizehn identifiziert, die eine bessere Hemmung zeigen als der ursprüngliche FGF2/Tec Inhibitor. Diese Verbindungen wurden als nächstes in einem zell-basierten Assay auf ihre Wirkung auf die Sekretion von FGF2 getestet. Aus den getesteten Verbindungen wurden zwei identifiziert, die einen stärkeren Sekretions-Phenotyp aufweisen als der ursprüngliche Inhibitor. Außerdem konnte durch das strukturierte Design der analogen Verbindungen, ein wertvoller Einblick in die Struktur-Aktivitäts-Eigenschaften des Inhibitors gewonnen werden. Diese Information ist von hohem Nutzen für die weitere Optimierung dieser Klasse von FGF2/Tec Inhibitoren mit dem Ziel einen potenten Wirkstoff zu entwickeln, der die biologische Funktion von FGF2 unter pathophysiologischen Bedingungen hemmt.

Table of Contents

A	Introduction.....	1
1	Protein secretion in eukaryotic cells.....	1
1.1	Classical protein secretion	1
1.2	Unconventional Protein Secretion.....	2
2	Fibroblast Growth Factor 2	5
2.1	Function and Structure of Fibroblast Growth Factor 2	5
2.2	Unconventional secretion pathway of FGF2	7
2.3	FGF2 in cancer	10
2.3.1	FGF2/FGFR deregulation	10
2.3.2	FGF2 as pro-angiogenic factor	11
2.3.3	FGF2 in tumours.....	11
2.4	Clinical Therapy Approaches targeting FGF2.....	12
3	Protein-Protein-Interaction inhibitors.....	15
4	Tec Kinase and FGF2 protein-protein interaction	17
4.1	Tec Kinase: structure, function and connection to FGF2	17
4.2	Tec Kinase in cancer	18
4.3	Identification of a small molecule inhibitor targeting FGF2 and Tec Kinase interaction.....	19
B	Aim	21
C	Medicinal Chemistry approach	23
D	Chemistry: Results and Discussion	25
1.1	Synthesis approach	25
1.2	Head group modification.....	27
1.2.1	Substituent group and position modification of the head group	27
1.2.2	Introducing bigger alkyl substituents on the C6 head group	32
1.2.2.1	Evaluation of Suzuki coupling reaction with compounds 40 and 41	34
1.2.2.2	Alkylation of pyridopyrimidone head group using the Suzuki reaction	36
1.2.2.3	Alkylation of 2-amino-6-bromopyridine with the Suzuki reaction ..	38
1.2.2.4	Linking alkylated pyridopyrimidone head groups with pyrrole	42
1.2.1	Multiple Substituents on head group modification.....	43
1.2.2	Elimination of C=O from the head group	46

1.3	Tail group modification.....	48
1.3.1	Synthesis of pyrrole rings with bigger ring substituents	48
1.3.2	Synthesis of less substituted pyrrole compounds and pyrrole isosteres	56
1.3.3	N-modification of C6	57
1.4	Linker modification.....	59
1.4.1	Amide Linker.....	59
E	C6 analogues: Evaluation and Validation	63
1	Results.....	63
1.1	¹ H-NMR analysis of C6: possible internal H-Bonds to influence structure rigidity.....	63
1.2	AlphaScreen® evaluation of the synthesised compound library	64
1.2.1	Structure-Activity Relationship: Round I	65
1.2.1.1	Effect of the substituent type and position modification of the head group	65
1.2.1.2	Introduction of methyl keton substituent.....	68
1.2.2	Structure-Activity Relationship Round II: Extending ester and adding head group substituents	69
1.2.2.1	Ethyl ester effect on tail group.....	69
1.2.2.2	Adding a substituent to head group of C6	71
1.2.2.3	Removing carbonyl group from head group	72
1.2.3	Structure-Activity Relationship Round III: Tail group and Linker modification	73
1.2.3.1	Increase the size of the alkyl substituents on the tail group	74
1.2.3.2	Alkylation of pyrrole on NH-position	74
1.2.3.3	Removing substituents and exchanging pyrrole tail group	75
1.2.3.4	Amide Linker	76
1.3	Quantification of inhibition of FGF2 secretion in cell-based biotinylation assay	77
2	Discussion	81
F	Conclusion and Outlook	85
G	Experimental Procedures Biochemistry.....	87
1	Alpha® assay.....	87
1.1	Protein constructs	87
1.1.1	His-FGF2Wt.....	87

1.1.2	GST- Δ N173Tec Kinase	87
1.2	Compound stock solution preparation	88
1.3	Principle of Alpha [®] assay	88
1.4	Alpha [®] Screen for IC50 determination	89
2	Compound Solubility Determination.....	91
3	Cell surface biotinylation assay to quantify FGF2 secretion.....	92
H	Experimental Procedures Chemistry	95
1	Chemicals and Analytical Methods	95
1.1	Chemicals.....	95
1.2	NMR	95
1.3	Biotage	95
1.4	TLC.....	95
1.5	HPLC	96
1.6	UHPLC-MS	96
2	Syntheses	97
2.1	General procedures.....	97
2.1.1	General procedure A (Suzuki Cross Coupling Reaction).....	97
2.1.2	General Procedure B (Pyrrole Synthesis Step I+II)	97
2.1.3	General Procedure C (Pyrrole Synthesis Step III)	98
2.1.4	General Procedure D (Pyrrole Synthesis Step IV: Ring closure)	98
2.1.5	General Procedure E (Pyrrole Synthesis Step V: Removal of benzyl protecting group by hydrogenation)	99
2.1.6	General procedure F (Pyridopyrimidone head group synthesis).....	99
2.1.7	General procedure G (Alkylation of pyrrole carboxylic acid)	100
2.1.8	General procedure H (Pyrrole N-alkylation).....	100
2.2	Syntheses of head group modified compounds	101
2.2.1	Substituent modification on head group.....	101
2.2.1.1	Syntheses of modified 2-(chloromethyl)-4H-pyrido[1,2-a]-4-pyrimidones.....	101
2-(chloromethyl)-6-methyl-4H-pyrido[1,2-a]pyrimidin-4-one (126)	101	
2-(chloromethyl)-6-ethyl-4H-pyrido[1,2-a]pyrimidin-4-one (159)	102	
2-(chloromethyl)-6,7-dimethyl-4H-pyrido[1,2-a]pyrimidin-4-one (161) ..	102	
2-(chloromethyl)-6,8-dimethyl-4H-pyrido[1,2-a]pyrimidin-4-one (162) ..	103	
2-(chloromethyl)-6,9-dimethyl-4H-pyrido[1,2-a]pyrimidin-4-one (163) ..	104	

7,9-dibromo-2-(chloromethyl)-6-methyl-4H-pyrido[1,2-a]pyrimidin-4-one (165)	105
7,9-dichloro-2-(chloromethyl)-4H-pyrido[1,2-a]pyrimidin-4-one (166) ...	106
3-(chloromethyl)-1H-pyrimido[1,2-a]quinolin-1-one (164)	107
6-bromo-2-(chloromethyl)-4H-pyrido[1,2-a]pyrimidin-4-one (138) (AM06-10)	108
7-bromo-2-(chloromethyl)-4H-pyrido[1,2-a]pyrimidin-4-one (139).....	108
8-bromo-2-(chloromethyl)-4H-pyrido[1,2-a]pyrimidin-4-one (140).....	109
9-bromo-2-(chloromethyl)-4H-pyrido[1,2-a]pyrimidin-4-one (141).....	110
2.2.1.2 Suzuki-Ring modification from Bromopyridine precursors.....	111
6-Ethylpyridin-2-amine (157).....	111
6-cyclopropyl-pyridin-2-amine (157)	112
2-(chloromethyl)-8-ethyl-4H-pyrido[1,2-a]pyrimidin-4-one (151)	113
2-(chloromethyl)-9-ethyl-4H-pyrido[1,2-a]pyrimidin-4-one (152)	114
2-(chloromethyl)-8-cyclopropyl-4H-pyrido[1,2-a]pyrimidin-4-one (154) .	115
2-(chloromethyl)-9-ethyl-4H-pyrido[1,2-a]pyrimidin-4-one (155)	116
2-(chloromethyl)-9-ethyl-4H-pyrido[1,2-a]pyrimidin-4-one (155)	117
2.2.1.3 Syntheses of head group modified methyl ester-pyrrole compounds	118
4-methyl 2-((6-methyl-4-oxo-4H-pyrido[1,2-a]pyrimidin-2-yl)methyl) 3,5-dimethyl-1H-pyrrole-2,4-dicarboxylate (10).....	118
4-methyl 2-((8-methyl-4-oxo-4H-pyrido[1,2-a]pyrimidin-2-yl)methyl) 3,5-dimethyl-1H-pyrrole-2,4-dicarboxylate (12).....	119
2-((6,7-dimethyl-4-oxo-4H-pyrido[1,2-a]pyrimidin-2-yl)methyl) 4-methyl 3,5-dimethyl-1H-pyrrole-2,4-dicarboxylate (72).....	120
2-((6,8-dimethyl-4-oxo-4H-pyrido[1,2-a]pyrimidin-2-yl)methyl) 4-methyl 3,5-dimethyl-1H-pyrrole-2,4-dicarboxylate (70).....	121
2-((6,9-dimethyl-4-oxo-4H-pyrido[1,2-a]pyrimidin-2-yl)methyl) 4-methyl 3,5-dimethyl-1H-pyrrole-2,4-dicarboxylate (74).....	122
2-((7,9-dichloro-4-oxo-4H-pyrido[1,2-a]pyrimidin-2-yl)methyl) 4-methyl 3,5-dimethyl-1H-pyrrole-2,4-dicarboxylate (169).....	123
4-methyl 2-((1-oxo-1H-pyrimido[1,2-a]quinolin-3-yl)methyl) 3,5-dimethyl-1H-pyrrole-2,4-dicarboxylate (68)	124
2-((6-bromo-4-oxo-4H-pyrido[1,2-a]pyrimidin-2-yl)methyl) 4-methyl 3,5-dimethyl-1H-pyrrole-2,4-dicarboxylate (40).....	125
2-((6-bromo-4-oxo-4H-pyrido[1,2-a]pyrimidin-2-yl)methyl) 4-methyl 3,5-dimethyl-1H-pyrrole-2,4-dicarboxylate (41).....	126

2.2.2	Structural modification of head group	127
2.2.2.1	Syntheses of imidazo-pyridines.....	127
	2-(chloromethyl)-5-methyl-imidazo[1,2-a]pyridine (171)	127
	2-(chloromethyl)-5,6-dimethyl-imidazo[1,2-a]pyridine (173).....	128
	5-bromo-2-(chloromethyl)imidazo[1,2-a]pyridine (172)	129
2.2.3	Syntheses of head group modified final compounds	130
	4-methyl 2-((5-methylimidazo[1,2-a]pyridin-2-yl)methyl) 3,5-dimethyl-1H-pyrrole-2,4-dicarboxylate (88)	130
	2-((5,6-dimethylimidazo[1,2-a]pyridin-2-yl)methyl) 4-methyl 3,5-dimethyl-1H-pyrrole-2,4-dicarboxylate (91)	131
	2-((5-bromoimidazo[1,2-a]pyridin-2-yl)methyl) 4-methyl 3,5-dimethyl-1H-pyrrole-2,4-dicarboxylate (95)	133
2.3	Pyrrole-Ring Modification.....	135
2.3.1	Substituent-Modification of pyrrole ring.....	135
2.3.1.1	Reagent Syntheses.....	135
	Benzyl 3-oxopentanoate (174).....	135
	Benzyl 4-methyl-3-oxopentanoate (226)	136
	Benzyl (E)-2-(hydroxyimino)-3-oxobutanoate (177)	137
	Benzyl (E)-2-(hydroxyimino)-3-oxopentanoate (177)	138
	Benzyl (E)-2-(hydroxyimino)-4-methyl-3-oxopentanoate (178)	138
2.3.1.2	Pyrrole ring syntheses.....	139
	2-benzyl 4-methyl 5-ethyl-3-methyl-1H-pyrrole-2,4-dicarboxylate (180)	139
	2-benzyl 4-methyl 3-ethyl-5-methyl-1H-pyrrole-2,4-dicarboxylate (179)	140
	2-benzyl 4-methyl 3,5-diethyl-1H-pyrrole-2,4-dicarboxylate (181)	141
	2-benzyl 4-ethyl 5-ethyl-3-methyl-1H-pyrrole-2,4-dicarboxylate (186) ..	142
	2-benzyl 4-ethyl 3-ethyl-5-methyl-1H-pyrrole-2,4-dicarboxylate (185) ..	143
	2-benzyl 4-ethyl 3,5-diethyl-1H-pyrrole-2,4-dicarboxylate (187)	144
	2-benzyl 4-methyl 5-isopropyl-3-methyl-1H-pyrrole-2,4-dicarboxylate (183)	145
	2-benzyl 4-methyl 3-isopropyl-5-methyl-1H-pyrrole-2,4-dicarboxylate (182)	146
	2-benzyl 4-methyl 3,5-diisopropyl-1H-pyrrole-2,4-dicarboxylate (184)..	147
	2-benzyl 4-ethyl 5-isopropyl-3-methyl-1H-pyrrole-2,4-dicarboxylate (187)	148

2-benzyl 4-ethyl 3-isopropyl-5-methyl-1H-pyrrole-2,4-dicarboxylate (188)	149
2-benzyl 4-ethyl 3,5-diisopropyl-1H-pyrrole-2,4-dicarboxylate (190).....	150
2.3.1.3 Benzyl ester deprotection of pyrrole	151
5-ethyl-4-(methoxycarbonyl)-3-methyl-1H-pyrrole-2-carboxylic acid (192)	151
3-ethyl-4-(methoxycarbonyl)-5-methyl-1H-pyrrole-2-carboxylic acid (191)	152
3,5-diethyl-4-(methoxycarbonyl)-1H-pyrrole-2-carboxylic acid (193)	153
4-(ethoxycarbonyl)-5-ethyl-3-methyl-1H-pyrrole-2-carboxylic acid (198)	154
4-(ethoxycarbonyl)-3-ethyl-5-methyl-1H-pyrrole-2-carboxylic acid (197)	155
4-(ethoxycarbonyl)-3,5-diethyl-1H-pyrrole-2-carboxylic acid (199)	156
5-isopropyl-4-(methoxycarbonyl)-3-methyl-1H-pyrrole-2-carboxylic acid (195)	157
3-isopropyl-4-(methoxycarbonyl)-5-methyl-1H-pyrrole-2-carboxylic acid (194)	158
3,5-diisopropyl-4-(methoxycarbonyl)-1H-pyrrole-2-carboxylic acid (196)	159
4-(ethoxycarbonyl)-5-isopropyl-3-methyl-1H-pyrrole-2-carboxylic acid (201)	160
4-(ethoxycarbonyl)-3-isopropyl-5-methyl-1H-pyrrole-2-carboxylic acid (200)	161
4-(ethoxycarbonyl)-3,5-diisopropyl-1H-pyrrole-2-carboxylic acid (202)	162
2.3.1.4 Pyrrole substituent modified final compounds	163
4-methyl 2-((6-methyl-4-oxo-4H-pyrido[1,2-a]pyrimidin-2-yl)methyl) 5-ethyl-3-methyl-1H-pyrrole-2,4-dicarboxylate (76).....	163
4-methyl 2-((6-methyl-4-oxo-4H-pyrido[1,2-a]pyrimidin-2-yl)methyl) 3-ethyl-5-methyl-1H-pyrrole-2,4-dicarboxylate (77).....	164
4-methyl 2-((6-methyl-4-oxo-4H-pyrido[1,2-a]pyrimidin-2-yl)methyl) 3,5-diethyl-1H-pyrrole-2,4-dicarboxylate (80).....	165
4-ethyl 2-((6-methyl-4-oxo-4H-pyrido[1,2-a]pyrimidin-2-yl)methyl) 5-ethyl-3-methyl-1H-pyrrole-2,4-dicarboxylate (78)	166
4-ethyl 2-((6-methyl-4-oxo-4H-pyrido[1,2-a]pyrimidin-2-yl)methyl) 3-ethyl-5-methyl-1H-pyrrole-2,4-dicarboxylate (79)	167
4-ethyl 2-((6-methyl-4-oxo-4H-pyrido[1,2-a]pyrimidin-2-yl)methyl) 3,5-diethyl-1H-pyrrole-2,4-dicarboxylate (81).....	168

4-methyl 2-((6-methyl-4-oxo-4H-pyrido[1,2-a]pyrimidin-2-yl)methyl) 5-isopropyl-3-methyl-1H-pyrrole-2,4-dicarboxylate (82)	169
4-methyl 2-((6-methyl-4-oxo-4H-pyrido[1,2-a]pyrimidin-2-yl)methyl) 3-isopropyl-5-methyl-1H-pyrrole-2,4-dicarboxylate (83)	170
4-methyl 2-((6-methyl-4-oxo-4H-pyrido[1,2-a]pyrimidin-2-yl)methyl) 3,5-diisopropyl-1H-pyrrole-2,4-dicarboxylate (86)	171
4-ethyl 2-((6-methyl-4-oxo-4H-pyrido[1,2-a]pyrimidin-2-yl)methyl) 5-isopropyl-3-methyl-1H-pyrrole-2,4-dicarboxylate (84)	172
4-ethyl 2-((6-methyl-4-oxo-4H-pyrido[1,2-a]pyrimidin-2-yl)methyl) 3-isopropyl-5-methyl-1H-pyrrole-2,4-dicarboxylate (85)	173
4-ethyl 2-((6-methyl-4-oxo-4H-pyrido[1,2-a]pyrimidin-2-yl)methyl) 3,5-diisopropyl-1H-pyrrole-2,4-dicarboxylate (87)	174
2.3.2 N-modified pyrrole compounds	175
4-methyl 2-((6-methyl-4-oxo-4H-pyrido[1,2-a]pyrimidin-2-yl)methyl) 1,3,5-trimethyl-1H-pyrrole-2,4-dicarboxylate (100)	175
4-methyl 2-((6-methyl-4-oxo-4H-pyrido[1,2-a]pyrimidin-2-yl)methyl) 1-ethyl-3,5-dimethyl-1H-pyrrole-2,4-dicarboxylate (101)	176
4-methyl 2-((6-methyl-4-oxo-4H-pyrido[1,2-a]pyrimidin-2-yl)methyl) 3,5-dimethyl-1-propyl-1H-pyrrole-2,4-dicarboxylate (102)	177
4-methyl 2-((6-methyl-4-oxo-4H-pyrido[1,2-a]pyrimidin-2-yl)methyl) 1-((2-methoxyethoxy)methyl)-3,5-dimethyl-1H-pyrrole-2,4-dicarboxylate (103)	178
4-methyl 2-((6-methyl-4-oxo-4H-pyrido[1,2-a]pyrimidin-2-yl)methyl) 3,5-dimethyl-1-(2-morpholinoethyl)-1H-pyrrole-2,4-dicarboxylate (105)	179
4-methyl 2-((6-methyl-4-oxo-4H-pyrido[1,2-a]pyrimidin-2-yl)methyl) 1-benzyl-3,5-dimethyl-1H-pyrrole-2,4-dicarboxylate (107)	180
4-methyl 2-((6-methyl-4-oxo-4H-pyrido[1,2-a]pyrimidin-2-yl)methyl) 1-(2-(tert-butoxy)-2-oxoethyl)-3,5-dimethyl-1H-pyrrole-2,4-dicarboxylate (104)	181
4-methyl 2-((6-methyl-4-oxo-4H-pyrido[1,2-a]pyrimidin-2-yl)methyl) 1-(2-((tert-butoxycarbonyl)Amino)ethyl)-3,5-dimethyl-1H-pyrrole-2,4-dicarboxylate (106)	182
2-(3-(methoxycarbonyl)-2,4-dimethyl-5-(((6-methyl-4-oxo-4H-pyrido[1,2-a]pyrimidin-2-yl)methoxy)carbonyl)-1H-pyrrol-1-yl)acetic acid (108)	183
4-methyl 2-((6-methyl-4-oxo-4H-pyrido[1,2-a]pyrimidin-2-yl)methyl) 1-(2-Aminoethyl)-3,5-dimethyl-1H-pyrrole-2,4-dicarboxylate (109)	184
2.3.3 Substituent subtraction of pyrrole	185
(6-methyl-4-oxo-4H-pyrido[1,2-a]pyrimidin-2-yl)methyl 1-methyl-1H-pyrrole-2-carboxylate (54)	185

(6-methyl-4-oxo-4H-pyrido[1,2-a]pyrimidin-2-yl)methyl pyrrole-2-carboxylate (55).....	3,5-dimethyl-1H-	186
(6-methyl-4-oxo-4H-pyrido[1,2-a]pyrimidin-2-yl)methyl carboxylate (56).....	1H-indole-2-	187
(6-methyl-4-oxo-4H-pyrido[1,2-a]pyrimidin-2-yl)methyl-1H-pyrrole-2-carboxylate (57).....		188
(6-methyl-4-oxo-4H-pyrido[1,2-a]pyrimidin-2-yl)methyl imidazole-5-carboxylate (58).....	1-methyl-1H-	189
(6-methyl-4-oxo-4H-pyrido[1,2-a]pyrimidin-2-yl)methyl imidazole-4-carboxylate (59).....	1-methyl-1H-	190
(6-methyl-4-oxo-4H-pyrido[1,2-a]pyrimidin-2-yl)methyl b]pyrrole-5-carboxylate (60).....	4H-furo[3,2-	191
(6-methyl-4-oxo-4H-pyrido[1,2-a]pyrimidin-2-yl)methyl carboxylate (64).....	1H-imidazole-4-	192
2.3.4 Ester group modification of pyrrole ring		193
2.3.4.1 Head-group modified compounds		193
4-ethyl 2-((6-methyl-4-oxo-4H-pyrido[1,2-a]pyrimidin-2-yl)methyl) pyrrole-2,4-dicarboxylate (66).....	3,5-	193
4-ethyl 2-((7-methyl-4-oxo-4H-pyrido[1,2-a]pyrimidin-2-yl)methyl) pyrrole-2,4-dicarboxylate (123).....	3,5-	194
4-ethyl 2-((8-methyl-4-oxo-4H-pyrido[1,2-a]pyrimidin-2-yl)methyl) pyrrole-2,4-dicarboxylate (119).....	3,5-	195
4-ethyl 2-((9-methyl-4-oxo-4H-pyrido[1,2-a]pyrimidin-2-yl)methyl) pyrrole-2,4-dicarboxylate (120).....	3,5-	196
4-ethyl 2-((6-ethyl-4-oxo-4H-pyrido[1,2-a]pyrimidin-2-yl)methyl) pyrrole-2,4-dicarboxylate (118).....	3,5-	197
4-ethyl 2-((8-ethyl-4-oxo-4H-pyrido[1,2-a]pyrimidin-2-yl)methyl) pyrrole-2,4-dicarboxylate (111).....	3,5-	198
4-ethyl 2-((9-ethyl-4-oxo-4H-pyrido[1,2-a]pyrimidin-2-yl)methyl) pyrrole-2,4-dicarboxylate (113).....	3,5-	199
4-ethyl 2-((8-cyclopropyl-4-oxo-4H-pyrido[1,2-a]pyrimidin-2-yl)methyl) pyrrole-2,4-dicarboxylate (115).....	3,5-	200
4-ethyl 2-((9-cyclopropyl-4-oxo-4H-pyrido[1,2-a]pyrimidin-2-yl)methyl) pyrrole-2,4-dicarboxylate (117).....	3,5-	201
2-((6,7-dimethyl-4-oxo-4H-pyrido[1,2-a]pyrimidin-2-yl)methyl) pyrrole-2,4-dicarboxylate (73).....	4-ethyl 3,5-	202
2-((6,8-dimethyl-4-oxo-4H-pyrido[1,2-a]pyrimidin-2-yl)methyl) pyrrole-2,4-dicarboxylate (71).....	4-ethyl 3,5-	203

2-((6,9-dimethyl-4-oxo-4H-pyrido[1,2-a]pyrimidin-2-yl)methyl) 4-ethyl 3,5-dimethyl-1H-pyrrole-2,4-dicarboxylate (75).....	204
2-((7,9-dichloro-4-oxo-4H-pyrido[1,2-a]pyrimidin-2-yl)methyl) 4-ethyl 3,5-dimethyl-1H-pyrrole-2,4-dicarboxylate (170).....	205
4-ethyl 2-((1-oxo-1H-pyrimido[1,2-a]quinolin-3-yl)methyl) 3,5-dimethyl-1H-pyrrole-2,4-dicarboxylate (69).....	206
2-((6-bromo-4-oxo-4H-pyrido[1,2-a]pyrimidin-2-yl)methyl) 4-ethyl 3,5-dimethyl-1H-pyrrole-2,4-dicarboxylate (67).....	207
2-((7-bromo-4-oxo-4H-pyrido[1,2-a]pyrimidin-2-yl)methyl) 4-ethyl 3,5-dimethyl-1H-pyrrole-2,4-dicarboxylate (65).....	208
2-((8-bromo-4-oxo-4H-pyrido[1,2-a]pyrimidin-2-yl)methyl) 4-ethyl 3,5-dimethyl-1H-pyrrole-2,4-dicarboxylate (121).....	209
2-((9-bromo-4-oxo-4H-pyrido[1,2-a]pyrimidin-2-yl)methyl) 4-ethyl 3,5-dimethyl-1H-pyrrole-2,4-dicarboxylate (122).....	210
4-methyl 2-((5-methylimidazo[1,2-a]pyridin-2-yl)methyl) 3,5-dimethyl-1H-pyrrole-2,4-dicarboxylate (89).....	211
2-((5,6-dimethylimidazo[1,2-a]pyridin-2-yl)methyl) 4-ethyl 3,5-dimethyl-1H-pyrrole-2,4-dicarboxylate (93).....	213
2-((5-bromoimidazo[1,2-a]pyridin-2-yl)methyl) 4-ethyl 3,5-dimethyl-1H-pyrrole-2,4-dicarboxylate (97).....	215
2.4 Amide linker modification.....	217
2.4.1 Amine Synthesis.....	217
2-((6-methyl-4-oxo-4H-pyrido[1,2-a]pyrimidin-2-yl)methyl)isoindoline-1,3-dione (Gabriel Step I) (209).....	217
2-((6-methyl-4-oxo-4H-pyrido[1,2-a]pyrimidin-2-yl)methyl)isoindoline-1,3-dione (Gabriel Step I) (210).....	218
2-(Aminomethyl)-6-methyl-4H-pyrido[1,2-a]pyrimidin-4-one (211).....	219
2-(Aminomethyl)-7-bromo-4H-pyrido[1,2-a]pyrimidin-4-one (212).....	220
2.4.2 Peptide coupling.....	220
4-acetyl-3,5-dimethyl-N-((6-methyl-4-oxo-4H-pyrido[1,2-a]pyrimidin-2-yl)methyl)-1H-pyrrole-2-carboxamide (61).....	220
Methyl 2,4-dimethyl-5-(((6-methyl-4-oxo-4H-pyrido[1,2-a]pyrimidin-2-yl)methyl) carbamoyl) -1H-pyrrole-3-carboxylate (62).....	222
Ethyl-2,4-dimethyl-5-(((6-methyl-4-oxo-4H-pyrido[1,2-a]pyrimidin-2-yl)-methyl)-carbamoyl)-1H-pyrrole-3-carboxylate (63).....	223
Methyl 5-(((7-bromo-4-oxo-4H-pyrido[1,2-a]pyrimidin-2-yl)methyl)carbamoyl)-2,4-dimethyl-1H-pyrrole-3-carboxylate (213).....	224

I	Appendix	225
1	Literature.....	225
2	Legends.....	235
2.1	Figures.....	235
2.2	Tables.....	237
2.3	Schemes.....	239
3	Abbreviation Index	241
4	Compound Index	244
J	Acknowledgment	255

A Introduction

As cancer is the second leading cause of death worldwide¹, developing specific treatments targeting different kinds of cancer is of high priority. Although a progress has been made in this area, these treatments often come with a significant number of side effects and can lead to drug resistance in tumours. Hence, research into the developments of drugs is on-going. Fibroblast Growth Factor 2 (FGF2), a potent pro-angiogenic mitogen, is overexpressed in a set of different cancer types, promotes tumour-induced angiogenesis and contributes to tumour survival². Unlike the majority of proteins secreted from cells, which utilise the classical secretion pathway, FGF2 follows a more unconventional route to reach the extracellular space³. Targeting this unusual secretion mechanism of FGF2 opens up a unique opportunity for the development of cancer therapeutics specific to this target protein.

1 Protein secretion in eukaryotic cells

1.1 Classical protein secretion

The conventional protein secretion pathway is a highly conserved within eukaryotic cells. It ensures the delivery of newly synthesised proteins to their target compartment within the cell as well as their transport to the extracellular space (**Scheme 1**). Protein translation starts with the binding of mRNA to cytosolic ribosomes. The translation stops upon the recognition and binding of signal recognition particle (SRP) to the N-terminal nascent signal polypeptide⁴ of the protein being translated. The SRP relocates the ribosome-polypeptide to the endoplasmic reticulum (ER) through its interaction with its receptor (SR) on the ER surface. This interaction initiates the co-translational translocation of the protein into the lumen of the ER via the Sec61 translocon⁵. After cleaving of the signal peptide, folding and potential posttranslational modifications, the protein is transported from the ER to the Golgi in COPII vesicles⁶, where further posttranslational modifications can take place. The Golgi (trans compartment)

¹ WHO Cancer, <https://www.who.int/news-room/fact-sheets/detail/cancer>; March **2021**.

² N. Turner, R. Grose, *Nat. Rev. Cancer*, **2010**, *10*(2), 116-129.

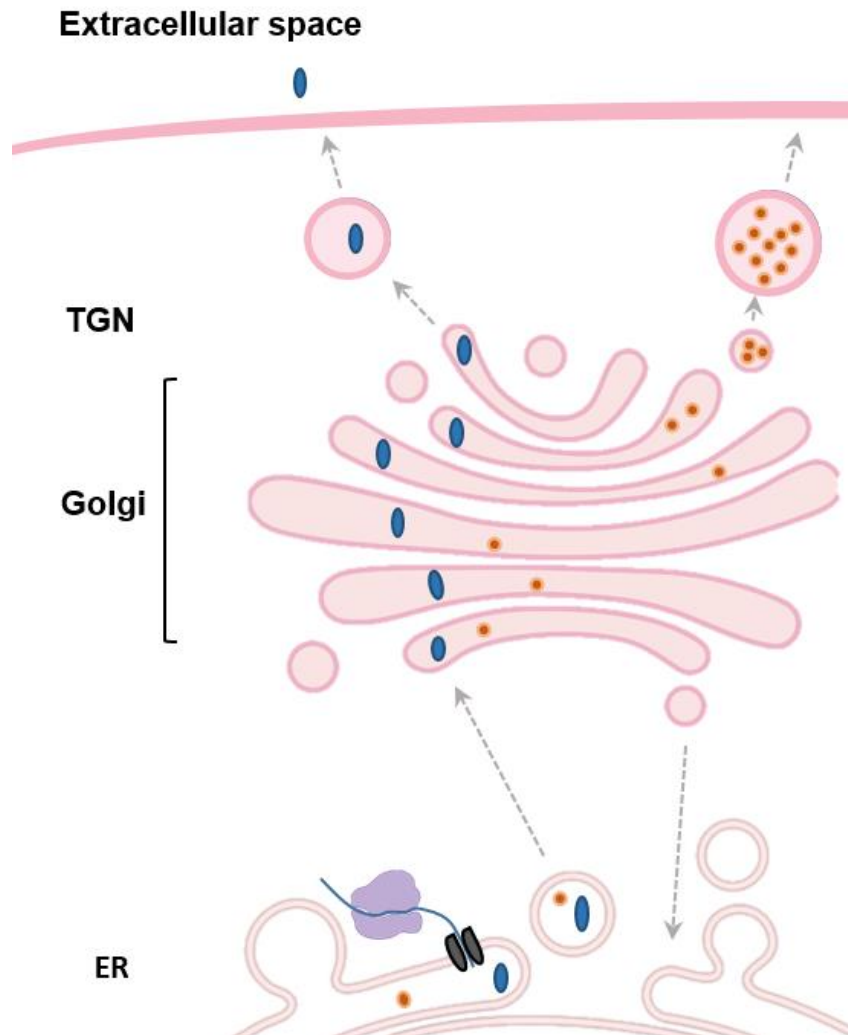
³ G. La Venuta, M. Zeitler, J. P. Steringer, H.-M. Müller, W. Nickel, *J. Biol. Chem.*, **2015**, *290*(45), 27015-27020.

⁴ P. Walter, *J. Cell Biol.*, **1981**, *91*(2), 557-561.

⁵ I. Saraogi, S. O. Shan, *Traffic*, **2011**, *12*(5), 535-542.

⁶ J. G. D'Arcangelo, K. R. Stahmer, E.A. Miller, *Biochimica et Biophysica Acta*, **2013**, *1833*(11), 2464-2472.

containing the modified proteins matures to the trans Golgi network (TGN), where proteins are sorted⁷ and from where they will be secreted via secretory vesicles to the plasma membrane⁸.



Scheme 1 Overview of conventional protein secretion from translation into the ER to the transport with secretory vehicles to the plasma membrane.

1.2 Unconventional Protein Secretion

Since the discovery of the first unconventionally secreted protein over 30 years ago, several other proteins have been discovered to also be secreted independent of the Golgi/ER pathway⁹. One distinctive feature of these proteins is the lack of a signal

⁷ F. Gu, C. M. Crump, G. Thomas, *Cell Mol. Life Sci.*, **2001**, 58(8), 1067-1084.

⁸ C. Viotti, "Unconventional Protein Secretion: Methods and Protocols, Chapter I: ER to Golgi-dependent Protein secretion: the conventional way", Editors: A. Pompa, F. De Marchis, **2016**, Springer New York: New York, NY.

⁹ W. Nickel, M. Seedorf, *Annu. Rev. Cell Dev. Biol.*, **2008**, 24, 287-308.

peptide. Yet some proteins containing a signal peptide are also secreted unconventionally by bypassing the Golgi¹⁰. While only a small number of these proteins have been investigated until now, it is worth noting that the predicted human secretome has classified 566 proteins without signal peptide as potentially secreted in an unconventional way¹¹.

To the group of unconventionally secreted proteins belong cytokines like interleukin 1 β ^{12,13}, FGF1 and FGF2¹⁴, extracellular matrix proteins like galectins¹⁵, HIV tat¹⁶ and many more. While they are secreted in an unconventional way, not all of them follow the same secretion pathway. So far, four distinct types of unconventional secretion have been identified and defined¹⁷ (**Scheme 2**), each using a different mechanism. Proteins following the UPS **Type I** secretion mechanism, are secreted by direct translocation over the plasma membrane through the formation of lipidic pores. Belonging to this group are for example FGF1¹⁸ and FGF2¹⁴. Other proteins, e.g. HASPB (hydrophilic acylated surface protein B)¹⁹, are modified through acylation which is recognized by ABC (ATP binding cassette) transporter proteins, leading to their translocation through the plasma membrane. Proteins following this secretion mechanism are in the UPS category **Type II**. To the group of **Type III** unconventional secretion belong cytoplasmic proteins that are secreted through autophagosome-like vesicles. Interleukin 1 β was one of the first proteins identified following this mechanism²⁰. In general, unconventionally secreted proteins can be separated in two distinct groups. The first group of proteins follow UPS **Type I-III**. They are classified as cytoplasmic leaderless proteins without a signal peptide or a transmembrane domain. The other group of proteins being secreted unconventionally follow UPS **Type IV**¹⁰. The proteins falling into this category of unconventional secretion do contain a signal

¹⁰ C. Rabouille, *Trends in Cell Biol.*, **2017**, 27(3), 230-240.

¹¹ K.K. Kandaswamy, G. Pugalenti, E. Hartmann, K.-U. Kalies, S. Moller, P. N. Suganthan, T. Martinez, *Biochem. Biophys. Res. Commun.*, **2010**, 391(3), 1306-1311.

¹² C. Eder, *Immunobiology*, **2009**, 214, 543-553.

¹³ M. Palotta, W. Nickel, *J. Cell Sci.*, **2020**, 133, jcs250449.

¹⁴ W. Nickel, *Traffic*, **2011**, 12, 799-805.

¹⁵ C. Seelenmeyer, S. Wegehingel, I. Tews, M. Künzler, M. Aebi, W. Nickel, *J. Cell Biol.*, **2005**, 171, 373-381.

¹⁶ F. Rayne, S. Debaisieux, A. Bonhoure, B. Beaumelle, *Cell. Biol. Int.*, **2010**, 34(4), 409-413.

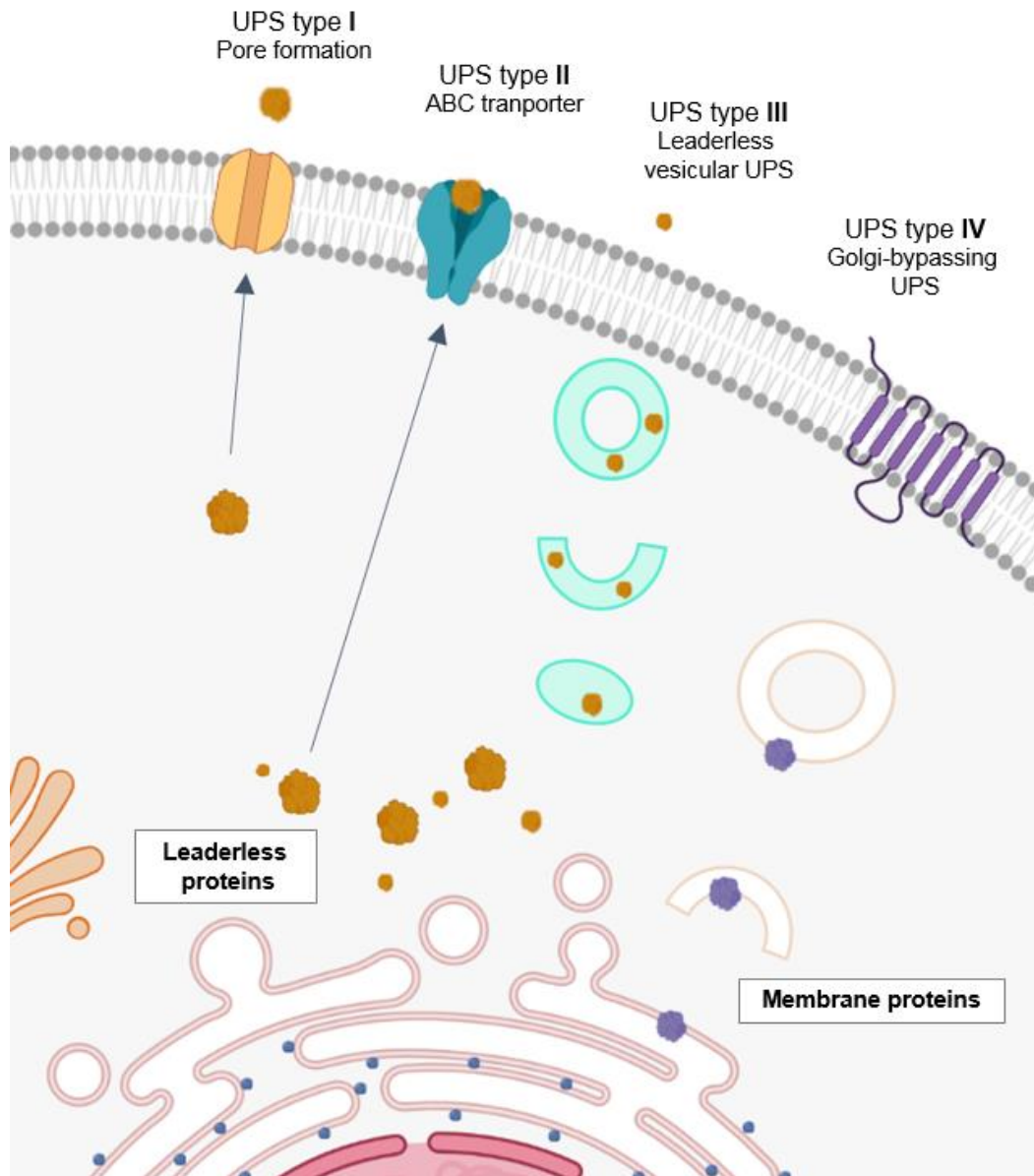
¹⁷ E. Dimou, W. Nickel, *Curr. Biol.*, **2018**, 28, R406-R410.

¹⁸ I. Prudovsky, D. Kacer, J. David, V. Shah, S. Jayanthi, I. Huber, R. Dakshinamurthy, O. Ganter, R. Soldi, D. Neivandt, O. Guvench, T. K. Suresh Kumar, *Biochemistry*, **2016**, 55(7), 1159-1167.

¹⁹ P. W. Denny, S. Gokool, D. G. Russel, M. C. Field, D. F. Smith, *J. Biol. Chem.*, **2000**, 275, 11075-11025.

²⁰ A. Rubartelli, F. Cozzolino, M. Talio, R. Sitia, *EMBO J.*, **1990**, 9, 1503-1510.

peptide and/or a trans-membrane domain and are synthesised in the ER. However, their secretion bypasses the Golgi and are directly delivered to the plasma membrane. This mechanism was discovered through experiments with Brefeldin A, a drug which inhibits ER-Golgi transport²¹, which couldn't stop the transport of this distinct group of proteins.



Scheme 2 Overview of unconventional protein secretion (UPS) mechanisms Type I-IV.

²¹ J. Lippencott-Schwartz, L. C. Yuan, J. S. Bonifacio, R. D. Klausner, *Cell*, **1989**, 56(5), 801–813.

While a small number of known UPS proteins are secreted constitutively, e. g. FGF2³ and HIV Tat^{22,23}, for the majority of unconventionally secreted proteins, the mechanism is triggered by inflammation, cellular, mechanical or nutrient stress¹⁰.

2 Fibroblast Growth Factor 2

Fibroblast growth factor 2, also known as basic Fibroblast growth factor (bFGF), is part of the fibroblast growth factor (FGF) family, which consists of 23 FGF signalling polypeptides. The whole protein family consists of very potent mitogens which play a role in embryonic development²⁴, wound healing²⁵ and angiogenesis^{26,27}.

2.1 Function and Structure of Fibroblast Growth Factor 2

In addition to the low molecular weight isoform of FGF2 (18kDa), four isoforms with higher molecular weight (HMW) have been identified (22, 22.5, 24, 34kDa). All isoforms are translated from the same *fgf2* mRNA using different start codons²⁸. The 18kDa isoform is translated from the canonical AUG start codon²⁹, while the translation of the HMW isoforms starts further upstream with different non-canonical CUG start codons. It follows that HMW FGF2s are N-terminal elongated versions of the 18kDa FGF2 isoform^{30,31}.

The 18 kDa isoform and the HMW isoforms are both used as signalling molecules³², but are performing this task in different compartments within the cell³². HMW FGF2s possess a nuclear location sequence (NLS) in their N-terminal extension which leads to them being primarily located in the nucleus. In recent years, some studies have indicated that they also might play a role during the proliferation of cancer cells³³. The

²² S. Debaisieux, F. Rayne, H. Yezid, B. Beaumelle, *Traffic*, **2012**, 13, 355-363.

²³ M. Zeitler, J. P. Steringer, H.-M. Müller, M. P. Mayer, W. Nickel, *J. Biol. Chem.*, **2015**, 290(36), 21976-21984.

²⁴ R. T. Böttcher, C. Niehrs, *Endocrine Rev.*, **2005**, 26(1), 63–77.

²⁵ R. Tsuboi, D. B. Rifkin, *J Exp. Med.*, **1990**, 172, 245-251.

²⁶ T. J. Stegmann, *BioDrugs*, **1999**, 11(5), 301–8.

²⁷ R. Cao, E. Bråkenhielm, R. Pawliuk, D. Wariaro, M. J. Post, E. Wahlberg, P. Leboulch, Cao Y, *Nature Medicine*, **2003**, 9(5), 604–13.

²⁸ M. Okada-Ban, J. P. Thiery, J. Jouanneau, *Int J. Biochem Cell Biol*, **2000**, 32(3), 263–267.

²⁹ O.A. Ibrahim, F. Zhang, A. V. Eliseenkova, R. J. Linhardt, M. Mohammadi, *Hum. Mol. Genet.*, **2004**; 13, 69-78.

³⁰ V. Sørensen, T. Nilsen, A. Wiedlocha, *Bioessays*, **2006**, 28(5), 504–514.

³¹ R. Z. Florkiewicz, A. Sommer, *PNAS*, **1989**, 86, 3978–3981.

³² P.-J. Yu, G. Ferrari, A. C. Galloway, P. Mignatti, G. Pintucci. *J Cell Biochem*, **2007**, 100(5), 1100-1108.

³³ F. Wang, L. Yang, L. Shi, Q. Li, G. Zhang, J. Wu, J. zheng, B. Jiao, *Oncotarget*, **2015**, 6(25), 21468-21478.

18 kDa isoform is found to be mainly in the cytosol and functions as an autocrine and paracrine signalling molecule³⁴.

From this point on in the text, the term 'FGF2' will exclusively refer to the 18kDa isoform.

FGF2 is one of the most extensively investigated members of the FGF family. FGF2 is a cytosolic protein that is secreted from the cell independently from the classical ER/Golgi pathway. Extensive research in the last two decades has given a significant insight into its secretion mechanism, which was determined to be direct translocation over the plasma membrane and therefore belongs to the group of proteins following UPS **Type I**³⁵. With crystallisation experiments, the structure of FGF2 was determined to contain 12 β -sheets³⁶ and an unstructured N-terminus not visible in the crystal structure data. Six of these anti-parallel β -sheets form a beta-sheet barrel, giving FGF2 its shape³⁷.

Autocrine and paracrine signalling of FGF2 is triggered through the formation of a tertiary complex with cell surface heparan sulfate proteoglycans (HSPGs) and a fibroblast growth factor receptor (FGFR). The formation of the tertiary complex causes the dimerization of FGFR, which leads to conformational changes. These changes trigger intermolecular transphosphorylation, which starts the signalling cascade within the cell. Through this interaction, downstream signalling pathways, including Ras, Raf, MAPK/ ERK³⁸ and PI3K/AKT³⁹, are activated promoting cell proliferation and survival. In addition to triggering signalling, the tertiary complex also hinders protein degradation⁴⁰. Five different FGF receptors have been identified in the literature so far. Four of these (FGFR 1-4) are highly conserved trans-membrane tyrosine kinase receptors⁴¹. With 23 different FGFs in the FGF family, specificity of the receptors is reached by alternative splicing of FGFR1-3 i their immunoglobulin(Ig)- like domains⁴².

³⁴ D. M Ornitz, N. Itoh, *Wiley Interdiscip Rev Dev Biol.*, **2015**, 4(3), 215–266.

³⁵ J. P. Steringer, W. Nickel, *Semin. Cell Dev. Biol.*, **2018**, 83(3), 3-7.

³⁶ H. Ago, Y. Kitagawa, A. Fujishima, Y. Matsuura, Y. Katsube, *J Biochem*, **1991**, 110(3), 360-363.

³⁷ J.S. Kastrup, E. S. Eriksson, H. Dalboge, H. Flodgaard, *Acta Crystallogr D Biol Crystallogr*, **1997**, 53, 160-168.

³⁸ O. A. Ibrahim, F. Zhan, S. C. Hrstka, M. Mohammadi, R. J. Linhardt, *Biochemistry (Mosc)*, **2004**; 43, 4724-4730.

³⁹ M. A. Karajannis, L. Vincent, R. Drenzo, S. V. Shmelkov, F. Zhang, E. J. Feldman, P. Bohlen, Z. Zhu, H. Sun, P. Kussie, S. Rafii, *Leukemia*, **2006**; 20, 979-986.

⁴⁰ S. Faham, R. E. Hileman, J. R. Fromm, R. J. Linhardt, and D. C. Rees, *Science*, **1996**, 271(5252), 1116–1120.

⁴¹ V. Eswarakumar, I. Lax, J. Schlessinger, *Cytokine Growth Factor Rev.*, **2005**; 16, 139-149.

⁴² M. Korc, R. E. Friesel, *Curr. Cancer Drug Targets*. **2009**; 9(5), 639-651.

While FGF1 binds promiscuously to all receptors, FGF2 only binds to FGFR1 (IIIb), FGFR1 (IIIc), FGFR2 (IIIc) and FGFR4⁴².

Through its effect as a potent mitogen and survival factor, FGF2 is involved in several processes including cell migration and proliferation as well as wound healing and neuro-differentiation⁴³ to name a few. FGF2 activates proliferation in all cells connected to angiogenesis, e.g. fibroblasts and endothelial cells⁴⁴. That makes FGF2 together with VEGF^{45, 46} one of the most potent pro-angiogenic factors⁴⁷. A number of different studies have shown that dysregulation of FGF2/FGFR signalling leads to aberrant cell growth and migration. This behaviour is seen in a number of different cancer Types⁴⁸.

2.2 Unconventional secretion pathway of FGF2

The lack of a signal peptide is the main characteristic associated with proteins bypassing the conventional secretion pathway for UPS. With FGF2 lacking a signal peptide, it was confirmed in the early 1990s with experiments blocking the classical secretion pathway by small molecule inhibitors Brefeldin A and Monensin⁴⁹, that FGF2 is using an unconventional secretion mechanism to be secreted from the cell. Since then, the mechanism it utilizes has been classified as UPS **Type I**⁵⁰. Furthermore, several interaction partners contributing to the secretion process have been identified through a genome wide RNAi screen and have been confirmed by biochemical reconstituted experiments³⁵. So far, ATP1A1, a subunit of the Na/K-ATPase, has been identified as a recruitment factor for FGF2 to the plasma membrane⁵¹. Furthermore, phosphatidylinositol-4, 5-bisphosphate (PI(4,5)P₂) was identified as the lipid binding

⁴³ A. Bikfalvi, S. Klein, G. Pintucci, D. B. Rifkin, *Endocr Rev*, **1997**, 18(1), 26–45.

⁴⁴ A. Beenken, M. Mohammadi, *Nat Rev Drug Discov*, **2009**, 8(3), 235–253.

⁴⁵ G. Seghezzi, S. Patel, C. J. Ren, A. Gualandris, G. Pintucci, E. S. Robbins, R. L. Shapiro, A. C. Galloway, D. B. Rifkin, P. Mignatti, *J Cell Biol*, **1998**, 141(7), 1659–1673.

⁴⁶ D. Ribatti, A. Vacca, M. Presta, *Gen Pharmacol.*, **2000**, 35(5), 227–231.

⁴⁷ P. Carmeliet, R. K. Jain, *Nature*, **2000**, 407(6801), 249–257.

⁴⁸ R. M. Akl, P. Nagpal, N. M. Ayoub, B. Tai, S. A Prabhu, C. M. Capac, M. Gliksman, A. Goy, K. S. Suh, *Oncotarget*, **2016**, 7(28), 44735–44762.

⁴⁹ P. Mignatti, T. Morimoto, D. B. Rifkin, *J Cell Physiol*, **1992**, 151(1), 81–93.

⁵⁰ G. La Venuta, M. Zeitler, J. P. Steringer, H.-M. Müller, W. Nickel, *J Biol Chem*, **2015**, 290(45), 27015–27020.

⁵¹ C. Legrand, R. Saleppico, J. Sticht, F. Lolicato, H.-M. Müller, S. Wegehingel, E. Dimou, J. P. Steringer, E. Ewers, I. Vattulainen, C. Freund, W. Nickel, *Commun Biol*, **2020**, 3, art n° 141.

FGF2 to the inner leaflet of the plasma membrane⁵². It was also determined that PI(4,5)P₂ binding is one of the driving factors for FGF2 oligomerisation, insertion and pore formation⁵³. The phosphorylation of FGF2 on tyrosine 81 by Tec Kinase was confirmed to be an upregulating factor for FGF2 secretion⁵⁴. Furthermore, two surface cysteine residues, C77 and C95, which are unique to FGF2 within the FGF family, are found to be a critical factor for the oligomerisation of FGF2 by forming intermolecular disulfide bridges. The mutation of both cysteine residues to alanine leads to a nearly complete loss of FGF2 secretion⁵⁵. Heparan sulphate proteoglycans (HSPGs), which are populating the cell surface, were found to extract FGF2 from the plasma membrane on the extracellular side and are able to retain it in the extracellular space close to the plasma membrane by binding FGF2 to its heparin sulphate chains⁵⁶.

Based on the identification of these cis and trans factors facilitating FGF2 secretion, a working model for the secretion mechanism was developed (**Scheme 3**). ATP1A1 (Na/K-ATPase subunit alpha-1) seems to be one of the first interaction partners of FGF2, leading to its recruitment to the plasma membrane. This interaction takes place independent of its normal function as part of the Na/K-ATPase⁵⁷. The residues on FGF2 crucial for the interaction with ATP1A1 were recently identified as lysine 54 and lysine 60 through ¹H-¹⁵N-HSQC-NMR experiments⁵¹. Mutation of these residues led to a 40% decrease of FGF2 secretion from cells⁵¹. This seems to indicate that an additional, as of yet unidentified factor might also play a role in FGF2 recruitment to the membrane. Once FGF2 is in close proximity to the plasma membrane, it binds to PI(4,5)P₂ rich domains on the inner leaflet. Once bound, FGF2 is phosphorylated on tyrosine 81 by Tec Kinase, which itself is recruited to the plasma membrane and is bound to PI(3,4,5)P₃. This phosphorylation, while not necessary for the secretion to occur, increases the secretion of FGF2 significantly. A mutation of tyrosine 81 to alanine showed a significantly decreased secretion phenotype⁵⁴ confirming the

⁵² K. Temmerman, A. D. Ebert, H.-M. Müller, I. Sinning, I. Tews, W. Nickel, *Traffic*, **2008**, *9*(7), 1204-1217.

⁵³ J. P. Steringer, S. Bleicken, H. Andreas, S. Zacherl, M. Laussmann, K. Temmerman, F. X. Contreras, T. A. M. Bharat, J. Lechner, H.-M. Müller, J. A. G. Briggs, A. J. Garcia-Saez, and W. Nickel, *J Biol Chem*, **2012**, *287*(33), 27659–27669.

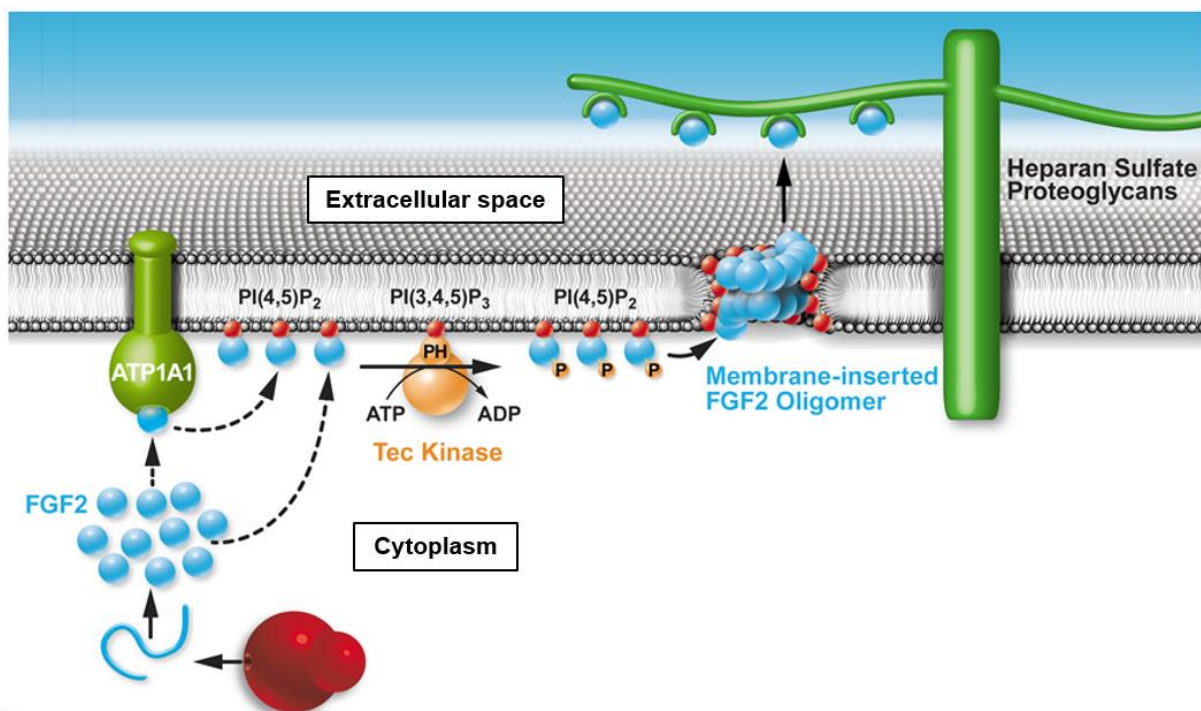
⁵⁴ A. D. Ebert, M. Laussmann, S. Wegehngel, L. Kaderali, H. Erfle, J. Reichert, J. Lechner, H.-D. Beer, R. Pepperkok, and W. Nickel, *Traffic*, 2010, *11*(6), 813–826.

⁵⁵ H.-M. Müller, J. P. Steringer, S. Wegehngel, S. Bleicken, M. Munster, E. Dimou, S. Unger, G. Weidmann, H. Andreas, A. J. Garcia-Saez, K. Wild, I. Sinning, W. Nickel, *J Biol Chem*, **2015**, *290*(14), 8925–8937.

⁵⁶ W. Nickel, *J Cell Sci*, **2007**, *120*(Pt 14), 2295–2299.

⁵⁷ R. Z. Florkiewicz, J. Anchin, A. Baird, *J Biol Chem*, **1998**, *273*(1), 544–551.

influence of Tec Kinase on FGF2 secretion. FGF2 binding to PI(4,5)P₂ induces oligomerisation and membrane insertion. The cone-like structure of PI(4,5)P₂ in combination with its abundance due to the oligomerisation of FGF2 bound to the inner leaflet, leads to a negative membrane curvature, easing the insertion process. The exact form of the pore is still under investigation, although two possibilities have been theorised¹⁰. The first theory is that a pore forms through which single FGF2 proteins are secreted. The second theory is that a continuous oligomerisation of FGF2 on the inner leaflet leads to a toroidal pore with FGF2 detaching on the outer leaflet with the help of HSPGs (as seen in **Scheme 3**). The HSPGs compete with the binding site of PI(4,5)P₂ on FGF2, which leads to FGF2 release and its storage in the extracellular space.



Scheme 3 Current model of FGF2 secretion mechanism showing the membrane recruitment through ATP1A1, FGF2 bound to PI(4,5)P₂ being phosphorylated by Tec Kinase leading to increased oligomerisation, insertion and finally translocation to the extracellular space facilitated by HSPGs. (courtesy: WN; adapted by author from Brough et al.⁵⁸)

While the ATP1A1 interaction as well as the phosphorylation through Tec Kinase, both lead to an upregulation of FGF2 secretion, the exact time point in the secretion mechanism still needs to be determined for both interactions.

⁵⁸ D.Brough, P. Pelegrin, W. Nickel, *J Cell Sci*, **2017**, *130*, 3197-3202.

2.3 FGF2 in cancer

In healthy cells, expression of FGF2 and FGFR are highly regulated. To stop FGF2 signalling, FGFRs are internalized^{42,59}. This mechanism however, when disturbed, can often cause aberrant FGF2/FGFR signalling in cancer cells, leading to the pathogenesis of many different cancer types.

2.3.1 FGF2/FGFR deregulation

This dysregulation of FGF2/FGFR signalling is often caused by FGFR amplification and/or upregulation⁶⁰. Through mutations in the FGFR, the receptor becomes insensitive to endocytosis, which leads to continued signal activation in cells⁶⁰.

Furthermore, germline point mutations of FGFR in human cancers have been connected with poor survival and chemoresistance⁶¹. Point mutations in the extracellular domain of FGFR can enhance the ligand binding ability and lead to over-activation. Meanwhile point mutations in the transmembrane/ kinase domain cause constitutive activation of the receptors⁶⁰.

FGFR2 amplification in cancer cells often occurs together with a truncation of its C-terminus, which in its normal state regulates endocytosis of the receptor to control FGF signalling. With this control mechanism destroyed additionally to FGFR2 upregulation, cancer types exhibiting these markers are generally connected to a poor outcome⁶².

Another factor in FGFR signalling dysregulation is alternative splicing of the Ig-domain of the receptor to more oncogenic isoforms. This process can result into the formation of an autocrine feedback loop instead of paracrine signalling^{63,64}, leading to more tumour growth. The switch of FGFR2-IIIb to its FGFR2-IIIc isoform is known to increase invasiveness in bladder cancer⁶⁵, for example.

⁵⁹ C. Powers, S. McLiskey, A. Wellstein, *Endocr. Relat. Cancer*, **2000**, *7*, 165–197.

⁶⁰ I. Ahmad, T. Iwata, H. Y. Leung, *Biochim Biophys Acta*, **2012**, *4*, 850-860.

⁶¹ C. Thussbas, J. Nahrig, S. Streit, J. Bange, M. Kriner, R. Kates, K. Ulm, M. Kiechle, H. Hoefler, A. Ullrich, N. Harbeck, *J Clin Oncol.* **2006**; *24*, 3747-3755.

⁶² J. H. Jang, K. H. Shin, J. G. Park, *Cancer Res.*, **2001**; *61*, 3541-3543.

⁶³ G. Yan, Y. Fukabori, G. McBride, S. Nikolaropolous, W.L. McKeenan, *Mol. Cell. Biol.*, **1993**, *13*, 4513-4522.

⁶⁴ P. Savagner, A.M. Valles, J. Jouanneau, K.M. Yamada, J.P. Thiery, *Mol. Biol. Cell*, **1994**, *5*, 851–862.

⁶⁵ C. L. Chaffer, J. P. Brennan, J. L. Slavin, T. Blick, E. W. Thompson, E.D. Williams, *Cancer Res.*, **2006**, *66*, 11271-11278.

2.3.2 FGF2 as pro-angiogenic factor

As previously mentioned, FGF2 is a very strong pro-angiogenic factor. For a tumour to grow, the supply of nutrients and oxygen to the cells needs to be ensured via its own blood supply.

Through the interaction with endothelial cells by paracrine signalling, FGF2 secreted from tumour cells causes the activation of the ERK1/2 and PKC signalling⁶⁶. This leads to cell proliferation, migration and finally angiogenesis. Furthermore, the degradation of the extracellular matrix (ECM) witnessed in tumour tissue⁶⁷ leads to excess release of FGF2 “stored” in the extracellular matrix (ECM), which exacerbates the paracrine signalling and leads to angiogenesis.

2.3.3 FGF2 in tumours

Dysregulation of proteins in cancer cells can be caused in two ways. One way is an activating mutations, leading to a more potent form of the protein, while the other one would be through upregulation of the transcription and translation. Because no activating mutation of FGF2 has been reported⁶⁸ yet, the main effect FGF2 exhibits in cancer cells is caused by overexpression. The main influence it holds comes through paracrine and autocrine signalling pathways. For example, in endometrial cancer a 10-20 fold increase of FGF2 expression can be witnessed⁶⁹. Also in number of different types of breast cancer, an elevation in FGF2 expression is noticeable^{70,71}.

FGF2 can also lead to chemoresistance of tumour tissues⁷². Paracrine FGF2 signalling between pericytes and endothelial cells plays an important role in maintaining the tumour vasculature in anti-VEGF therapy-resistant tumours like prostate cancer⁷³: The epithelium tissue, which can easily form tumours, is normally regulated by steroid hormones. It follows that these tumours are steroid-dependent and can be targeted with an anti-hormonal treatment. The upregulation of FGFR3 in combination with

⁶⁶ M. Presta, L. Tiberio, M. Rusnati, P. Dell’Era, G. Ragnotti, *Cell Regul.* **1991**, 2, 719-726.

⁶⁷ P. Lu, K. Takai, V. M. Weaver, Z. Werb, *Cold Spring Harb Perspect Biol.*, **2011**, 3(12), a005058.

⁶⁸ D. Ribatti, A. Vacca, M. Rusnati, M. Presta, *Cytokine Growth Factor Rev.*, **2007**; 18(3-4), 327-334.

⁶⁹ B. Dobrzycka, B. Mackowiak-Matejczyk, M. Kinalski, S. J. Terlikowski, *Gynecol Oncol.*, **2013**, 128, 454-460.

⁷⁰ M. Relf, S. LeJeune, P. A. Scott, S. Fox, K. Smith, R. Leek, A. Moghaddam, *Cancer Res.*, **1997**, 57, 963-969.

⁷¹ D. Visscher, F. DeMattia, S. Ottosen, F. Sarkar, J. Crissman, *Mod Pathol.*, **1995**; 8, 665-670.

⁷² R. Kurimoto, S. Iwasawa, T. Ebata, T. Ishiwata, I. Sekine, Y. Tada, K. Tatsumi, S. Koide, A. Iwama, Y. Takiguchi, *Int J Oncol*, **2016**, 48, 1825-1836.

⁷³ K. Ichikawa*, S. W. Miyano, Y. Minoshima, J. Matsui, Y. Fun, *Sci Rep*, **2020**, 10, art n°2939.

FGF2 witnessed in prostate cancer⁷⁴ leads to an autocrine signalling loop, through which the tumour becomes steroid independent. With this, the anti-hormonal treatment becomes redundant and new treatments option have to be explored. FGF2 is also investigated as a prognostic biomarker in different solid cancer types as well as in haematological tumours⁴⁸.

Additionally, FGF2 can function as an anti-apoptotic cell survival factor in tumour cells. In immune resistant cancer cells, the upregulation of FGF2 signalling has been linked to API5 (Apoptosis Inhibitor 5), an apoptotic suppressor and widely recognized as an immune escape gene⁷⁵. It has been shown that FGF2 and API5 exhibit a near 1:1 correlation in their expression levels in a number of different cancer types providing further proof that these two proteins are working in tandem to cause immune resistance in cancer cells. By blocking FGF2 with an antibody, the downregulation of FGF2/FGFR signalling through the downstream mediators PKC δ /ERK, was observed leading to BIM, a pro-apoptotic factor, to be increasingly expressed⁷⁵.

2.4 Clinical Therapy Approaches targeting FGF2

Until now, two approaches have been employed to target FGF2 and its effect in cancer cells. One approach is to target FGF2 directly, while the alternative targets the FGF2 signalling by inhibiting the FGF receptors.

Alternative ways to target FGF2 directly have been explored with varying degree of success. The development of a ligand trap to sequester FGF2 is one method having finished a Phase I clinical trial successfully⁷⁶. A soluble FGFR receptor fusion protein was designed to bind all mitogenic FGFs, including FGF2, with the exception of the metabolic hormone FGFs (FGF19/21/23)⁷⁷. This approach was found to inhibit *in vitro* cell proliferation and *in vivo* the growth of a variety of tumours was inhibited. Small molecules have been developed targeting HSPGs as a binding partner for FGF2.

⁷⁴ G. Yan, Y. Fukabori, G. McBride, S. Nikolaropolous, W. L. McKeegan, *Mol. Cell. Biol.*, **1993**, *13*, 4513-4522.

⁷⁵ K. H. Noh, S.-H. Kim *et al.*, *Cancer Res.* **2016**, *76*(22), 6471–6482.

⁷⁶ E. M. J. van Brummelen, E. Levchenko, M. Dómine, D. A Fennell, H. L. Kindler, S. Viteri, S. Gadgeel, P. G. López, V. Kostorov, D. Morgensztern, S. Orlov, M. G. Zauderer, J. F. Vansteenkiste, K. Baker-Neblett, J. Vasquez, X. Wang, D. I. Bellovin, J. H. M. Schellens, L. Yan, I. Mitrica, M. P. DeYoung, J. Trigo, *Invest New Drugs*, **2020**, *38*(2), 457-467.

⁷⁷ T. C. Harding, L. Long, S. Palencia, H. Zhang, A. Sadra, K. Hestir, N. Patil, A. Levin, A. W. Hsu, D. Charych, T. Brennan, J. Zanghi, R. Halenbeck, S. A. Marshall, M. Qin, S. K. Doberstein, *Sci Transl Med.*, **2013**, *5*, 3005414.

Sm27 directly inhibits the heparin-binding site on FGF2, effectively stopping the interaction with FGFR⁷⁸. In comparison, Suramin works as a FGF2 antagonist by inhibiting heparanase activity⁷⁹. It effectively stops the release of FGF2 from its storage in the extracellular matrix. Another approach that has been explored is to target FGF2 interaction partners like the Na/K-ATPase using a small molecule inhibitor, called anvirzel, to hinder FGF2 secretion⁸⁰.

Different methods to hinder FGF2 transcription have also been investigated. Peginterferon α -2b (IFN- α) works as an inhibitor of FGF2 expression in bladder cancer and melanoma⁸¹. Additionally, a number of small molecule inhibitors have also been identified to inhibit FGF2 transcription and therefore reduce angiogenesis significantly, an example for this is thalidomide⁸². The exact mechanism of its effects within the cell have yet to be fully elucidated, although a theory has been proposed to explain the anti-angiogenic effect that it shows. Thalidomide is theorized to bind into the GC box of the *fgf2* gene promoter, effectively stopping its transcription⁸³.

Targeting FGF receptors directly through either small molecule inhibitors or antibodies has shown great promise for hindering FGF2 signalling⁴⁸. FGFR belongs to the family of tyrosine kinases. Developing inhibitors targeting specific tyrosine kinases is difficult due to the highly conserved ATP-binding pocket⁸⁴. This can lead to severe off-target effects.

The first iteration of FGFR inhibitors, that have been developed were nonspecific inhibitors which also targeted other kinase receptors such as vascular endothelial growth factor receptor (VEGFR) and platelet-derived growth factor receptor (PDGFR)^{85,86}, because of the highly conserved ATP binding site. Lenvatinib is one of these inhibitors. It has been approved for the treatment of progressive radioactive iodine-

⁷⁸ G. Colombo, B. Margosio, L. Ragona, M. Neves, S. Bonifacio, D. S. Annis, M. Stravalaci, S. Tomaselli, R. Giavazzi, M. Rusnati, M. Presta, L. Zetta, D. F. Mosher, D. Ribatti, M. Gobbi, G. Taraboletti, *J Biol Chem.*, **2010**; *285*, 8733-8742.

⁷⁹ A. Tayel, K. H. Abd El Galil, M. A. Ebrahim, A. S. Ibrahim, A. M. El-Gayar, M. M. Al-Gayyar MM, *Eur J Pharmacol.*, **2014**, *72*, 151-160.

⁸⁰ J. A. Smith, T. Madden, M. Vijjeswarapu, R. A. Newman, *Biochem Pharmacol.*, **2001**, *62*, 469-472.

⁸¹ J. W. Slaton, P. Perrotte, K. Inoue, C. P. Dinney, I. J. Fidler, *Clin Cancer Res.*, **1999**, *5*, 2726-2734.

⁸² S. Zhou, F. Wang, T. C. Hsieh, J. M. Wu, E. Wu, *Curr Med Chem.*, **2013**, *20*, 4102-4108.

⁸³ T. D. Stephens, C. J. Bunde, B. J. Fillmore, *Biochem Pharmacol.*, **2000**, *59*(12), 1489-1499.

⁸⁴ C. Pottier, M. Fresnais, M. Gilon, G. Jerusalem, R. Longuespee, N. E. Sounni, *Cancers*, **2020**, *12*, 731-748.

⁸⁵ C. Lieu, J. Heymach, M. Overman, H. Tran, S. Kopetz, *Clin Cancer Res.*, **2011**, *17*, 6130-6139.

⁸⁶ V. K. Jain, N. C. Turner, *Breast Cancer Res.*, **2012**, *14*, 208-217.

refractory thyroid cancer⁸⁷. Beside FGFR, it also blocks signalling via vascular endothelial growth factor receptor (VEGFR) and platelet-derived growth factor receptor (PDGFR). Nintedanib, approved for the treatment of non-small-cell lung cancer, has a similar activity profile⁸⁸ as Lenvatinib. With VEGF also being a strong pro-angiogenic factor⁸⁹ like FGF2 and PDGF enhancing cell proliferation⁹⁰, the use of nonspecific inhibitors targeting all three receptors is a more comprehensive way of suppressing angiogenesis and slowing down or stopping tumour growth.

The second iteration of FGFR inhibitors have a more specific profile and are designed to target solely the FGF receptor family. One of these small molecule inhibitors is Debio 1347 which inhibits autophosphorylation of FGFR1-3. It is an orally bioavailable inhibitor and has been evaluated for safety and tolerability in patients in a phase I clinical trial for the treatment of advanced solid tumours⁹¹. Targeting breast cancer and gastric cancer, a small molecule inhibitor developed by AstraZeneca also targeting FGFR1-3 is being tested. Unlike Debio 1347, this inhibitor targets the kinase activity of FGFR1-3⁹².

Because of the highly conserved structure of tyrosine kinases, inhibitors can often have side effects and chemo-resistance can develop⁸⁴. Using unique residues within the active site or the vicinity thereof, leads to the development of more selective inhibitors. Taking advantage of such residues are irreversible inhibitors which can bind covalently to their interaction site. The most commonly targeted residue by covalent inhibitors is the side chain of cysteine. The covalent binding of the inhibitor leads to a slower off-rate, allowing a lower drug dosage. Furthermore, the use of these inhibitors limit the off-target effects and are very potent⁸⁴. A couple of such inhibitors have been developed to target FGFR. One of them is TAS-120 to treat advanced solid tumours, multiple myeloma⁹³ currently in phase I/II clinical trials.

⁸⁷ J. Matsui, Y. Funahashi, T. Uenaka, T. Watanabe, A. Tsuruoka, M. Asada, *Clin Cancer Res.*, **2008**; *14*, 5459-5465.

⁸⁸ S. Popat, A. Mellemaard, K. Fahrback, A. Martin, M. Rizzo, R. Kaiser, I. Griebisch, M. Reck, *Future Oncol.*, **2015**, *11*, 409-420.

⁸⁹ M. Shibuya, *Genes Cancer.*, **2011**, *2*(12), 1097-1105.

⁹⁰ C. Gialeli, D. Nikitovic, D. Kletsas, A. D. Theocharis, G. N. Tzanakakis, N. K. Karamanos, *Curr. Pharm. Des.*, **2014**, *20*(17), 2843-8.

⁹¹ Y. Nakanishi, N. Akiyama, T. Tsukaguchi, T. Fujii, K. Sakata, H. Sase, T. Isobe, K. Morikami, H. Shindoh, T. Mio, *Mol Cancer Ther.*, **2014**, *13*, 2547-2558.

⁹² P. R. Gavine, L. Mooney, E. Kilgour, A.P. Thomas, K. Al-Kadhimi, S. Beck, C. Rooney, T. Coleman, D. Baker, M. J. Mellor, A. N. Brooks, T. Klinowska, *Cancer Res.*, **2012**, *72*(8), 2045-56.

⁹³ H. Ochiwa, H. Fujita, K. Itoh, H. Sootome, A. Hashimoto, Y. Fujioka, Y. Nakatsuru, N. Oda, K. Yonekura, H. Hirai, *Mol Cancer Ther.*, **2013**, *12*, A270-A270.

Targeting one specific FGFR isoform within the receptor family is difficult due to the highly conserved kinase structure. Bayer has developed an antibody designed to specifically target FGFR3, which has been tested for safety and tolerability as an intravenous medication to treat advanced refractory solid tumours⁹⁴.

With the exception of one compound targeting Na/K-ATPase⁸⁰, there are no reports of research into developing inhibitors targeting the unique secretion mechanism of FGF2.

3 Protein-Protein-Interaction inhibitors

Crucial biological processes, like DNA replication, transcription, translation and transmembrane signalling are often regulated through protein complexes, which are formed through protein-protein interactions (PPI)⁹⁵. All PPI's are summarized under the term "interactom"⁹⁶.

The near ubiquitous involvement of PPI's in cellular processes can lead to severe medical conditions when these interactions are disturbed. Targeting PPIs creates a new avenue for drug discovery⁹⁷. Developing PPI inhibitors however comes with its own set of difficulties. Traditional drug discovery targets pockets and deep groves, like the ATP-binding pocket in kinases. Targeting PPIs on the other hand tends to be more difficult because the interaction surface is often flat and lacks pockets where small molecules can easily bind^{98,99}. Furthermore, the area the inhibitor needs to target is larger^{100,101} and often highly hydrophobic¹⁰⁰ compared to for example the ligand-binding area of a receptor. Additionally, the interaction between two proteins often exhibits high affinities that small molecules often cannot compete with¹⁰². In traditional drug discovery, known endogenous ligands of the target site are often used as

⁹⁴ J. Qing, X. Du, Y. Chen, P. Chan, H. Li, P. Wu, S. Marsters, S. Stawicki, J. Tien, K. Totpal, *J Clinical Invest.*, **2009**, 119, 1216.

⁹⁵ U. Stelzl, U. Worm, M. Lalowski, C. Haenig, F. H. Brembeck, H. Goehler, M. Stroedicke, M. Zenkner, A. Schoenherr, S. Koeppen, J. Timm, S. Mintzlaff, C. Abraham, N. Bock, S. Kietzmann, A. Goedde, E. Toksöz, A. Droege, S. Krobitsch, B. Korn, W. Birchmeier, H. Lehrach, E. E. Wanker, *Cell*, **2005**, 122, 957–968.

⁹⁶ G. C. Koh, P. Porras, B. Aranda, H. Hermjakob, S. E. Orchard, *J. Proteome Res.*, **2012**, 11, 2014–2031.

⁹⁷ D. E. Scott, A. R. Bayly, C. Abell, J. Skidmore, *Nat. Rev. Drug Discov.*, **2016**, 15, 533–550.

⁹⁸ B. I. Diaz-Eufracio, J. J. Naveja, J. L. Medina-Franco, *Adv. Protein Chem. Struct. Biol.*, **2018**, 110, 65–84.

⁹⁹ P. Buchwald, *IUBMB Life*, **2010**, 62, 724–731.

¹⁰⁰ M. C. Smith, J. E. Gestwicki, *Expert Rev. Mol. Med.*, **2012**, 14, e16.

¹⁰¹ A. C. Cheng et al. *Nat. BioTechnol.*, **2007**, 25, 71–75.

¹⁰² A. A. Ivanov, F. R. Khuri, H. Fu, *Trends Pharmacol. Sci.*, **2013**, 34, 393–400.

template for drug development, which for PPI's do not exist¹⁰³. Since PPI inhibitors need to target a bigger area, they tend to have a higher molecular weight than traditional inhibitors which often makes following the Lipinski rules a challenge⁹⁹. Due to all of these challenges; for a long time PPI's were considered to be 'undruggable'¹⁰².

An important step in designing PPI inhibitors is the identification of the so-called 'hot-spots' in the interaction area. These are the amino acids in the interaction site which play a significantly role in the interaction¹⁰⁴. These interaction sites can be identified by NMR⁵¹ analysis of the interaction and confirmed by point-mutations. The most common amino acids found in these spots are tryptophan, arginine and tyrosine¹⁰⁴.

A few approaches have been developed to help with the design and identification of PPI inhibitors. One approach is to develop a high-through put screen (HTS) of small molecule libraries containing a wide range of compounds¹⁰⁵. Another approach is to screen the PPI area with a fragment library. The goal of this approach is to target the separate hot-spots¹⁰⁶ in the interaction. Further information of where the identified fragments bind can be achieved by different methods like NMR or surface plasmon resonance (SPR). The information obtained can be used to link the fragments and optimize the inhibitor design. Other approaches are virtual screening or structure-based design, if a crystal structure is known.

Even with all these different methods, the development of specific PPI inhibitor is difficult but not impossible. In the last two decades, a number of PPI inhibitors have been developed and successfully brought to market or are currently in clinical trials¹⁰⁷. The rapid development of methods in structural biology enabled a better understanding of PPIs which has significantly sped up the design process of inhibitors¹⁰⁷.

Amongst the approved inhibitors, Maraviroc can be found to treat HIV¹⁰⁸. It blocks the binding of the viral envelop Gp120 to CCR5, which prevents the membrane fusion needed for virus entry into the cell. The PPI inhibitor is highly selective for CCR5 and showed a geometric 90% inhibition at 2nM concentration for CCR5-tropic HIV-1 viruses. Another example for a small molecule PPI inhibitor is Apabetalone, which is

¹⁰³ A. G. Coyne, D. E. Scott, C. Abell, *Curr. Opin. Chem. Biol.*, **2010**, *14*, 299–307.

¹⁰⁴ I. S. Moreira, P. A. Fernandes, M. J. Ramos, *Proteins*, **2007**, *68*, 803-812.

¹⁰⁵ J. A. Wells, C. L. McClendon, *Nature*, **2007**, *450*, 1001–1009.

¹⁰⁶ P. J. Hajduk, J. A. Greer, *Nat. Rev. Drug Discov*, **2007**, *6*, 211–219.

¹⁰⁷ H. Lu, Q. Zhou, J. He, Z. Jiang, C. Peng, R. Tong, J. Shi, *Sig Transduct Target Ther.*, **2020**, *5*, 213.

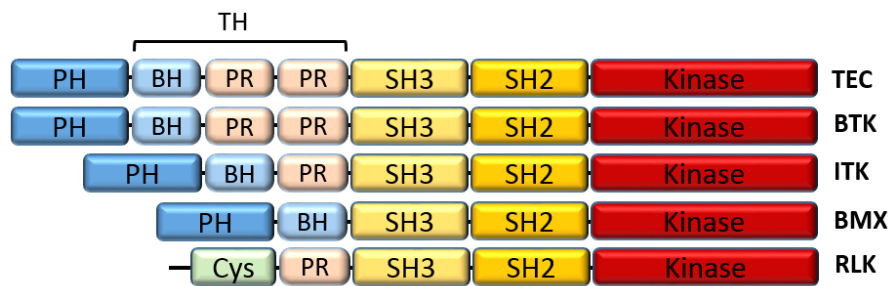
¹⁰⁸ P. Dorr *et al.* *Antimicrob. Agents Chemother* **2005**, *49*, 4721–4732.

currently in phase III clinical trials¹⁰⁹. It targets the BET protein BRD4 which is indicated as epigenetic driver of inflammation and atherogenesis. The inhibitor hinders the BET-dependent transcription induced by multiple inflammatory triggers by blocking interaction with enhancers and promoters¹¹⁰.

4 Tec Kinase and FGF2 protein-protein interaction

4.1 Tec Kinase: structure, function and connection to FGF2

The Tec Kinase family is made up of 5 members called Tec, Btk, Itk, Bmx, and Rlk¹¹¹. They belong to the group of *non-receptor* tyrosine kinases and are the second largest subgroup of this kind¹¹².



Scheme 4 Overview of Tec kinase family showing their structural similarities and differences.

The structure of Tec can be divided in 5 subdomains with a N-terminal plekstrin homology domain (PH), a Tec homology (TH) domain, and three Src homology domains SH3, SH2 and at the C-terminus SH1 (**Scheme 4**).

The N-terminal PH domain is a binding site for phosphoinositide-(3,4,5)-trisphosphate PI(3,4,5)P₃ and facilitates the transient binding of Tec to the inner leaflet of the plasma membrane. The TH domain contains a Btk motif (BH) and two proline rich regions (PRR)¹¹¹. The SH3 domain recognizes proline rich regions and interacts with the TH domain stabilizing Tec in its possibly inactive conformation¹¹². The deletion of the SH3 domain led to a constitutively active enzyme¹¹¹ further strengthening this hypothesis. The SH2 domain has been identified to bind phosphotyrosine residues on other

¹⁰⁹ D. Bailey *et al.*, *J. Am. Coll. Cardiol.*, **2010**, 55, 2580-2589.

¹¹⁰ L. M. Tsujikawa, L. Fu, S. Das *et al.*, *Clin Epigenet*, **2019**, 11, art n°102.

¹¹¹ H. Mano, *Cytokine Growth Factor Rev.*, **1999**, 10(3-4), 267-280.

¹¹² J. M. Bradshaw, *Cell Signal*, **2010**, 22(8), 1175-84.

ligands¹¹³. The catalytic domain of Tec is located in the SH1 domain, which contains the ATP-binding pocket to facilitate its phosphorylation activity.

Tec Kinases function downstream of several cell surface receptors, e.g. cytokine receptors and G-protein coupled receptors and are therefore involved in many cellular processes¹¹¹. Tec Kinase phosphorylates several substrates, of which PLC- γ 2 is one of them. While PLC- γ 2 is also phosphorylated by other members of the Tec kinase family, STAB (BRDG1) is phosphorylated exclusively by Tec Kinase¹¹¹.

Tec Kinase is activated by phosphorylation of Src kinases but also has the ability to autophosphorylate¹¹². With PI3K upregulation in several cancer types, it might have a connection to Tec Kinase upregulated FGF2 secretion¹¹⁴. PI3K catalyzes PI(3,4,5)P3 formation which facilitates the recruitment of Tec Kinase. This may lead to an increase of binding of Tec Kinase to the inner leaflet-of the plasma membrane leading to an upregulation of FGF2 secretion.

The amino acid residues responsible for the interaction between FGF2 and Tec Kinase have not been identified. However, the interaction surface on Tec Kinase was narrowed down to its kinase domain¹¹⁵.

4.2 Tec Kinase in cancer

Tec kinase is known to be a regulator for cell growth and differentiation in hematopoietic cells, like for example myeloid lineage cells, and has also been linked to T and B cell receptor signaling¹¹⁶. Tec has also been connected to tumorigenesis and is found to be overexpressed in amongst other cancer types also in hepatocellular carcinomas¹¹⁷. In these types of cancers, Tec kinase is found to be a regulator controlling development in an FGF2 dependent manner. Furthermore, it was shown that in acute myeloid leukemia (AML) Tec Kinase, through overexpression, contributes significantly to the FGF2- dependent chemoresistance that occurs after prolonged

¹¹³ L. E. Marengere, T. Pawson, *J Cell Sci. Suppl*, **1994**, 18, 97–104.

¹¹⁴ P. Liu, H. Cheng, T. M. Roberts, J. J. Zhao, *Nat. Rev. Drug Discov.*, **2009**, 8, 627–644.

¹¹⁵ G. La Venuta, S. Wegehingel, P. Sehr, H.-M. Müller, E. Dimou, J. P. Steringer, M. Grotwinkel, N. Hentze, M. Mayer, D. W. Will, U. Uhrig, J. D. Lewis, W. Nickel, *J. Biol. Chem.*, **2016**, 291(34), 17787-17803.

¹¹⁶ L. Yu, O. E. Simonson, A.J. Mohamed, C. I. Smith, *FEBS J.*, **2009**, 276, 6714–6724.

¹¹⁷ T. Vanova, Z. Konecna, Z. Zbonakova, G. La Venuta, K. Zoufalova, S. Jelinkova, M. Varecha, V. Rotrekl, P. Krejci, W. Nickel *et al.*, *Stem Cells*, **2017**, 35, 2050–2059.

treatment with FLT3 inhibitors¹¹⁸. It was found that the inhibition of FGF2/FGFR1 signalling leads to the sensitivity against FLT3 drugs in AML cells to reoccur.

4.3 Identification of a small molecule inhibitor targeting FGF2 and Tec Kinase interaction

To target the interaction of FGF2 and Tec Kinase, an assay was developed with high-throughput screening (HTS) capabilities¹¹⁵. The assay was based on the Alpha Assay® using immobilized proteins on donor and acceptor beads to evaluate the effect of small molecules on the interaction.

A library of 79 000 compounds was screened at 40µM¹¹⁵, after deselection of known promiscuous inhibitors, 141 compounds were identified with an inhibition of >40%¹¹⁵. For these compounds a dose-response curve was determined using the Alpha® Technology, to yield 28 compounds with an IC₅₀ of >100µM.

In addition to three structurally related compounds, also two inactive derivatives were identified (**Fig. 1**). Their inhibition levels were determined in the Alpha assay separately from the screening set-up to give IC₅₀ values in the low micromolar range. All of these compounds showed no pleiotropic effects on cell proliferation¹¹⁵. Furthermore, it was shown that they exhibit specificity for the inhibition of the interaction of Tec Kinase and FGF2. The phosphorylation of STAB, another substrate of Tec Kinase, took place in the presence of all compounds, showing no inhibitory activity¹¹⁵. The influence of these compounds on FGF2 secretion was also determined. The results showed a 50% reduction of FGF secretion at a concentration of 25µM for **C6**, while **C14** exhibited a 30% reduction and **C21** only a 25% reduction¹¹⁵.

These results show that the development of a small molecule inhibitor for the protein-protein interaction of Tec Kinase and FGF2 can be successfully executed, with a possible application in cancer therapy or as a tool compound to further study the effect of Tec Kinase on FGF2 secretion.

¹¹⁸ E. Traer, J. Martinez, N. Javidi-Sharifi, A. Agarwal, J. Dunlap, I. English, T. Kovacovics, J. W. Tyner, M. Wong, B. J. Druker, *Cancer Res.*, **2016**, 76(22), 6471-6482.

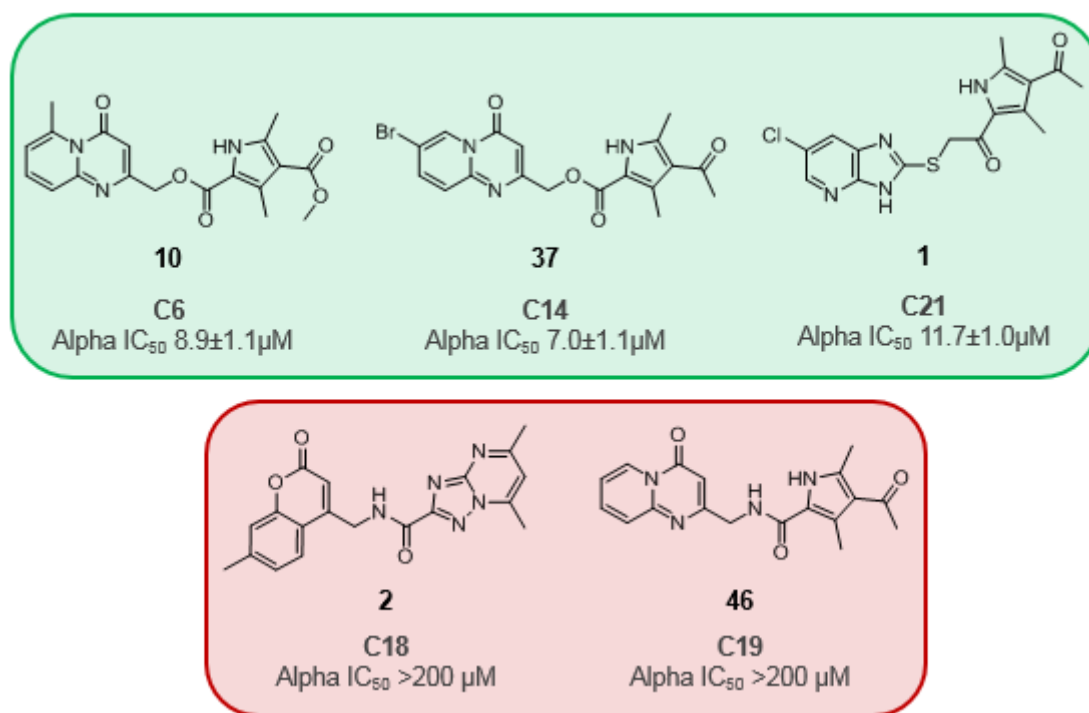


Fig. 1 HTS identified small molecule inhibitors and control compounds for the PPI of Tec Kinase and FGF2; green box: inhibitors; red box: inactive control compounds.

B Aim

Based on the inhibitors targeting the protein-protein interaction of Tec Kinase and FGF2 identified and validated in La Venuta *et al.*¹¹⁵, a comprehensive study of the structure-activity-relationship (SAR) of the hit compound “**C6**” was needed. The goal was to improve the IC₅₀ of **C6** from the low micromolar into the nanomolar range by modifying its structure.

To achieve this, a library of **C6** derivatives needed to be synthesised. The first step was to develop a comprehensive medicinal chemical approach detailing the planned modifications in each of the different sections of the molecule. Additionally, a synthesis plan to achieve the needed structural modifications needed to be developed. The total synthesis needed to be flexible enough to allow the combination of separate modifications. To validate the effect of the compounds, all compounds were tested in the AlphaScreen^{®119} protein-protein interaction assay giving a dose-response curve. Additionally, the compounds identified in the Alpha assay with a similar or lower IC₅₀ than **C6** were validated in a cell-based assay to determine their effect on FGF2 secretion.

¹¹⁹ Perkin Elmer, May 2016, “User’s Guide To Alpha Assays: Protein:Protein Interactions” https://www.perkinelmer.com/lab-solutions/resources/docs/009625A_01_GDE.pdf; (15.01.2020).

C Medicinal Chemistry approach

La Venuta *et al*¹¹⁵ identified a small molecule inhibitor **C6**, which disrupts the protein-protein interaction between Tec Kinase and FGF2, leading to a decrease of FGF2 secretion. It was decided to investigate the structure-activity-relationship (SAR) of **C6** to find new analogues with an improved potency and selectivity towards this PPI. This effort was also undertaken with an eye on the possibility of developing therapeutics based on the **C6** structure, so some modifications were made to improve its metabolic stability.

For a comprehensive design approach of new analogues of **C6**, its structure was divided into three subunits which could be modified individually and combined to give an optimal final molecule. The design approach used is summarized in **Fig. 2**.

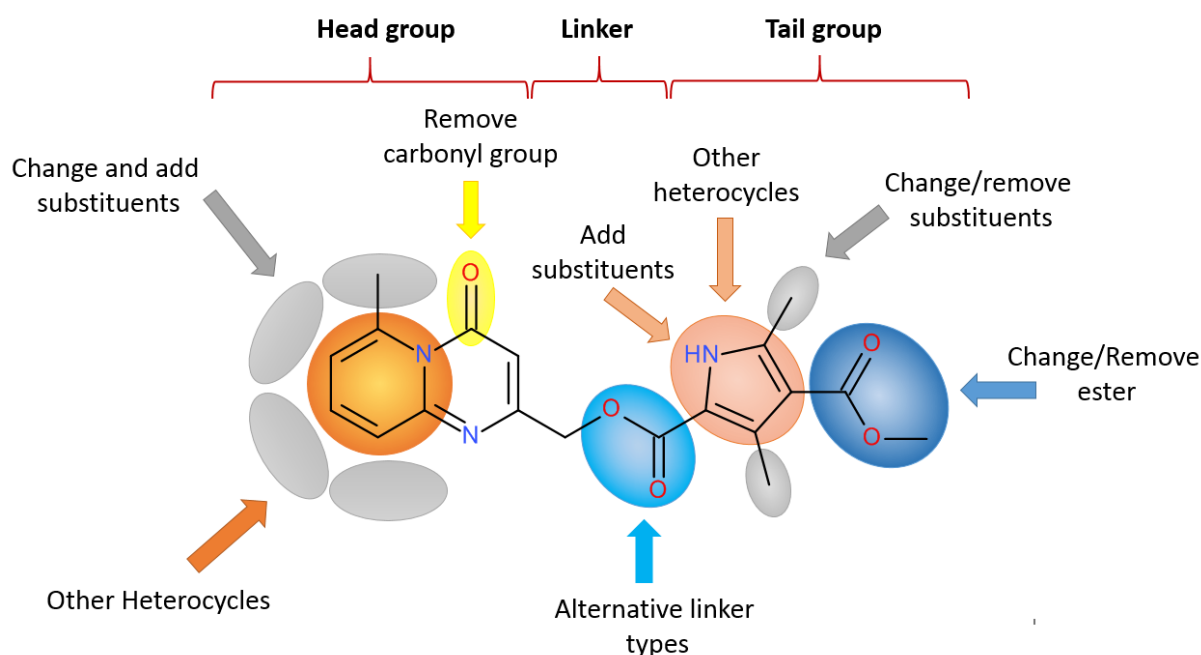


Fig. 2 Overview of planned SAR for **C6**; Changes of the ring structure and substituents in both head and tail group as well as changing the linker between both.

The **C6** structure was subdivided into a so-called head group, the linker region and the tail group.

The head group is composed of a substituted pyridopyrimidone scaffold. Changes to the head group were primarily focused on finding the optimal position and type of substituent on the scaffold ring. Adding an additional substituent was also investigated,

as well as removing the carbonyl group to modify the aromatic structure of the scaffold itself.

The ester function in the linker region can potentially undergo metabolic cleavage *in vivo* by plasma esterases as well as esterase degradation within the cell, making the replacement of the ester function to an amide a priority.

The tail group is composed of a tetrasubstituted pyrrole where only the N1 is unsubstituted. To determine the importance of the different substituents on the tail group, pyrrole analogues were synthesised where substituents were removed or increased in size. Another set of compounds was synthesised with an added substituent on the N1 to determine its effect. Furthermore, the exchange of the whole pyrrole tail group with other heterocycles was done to determine its importance in the C6 structure.

D Chemistry: Results and Discussion

1.1 Synthesis approach

A retrosynthetic evaluation of the C6 structure was necessary to determine the best synthesis approach to allow modification with the least amount of reaction steps necessary.

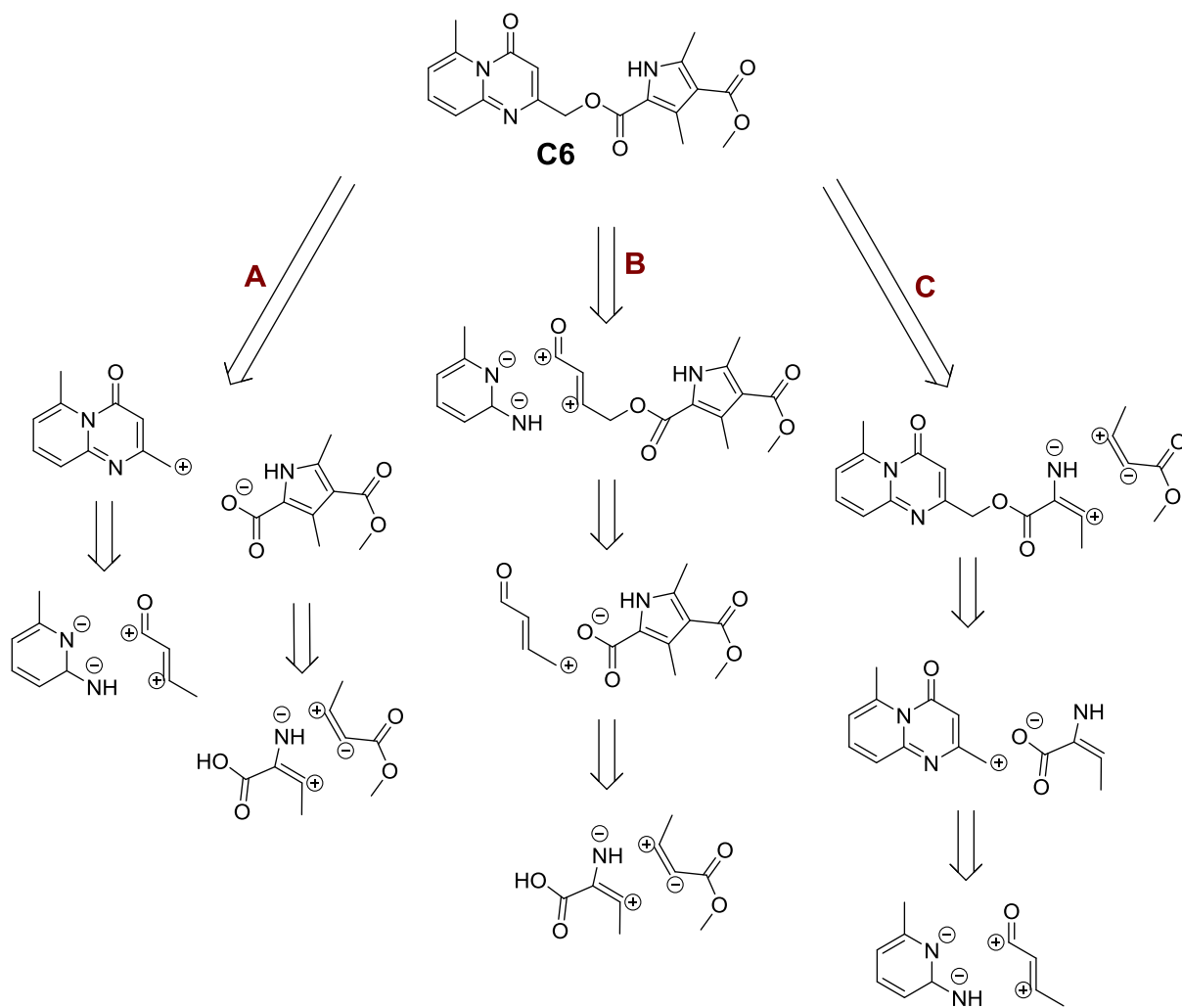
Three synthetic pathways are feasible (**Scheme 5**). With path **A**, the linker region is used to split **C6**. One half contains the head group and the other the tail group. Both of these groups can be synthesised in parallel and combined in different combinations. This leads to a diverse set of compounds with single or combined modifications to determine the SAR. Path **B** and **C** follow a linear synthetic route. Path **B** starts with the synthesis of the pyrrole ring and adds step-by-step the reagents to reach the final structure. Alternatively the synthesis pathway can start on the other end of the molecule with the aminopyridine (**path C**) as starting material. Through successive reaction steps to each of the starting materials, **C6** can be synthesised. For these linear reaction pathways the total sum of reaction steps is the same as path **A**. However, for the synthesis of a library of modified structures the total of all reactions steps needed would be considerably more. Furthermore with the linear synthesis routes, the possibility of having to introduce protective groups for some of the functional groups along the pathway increases and would add more reaction steps.

Considering the synthesis pathways, the most efficient route for the development of a compound library to investigate the structure-activity relationship of C6 is path **A**.

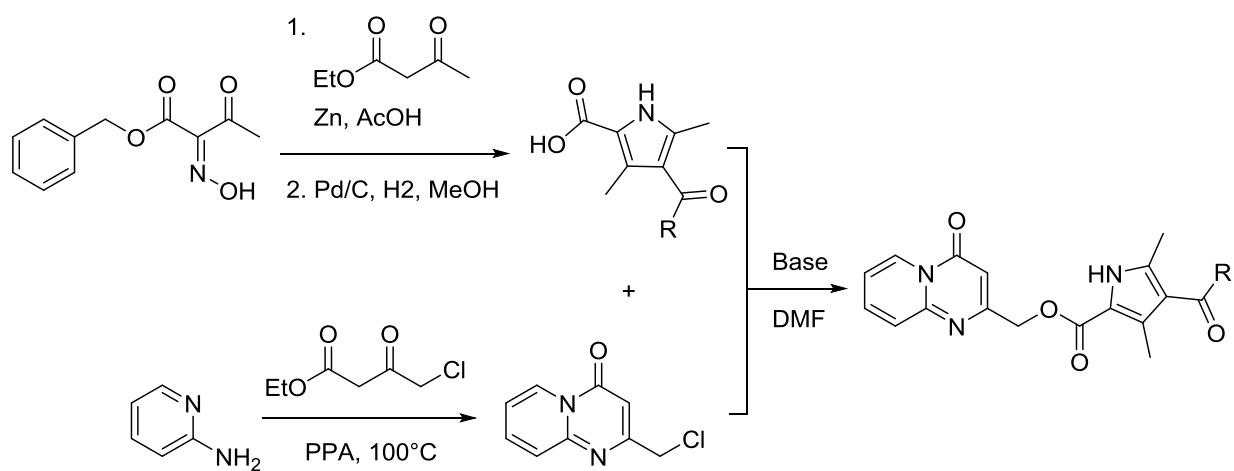
Following the retro-synthesis path **A**, a synthetic route was developed based on literature known reactions (**Scheme 6**). To synthesise the pyridopyrimidone, the cyclisation reaction following the procedure by Ferrarini *et al.*¹²⁰ was used followed by an alkylation reaction to link the pyrrole to the head group. To synthesise pyrrole analogues, the Knorr-Synthesis by Shiner *et al.*¹²¹ was used.

¹²⁰ P. L. Ferrarini, C. Mori, O. Livi, G. Biagi, A. M. Marini, *J. Heterocyclic Chem.*, **1983**, *20*, 1053-1057.

¹²¹ C. M. Shiner, T. D. Lash, *Tetrahedron*, **2005**, *61*, 11628-11640.



Scheme 5 Retrosynthesis overview for C6.



Scheme 6 Synthetic steps for C6 analogues.

1.2 Head group modification

1.2.1 Substituent group and position modification of the head group

To synthesise the pyridopyrimidone head group, the reaction protocol by Ferrarini *et al.*¹²⁰ was adapted and utilized. A set of differently substituted 2-aminopyridine compounds were each mixed with ethyl 4-chloroacetoacetate and polyphosphoric acid (PPA) before being stirred at 90-100°C for 2h.

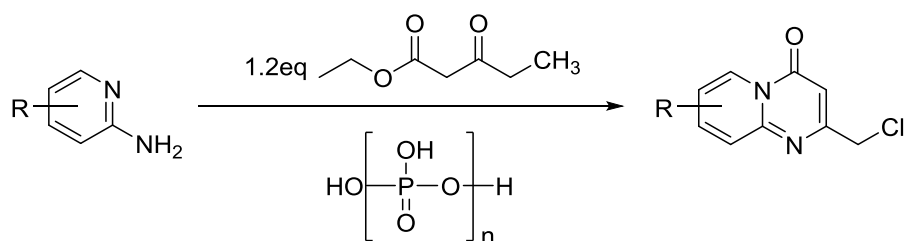
The yields of all synthesised compounds vary greatly (**Table 1**). The substituent as well as the position on the ring seems to affect the product yield. Comparing the yields of all reactions, it is clear that the yields for all compounds with a trifluoromethyl substituent (**130-133**) are distinctly lower than for other substituents. An explanation can be found by examining the proposed reaction mechanism¹²² in

Scheme 7. For the first reaction step to occur, the N1 on the pyridine needs to be protonated, which leads to the formation of a positively charged intermediate **I** that is stabilized through resonance structures to form the actual reactive compound **II** needed for the first step in the reaction. A lot of energy is needed to compensate for the loss of the aromaticity of the pyridine ring to form the likely not very stable intermediate **II**. Adding a substituent to the pyridine ring can help to stabilize intermediate **I**, if substituents can contribute additional resonance structure through their positive mesomeric effect ((+)-M-Effect). While deactivating substituents like Br Cl and trifluoromethyl should all have a negative effect on the formation of intermediate **II**, the weak (+) M-effect that chloro and bromo substituents can exhibit, seems to compensate. Considering this, it is of no surprise that compounds with a trifluoromethyl group exhibiting a negative inductive and negative mesomeric effect have a distinctive lower yield. The attempt to introduce a nitrile group as substituent (**145**) didn't give any product. The nitrile group was likely hydrolysed under the highly acidic reaction conditions to form the carboxylic acid¹²³.

¹²² S.N. Basahel, N. S. Ahmed, K. Narasimharao, M. Mokhtar, *RSC Adv.*, **2016**, 6, 11921-11932.

¹²³ V. K. Kriebel, C. I. Noll, *J. Am. Chem. Soc.*, **1939**, 61, 560-563.

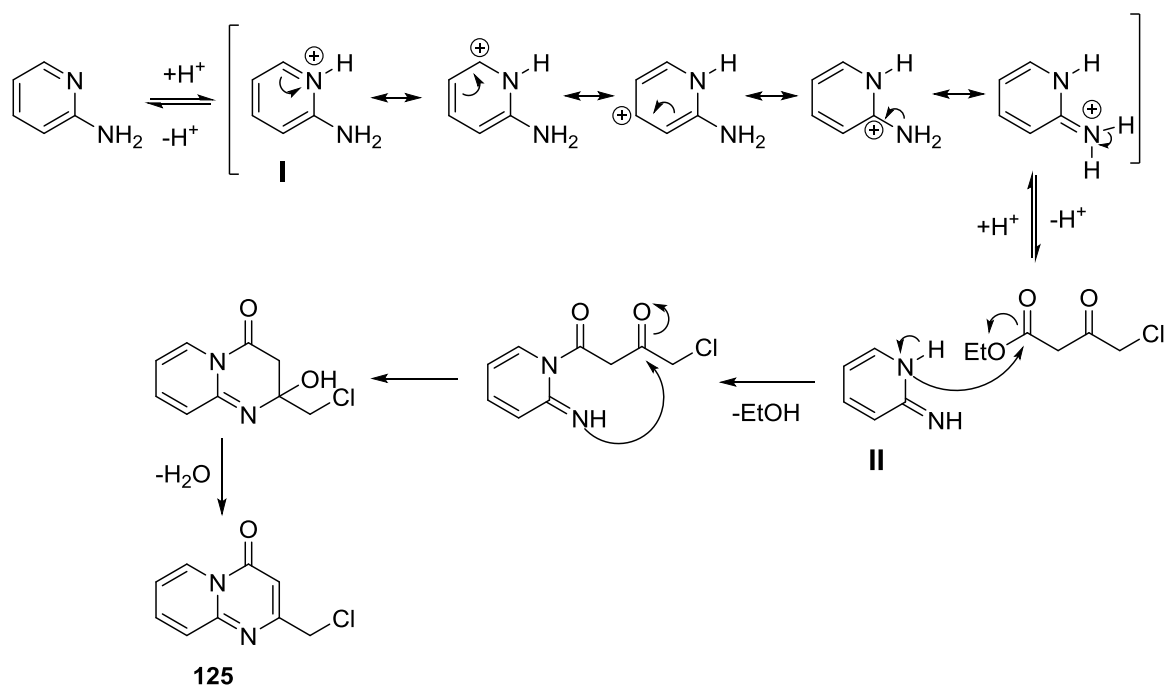
Table 1 Overview of pyridopyrimidone synthesis with different substituents.



	N°	R	Time [h]	Temp [°C]	Yield [%]
	125	H	2	125	73 ^a
	126	Me	2	100	56
	130	CF ₃	2	125	26 ^a
	134	OMe	2	125	65 ^a
	138	Br	2	125	76 ^a
		Br	2	95	91
	127	Me	2	125	62 ^a
	131	CF ₃	2	125	31 ^a
	135	OMe	3	95	50 ^b
	142	Cl	2	125	81 ^a
	139	Br	2	125	38 ^a
		Br	2	100	87
	145	CN	2	100	--
	128	Me	2	125	49 ^a
	132	CF ₃	2	125	27 ^a
	136	OMe	2	125	30 ^a
	143	Cl	2	125	76 ^a
	140	Br	2	125	22 ^a
		Br	2.5	100	31
	129	Me	2	125	66 ^a
	133	CF ₃	2	125	6 ^a
	137	OMe	2	125	65 ^a
	144	Cl	2	125	34 ^a
	141	Br	2	125	65 ^a

^a crude yield, experiment conducted by M. Mößer¹²⁴; ^b experiment conducted by I. Ferreira.

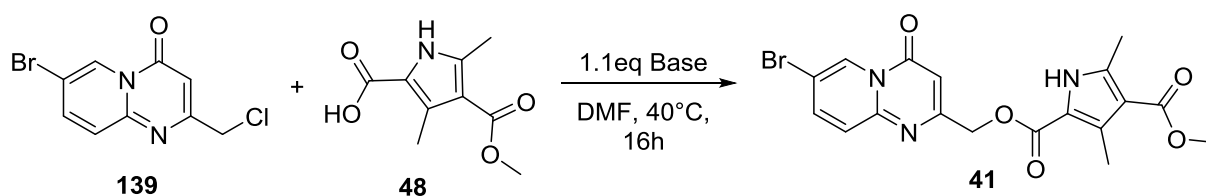
¹²⁴ M. Mößer, "Synthesis of Tec-Kinase Inhibitors as a novel class of anti-angiogenic drugs for cancer therapy", 2015, Bachelor thesis, Universität Heidelberg.



Scheme 7 Plausible reaction mechanism of the pyridopyrimidone synthesis of **125**.

To synthesise the final compounds, the head and the tail group are linked together by alkylation of the carboxylic acid of the pyrrole tail group. A set of inorganic bases were tested to establish the reaction conditions. The educts were stirred in DMF with each base at 40°C overnight.

Table 2 Overview of test reactions for ester linker of **41**¹²⁵.



Test reaction	Pyrrole	Base	Time [h]	Temp [°C]	Yield [%]
I	1.1eq	NaCO ₃	16	40	<1
II	1.1eq	NaHCO ₃	16	40	--- ^a
III	1.1eq	Cs ₂ CO ₃	16	40	39
IV	1.1eq	Ag ₂ O	16	40	-- ^a

^a not determined, analysis via UPLC-MS and TLC shows formation of product and side products

As can be seen in **Table 2**, the base leading to the product formation in a reasonable yield was cesium carbonate (entry **III**). While silver oxide (entry **IV**) and sodium

¹²⁵ unpublished data; reactions conducted by M. Mößer.

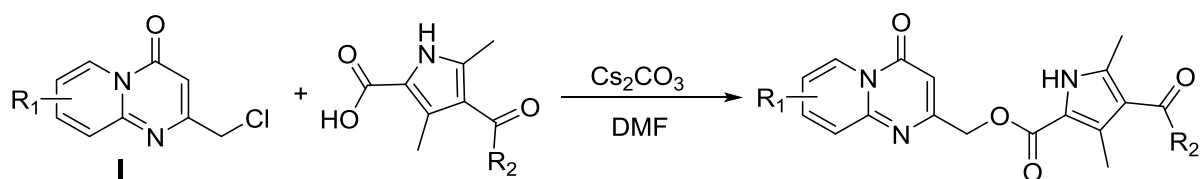
biscarbonate (entry **II**) lead to some product formation, the analysis of their UPLC-MS reaction controls after 16h show low conversion and presence of a side product. The reaction with sodium carbonate (entry **I**) was almost complete after 16h with a significant lower yield caused by issues during the work-up. Comparing the UPLC-MS reaction controls of **I** and **III** after 2h showed that the reaction with cesium carbonate was faster when comparing the consumption of the educts, which is why the reaction with sodium carbonate was not repeated. NMR analysis additionally confirmed that the intended O-alkylated product was formed and not the N-alkylated isomer. There was no evidence of the potential pyrrole N-alkylation side reaction with cesium carbonate as base.

The established conditions were used to link the synthesised pyridopyrimidones **124-144** to different pyrrole building blocks. The pyrrole building blocks **48**, **52** and **53** were each stirred with the educt **I** in the presence of cesium carbonate at 40°C in DMF. After the aqueous work-up, the purity of the synthesised compounds was determined by NMR and UPLC-MS and the products purified if needed.

As can be seen in **Table 3**, the isolated yields for the reactions linking the pyridopyrimidone head groups to a selection of pyrrole building blocks range from low to excellent. This disparity of results can be attributed to poor solubility of several compounds causing complications during the aqueous work-up, e.g. compounds **22**, **24** and **27**. Furthermore, in some cases the product required purification by preparative HPLC, which resulted in further product loss and a further reduced yield. No particular pattern is discernible when the yields of compounds differing in the pyrrole building block are compared, which indicates that they don't have an influence on the reaction. While most reactions were run overnight for convenience, compounds **121-123** show clearly that a shorter reaction time can be achieved by slightly modified reaction conditions. Furthermore, the entries for compound **40** and **41** show that a slight increase of base, led to an increase of isolated product.

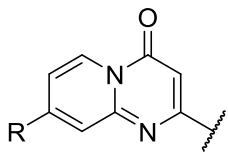
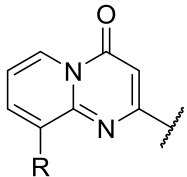
The established two-step synthesis for **C6** analogues containing a variety of substituents on the head group starting from their 2-aminopyridine educts, gave good overall yields for the majority of synthesised compounds. The exceptions, e.g. compounds containing a trifluoromethyl group, were mostly due to solubility issues during the work-up. In conclusion, it can be said that this synthesis pathway is a very efficient way to obtain a wide variety of compounds in a fast and expedient manner.

Table 3 Syntheses of C6 analogues with pyridopyrimidines **124-144** in combination with pyrrole building blocks **48**, **52** and **53^a**.



	N°	R ₁	R ₂	Pyrrole [eq]	Cs ₂ CO ₃ [eq]	Time [h]	Temp [°C]	Yield ^c [%]	
	4	H	Me	1.1	1.1	16	40	65 ^a	
	5	H	OMe	1.1	1.1	16	40	38 ^a	
	6	Me	Me	1.1	1.1	16	40	6 ^{a,d}	
	10	Me	OMe	1.1	1.1	16	40	58	
	66	Me	OEt	1.1	1.1	17	40	98	
	14	CF ₃	Me	1.1	1.1	16	40	6 ^{a,d}	
	18	CF ₃	OMe	1.1	1.1	16	40	4 ^{a,d}	
	28	OMe	Me	1.1	1.1	16	40	44 ^a	
	32	OMe	OMe	1.1	1.1	16	40	19 ^a	
	36	Br	Me	1.1	1.1	16	40	46 ^a	
	40	Br	OMe	1.1	1.1	16	40	62	
			Br	OMe	1.1	1.5	17	40	75 ^b
	67	Br	OEt	1.1	1.1	17	40	93	
	7	Me	Me	1.1	1.1	16	40	39 ^a	
	11	Me	OMe	1.1	1.1	16	40	19 ^a	
	123	Me	OEt	1.5	2	2	50	52 ^e	
	15	CF ₃	Me	1.1	1.1	16	40	9 ^{a,d}	
	19	CF ₃	OMe	1.1	1.1	16	40	3 ^{a,d}	
	29	OMe	Me	1.1	1.5	17	40	43 ^a	
	33	OMe	OMe	1.1	1.5	17	40	85 ^b	
	22	Cl	Me	1.1	1.1	16	40	4 ^a	
	25	Cl	OMe	1.1	1.1	16	40	30 ^a	
	37	Br	Me	1.1	1.1	16	40	44 ^a	
	41	Br	OMe	1.1	1.1	16	40	77	
			Br	OMe	1.1	1.6	17	40	81 ^b
	65	Br	OEt	1.1	1.1	16	40	99	

Table 3 continued ^a

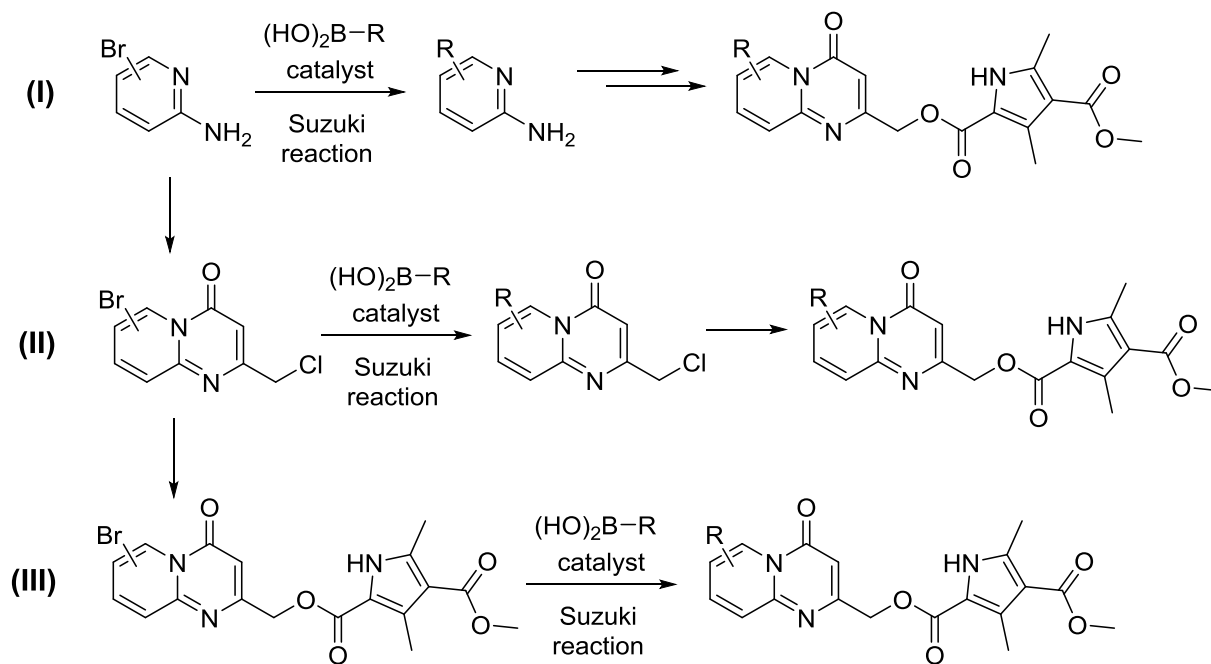
	N°	R	R ₂	Pyrrole [eq]	Cs ₂ CO ₃ [eq]	Time [h]	Temp [°C]	Yield ^b [%]
	8	Me	Me	1.1	1.1	16	40	43 ^a
	12	Me	OMe	1.2	1.2	16	40	41 ^a
	119	Me	OEt	1.2	1.2	15	40	67
	16	CF ₃	Me	1.1	1.1	16	40	2 ^{a,d}
	20	CF ₃	OMe	1.1	1.1	16	40	7 ^{a,d}
	30	OMe	Me	1.1	1.1	16	40	38 ^a
	34	OMe	OMe	1.1	1.1	16	40	1 ^{a,d}
	23	Cl	Me	1.1	1.1	16	40	42 ^a
	26	Cl	OMe	1.1	1.1	16	40	12 ^a
	38	Br	Me	1.1	1.1	16	40	32 ^a
	42	Br	OMe	1.1	1.1	16	40	59 ^a
	121	Br	OEt	1.5	2	1.5	50	63
	9	Me	Me	1.1	1.1	16	40	8 ^a
	13	Me	OMe	1.1	1.1	16	40	59 ^a
	120	Me	OEt	1.2	1.2	15	40	38
	21	CF ₃	OMe	1.1	1.1	16	40	1 ^{a,d}
	31	OMe	Me	1.1	1.1	16	40	64 ^a
	35	OMe	OMe	1.1	1.1	16	40	31 ^a
	24	Cl	Me	1.1	1.1	16	40	8 ^a
	27	Cl	OMe	1.1	1.1	16	40	11 ^a
	39	Br	Me	1.1	1.1	16	40	56 ^a
	43	Br	OMe	1.1	1.1	16	40	62 ^a
	122	Br	OEt	1.5	2	1.5	50	36 ^d

compound synthesised by ^a M. Mößer¹²⁴ and ^b I. Ferrara¹³³; ^c crude yield; purified by ^d HPLC or ^e silica column chromatography.

1.2.2 Introducing bigger alkyl substituents on the C6 head group

To synthesise C6 analogues containing a larger alkyl substituent on the pyridopyrimidone head group, the Suzuki cross coupling reaction with its less-toxic and

comparatively mild reaction conditions^{126,127,128} was utilized. Additionally its high compatibility with a number of functional groups¹²⁹ offers the possibility of introducing the alkyl group at later points during the synthetic pathway. Seeing as the Suzuki reaction generally performs well with bromo substituted starting materials, the already synthesised bromo compounds, e.g. **40** or **138**, can be used. Considering the two-step synthesis needed to obtain a **C6** analogues, three different possibilities to introduce the alkyl group are conceivable as can be seen in **Scheme 8**.



Scheme 8 Schematic overview of the different approaches possible to introduce alkyl group via Suzuki reaction.

The most efficient way to introduce a variety of different alkyl groups would be after the reaction step linking the head and the tail building blocks together (**Scheme 8 (III)**). Using this approach would be preferable as this would keep the reaction steps needed to attain a range of differently substituted analogues at a minimum. Alternatively, the Suzuki reaction can be performed on the pyridopyrimidone head group before it is attached to the tail group (**Scheme 8 (II)**). This approach adds to the total number of reactions steps required to synthesise a variety of compounds but also opens up the possibility of linking the new head groups to a range of different tail group building blocks extending the scope of possible compounds to make. The third approach would

¹²⁶ S. R. Chemler, D. Trauner, S. J. Danishefsky, *Angewandte Chem. Intl. Ed.*, **2001**, 40(24), 4544-4568.

¹²⁷ N. Miyaura, A. Suzuki, *Chem. Rev.*, **1995**, 95(7), 2457-2483.

¹²⁸ S. s. Gujral, S. Kathri, P. Riyal, *Indo Global J. Pharm. Sci.*, **2012**, 2(4), 351-367.

¹²⁹ S. W. Wright, D. L. Hageman, L. D. McClure, *J. Org. Chem.*, **1994**, 59(20), 6095-6097.

be to modify the 2-aminopyridine directly before it is transformed into the pyridopyrimidone head group followed by the attachment of the pyrrole ring (**Scheme 8 (I)**). Utilizing this path would require the largest number of reaction steps needed to create a number of new compounds and with that is the most undesirable approach.

1.2.2.1 Evaluation of Suzuki coupling reaction with compounds **40** and **41**

To investigate the coupling reactivity of the bromines close to the bridging nitrogen, test reactions with compounds **40** and **41** with phenyl boronic acid under a variety of conditions were conducted. A range of catalyst/ligand systems based on Fu *et al.*¹³⁰ were tested in combination with different solvents^{131,132} to evaluate their effectiveness.

While one reaction condition in **Table 4** (entry **V**) led to the isolation of compound **147** in a moderate yield, **146** could not be synthesised under the same reaction conditions even though a longer reaction time and a higher reaction temperature were employed. A range of catalysts were tested to synthesise **146** with no success. A possible explanation could be that the carbonyl group sterically hinders the reaction or that the reactivity of that position was not high enough¹³².

Considering these preliminary results, it was likely that a modification of compound **40** with alkyl boronic acids, which are known to be less reactive, would likely not yield any product. However, based on the success of synthesizing compound **147**, further experiments were conducted to test coupling alkyl boronic acids to compound **40**¹³³. Optimization of the reaction conditions were undertaken yielding the successful alkylation products **45**, **47** and **148** (**Scheme 9**). While the alkylation of compound **40** proceeded successfully with a range of alkyl boronic acids, the isolated yields were not deemed satisfactory enough. The decision was made to abandon this reaction pathway and continue to test the alkylation via the Suzuki reaction on the pyridopyrimidone head group (**Scheme 8 (II)**).

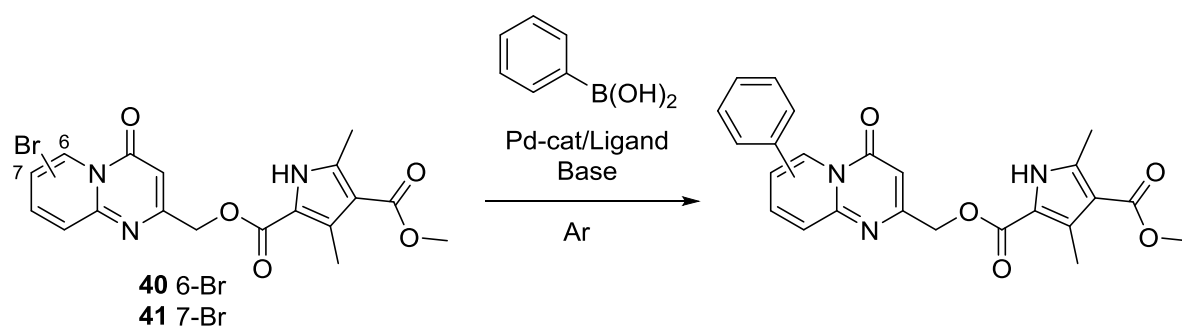
¹³⁰ G. C. Fu, *Acc. Chem. Res.*, **2008**, *41*(11), 1555-1564.

¹³¹ H. Doucet, *Eur. J. Org. Chem.*, **2008**, *12*, 2023-2030.

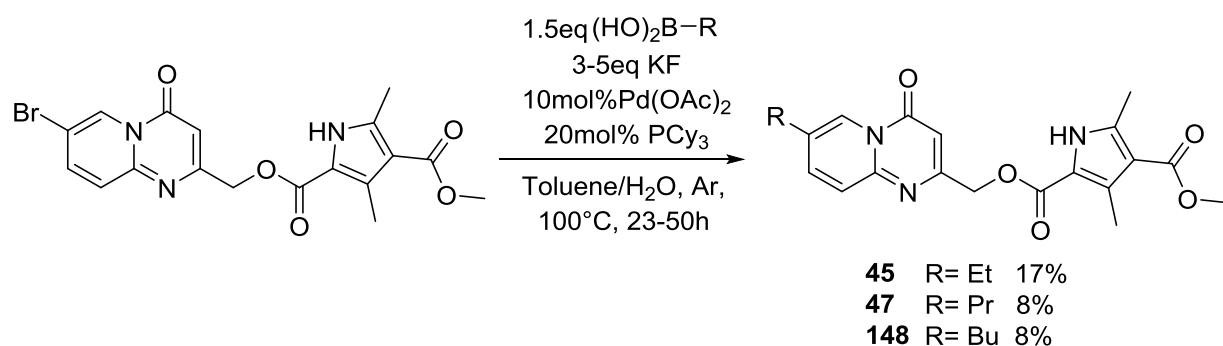
¹³² A. Molnár, A. Kapros, L. Párkányi, Z. Mucsi, G. Vlád, I. Hermeicz, *Org. Biomol. Chem.*, **2011**, *9*, 6559-6565.

¹³³ I. Ferrara, "Synthesis of small molecule inhibitors targeting the interaction of TecKinase and Fibroblast Growth Factor 2 (FGF2) in order to develop new anti-angiogenic drugs", **2018**, Universität Heidelberg.

Table 4 Test reaction of Aryl-Aryl Suzuki coupling conditions.



	Catalyst	Ligand	Base	Solvent	Time [h]	Temp [°C]	Yield [%]
 146	I 10mol% Pd(OAc) ₂	20mol% PCy ₃	3eq KF	THF	72	40	--
	II 10mol% Pd(PPh ₃) ₄	--	3eq KF	DMF/THF F (2:1)	48	RT	--
	III 10mol% Pd(dba) ₂	20mol% HPt-Bu ₃ BF ₄	3eq KF	THF	48	RT	--
	IV 10mol% PdCl ₂ (PPh ₃) ₂ *DCM	--	3eq KF	DMF/THF F (2:1)	48	RT	--
 147	V 10mol% Pd(OAc) ₂	20mol% PCy ₃	3eq KF	THF	48	RT	38
	VI 10mol% Pd(dba) ₂	20mol% HPt-Bu ₃ BF ₄	3 eq KF	THF	72	RT	--

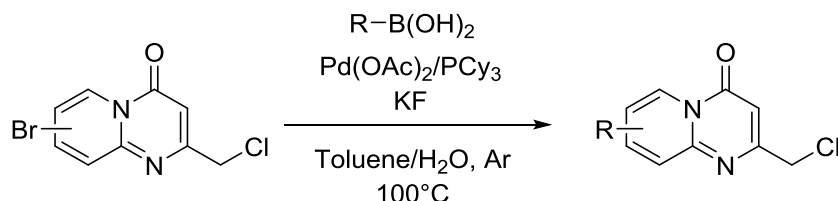


Scheme 9 Alkylation of **40** via Suzuki reaction.

1.2.2.2 Alkylation of pyridopyrimidone head group using the Suzuki reaction

The reaction conditions previously established to alkylate compound **40** were tested with the bromo-substituted pyridopyrimidones (**138-141**) as starting material. The educts were stirred together with the alkyl boronic acid, potassium fluoride and the catalyst system ($\text{Pd}(\text{OAc})_2/\text{PCy}_3$) under an argon-atmosphere at 100°C in a toluene/water-mixture.

Table 5 Suzuki reaction with pyridopyrimidones **138-141**.



	N°	R	$\text{Pd}(\text{OAc})_2/\text{PCy}_3$	Boronic Acid	Base	Temp [°C]	Time	Yield [%]
	149	Cyclopr	10mol%/20mol%	1.5eq	3eq KF	100	4d	32 ^{a,b}
	150	Et	10mol%/20mol%	1.5eq	3eq KF	100	26h	53 ^a
	153	Cyclopr	10mol%/20mol%	1.5eq	3eq KF	100	20h	59 ^a
	151	Et	1mol%/2mol%	1.5eq	3eq KF	100	26h	83
	154	Cyclopr	1mol%/2mol%	1.5eq	3eq KF	100	26h	75
	152	Et	1mol%/2mol%	1.5eq	3eq KF	100	5d	35
		Et	10mol%/20mol%	2.5eq	3eq KF	95	3d	22
	155	Cyclopr	1mol%/2mol%	1.5eq	3eq KF	100	5d	43
		Cyclopr	1mol%/2mol%	1.5eq	3eq K_3PO_4	100	3d	84
		Cyclopr	1mol%/2mol%	1.5eq	3eq Cs_2CO_3	100	3d	51 ^c

^a conducted by I. Ferrara¹³³; ^b isolated product yield has 60% purity; ^cyield calculated from $^1\text{H-NMR}$;

Using the Suzuki reaction to functionalise the pyridopyrimidone educts with an alkyl group gave moderate to good yields (**Table 5**). In all positions along the ring the reaction gave good yields with the cyclopropyl boronic acid as reagent, except at the 6-position. While the reaction took an undesirably long time at a comparatively high

catalyst load, the isolated product additionally couldn't be fully purified by chromatography and retained 40% impurities, making this reaction unsuitable for further investigation. The reactions involving the 7- and 8-position gave good yields for both boronic acids in a short reaction time, even with a low catalyst load for compounds **151** and **154** indicating that this might be an option for other positions on the ring as well. Introducing the alkyl groups in the 9 position was significantly slower than in the other sites. Furthermore, trying to increase the yield of **152** by using more catalyst and boronic acid led to the formation of a hydrodehalogenated side product which was identified by UPLC-MS (**Fig. 3**).

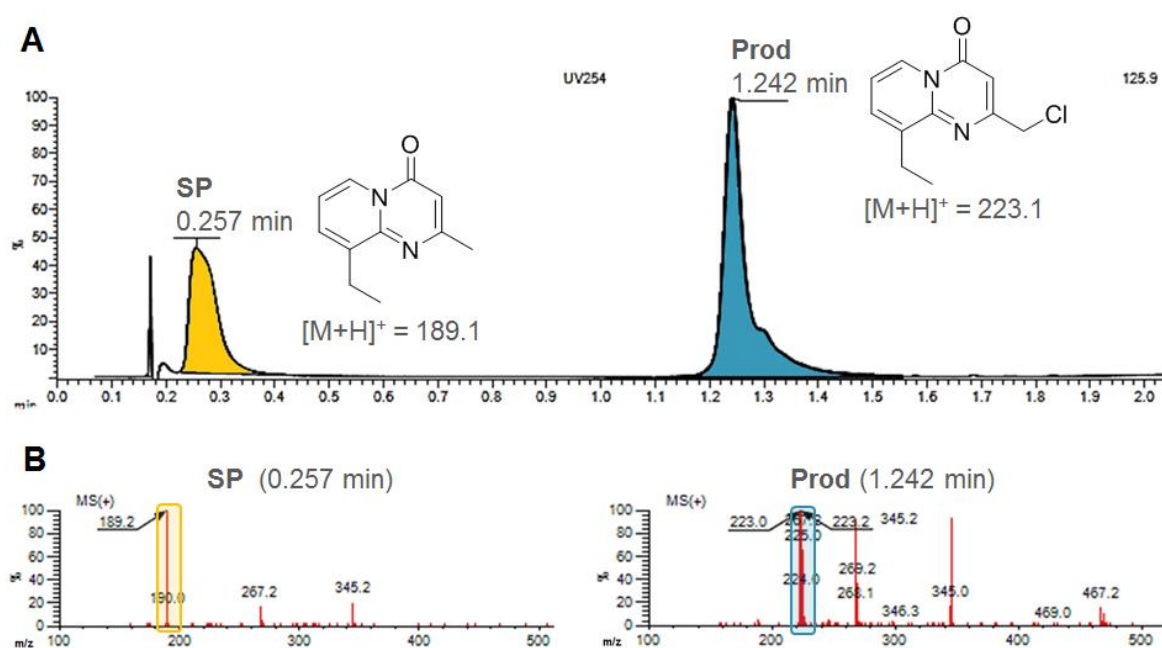


Fig. 3 UPLC-MS analysis of mixed fraction during column purification of X5; A.) UV254nm chromatogram of UPLC-MS with SP (yellow) and Prod (blue) peaks including their chemical structures and the expected protonated MW; B.) MS spectra of SP and Prod peaks with respective highlighted Mass peaks.

This indicated that the reaction was finished at an earlier time point and has to be carefully monitored. The order of reactivity of the halides in Suzuki reactions, which is $I > Br > Cl$ ¹³⁴, explains the primary formation of the product before an attempted second alkylation at the chlorine atom led to the side product formation. This side reaction might be circumvented by changing the base¹³⁵. As can be seen for the synthesis of **155**, the use of K_3PO_4 led to a higher yield during a shorter reaction time than the use

¹³⁴ P. Fitton, E. A. Rick, *J. Organomet. Chem.*, **1971**, 28(2), 287-291.

¹³⁵ L. Jedinák, R. Zátoková, H. Zemánková, A. Šustková, P. Cankař, *J. Org. Chem.*, **2017**, 82(1), 157-169.

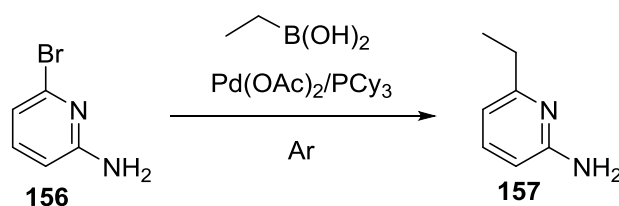
of KF, which might also be of interest to increase the yield for the synthesis of **152**. It is apparent that the conditions for the alkylation of pyridopyrimidones via the Suzuki reaction need to be adjusted depending on the position that is targeted on the ring, which confirms that a distinct difference in their reactivity exists. Due to the disappointing result for the Suzuki reaction in the 6-position on the pyridopyrimidone ring, approach **(I)** in **Scheme 8** needed to be investigated.

1.2.2.3 Alkylation of 2-amino-6-bromopyridine with the Suzuki reaction

A comprehensive optimisation for the alkylation of 2-amino-6-bromo-pyridine with ethyl and cyclopropyl boronic acid was conducted, employing a variety of bases and different heating methods with a range of different catalyst loads. All reactions were conducted under Argon atmosphere with degassed solvents and stirred at 90°C or 160°C in a microwave reactor.

As can be seen in **Table 6** the synthesis of **157** was very slow even when increasing the amount of catalyst/ligand ten-fold (entries **II** and **XII**). The first and rate-determining reaction step of the catalytic mechanism is the oxidative addition of the halide to the catalyst. The addition can strongly be influenced by the electron density of the Pd/Ligand-complex used¹³⁰. A comprehensive screen of catalyst systems might therefore lead to a reaction condition with an increased reaction speed. Using a toluene/water mixture as solvent enables the reaction to run at a higher temperature increasing the reaction rate and resulted in none of the product formation seen in dioxane/water. Changing the ratio of toluene and water from 5:1 to 2:1 also led to a slight increase in yield (**XII** to **XIII**). A significant decrease in reaction time is obtained by using a microwave reactor (**V**) as heating source instead of a heat block (**XII**), which allowed the reaction to run at a higher temperature. Additionally, the reaction took place with notably lower catalyst load and produced the product in a similar yield. Surprisingly, it was found that some/all of the products were volatile and were largely lost during evaporation of the solvents *in vacuo*. Using N₂-flow to fully dry the product led to an increase in isolated yield (**XII**, **XIII**). Even with a high catalyst load, the tested reaction conditions didn't lead to a full conversion of the educt **156**. With ethyl boronic acid being less reactive and having the ability to undergo an elimination reaction during the catalytic reaction cycle, increasing the amount used might improve the product yield.

Table 6 Synthesis of **157**.

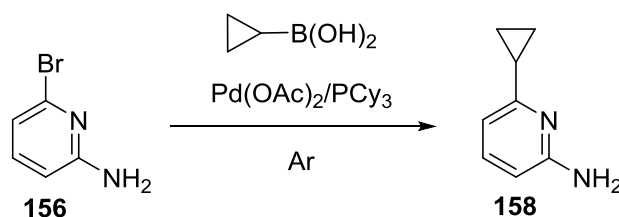


	Cat/Ligand	Boronic acid	Base	Solvent	Time	Temp [°C]	Yield [%]
I	1 mol%Pd(OAc) ₂ / 2 mol%PCy ₃	1.5eq	3eq KF	Toluene/H ₂ O (6mL +3μL)	40h	90	--
II	1 mol%Pd(OAc) ₂ / 2 mol%PCy ₃	1.5eq	3eq K ₃ PO ₄	Toluene/H ₂ O (5:1)	5d	90	-- ^a
III	1 mol%Pd(OAc) ₂ / 2 mol%PCy ₃	1.5eq	3eq K ₃ PO ₄	THF/H ₂ O (5:1)	5d	65	-- ^a
IV	1 mol%Pd(OAc) ₂ / 2 mol%PCy ₃	1.5eq	3eq Cs ₂ CO ₃	Toluene/H ₂ O (5:1)	5d	90	--- ^a
V	1 mol%Pd(OAc) ₂ / 2 mol%PCy ₃	1.5eq	3eq K ₃ PO ₄	Toluene/H ₂ O (5:1)	2h	160 ^b (μW)	18
VI	1 mol%Pd(OAc) ₂ / 2 mol%PCy ₃	1.5eq	3eq K ₃ PO ₄	Dioxane/H ₂ O (5:1)	2h	160 ^b (μW)	--
VII	5 mol%Pd(OAc) ₂ / 10 mol%PCy ₃	1.5eq	3eq K ₃ PO ₄	Toluene/H ₂ O (5:1)	72h	90	3 ^c
VIII	5 mol%Pd(OAc) ₂ / 10mol%PCy ₃	1.5eq	3eq KF	Toluene/H ₂ O (5:1)	72h	90	-- ^c
IX	5 mol%Pd(OAc) ₂ / 10 mol%HPCy ₃ BF ₄	1.5eq	3eq K ₃ PO ₄	Toluene/H ₂ O (5:1)	72h	90	10 ^c
X	5 mol%Pd(OAc) ₂ / 10 mol%PCy ₃	1.5eq	3eq K ₃ PO ₄	Toluene/H ₂ O (5:1)	3h	160 (1h, μW) + 140 (2h, μW) ^b	23 ^c
XI	10 mol%Pd(OAc) ₂ / 20 mol% PCy ₃	1.5eq	3eq K ₃ PO ₄	Toluene/H ₂ O (5:1)	72h	95	3 ^c
XII	10 mol%Pd(OAc) ₂ / 20 mol% PCy ₃	1.5eq	3eq K ₃ PO ₄	Toluene/H ₂ O (5:1)	72h	100	29 ^d
XIII	10 mol%Pd(OAc) ₂ / 20 mol% PCy ₃	1.5eq	3eq K ₃ PO ₄	Toluene/H ₂ O (2:1)	72h	100	18 ^d

^a minimal amount of impure product isolated; ^b reaction conducted with microwave reactor at 160°C/140°C, 35W, 6bar/3.5bar; ^c yield in reality higher, product partially co-evaporated under reduced pressure; ^d product dried with N₂-stream;

To synthesise **158**, the catalyst with all reagents were weighed into a flask under Argon atmosphere and stirred at 90-100°C with the degassed solvents.

Table 7 Synthesis of **158**.



	Cat/Ligand	Boronic acid	Base	Solvent	Time	Temp [°C]	Yield [%]
I	1 mol%Pd(OAc) ₂ / 2 mol% PCy ₃	1.5eq	3eq KF	Toluene/H ₂ O (3mL+30μL)	24h	90	--
II	1 mol%Pd(OAc) ₂ / 2 mol%PCy ₃	1.5eq	3eq K ₃ PO ₄	Toluene/H ₂ O (5:1)	5d	90	35 ^c
III	1 mol%Pd(OAc) ₂ / 2 mol%PCy ₃	1.5eq	3eq K ₃ PO ₄	THF/H ₂ O (5:1)	5d	65	28 ^c
IV	1mol%Pd(OAc) ₂ / 2 mol%PCy ₃	1.5eq	3eq Cs ₂ CO ₃	Toluene/H ₂ O (5:1)	5d	90	16 ^c
V	5 mol%Pd(OAc) ₂ / 10 mol%PCy ₃	1.5eq	3eq K ₃ PO ₄	Toluene/H ₂ O (5:1)	72h	90	9 ^d
VI	5 mol%Pd(OAc) ₂ / 10mol%PCy ₃	1.5eq	3eq KF	Toluene/H ₂ O (5:1)	72h	90	9 ^{c,d}
VII	5 mol%Pd(OAc) ₂ / 10 mol%HPCy ₃ BF ₄	1.5eq	3eq K ₃ PO ₄	Toluene/H ₂ O (5:1)	72h	90	3 ^{c,d}
VIII	5 mol%Pd(OAc) ₂ / 10 mol%PCy ₃	1.5eq	3eq K ₃ PO ₄	Toluene/H ₂ O (5:1)	3h	140 (μW) ^b	16 ^{c,d}
IX	5 mol%Pd(OAc) ₂ / 10 mol% PCy ₃	1.5eq	3eq K ₃ PO ₄	Toluene/H ₂ O (5:1)	24h	95	49 ^a
X	10 mol%Pd(OAc) ₂ / 20 mol% PCy ₃	2eq	4eq K ₃ PO ₄	Toluene/H ₂ O (16:1)	24h	100	54 ^e

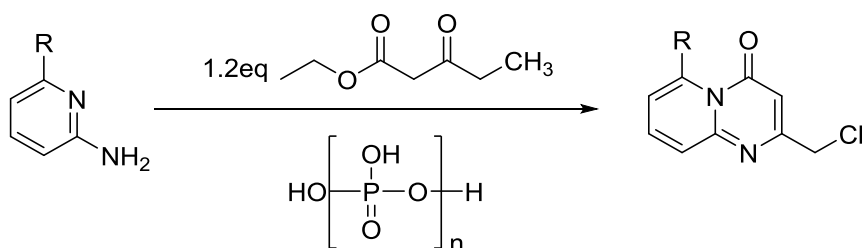
^a product dried with N₂-stream; ^b reaction conducted with microwave reactor at 140°C, 35W, 3-4bar; ^c SM not fully converted, yield calculated excluding reisolated educt; ^d yield in reality higher, product partially co-evaporated under reduced pressure; ^e experiment conducted by I. Ferrara.

Table 7 shows clearly that the synthesis of compound **158** can happen under a variety of conditions resulting in a range of different yields. The product was formed with all catalyst loads tested from 1-10mol%, whose increase was accompanied with a decreasing reaction time and full conversion with ≥ 5mol% catalyst load. As could already be seen in the synthesis of **157**, the toluene/water mixture as solvent gives

higher yields and no side product formation was observed. Furthermore, the use of different bases showed that potassium phosphate is the best choice for this reaction. As was also observed with **157**, an extended time under high vacuum to dry the product led to a significant loss in yield (**V-VIII**) due to co-evaporation of the product. Using a N₂ stream to dry the product increased the yields significantly (**IX, X**). Using the microwave oven to heat the reaction also led to a significant reduction of reaction time (**VIII**) because the reaction can run at a higher temperature which speeds up the reaction significantly. Alkylation in 6-position via the Suzuki reaction worked better with the cyclopropyl boronic acid than ethyl boronic acid. This can be clearly seen in the yields documented in **Table 6** and **Table 7**. This result was to be expected by comparing the respective stability and the reactivities of both boronic acids. The cyclopropyl group with its ring tension is more reactive than the ethyl boronic acid, which leads to a faster reaction and therefore to full conversion of the educt. It is notable that the reactivity of boronic acid as well as the base, catalyst/ligand and solvent can have a significant influence on the reaction rate and product formation and need to be chosen carefully.

Following the Suzuki alkylation, pyridopyrimidone structure was synthesised with **157** and **158** as educts using method of Ferrarini *et al.*¹²⁰. The educt and the reagent were stirred at 100°C in PPA for 2h before an aqueous work-up was conducted.

Table 8 Synthesis of compounds **159** and **160**.



N°	R	Time [h]	Temp [°C]	Yield [%]
159	Et	2	100	41-63
160	Cyclopropyl	2	100	--

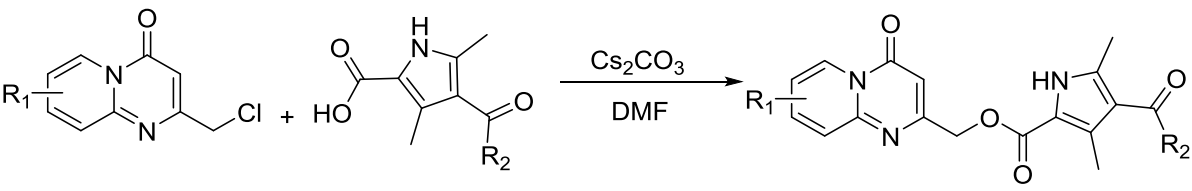
The formation of **159** proceeded in good yield as can be seen in **Table 8**, whereas no product could be isolated for the synthesis of **160**. The UHPLC-MS analysis of the

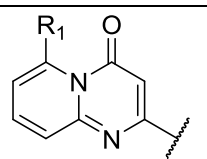
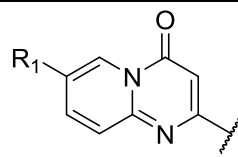
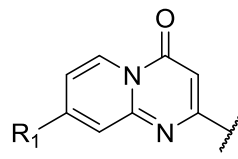
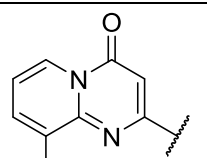
aqueous and organic phase during the work-up of its synthesis showed minimal amount of product in both phases. Furthermore a substantial amount of the educt was identified in the aqueous phase indicating a slower reaction rate for **160** than **159**. Looking at the reaction mechanism (**Scheme 7**), it is possible that the cyclopropyl group is too sterically hindering for the intermediate **II** to be able to initiate the first reaction step with the reagent.

1.2.2.4 Linking alkylated pyridopyrimidone head groups with pyrrole

To link the synthesised head groups with larger alkyl substituents to the pyrrole ring the conditions established in **Table 2** were used.

Table 9 Synthesis of C6 analogues containing larger alkyl substituents on the head group.



	N°	R1	R2	Pyrrole [eq]	Cs ₂ CO ₃ [eq]	Time [h]	Temp [°C]	Yield [%]
	51	Et	Me	1.1	1.5	16	40	35 ^a
	118	Et	Et	1.5	1.5	15	50	92
	45	Et	Me	1.1	1.5	16	40	33 ^a
	44	Cyclopr	Me	1.3	1.7	16	40	46 ^a
	110	Et	Me	1.2	1.2	17	40	90
	111	Et	Et	1.2	1.2	3	50	86
	114	Cyclopr	Me	1.2	1.2	4	40	78
	115	Cyclopr	Et	1.2	1.2	5	40	65
	112	Et	Me	1.2	1.2	15	40	75
	113	Et	Et	1.2	1.2	15	40	67
	116	Cyclopr	Me	1.2	1.2	4	40	64
	117	Cyclopr	Et	1.2	1.2	5	40	56

^a experiment conducted by I. Ferrara¹³³;

As can be seen in **Table 9**, the **C6** analogues containing larger alkyl substituents were isolated in good to excellent yield. As was already discussed in **Table 3**, while running the reaction overnight is more convenient, the actual reaction time is significantly shorter.

Substituting the methyl group of compound **C6** with bigger alkyl groups as well as introducing these groups at other positions on the pyrimidine head group via the Suzuki cross coupling reaction was successfully accomplished. A minor downside of this method is the continuous adjustments of the reaction conditions that are needed, depending on the boronic acid or halide that are used. In total, it can be said that using the Suzuki cross coupling reaction to introduce the bigger alkyl groups gave good overall yields for the majority of synthesised compounds and can therefore be considered a very good option for this modification.

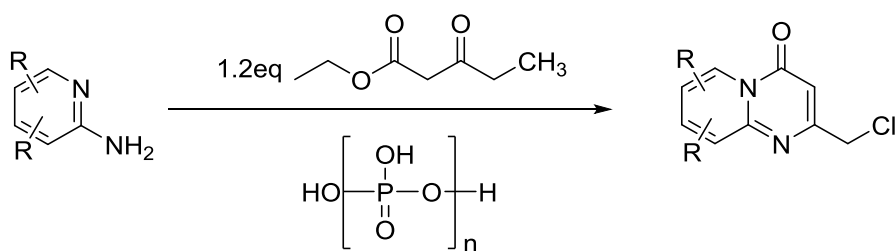
1.2.1 Multiple Substituents on head group modification

To introduce multiple substituents on the head group, 2-aminopyridines with the desired substitution pattern were transformed into the corresponding pyridopyrimidone head group following the method by Ferrarini *et al*¹²⁰. The 2-amino pyridines /2-amino quinoline were stirred for 2h at 90°C with ethyl 4-chloroacetoacetate in **PPA** to give the product compounds.

Compounds with multiple substituents yielded isolated product in a wide range from moderate to excellent (**Table 10**). The isolated yields for the double alkyl substituted compounds all show an excellent yield, except for **162**, which has a decreased yield caused by issues during the purification process. Compounds containing two negative inductive substituents (**165**, **166**) were isolated in a significantly lower yield than their alkyl counter parts. Comparing the yield for **166** to the conditions used which gave a yield of 77%¹³⁶ documented in the literature; it is noticeable that a lower reaction temperature and shorter reaction time led to a 5-fold decrease in isolated product. The accumulation of deactivating groups on the pyridine ring seems to increase the energy needed to for intermediate **II** to react (see **Scheme 7**). A similar issue likely led to the low yield of compound **165**.

¹³⁶ Y. Kabri, M. D. Crozet, N. Primas, P. Vanelle, *Eur. J. Org. Chem.*, **2012**, 2012(28), 5595-5604.

Table 10 Synthesis of multiply substituted pyridopyrimidones.



N°	SM	Reagent [eq]	Temp [°C]	Time	Yield [%]
161		1.1	100	2h	60
162		1.1	95	2h	18
163		1.1	100	2h	79
164		1.1	95	2h	38
165		1.1	95	2h	15
		1.25	105	3h	24
166		1.1	100	2h	16

To complete this set of compounds, **161-166** were linked to the two pyrrole building blocks **48** and **52**, by stirring at 40°C with an excess of caesium carbonate in DMF.

As can be seen in **Table 11**, the isolated yields of the multiple substituted **C6** derivatives varied greatly. Compounds with alkyl substituents all gave excellent yields, except for **72** and **75**, which had a decreased yield due to product loss during the purification step. Compound **167** and **168** were very unstable under the reaction

conditions. This can be shown by comparing the UHPLC-MS traces after 2h and 17h (Fig. 4). After 2h reaction time and direct purification of the reaction mixture via HPLC **168** was isolated. As both compounds were unstable, they were not tested in any subsequent biochemical assays.

Table 11 Synthesis of C6 analogues with multiple substituents on the head group.

SM	N°	R1	Pyrrol [eq]	Time	Yield [%]
	72	Me	1.4	3.5h	46
	71	Et	1.5	3.5h	77
	70	Me	1.5	2.5h	75
	71	Et	1.5	2.5h	85
	74	Me	1.5	3.5h	72
	75	Et	1.5	3.5h	38
	68	Me	1.5	2.5h	30
	69	Et	1.5	2.5h	28
	167	Me	1.5	2.5h	--
	168	Et	1.5	2.5h	5
	169	Me	1.5	15h	6
	170	Et	1.5	15h	7

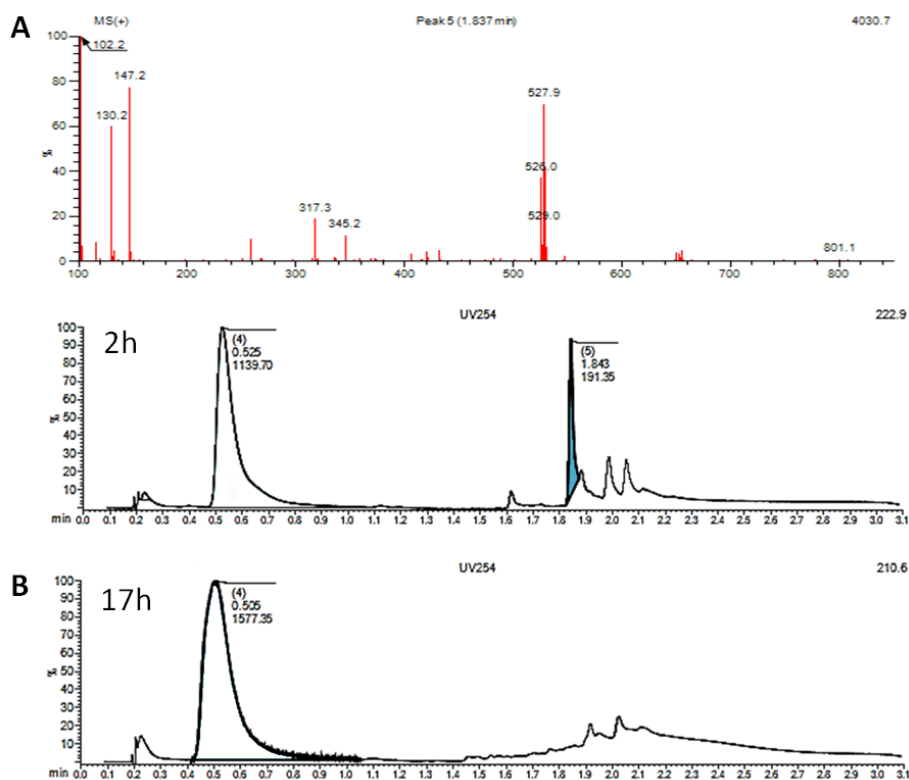


Fig. 4 UPLC-MS measurements of **167** after **A** 2h with **167** (blue peak) its corresponding mass spectra and **B** 17h without product peak.

1.2.2 Elimination of C=O from the head group

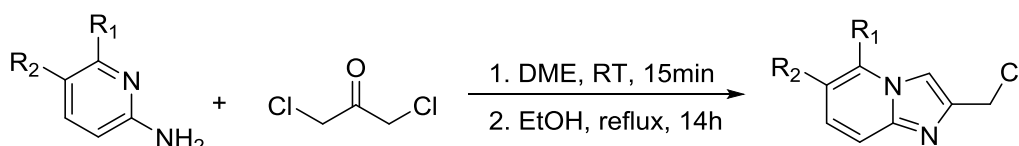
To investigate the importance of the carbonyl in the head group of **C6**, compounds lacking this feature, so called imidazopyridines were synthesised following the method of Henry *et al*¹³⁷. First the substituted 2-amino pyridine was dissolved in dimethoxyethane (DME) before 1,3-dichloropropanone was added. After 15min the solvent was evaporated and the reaction mixture refluxed in ethanol.

The yields of this reaction were moderate for the products containing alkyl substituents (**Table 12**). Comparing the literature yield of 77% for the unsubstituted product with **171** and **173** the substituents seem to have a negative effect on the speed of the product formation. Under slightly modified conditions than used here, the yield for **171** documented in the literature is 26%¹³⁸, which is significantly less than noted in **Table 12**, showing that the method of Henry *et al*¹³⁷ is better for this educt

¹³⁷ N. Henry, E. Thiery, J. Petriguet, H. Halouchi, J. Thibonnet, M. Abarbri, *Eur. J. Org. Chem.*, **2012**, *2012* (31), 6212-6217.

¹³⁸ H. Mitsudera, K. Otaka, J. Fujiwara, World Intellectual Property Organization, WO2005068432 A1, 2005-07-28.

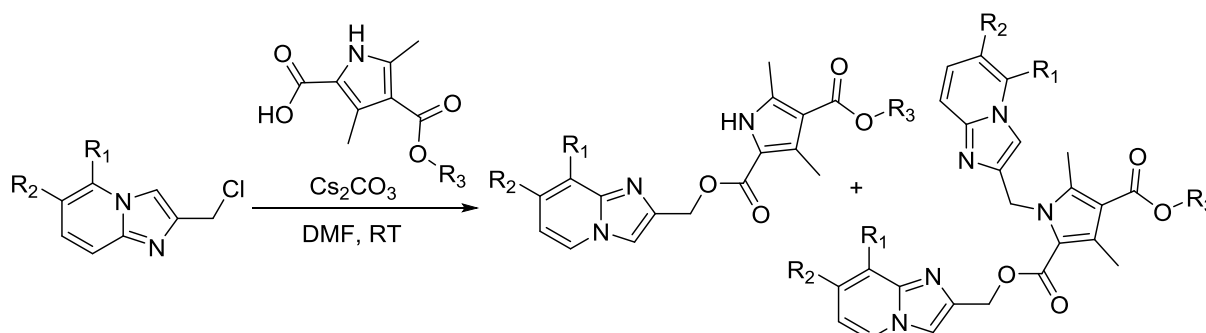
Table 12 Syntheses of imidazopyridines **171**, **172** and **173**.



	R ₁	R ₂	Reagent [eq]	Time [h]	Yield [%]
171	Me	H	2	14	44
172	Br	H	2	14	90
173	Me	Me	2	14	35

To connect the pyrrole building blocks **48** and **52** with the modified head groups **171-173**, similar reaction conditions were used to those established in **Table 2**.

Table 13 Syntheses of **C6** analogues missing the carbonyl group in the head group.



Prod/SP N°	Pyrrole			Cs ₂ CO ₃ [eq]	Time [h]	Prod [%]	SP [%]	
	R ₁	R ₂	R ₃					
88	Me	H	Me	1.5	3	13	28	-- ^a
89/ 90	Me	H	Et	1.5	3	18	22	63
95/ 96	Br	H	Me	1.5	3	13	30	54
97/ 98	Br	H	Et	1.5	3	18	19	35
91/ 92	Me	Me	Me	1.5	3	13	34	56
93/ 94	Me	Me	Me	1.5	3	18	26	44

^a Yield of SP not determined.

The product yields for all reactions were only moderate (**Table 13**). Surprisingly, in contrast to the original scaffold, this reaction led to significant N-alkylation of the pyrrole. The structure of the side product was confirmed by NMR and UPLC-MS. Even

though pyrrole building blocks **48** and **52** were used in excess, the main compound formed was the side product. NMR analysis of the single substituted compounds, confirmed the formation of the intended compound and not the N- modified isomer (**Fig. 5**). It seems that the pyridopyrimidones **171-173** are less sterically hindered, due to the absence of the carbonyl group, than pyridopyrimidone **126**, permitting the second alkylation. Reducing the amount of base as well as changing the order of addition of the reagent will likely improve the product yields. Alternatively, the addition of a protecting group to the N1 of the pyrrole will hinder the side product formation. Nonetheless, sufficient amounts of the desired products were obtained for biological testing.

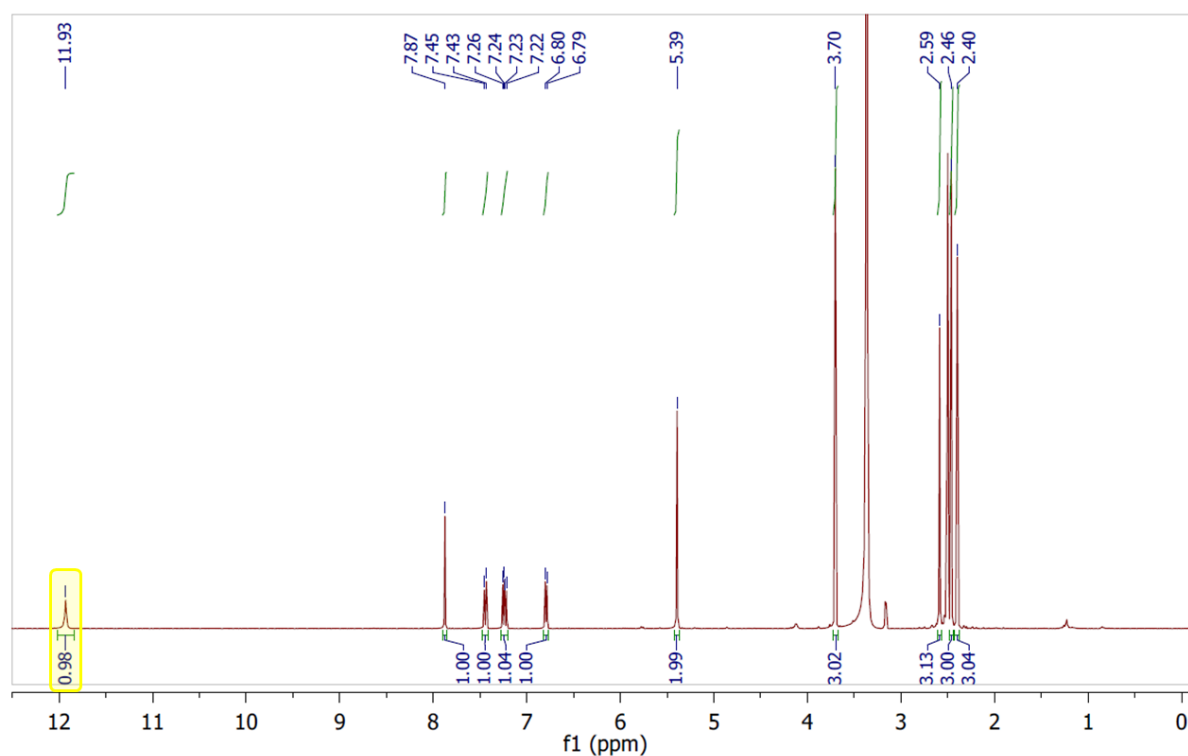
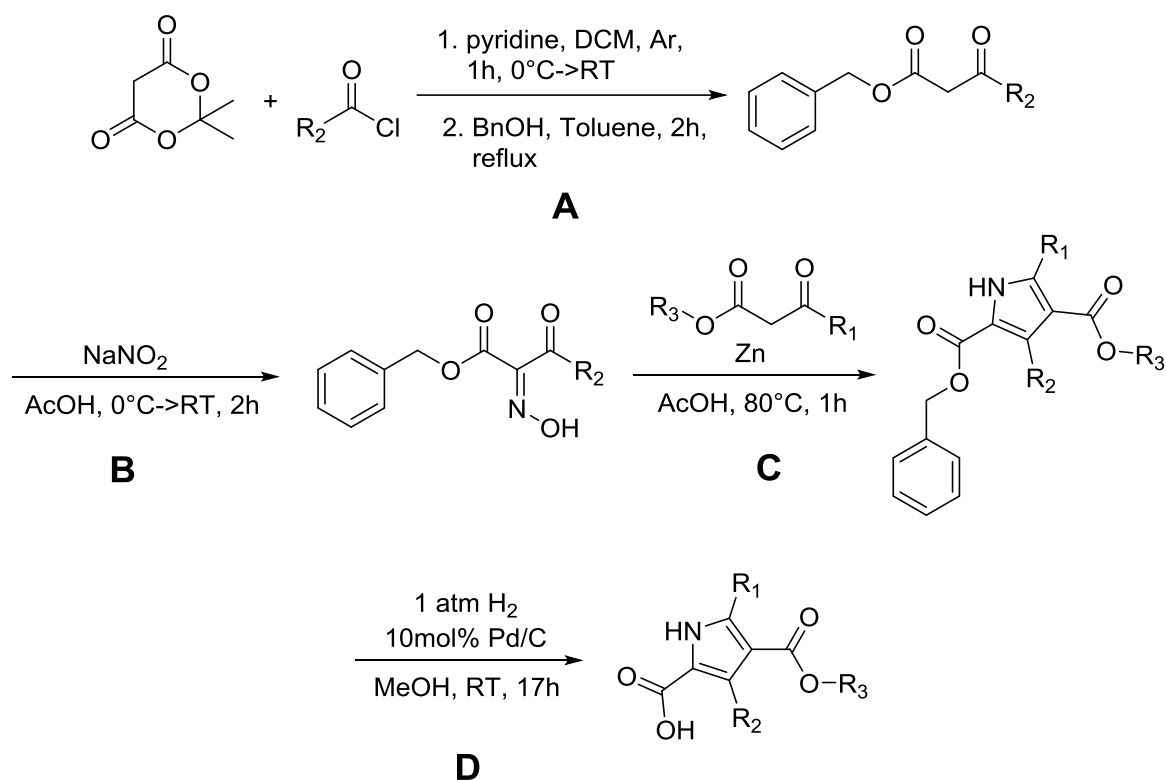


Fig. 5 $^1\text{H-NMR}$ of **88** in DMSO-d_6 with the identified NH -proton peak (yellow).

1.3 Tail group modification

1.3.1 Synthesis of pyrrole rings with bigger ring substituents

In addition to the changes in the head group of the lead compound **C6**, the influence of the size of the substituents on the tail group were investigated. To introduce larger substituents on the pyrrole, the synthetic route in **Scheme 10** was used.



Scheme 10 Synthesis route for substituted pyrrole carboxylic acids.

Reaction of Meldrum's acid with the appropriate acyl chloride (**A**) gave asymmetric β -keto esters which were then directly nitrosylated (**B**). These educts were then used to synthesise the pyrrole ring with the Knorr-Pyrrole-Synthesis (**C**). This reaction was followed by the hydrogenolysis of the benzyl ester to give the corresponding carboxylic acid (**D**).

For the first step in the synthetic pathway, the method of Y. Oikawa *et al.*¹³⁹ was used to form the asymmetric β -keto ester. Introduction of the modification was achieved by the reaction of the corresponding acyl acid with Meldrum's acid and pyridine as base in DCM. The generated intermediate was then reacted without purification with benzyl alcohol under reflux in toluene to yield the products **174** and **175**.

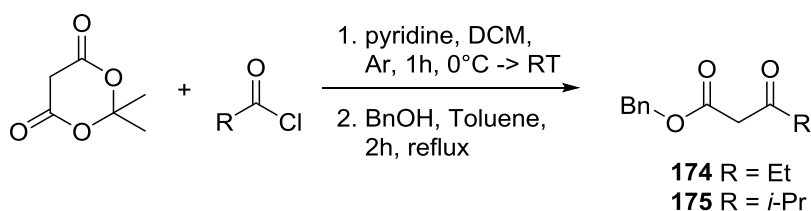
While both compounds were isolated in a lower yield than given in the literature, both 74%^{[139], 140}, the products were still isolated in an acceptable yield, as can be seen in

Table 14.

¹³⁹ Y. Oikawa, K. Sugano, O. Yonemitsu, *J. Org. Chem.*, **1978**, *43*, 2087-2088.

¹⁴⁰ G. Giacomelli, A. Porcheddu, M. Salaris, M. Taddei, *Eur. J. Org. Chem.*, **2003**, *3*, 537-541.

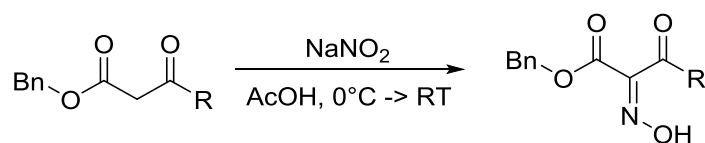
Table 14 Synthesis of β -keto ester.



N°	R	Acylchloride [eq]	BnOH [eq]	Time	Yield [%]
174	Et	1.1	3	0°C (30'') → 30min RT	63 - 66%
175	<i>i</i> -Pr	1.1	3	30min 0°C → 30min RT	41 - 49%

The β -keto esters were directly transformed with sodium nitrite in glacial acetic acid to **176-178** following the method of Paine *et al*¹⁴¹.

Table 15 Synthesis of nitrosylated β -keto ester.



N°	R	NaNO ₃ [eq]	Time [h]	Yield [%] ^a
176	Me	1.5	17h	98%
177	Et	1.5	16h	97%
178	<i>i</i> -Pr	1.5	17h	99%

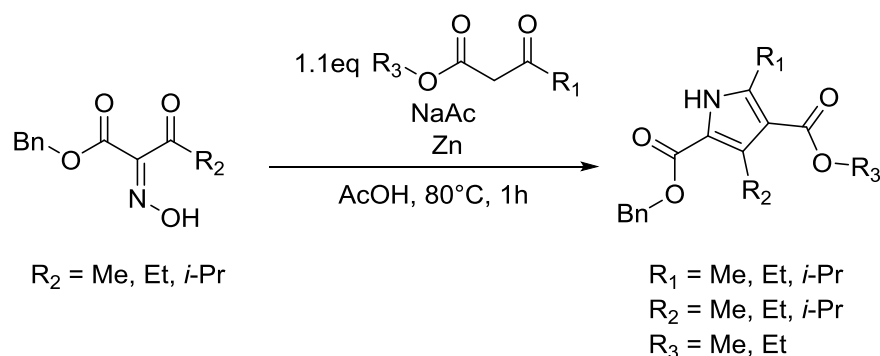
^a crude yield.

As can be seen in **Table 15**, the reaction led to near quantitative yields for all educts. Due to their clean transformation during the reaction, purification of the formed products was not necessary and the crude was used in the following reaction steps.

To form the pyrrole ring, the Knorr-pyrrole synthesis was used¹²¹. A β -keto ester dissolved in glacial acetic acid with anhydrous sodium acetate was stirred at 70°C before the oxime dissolved in 50% acetic acid was added in small increments alternately with zinc. The mixture for 1h before the excess of zinc was filtered off and the hot filtrate poured into ice water.

¹⁴¹ J.B. Paine, D. Dolphin, *J. Org. Chem.*, **1988**, *53*, 2787-2795.

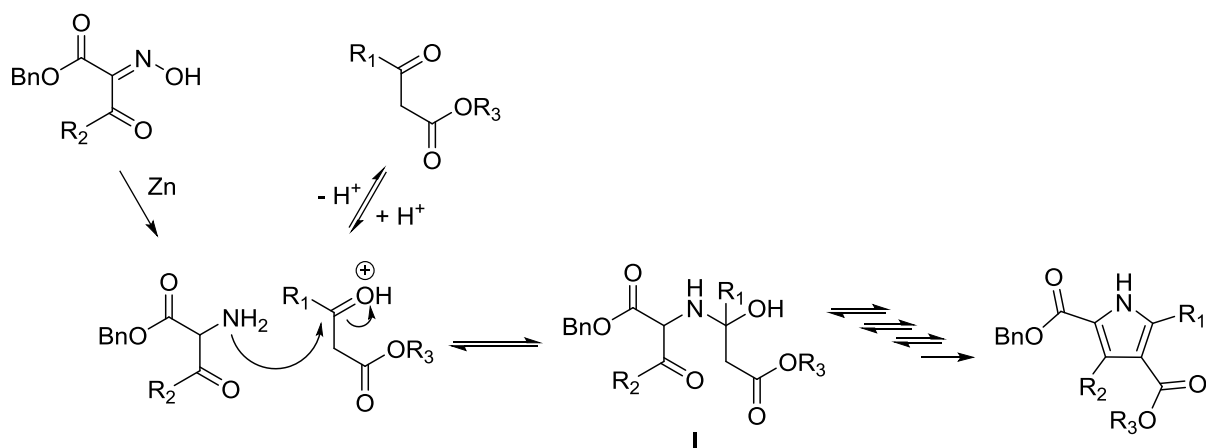
Table 16 Knorr-Pyrrole Synthesis.



N°	R ₁	R ₂	R ₃	NaOAc [eq]	Zn [eq]	Time [h]	T [°C]	Yield [%] ^a
179	Me	Et	Me	1.25	3	1h	70°C	54
180	Et	Me	Me	--	2	1h	80°C	18
	Et	Me	Me	1.25	3	1.5h	80°C	27
181	Et	Et	Me	1.25	3	1h	70°C	38
182	Me	<i>i</i> -Pr	Me	1.25	3	1h	70°C	35
183	<i>i</i> -Pr	Me	Me	1.25	3	1h	80°C	8
184	<i>i</i> -Pr	<i>i</i> -Pr	Me	1.25	3	1h	70°C	28
185	Me	Et	Et	1.25	3	1h	75°C	36
186	Et	Me	Et	1.25	3	1h	80°C	32
187	Et	Et	Et	1.25	3	1h	75°C	27
188	Me	<i>i</i> -Pr	Et	1.25	3	1h	70°C	37
189	<i>i</i> -Pr	Me	Et	1.25	3	1h	80°C	8
	<i>i</i> -Pr	Me	Et	1.25	3	1h	75°C	7
190	<i>i</i> -Pr	<i>i</i> -Pr	Et	1.25	3	1h	70°C	27

Table 16 shows that the formation of the pyrrole building blocks containing larger alkyl substituents using the Knorr Synthesis gave overall moderate to good yields. Adding sodium acetate to the reaction mixture the product yield increased. A larger substituent in the R1 position leads to a decrease of product formation which can be explained by

considering the reaction mechanism (**Scheme 11**)¹⁴². It shows that the first reaction step to form intermediate **I** can be sterically hindered by bigger substituents and so contribute to a lower product formation. Furthermore, the different ester substituents do not influence on yields, while a lower reaction temperature and a shorter reaction time increased the product yield.



Scheme 11 Schematic overview of first reaction step in the mechanism of the Knorr synthesis forming intermediate **I**.

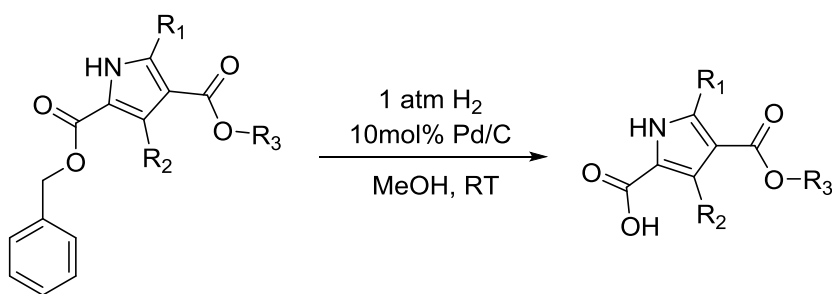
To finish the synthesis of the pyrrole building blocks, the benzyl ester is cleaved by hydrogenolysis using palladium on carbon as catalyst in MeOH. The reaction proceeded with quantitative or near quantitative yield for all compounds as can be seen in **Table 17**. This concurred with the yields documented in literature for reactions of similar compounds^{141,143,144}.

¹⁴² J. W. Harbuck, H. Rapoport, *J.Org.Chem.*, **1971**, 36(6), 853-855.

¹⁴³F. Micheli, R. Di Fabio, P. Cavanni, J. M. Rimland, A. M. Capelli, C. Chiamulera, M. Corsi, C. Conrti, D. Donati, A. Feriani, F. Ferraguti, M. Maffei, A. Missio, E. Ratti, A. Paio, R. Pachera, M. Quartaroli, A. Reggiani, F. M. Sabbatini, D. G. Trist, A. Ugolini, G. Vitulli, *Bioorg. Med. Chem.*, **2003**, 11, 171-183.

¹⁴⁴ A. C. Zuniga, *Heterocycles*, **2004**, 63, 2071-20MS77.

Table 17 Benzyl ester hydrogenolysis to give pyrrole building blocks **191-202**.

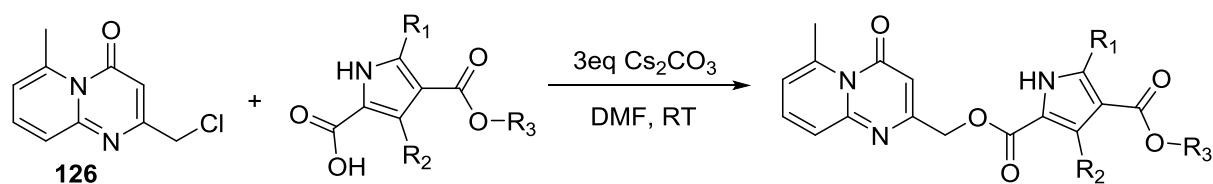


	R ₁	R ₂	R ₃	Time [h]	Yield [%]
191	Me	Et	Me	17	92
192	Et	Me	Me	16	83-87
193	Et	Et	Me	18	97
194	Me	<i>i</i> -Pr	Me	17	99
195	<i>i</i> -Pr	Me	Me	18	99
196	<i>i</i> -Pr	<i>i</i> -Pr	Me	17	90
197	Me	Et	Et	18	102
198	Et	Me	Et	17	78
199	Et	Et	Et	17	100
200	Me	<i>i</i> -Pr	Et	18	100
201	<i>i</i> -Pr	Me	Et	17	102
202	<i>i</i> -Pr	<i>i</i> -Pr	Et	17	97

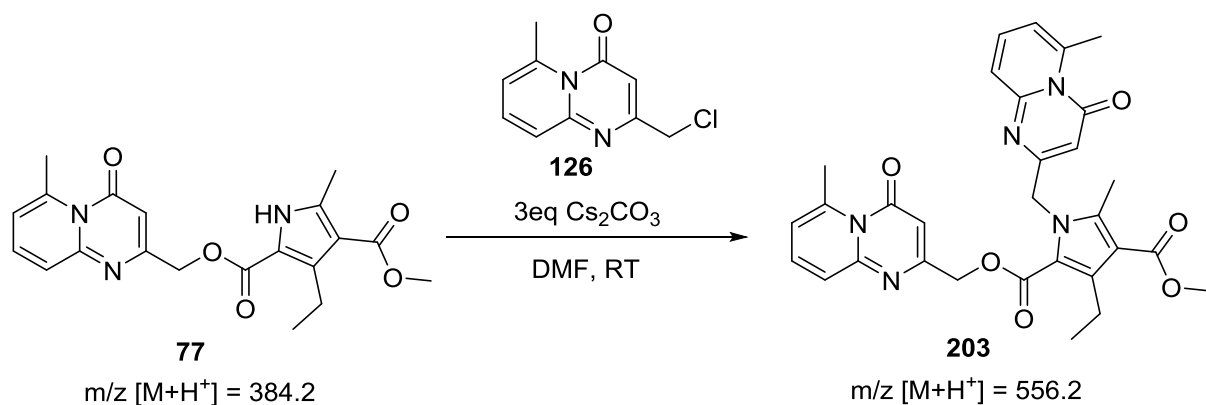
To finish the synthesis of **C6** analogues containing larger alkyl groups, the pyridopyrimidone **126** was linked to the pyrrole building blocks **191-202** in the presence of caesium carbonate while being stirred in DMF at RT.

Table 18 shows the reaction to give moderate to good yields. The use of an excess of **126** led a second alkylation of the product on N1 of the pyrrole, decreasing the isolated yield of the product (**Scheme 12**). The identity of the side product was confirmed by evaluating the UHPLC-MS spectra of the reaction mixture (**Fig. 6**). The respective mass spectra of the two peaks visible in the chromatogram correspond to the expected masses for compounds **77** and **203**.

Table 18 Synthesis of **C6** analogues **76-87**.



	R ₁	R ₂	R ₃	Comp 126 [eq]	Pyrrole [eq]	Time	Yield [%]
77	Me	Et	Me	1.5	1	17	35
76	Et	Me	Me	1.5	1	16	41
80	Et	Et	Me	1.5	1	17	55
83	Me	<i>i</i> -Pr	Me	1.5	1	16	41
82	<i>i</i> -Pr	Me	Me	1.5	1	16	77
86	<i>i</i> -Pr	<i>i</i> -Pr	Me	1.5	1	17	76
79	Me	Et	Et	1.2	1	17	63
78	Et	Me	Et	1.2	1	16.5	62
81	Et	Et	Et	1.2	1	16	61
85	Me	<i>i</i> -Pr	Et	1.5	1	14	87
84	<i>i</i> -Pr	Me	Et	1.2	1	16	75
87	<i>i</i> -Pr	<i>i</i> -Pr	Et	1.5	1	17	55



Scheme 12 Second alkylation reaction of **77**.

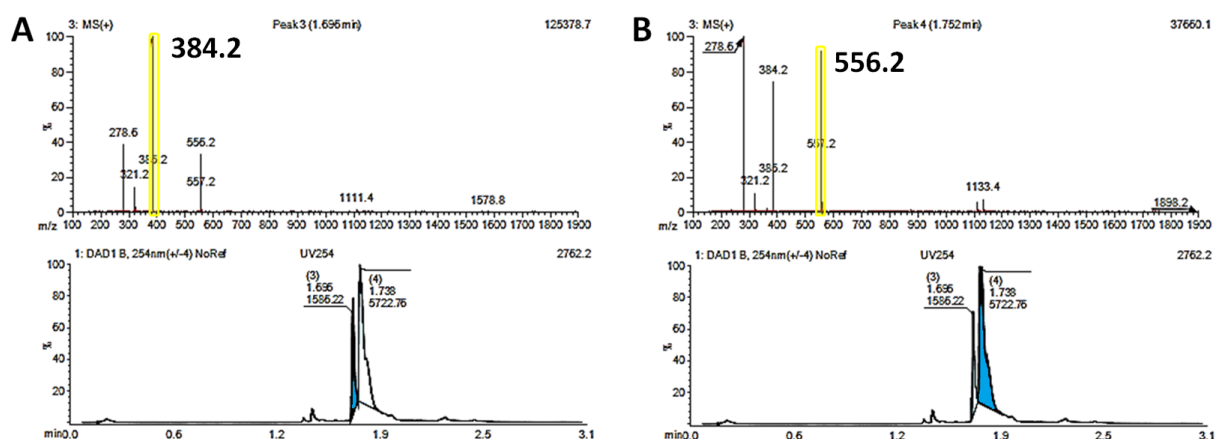


Fig. 6 UHPLC-MS graphs of reaction mixture of to synthesise **77** after 17h; **A**, MS spectrum (ESI⁺) with main peak (yellow box) corresponding to MW of **77** in chromatogram at 1.636min (blue in lower panel); **B** MS spectrum (ESI⁺) with main peak (yellow box) corresponding to MW of **203** in chromatogram at 1.752min (blue in lower panel).

In **Fig. 7**, it is shown that a larger substituent as R₁ position leads to a decreased formation of side product due to steric hindrance. The qualitative examination of the peak areas for the side products are shown to decrease from compound **203** to **205**.

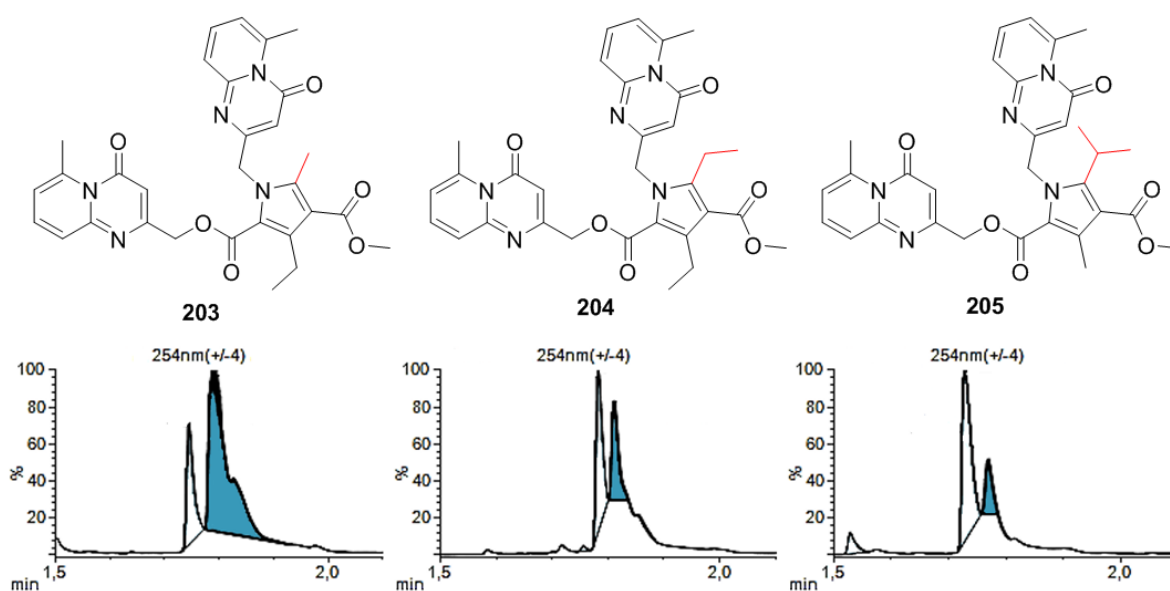
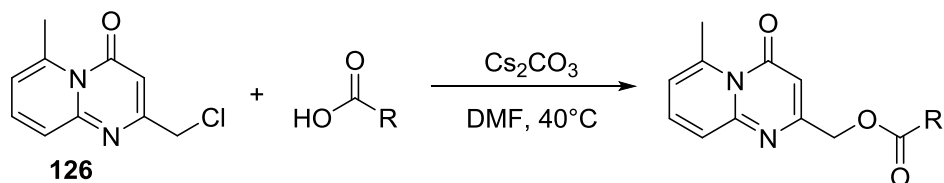


Fig. 7 UPLC chromatogram of reaction control after 16-17h showing the qualitative peak size (blue) of the **203**, **204** and **205** formed in each reaction.

1.3.2 Synthesis of less substituted pyrrole compounds and pyrrole isosteres

Some commercially available pyrrole and pyrrole isostere building blocks were utilized to synthesise **C6** derivatives using the previously established reaction conditions (Table 2).

Table 19 Synthesis of **C6** analogues **54-60** and **64**¹⁴⁵.



	R	Acid [eq]	C ₂ CO ₃ [eq]	Time [h]	Yield [%] ^a
54		1.1	1.5	16	93
55		1.1	1.5	16	99
56		1.1	1.5	16	97
57		1.1	1.5	15.5	93
58		1.1	1.5	16	96
59		1.1	1.5	15	97
60		1.1	1.5	18	15 ^b
		1.7	2.5	18	22 ^b
64		2.2	3	40	--
		2.2	3	96 (60°C)	7 ^b

^a crude yield; ^b HPLC purified;

¹⁴⁵ experiments conducted by I. Ferrara.

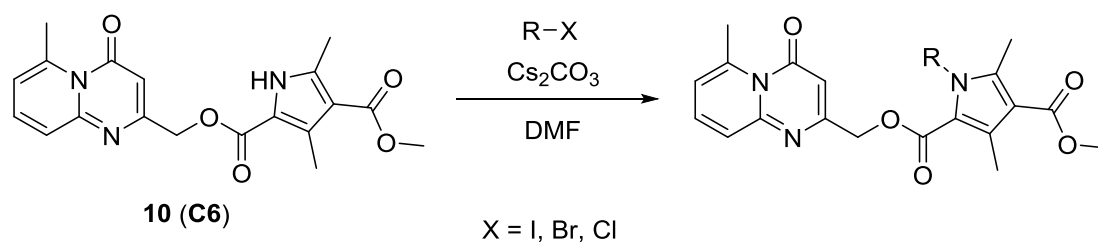
As can be seen in **Table 19**, the majority of the synthesised compounds gave an excellent yield with a very high purity and were used without any further purification. The exceptions are compound **60** and **64**, which gave a comparatively low yield, caused by a high reactivity of the N1 of the tail building block leading to double modification even when compound **126** is used in excess. To increase the yield of both compounds the introduction of a protecting group is necessary. This approach was not employed however, because the compounds could be isolated in a sufficient amount to carry out a full characterisation and to test them in biochemical applications.

1.3.3 N-modification of C6

Another type of modification of **C6** was the alkylation of N1 in the pyrrole ring. As was already described in previous chapters, the use of an excess of Cs₂CO₃ led to double alkylation on N1 of the pyrrole group (**Scheme 12**). This observation was used to alkylate **C6** with alkyl halides in the presence of caesium carbonate.

The alkylation of **C6** (**10**) in the N1 position of the pyrrole proceeded in good to excellent yields, except for compounds **103** and **207** (**Table 20**), whose reactions didn't give any product. The reaction seems to be sterically hindered by the methyl group neighbouring the N1 position and the secondary carbon of the alkylation agents the nitrogen has to react with. Furthermore, alkylation reagents containing electron withdrawing groups close to the reacting carbon, e.g. **104**, show an increased reactivity and proceed at RT giving a good yield.

Table 20 N1-Alkylation of pyrrole tail group of **C6**.

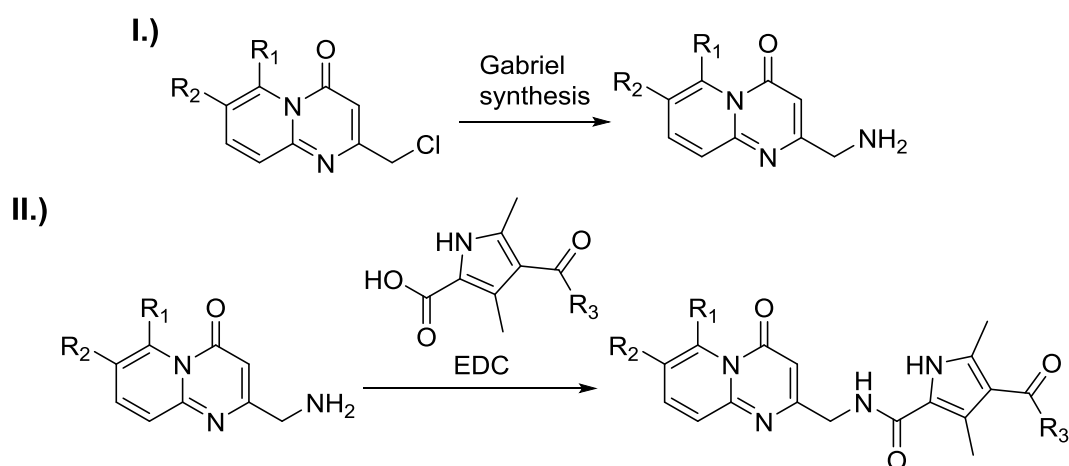


	R	X	Reagent	Cs ₂ CO ₃	Temp	Time	Yield [%]
100		I	1.5 eq	3 eq	RT	15h	76
101		Br	2 eq	3 eq	RT	24h	73
206		Br	1.5eq	3 eq	40°C	24h	--
102		Br	1.6 eq	3 eq	RT	24h	68
207		Br	1.5 eq	3 eq	50°C	5d	--
103		Cl	2.5 eq	3 eq	RT	48h	33
		Cl	2 eq	2 eq	40°C	18h	50
208		Br	1.5eq	2	40°C	4d	--
106		Br	4 eq	3 eq	50°C	72h	75
		Br	3.5 eq	5 eq	60°C	44h	75
104		Br	1.5 eq	3 eq	RT	16h	87
107		Br	1.5 eq	3 eq	RT	2h	98
105		Cl	1.5 eq	4 eq	50°C	16h	57

1.4 Linker modification

1.4.1 Amide Linker

To modify the structure of **C6** with an amide linker, the 2-(chloromethyl)-pyridopyrimidone **126** was first transformed into an amine with the Gabriel synthesis (**Scheme 13**). The amine was then reacted with the carboxylic acid of the pyrrole building block in a peptide synthesis step using the coupling reagent EDC.



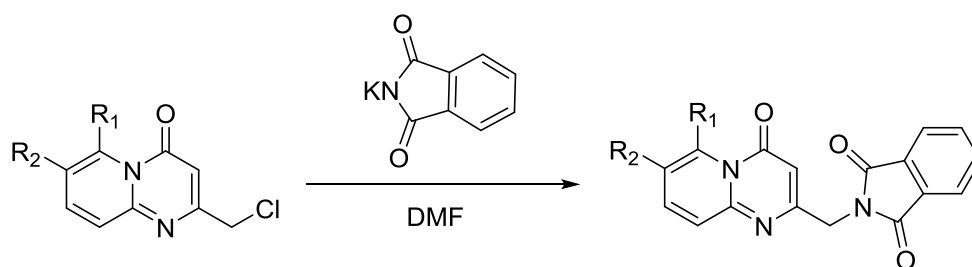
Scheme 13 Synthesis route for a C6 analogue containing an amide linker; **I.**) functionalization of 2-(chloromethyl)-pyridopyrimidones with an amine using the Gabriel Synthesis; **II.**) amide linker formation using the peptide coupling reagent EDC.

The Gabriel synthesis is a well-known two-step procedure to transform a halide into an amine. In the first step of the Gabriel synthesis, the 2-(chloromethyl)-pyridopyrimidones were modified with potassium phthalimide in dry DMF following the method of Sheehan *et al*¹⁴⁶

As can be seen in **Table 21**, compounds **209** and **210** were synthesised in excellent yields. These results correspond well with the yield found in literature (89%^{Error! Bookmark not defined.}) for a similar reaction.

¹⁴⁶ J. C. Sheehan, W. A. Bolhofer, *J. Am. Chem. Soc.*, **1950**, 72 (6), 2786–2788.

Table 21 Gabriel Synthesis Step I.

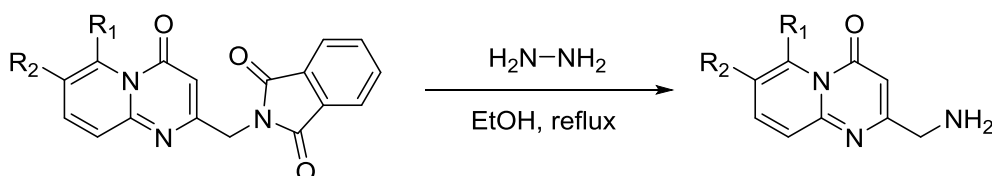


	R ₁	R ₂	Reagent [eq]	Temperatur [°C]	Time [h]	Yield [%]
209	Me	H	1.05	85	1.5	61 ^a
	Me	H	1.1	RT	18	88-98 ^b
210	H	Br	1.05	85	1.5	82

^a some product lost during purification; ^b crude yield; experiments conducted by I. Ferreira.

In the second step in the Gabriel synthesis, the phthalimido was cleaved to give the amine. With the modified conditions from Smits *et al*¹⁴⁷, compounds **209** and **210** underwent hydrazinolysis.

Table 22 Overview of Gabriel synthesis step II.



	R ₁	R ₂	Reagent [eq]	Temp. [°C]	Solvent	Time [h]	Yield [%]
211	Me	H	2.5	80	EtOH	3	99
	Me	H	3	RT	MeOH	34	76 ^a
	Me	H	5	RT	EtOH	19	100 ^a
	Me	H	5	RT	80%EtOH/ 20%MeOH	16	85 ^a
212	H	Br	2.5	80	EtOH	3	41
	H	Br	2.5	40	EtOH	16	54

^a crude yield, experiments conducted by I. Ferreira;

¹⁴⁷ R. A. Smits, M. Adami, E. P. Istyastono, O. P. Zuiderveld, C. M. E. van Dam, F. J. J. de Kanter, A. Jongejan, G. Coruzzi, R. Leurs, I. J. P. de Esch, *J. Med. Chem.* **2010**, 53, 2390–2400.

Table 22 shows near quantitative yield for the synthesis of compound **211** with ethanol as solvent, while compound **212** was isolated in a moderate yield under the same reaction conditions.

To form the amide linker, a peptide synthesis step using EDC coupling reagent was used. Different combinations of EDC with additives, which are documented in the literature^{148,149}, were tested to establish the best reaction conditions to link the 2-(methylamine)-pyridopyrimidones **211** and **212** with the carboxylic acid of the pyrrole building block. To activate the carboxylic acid, the pyrrole compound was dissolved in dry DMF with the coupling reagents and stirred at 0°C for 15 min before the amines dissolved in DMF was added and the reaction continued to be stirred at RT.

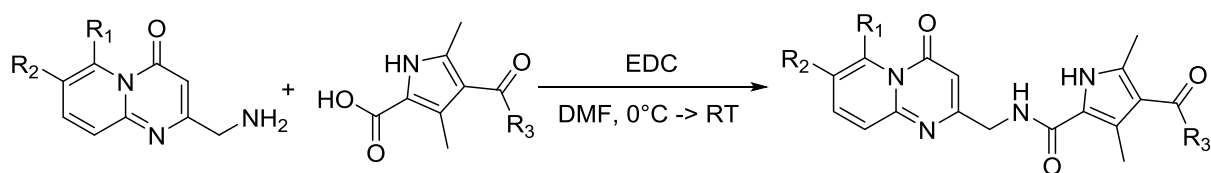
Table 23 shows moderate to good yields for the formation of amide linked compounds **61-63** and **213**. Several peptide coupling reagents were tested with a combination of EDC, HOBt and DIPEA giving the most promising results, even though the reaction took a long time to reach full conversion in some cases. It is imperative to mention that the best documented yields for the syntheses of **61**, **62** and **63** are crude yields, isolated from the aqueous phase as solids during the reaction work-up because the products exhibit very poor solubility in a number of organic solvents.

The use of other, more powerful peptide coupling reagents was not attempted and may be an approach to improve the yields of these compounds.

¹⁴⁸ S. Montalvao, T. O. Leino, P.S. Kiuru, K.-E. Lillsunde, J. Y. Kauhaluoma, P. Tammela, *Arch. Pharm. Chem. Life Sci.*, **2016**, *349*, 137–149.

¹⁴⁹ M.Hügler, X. Lucas, D. Ostrovskiy, P. Regenass, S. Gerhardt, O. Einsle, M. Hau, M. Jung, B. Breit, S. Günther, D. Wohlwend, *Angew.Chem.Int. Ed.*, **2017**, *56*,12476 –12480.

Table 23 Synthesis of **C6** analogues containing an amide linker.



N°	R ₁	R ₂	R ₃	SM	Pyrrole	Coupling reagents	Time	Yield [%]
61	Me	H	Me	1eq	1.1eq	1.1eq EDC/ 4eq NEt ₃	5d	--
	Me	H	Me	1.3eq	1eq	1.5eq EDC/1.1eq HOBt	19h	--
	Me	H	Me	1.1eq	1eq	1.3eq EDC/1.1eq HOBt/ 5eq DIPEA	18h	15 ^a
	Me	H	Me	1.1eq	1eq	1.3eq EDC/1.1eq HOBt/ 5eq DIPEA	18h	18 ^a
62	Me	H	OMe	1.2eq	1eq	1eq EDC/ 2eq DMAP	22h	--
	Me	H	OMe	1eq	1.1eq	1.1eq EDC/ 4eq NEt ₃	5d	3
	Me	H	OMe	1.2eq	1eq	1.3eq EDC/1.1eq HOBt/ 5eq DIPEA	3d	35 ^a
63	Me	H	OEt	1eq	1.1eq	1eq EDC/ 4eq NEt ₃	5d	6
	Me	H	OEt	1.2eq	1eq	1.3eq EDC/1.1eq HOBt/ 5eq DIPEA	3d	54 ^a
213	H	Br	OMe	1eq	1eq	1eq EDC/ 2eq DMAP	24h	13
	H	Br	OMe	1eq	1eq	1eq EDC/ 2eq DMAP	22h	8

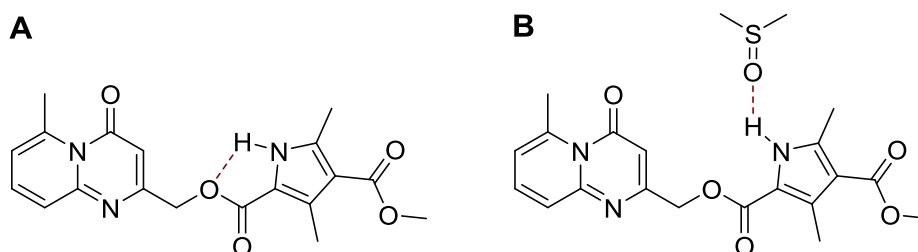
^a crude yield; synthesised by I. Ferrara;

E C6 analogues: Evaluation and Validation

1 Results

1.1 ¹H-NMR analysis of C6: possible internal H-Bonds to influence structure rigidity

When studying the structure of **C6**, it was apparent that a possible intramolecular hydrogen bond could be formed between N1 of the pyrrole ring and the ester in the linker (**Scheme 14**). If the hydrogen bond exists, the structure of **C6** would be more rigid and exchanging the ester linker would be undesirable. To investigate this hypothesis, the method of Jansma *et al.*¹⁵⁰ was used. It utilises the significant downfield shift that occurs when there is deshielding caused by hydrogen bond interactions¹⁵¹. DMSO interacts with the proton on N1 and leads to a significant shift of the signal compared to CDCl₃ when there is no internal interaction. In case of an interaction the DMSO molecule would not be able to compete with the intramolecular interaction causing the signal to shift minimally.



Scheme 14 C6 structure with **A** possible intramolecular H-Bond and **B** intermolecular H-bond with DMSO.

Comparing the ¹H-shifts of the NH peak of **C6** measured in CDCl₃ and DMSO-d₆, showed a significant downfield shift of 2.9ppm (**Fig. 8**), indicating no intramolecular interaction. An exchange of the pyrrole and ester linker was therefore not predicted to cause an unintended structural change, leading to inhibition loss.

¹⁵⁰ A. Jansma, Q. Zhan, B. Li, Q. Ding, T. Uno, B. Bursulaya, Y. Liu, P. Furet, N. S. Gray, B. H. Geierstanger, *J. Med. Chem.*, **2007**, *50*, 5875-5877.

¹⁵¹ G. Wagner, A. Pardi, K. Wüthrich, *J. Am. Chem. Soc.*, **1983**, *105*, 5948-5949.

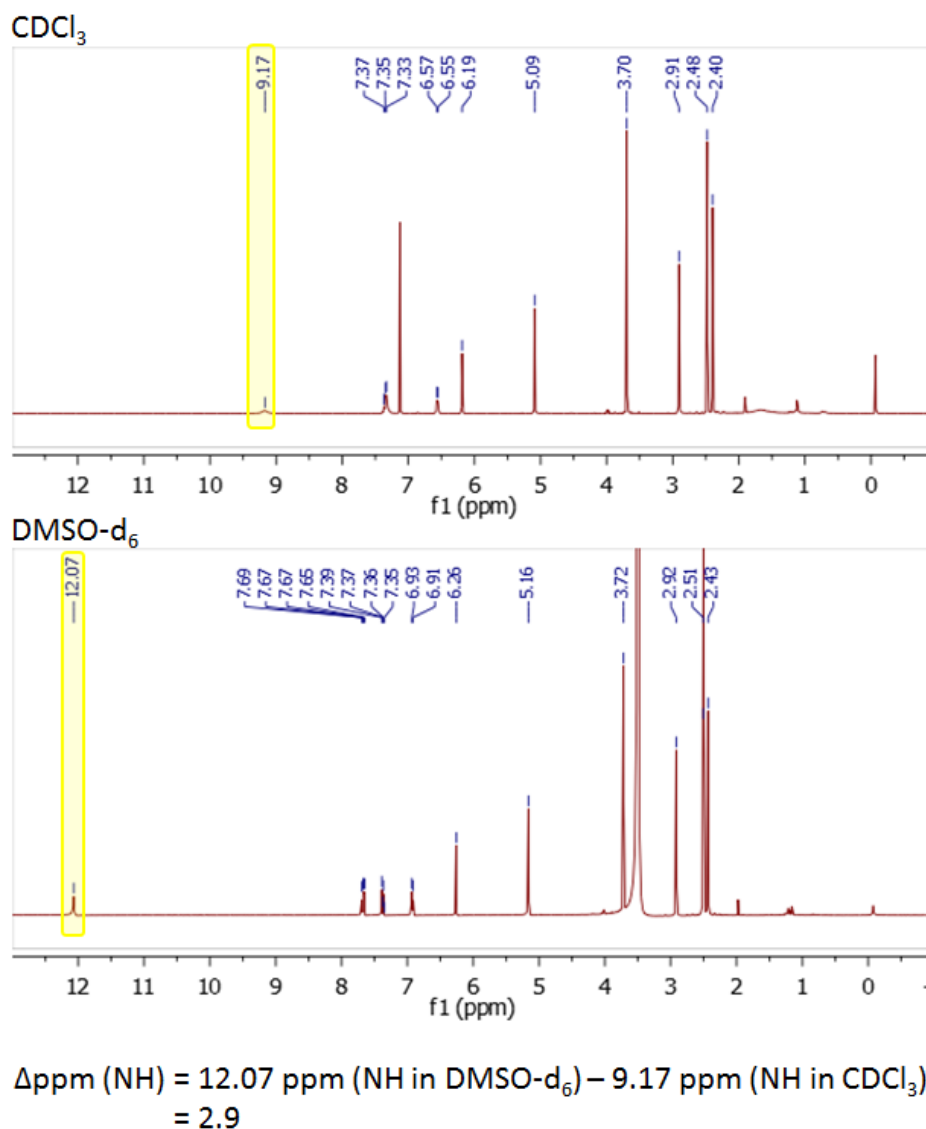


Fig. 8 ¹H-NMR (400MHz) of **C6** at RT in CDCl₃ and DMSO-d₆ with the NH peak highlighted (yellow).

1.2 AlphaScreen[®] evaluation of the synthesised compound library

As a first step to evaluate the biological activity of the **C6** analogues, the compounds were tested in an AlphaScreen[®] (see section **G1**). This biochemical assay is used to investigate protein-protein interactions and can therefore also be used to determine inhibition of such interactions. The PPI proteins are bound to an acceptor-/ donor- pair of Alpha Screen beads. The donor bead is excited by a laser causing a chemical reaction on its surface leading to the release of singlet oxygen. The singlet oxygen diffuses and on reaching the surface of the acceptor bead reacts with a thioxene derivative, generating a light emission, which is then detected. For the emission to occur, the beads need to be in close proximity due to the short half-life of the excited

oxygen species. The level of light emission is measured and used to determine the level of interaction. If the interaction of the proteins is inhibited, the emitted light is decreased significantly and can be used to determine the IC₅₀ of each compound. Recombinant Tec Kinase and FGF2 were bound to a donor/acceptor bead pair to test the effects of the compounds on their protein-protein interaction. All compounds were tested with a 10 step 1:3 dilution series spanning concentrations of 200µM to 3nM. For each compound two replicates were measured with each containing three technical replicates to determine their IC₅₀ value for protein-protein interaction of Tec Kinase and FGF2. Additionally, the solubility of the compounds was evaluated in the alpha assay buffer (see chapter **G2**) using the NEPHELOstar Nephelometer to comprehensively evaluate the measured data set, in case solubility issues influenced the measurements.

Graphs showing an inhibition level of >50% forming two plateaus were considered to give the actual IC₅₀. Compounds with solubility issues could be easily identified by the form of their graphs. The precipitation of compounds in the assay buffer at higher concentrations was visible in the decreasing inhibition values. Another possibility was a high variance in the inhibition values between the technical replicates at higher concentrations.

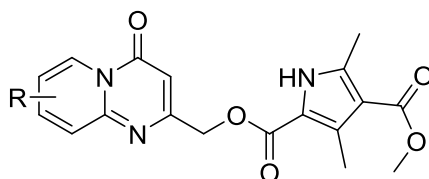
1.2.1 Structure-Activity Relationship: Round I

In La Venuta *et al.*¹¹⁵, compounds **C6 (10)** and **C14 (37)** (**Fig. 1**) were identified as PPI inhibitors for Tec Kinase and FGF2 which differ in their substitution on the pyridopyrimidine head group as well as in the tail group, making the exploration of the effects of those groups the first priority.

1.2.1.1 Effect of the substituent type and position modification of the head group

The first set of compounds tested contained a variety of substituents in different positions along the pyridopyrimidone scaffold. Additionally compounds without a substituent and lacking the whole head group were analysed as well as to their importance for the IC₅₀ of **C6 (10)**.

Table 24 Overview of solubility and IC₅₀ values of C6 derivatives with position and substituent modification on head group.



Head Group	N°	R	Solubility [μM]	Alpha IC ₅₀ ^a [μM]	Head Group	N°	R	Solubility [μM]	Alpha IC ₅₀ ^a [μM]
	3	--	>200	>200		11	Me	>200	11.8±0.2
						45	Et	>200	42.2±2.2
	5	H	>200	60.1±8.6		47	Pr ^b	43.6	25.9±3.2*
	10	Me	>200	22.3±3.1		44	Cyclopr	15.8	>200 [#] /16.
	51	Et	51.0	16.5±1		46	Bu ^b	65.4	>200
	49	Pr ^b	54.5	>200		33	OMe	>200	16±1.1
	52	Bu ^b	36.6	>200		19	CF ₃	64.6	>200 ^c
	32	OMe	63.3	20.2±1.6		41	Br	43.3	32.6±4.2*
	18	CF ₃	50	>200 ^c		25	Cl	101.2	22.8±0.8*
	40	Br	39.9	3.18±0.5		126	Bn	-- ^e	39±6.2 ^d
	12	Me	>200	13.9±2.8		13	Me	>200	17.2±0.9
	110	Et	55	52.3±5.7		112	Et	39.5	13±3.4
	114	Cyclopr	60	5.46±1.4 [#]		116	Cyclopr	46.4	23.7±3.2
	34	OMe	83.3	>200 ^c		35	OMe	36.46	34.2±1.3
	20	CF ₃	38.8	>200 ^c		21	CF ₃	81.2	>200 ^c
	42	Br	>200	14.6±0.2		43	Br	49.6	34.5±1.6
	26	Cl	>200	26.3±1		27	Cl	>200	19.7±2.1

^a data from two replicates with each three technical replicates; ^b synthesised by I. Ferrara¹³³; ^c data from M. Mößer Bachelor thesis; experiments conducted by P. Sehr at CBCF EMBL Heidelberg¹²⁴; ^d two data sets pipetted by hand; ^e data not recorded; * Inhibition level in Graph <50%, IC₅₀ likely higher than calculated; [#] solubility issues during assay;

Using a resynthesised **C6 (10)** as control and reference in the Alpha assay, several compounds were identified giving similar or lower IC_{50} value, e.g. **51**, **11**, **40**,... (labelled red in **Table 24**). Moving the methyl group along the head group scaffold gave improved IC_{50} values, whereas removing the substituent led to a 3-fold loss of activity. Increasing the size of the methyl group to an ethyl substituent led to a reduction of activity in the 7- and 8- position. The introduction of the propyl group in 6-position led to a loss of all activity whereas in 7-position an IC_{50} slightly higher than **C6 (10)** was measured. The introduction of a cyclopropyl group caused very low solubility in some positions, leading to the decision to test one of them in a hand-pipetted alpha assay, which led to the preliminary result of an IC_{50} value of $16.77\mu\text{M}$ (**Fig. 9 A and B**). This shows that for a number of compounds with a lower solubility, precipitation at higher concentrations can give a distorted picture of the real IC_{50} (**Fig. 9 D**). Compounds containing a methoxy group only gave an improved IC_{50} value in the 6- and 7- position on the scaffold. The analysis of the compounds containing a bromo substituent led with compound **40** to the most improved IC_{50} value measured.

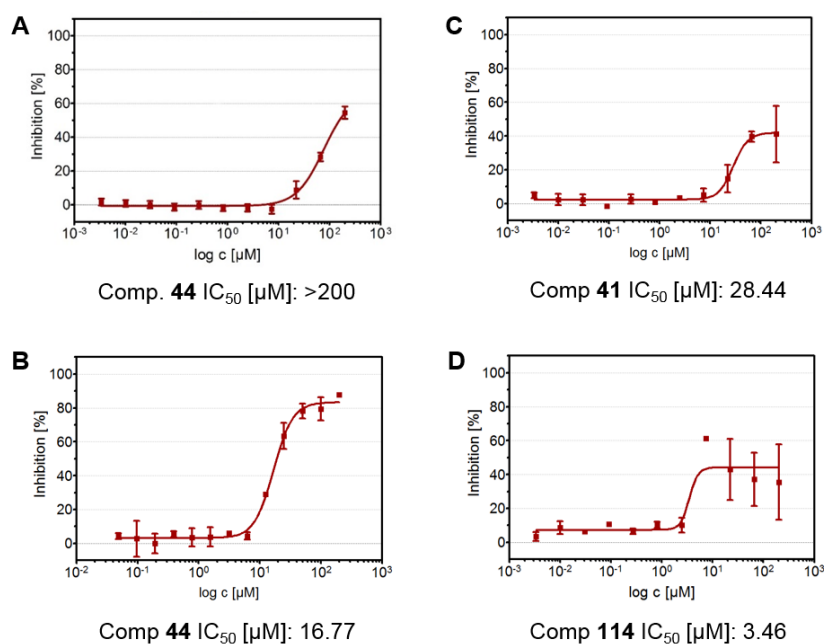
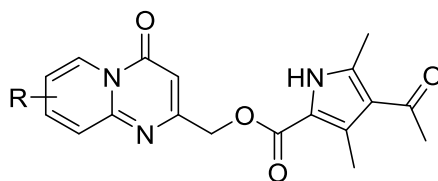
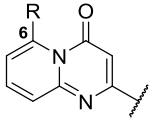
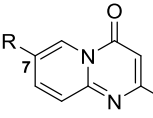
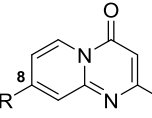
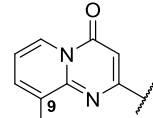


Fig. 9 IC_{50} graphs of Alpha Assay (3 techn. replic.): **A** Comp 44 graph of machine supported assay; **B** Comp 44 graph (hand pipetted); **C** Comp 41 with inhibition of <50%; **D** Precipitation of compound visible in graph at higher concentration for Comp 114.

In general, it is apparent that compounds containing an alkyl group give a better inhibition level, though no particular preference of the substituent position on the ring is noticeable (**Fig. 10**). For compounds with polar substituents most analogues don't

Table 25 Overview of solubility and IC₅₀ values of compounds with position and substituent modification on head group and the ketone on the pyrrole tail group.



Head Group	N°	R	Solubility [μM]	Alpha IC ₅₀ ^a [μM]	Head Group	N°	R	Solubility [μM]	Alpha IC ₅₀ ^a [μM]
	4	H	66	17.5±1.9*		7	Me	50.8	>200
	6	Me	>200	>200		29	OMe	49.7	50.1±0.3
	28	OMe	66	27.1±0.9		15	CF ₃	79	>200 ^b
	14	CF ₃	>200	>200 ^b		37	Br	66	24±4.1 ^d
	36	Br	22	10±0.4		22	Cl	>200	76±7.5
	8	Me	>200	>200		9	Me	63.1	>200
	30	OMe	50	75.9±3.1		31	OMe	>200	>200
	16	CF ₃	70	>200 ^b		17	CF ₃ ^c	--	--
	38	Br	>200	34.2±3.2		39	Br	22	32.5±0.2
	23	Cl	>200	40.2±0.8		24	Cl	30	38.4±0.7

* Inhibition level <50% IC₅₀ likely higher; ^a average±st.dev of two replicates (each three technical replicates); ^b data from M. Mößer Bachelor thesis; experiments conducted by P. Sehr at CBCF EMBL Heidelberg¹²⁴; ^c not enough compound to test; ^d assay pipetted by hand (2 repl. each three techn. repl.);

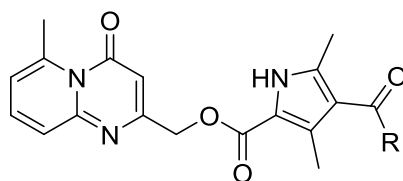
1.2.2 Structure-Activity Relationship Round II: Extending ester and adding head group substituents

Based on the data obtained in the first round of SAR, the introduction of a larger ester substituent on the tail group was investigated as well as introducing an additional substituent on the head group scaffold.

1.2.2.1 Ethyl ester effect on tail group

Due to the positive effect the methyl ester had on the activity of **C6** (**10**) compared to the ketone derivative (**7**), a further extension of the ester group was undertaken by introducing an ethyl ester.

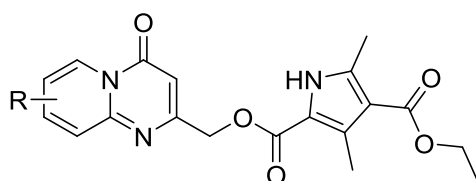
Table 26 Comparison of IC₅₀ values of **C6** with an ethyl ester on pyrrole ring.



N°	R	Solubility [μM]	Alpha ^a IC ₅₀ [μM]
7	Me	>200	>200
10 (C6)	OMe	>200	22.3±3.1
66	OEt	>200	15.2±1.6

As can be seen in **Table 26** the IC₅₀ value decreases significantly with an increasing size of the ester on the tail group. Based on this result, the most promising compounds from **Table 24** were modified accordingly and tested.

Table 27 Ethyl ester modification of most promising C6 derivatives with position and substituent modification on head group.



Head Group	N°	R	Solubility [μM]	Alpha IC ₅₀ ^a [μM]	Head Group	N°	R	Solubility [μM]	Alpha IC ₅₀ ^a [μM]
	66	Me	57.7	15.2±1.6		123	Me	-- ^b	55.41 ^c
	118	Et	39.6	>200		50	Pr	42.2	>200
	67	Br	34.7	30.8±3.0		65	Br	52.2	16.8±0.4
	119	Me	>200	10.1±2.0*		120	Me	57.2	9.0±0.1
	111	Et	64.9	11.0±0.7*		113	Et	52.9	26.8±0.1
	115	Cyclopr	52.8	44.2±1.6*		117	Cyclopr	45.6	>200
	121	Br	>200	18.5±0.4		122	Br	41.4	53.8±6.8

* Inhibition level <50% IC₅₀ likely higher; precipitation visible in technical triplicates; ^a average±st.dev of two replicates (each three technical replicates); ^b data not recorded; ^c one replicate pipetted by hand containing three technical replicates;

Table 27 shows a clear improvement of IC₅₀ values for compounds with a methyl substituent. However, compounds containing the larger alkyl substituent on the head group exhibit a reduced or full loss of their activity. A similar trend is notable concerning the bromo analogues **67** and **122**, while compounds **65** and **121** retain their activity or increase it. While the introduction of the ethyl ester on the pyrrole group led to a improved IC₅₀ for the methyl analogues, compounds with larger groups mostly lost activity. Through the ambivalent effect the ethylester substituent exhibited in combination with different head groups, it was further evaluated with other **C6** scaffolds.

1.2.2.2 Adding a substituent to head group of **C6**

Looking at the IC₅₀ values of the compounds containing one methyl group in different positions on the head group scaffold, the next step was to try to combine their effects by adding a second methyl group. In addition, the effect of adding another aromatic ring to the pyridopyrimidone head group was investigated. The new head groups were also tested in combination with two different pyrrole tail groups, one containing the methyl ester and the other the ethyl ester substituent.

Table 28 shows clearly that the addition of a second substituent on the **C6** scaffold led to loss of inhibition for all position except for the 8-position, compound **70**, which exhibits a similar activity than **C6**. The introduction of an additional aromatic ring (**68**) gives at first glance a promising IC₅₀ value but as can be seen in **Fig. 11 C**, the inhibition level reached is only 30%. However, the trend seen in **Table 26** showing an improvement of the IC₅₀ on introduction of the ethyl ester on the tail group, continues for all compounds with a second methyl group, leading to the identification of promising compounds **71** and **73**. For compounds **74** and **75**, although having a supposed solubility of >200µM, precipitation can be seen in the graphs distorting the true IC₅₀ value (**Fig. 11 A and B**).

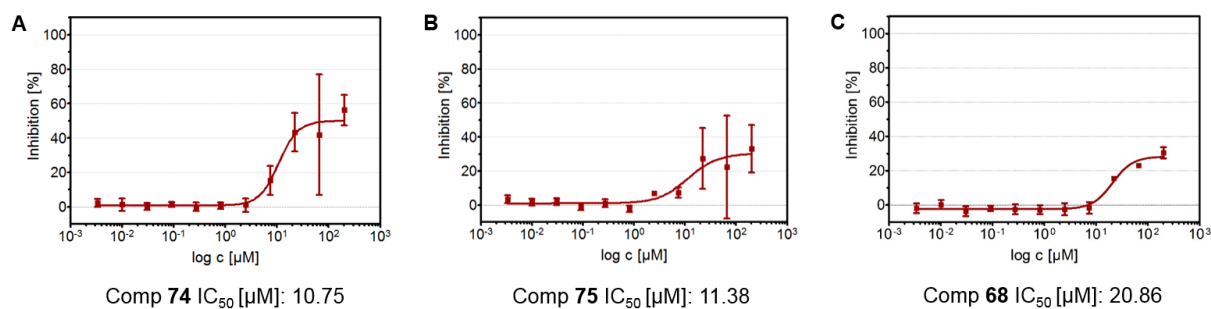
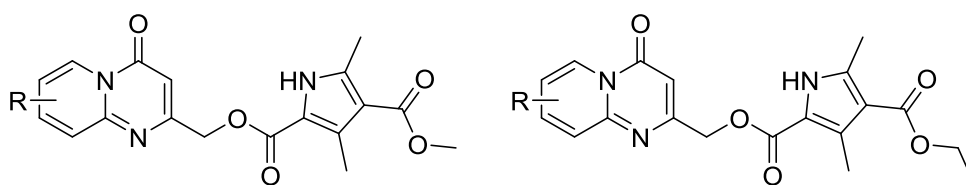


Fig. 11 Alpha assay graphs for **A** comp **74** and **B** comp **75** with a high variance of measured data between the technical replicates leading to possible incorrect IC₅₀ values; **C** Graph of comp **68** only giving an inhibition level of 30%.

Table 28 IC₅₀ and solubility values of compounds with multiple substituents and bigger groups.



Pyrrrole methylester tail group

Pyrrrole ethylester tail group

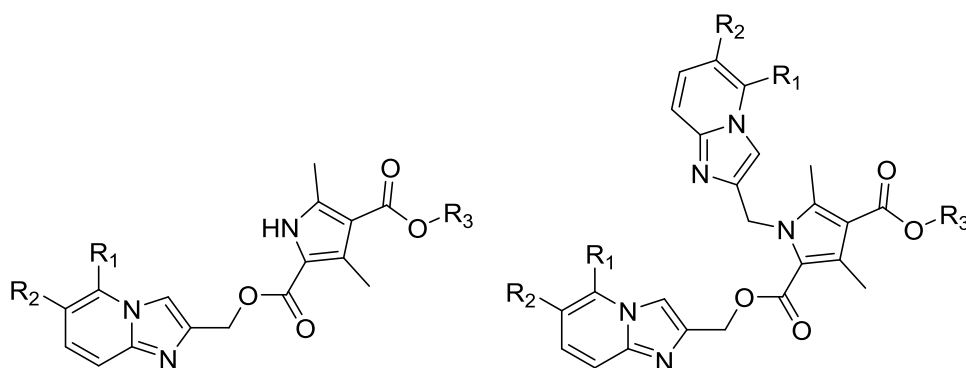
Head Group	N°	Solubility [μM]	Alpha IC ₅₀ [μM]	N°	Solubility [μM]	Alpha IC ₅₀ [μM]
	72	>200	51.2±3.5	73	>200	5.9±0.8
	70	>200	26.6±3.2	71	42.3	14.4±0.1
	74	>200	14.1±1.5*,#	75	>200	7.7±3.7*,#
	68	70	19.3±1.62*	69	70	>200

*Inhibition in Graph <50%, IC₅₀ likely higher; # high variance in data sets between technical replicates

1.2.2.3 Removing carbonyl group from head group

Changing the head group structure from a pyrimidopyrimidone to an imidazopyridine was needed to get an idea of how much of an influence the carbonyl group has on the IC₅₀ value. For this, the most promising compounds **40**, **73** and **C6 (10)** were modified.

Table 29 IC₅₀ and solubility results of compounds with imidazopyridines head groups.



R ₁	R ₂	R ₃	Single Modif.	Solubility [μM]	Alpha ^a IC ₅₀ [μM]	Double Modif.	Solubility [μM]	Alpha ^a IC ₅₀ [μM]
Me	H	Me	88	73.57	>200	--	--	--
Br	H	Me	95	68.3	>200	96	67.2	12.5±1
Me	Me	Me	91	>200	16.4±5.1*	92	--	--
Me	H	Et	89	>200	>200	90	100	16.5±1.8
Br	H	Et	97	100	28.2±2.8*	98	15	4.69±0.5**
Me	Me	Et	93	>200	8.3±0.1**	94	37.58	3.12±0.1**

^aaverage±st.dev of minimum two replicates (each three technical replicates); *at least one replicate: Inhibition level <50%, precipitation visible in technical triplicates; **Inhibition level >25%, precipitation in graph visible.

In **Table 29** IC₅₀ and solubility results of compounds with imidazopyridines head groups. **Table 29** it is notable that the removal of the carbonyl group led to a total loss of activity for compounds **88** and **95** containing the single methyl group. The IC₅₀ for the double substituted head group however decreased compared to the pyridopyrimidone containing compound **72** (**Table 28**). The introduction of the ethyl ester on the pyrrole ring led to a reactivation of activity for compound **97**. The addition of another head group to the prospective pyrrole ring, led to a higher inhibition. With the double modification causing a decrease of solubility, the IC₅₀ results for compounds **98** and **94** are likely higher than noted.

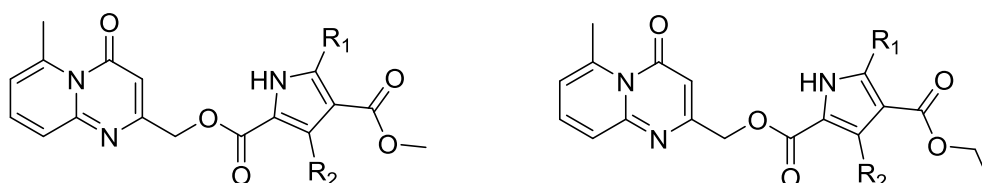
1.2.3 Structure-Activity Relationship Round III: Tail group and Linker modification

After the extensive examination of the effects of changes to head group scaffold, changes to the pyrrole and linker structure and their effects were investigated next.

1.2.3.1 Increase the size of the alkyl substituents on the tail group

After establishing the trend for increased inhibition by extending the ester substituent on the tail group into an ethyl ester, a closer look at the other substituents was needed. To evaluate the importance of the methyl substituents, they were exchanged with ethyl- and *iso*-propyl groups (**Table 30**).

Table 30 IC_{50} data for increased alkyl substituents on the tail group.



Pyrrole methylester tail group

Pyrrole ethylester tail group

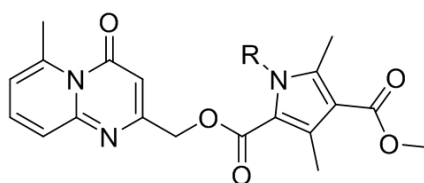
R ₁	R ₂	N°	Solubility [μM]	Alpha IC ₅₀ [μM]	N°	Solubility [μM]	Alpha IC ₅₀ [μM]
Et	Me	76	>200	>200	78	>200	>200
Me	Et	77	43.7	>200	79	>200	>200
Et	Et	80	10	>200	81	53.8	>200
<i>i</i> Pr	Me	82	53.8	>200	84	51.12	>200
Me	<i>i</i> Pr	83	>200	>200	85	65.51	>200
<i>i</i> Pr	<i>i</i> Pr	86	66.68	>200	87	66	>200

The replacement of the methyl group with an ethyl substituent for each separately and in combination led to a full loss of inhibitory activity (**76**, **77**, **80**). The same was observed for the introduction of the *iso*-propyl substituent respectively (**82**, **83**, **86**) and in combination. Even the combination with the ethyl ester group doesn't restore the activity (**Table 30** right side).

1.2.3.2 Alkylation of pyrrole on NH-position

The increase of inhibitory activity through the double modification on the nitrogen of the pyrrole ring shown in **Table 29**, suggested that a modification in that position might influence the inhibition of Tec Kinase and FGF2 positively. A range of alkyl groups, some containing a variety of functional groups designed to enhance solubility, were introduced (**Table 31**) on N1 of the pyrrole ring.

Table 31 IC_{50} values for N-modified tail group modifications.



N°	R	Solubility [μ M]	Alpha ^a IC_{50} [μ M]	N°	R	Solubility [μ M]	Alpha ^a IC_{50} [μ M]
100	Me	66	23.3±2.3	107	Bn	62.5	>200
101	Et	59.1	>200	108	CH ₂ COOH	>200	>200
102	Pr	47.9	>200	109	CH ₂ CH ₂ NH ₃	>200	>200
103	MEM	35	>200	106		53.8	85.2±12.7*
104	CH ₂ C=OOtBu	37.5	>200	99		43.4	45.6±6.6
105		66.1	40.6±1.1				

^a average±st.dev of two replicates (each three technical replicates); *Inhibition in Graph <50%, IC_{50} likely higher;

Modifying compound **C6** with alkyl groups led to full loss of activity for the majority of compounds (**101-104**, **107-109**). Some compounds still show inhibition (**105**, **106**, **99**) but compared to the IC_{50} of 22.3±3.1 μ M for **C6**, a 2- to 4-fold loss of activity was noticeable. Only the methyl-modified compound **100** retained the same IC_{50} value as **C6**, indicating that N1 is not essential for the inhibitory activity. The introduction of the morpholine group (**105**) or the MEM group (**104**), intended to increase the solubility, had the opposite effect and led to loss of activity. Interestingly, double modification of **C6** with a second head groups led to a two-fold loss of inhibition (**99**), exhibiting the opposite effect than the compounds with an imidazopyridine head group (**Table 29**).

1.2.3.3 Removing substituents and exchanging pyrrole tail group

After increasing the size of substituents and adding additional ones, it was also of interest to investigate the removal of the aforementioned substituents and substitute the pyrrole ring with other heterocycles like imidazoles or indole.

Table 32 IC₅₀ values for compounds **54-60** and **64**.

N°	R	Solubility [μM]	Alpha ^a IC ₅₀ [μM]	N°	R	Solubility [μM]	Alpha ^a IC ₅₀ [μM]
54		22	70.1±22.6	58		>200	>200
55		66.6	>200	59		>200	>200
56		32.8	>200 ^b	60		>200	>200
57		>200	>200	64		>200	>200

^a average±St.dev. of minimum two replicates (each three technical replicates); ^b one replicate with 3 technical replicates; * Inhibition in Graph <50%, IC₅₀ likely higher;

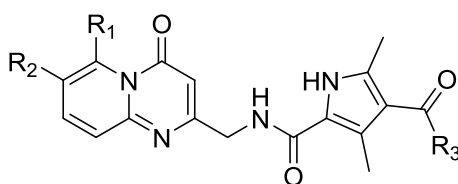
As can be seen in **Table 32**, all compounds, except for **54**, had no inhibitory effect on the interaction of Tec Kinase and FGF2. Of interest was especially the full loss of activity by removing the ester substituent from the tail group as was shown with compound **55**. The introduction of alternate heterocycles (**56**, **58-60**, **64**) also led to a full loss of inhibition.

1.2.3.4 Amide Linker

Through the existence of esterases in the human body, having an ester linker in a potential drug may lead to rapid clearance from the body. The introduction of an amide linker would increase plasma and cell stability. Furthermore, in the initial screen, an inactive compound (**C19**) lacking the methyl substituent on the head group and containing an amide linker was identified. The amide linker was introduced into the bromo containing compound **C14** (**37**) and methyl group containing compounds **6**, **C6** (**10**) and **66**.

#

Table 33 IC_{50} of amide linked compounds **61-63** and **124**.



N°	R ₁	R ₂	R ₃	Solubility [μ M]	Alpha ^a IC_{50} [μ M]
61	Me	H	Me	52.5	>200
62	Me	H	OMe	39.6	>200
63	Me	H	OEt	67.4	>200
124	H	Br	OMe	-- ^b	>200 ^c

^a average \pm st.dev. of two replicates (each three technical replicates), ^b data not recorded; ^c average+st dev. of two replicates (each three technical replicates) pipetted by hand

In **Table 33** it is clear that the exchange of the ester to an amide group was the cause for the full loss of any inhibition as was also seen in the control compound **C19**. Additionally the recorded solubility for compounds **61-63** are significantly lower than for compound **C6 (10)** with a solubility of >200 (**Table 24**).

1.3 Quantification of inhibition of FGF2 secretion in cell-based biotinylation assay

The compounds with the most promising inhibition levels determined in the biochemical alpha assay and the amine linked C6 derivative were tested in the cell surface biotinylation assay (see chapter **G3**) analysing their influence on FGF2 secretion from cells. The assay is commonly used to determine the amount of protein staying close to the cell surface after secretion. With FGF2 being bound to HSPG in the ECM¹⁵², this assay can be used to quantify the influence of each compound on FGF2 secretion.

A stable CHO cell line expressing FGF2-GFP in a doxycycline dependent manner was treated with **C6**, **control C19**, **51**, **62**, **66**, **67** and **71** at 50 μ M, 25 μ M, 10 μ M and 5 μ M in

¹⁵² C. Zehe, A. Engling, S. Wegehngel, T.Schäfer, W.Nickel, Proc. Natl. Acad. Sci. U.S.A., **2006**, *103*, 15479-15484.

0.5% DMSO (**Fig. 14**). All compounds identified in the alpha assay were tested with a compound concentration of 25 μ M in 0.5% DMSO (**Fig. 12**).

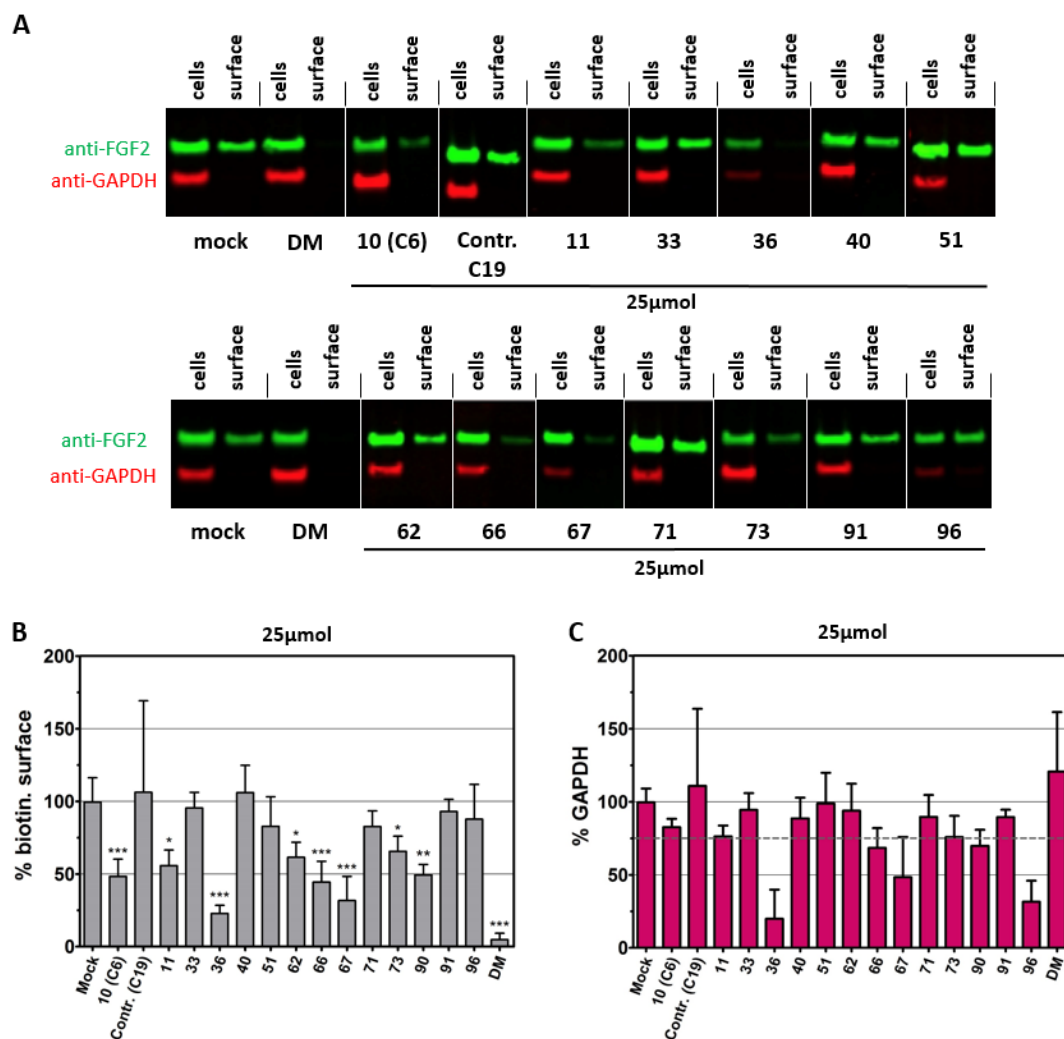


Fig. 12 Surface biotinylation levels of FGF2-GFP and GAPDH cell lysate quantification in CHO cells expressing FGF2Wt-GFP (mock) and FGF2C77/95A-GFP as cell control (DM) after incubation with compounds for 16h at 37°C; **A Western Blot of full cell lysate (cell) and surface population of FGF2 treated with no compound (mock, cell control (DM) and 25 μ M of compounds, proteins labelled with anti-FGF2(green) and anti-GAPDH (red) antibodies; **B** average and st.dev. of surface biotinylation levels at 25 μ M for all PPI inhibitors identified in alpha assay with **C** their GAPDH level; all data sets were normalized to average mock set to 100%. data sets calculated from min. 4 independent replicates (three repl.: 11; five repl.: 96; six repl.: 66, 10(C6); seven repl.: 33, 40, 71; eight repl.: 51, 90); experiments conducted by S.Wegehingel.**

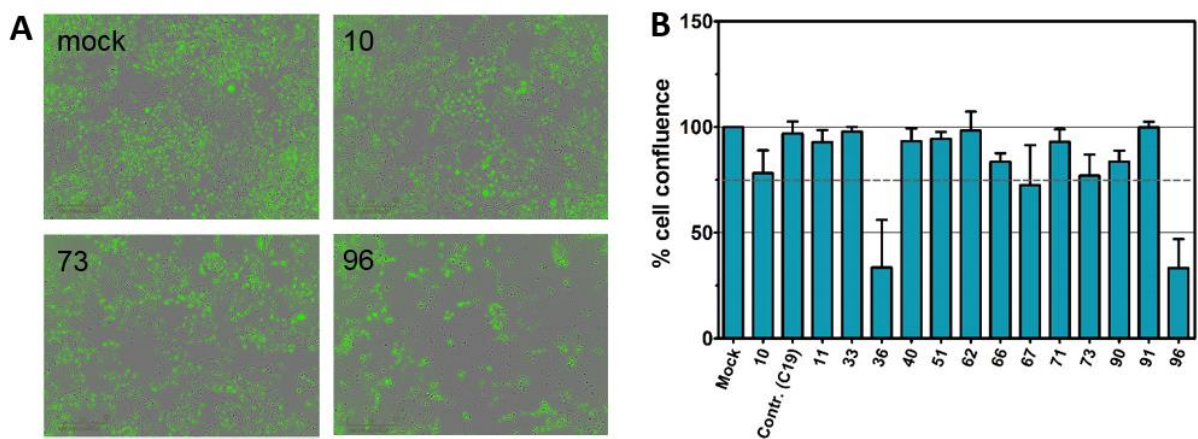


Fig. 13 Cell confluence of CHO cells after incubation with 25 μ M of compounds for 40h at 37 $^{\circ}$ C;
A microscopy pictures of mock and compounds **10**, **73** and **96**; **B** Graph of average \pm SD of cell confluence in % calculated from min. 3 repl. (4 repl.: **33**, **40**, **62**, **67**, **73**, **96**; 7 repl.: **10**(C6), **51**, **66**, **71**); confluence was normalized to average of mock set to 100%; Pictures and data was obtained by S. Wegehingel.

After the incubation of the cells with the small molecule inhibitors, the cell confluence of all samples was measured (**Fig. 13**) to check for cell health before their surface population of proteins was biotinylated. The biotinylated proteins were extracted with streptavidin beads from the total cell lysate. The purified surface population of FGF2 and the FGF2 amount in the total cell lysate were analysed via SDS-PAGE/Western blot and visualised with polyclonal GFP-antibodies (**Fig. 12 A**). GAPDH was used as an experimental control to confirm the integrity of each replicates, because as an intracellular protein it should not be found in the surface sample. However, it can also give an indication if cell growth might be influenced by the compounds (**Fig. 12 B**). For the quantification of FGF2 and GAPDH both were labelled with a different fluorescent secondary antibody. As can be seen in **Fig. 12**, not all compounds identified as inhibitors to the protein-protein interaction of Tec Kinase and FGF2 in the Alpha assay seem to have an effect on FGF2 secretion from cells. At 25 μ M compound concentration (**Fig. 12 B, C**) seven of the thirteen compounds caused a significant difference in secretion. Only compounds **36**, **66** and **67** inhibited FGF2 secretion better than compound **10** (C6). As can be seen in **Fig. 12 C** and **Fig. 13 B** for these compounds however, the low level of GAPDH and lower level of cell confluence indicated that **36** might be cytotoxic. Other compounds like **33**, **40**, **71** and **91** didn't seem to have any effect on the secretion at all, even though they all gave lower IC₅₀ values in the alpha assay, indicating differences in cell permeability for these compounds. Compound **11** and **90** have a similar effect on the secretion of FGF2 as **10** (C6). Compound **62**, showing no effect in the alpha assay, was tested as a control

compound but gave a significant reduction of FGF2 secretion. All of the compounds seeming to have a cell toxic/ hindering cell growth (**36**, **96**) when looking at their cell confluence and GAPDH levels contain a bromo substituent. Comparing the influence of select compounds at different concentrations showed a dose-response effect for most compounds tested as can be seen in **Fig. 14 A** and **B**. For compound **51** and **C6** a similar inhibition level of secretion can be seen at 25 μ M and 10 μ M. Comparing the GAPDH levels at those concentrations for both compounds indicates less toxicity.

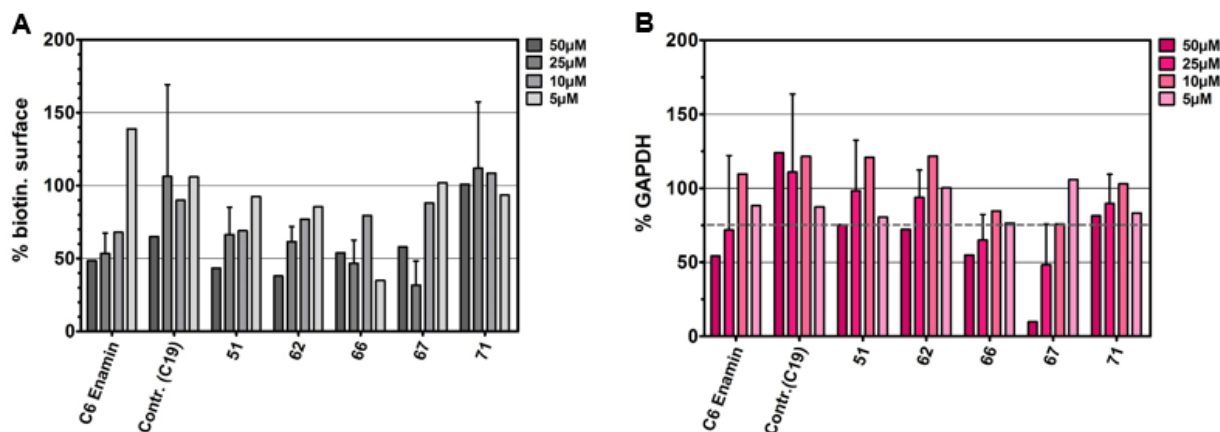


Fig. 14 Surface biotinylated FGF2-GFP population and GAPDH cell lysate quantification in CHO cells expressing FGF2Wt-GFP (mock) after incubation with compounds at 50 μ M, 25 μ M, 10 μ M and 5 μ M for 16h at 37 $^{\circ}$ C; all data sets; **A average of surface population of FGF2Wt normalized to mock set to 100% for 50 μ M, 10 μ M and 5 μ M and average \pm SD for 25 μ M; **B** average of GAPDH level in cell lysate for 50 μ M, 10 μ M and 5 μ M, average \pm SD for 25 μ M of compound conc.; all data sets were normalized to the average of mock set to 100%; average for 50 μ M, 10 μ M and 5 μ M calculated from 2 repl.; average \pm SD for 25 μ M calculated from 4 repl.; experiments were conducted by S.Wegehingel.**

2 Discussion

The alpha assay data gave a good overview of the SAR for **C6** (Fig. 15) so far.

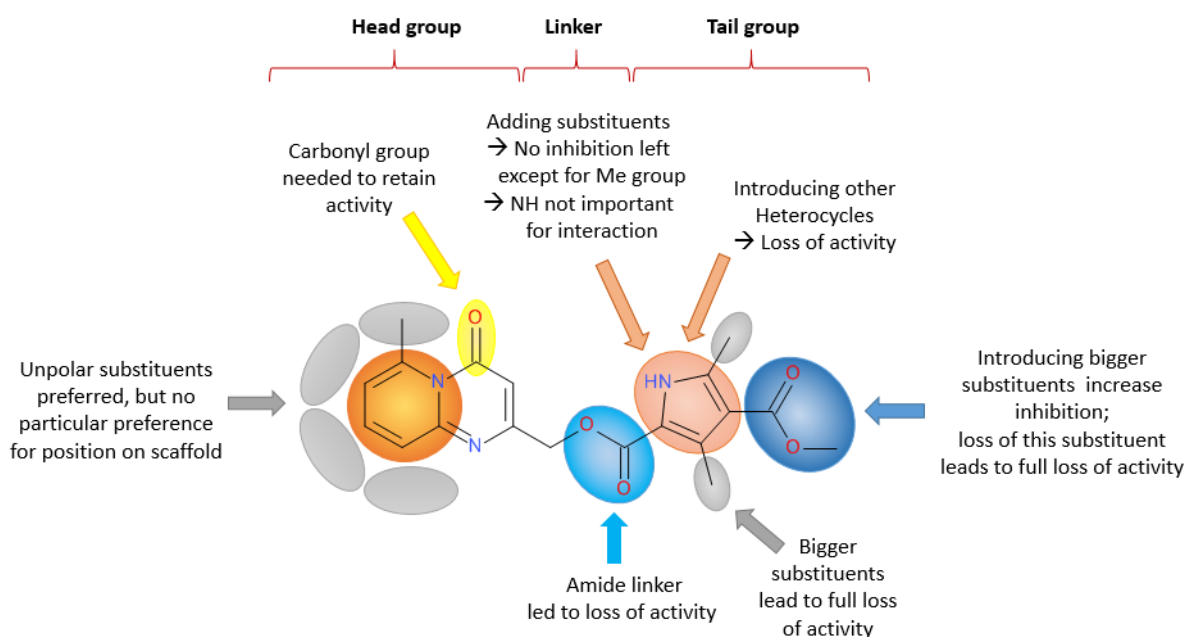


Fig. 15 SAR results of the alpha assay for C6.

Looking at the head group substituents, it showed clearly that non polar substituents improved potency indicating the surrounding of the molecule in the interaction site is likely lipophilic and will not tolerate polar groups. Larger non-polar substituents (e.g ethyl, cyclopropyl) increased the inhibition further. However, exchanging the methyl ester on the tail group for the ethyl ester for these compounds led to loss of inhibition. The interaction site on the protein only seems to be able to accommodate a larger substituent on either the head group or the tail group but not on both at the same time. A similar effect is noticeable for compounds containing a bromo substituent. Furthermore, adding another alkyl substituent on the head group did not have a full additive effect on the inhibition level, but only slightly improved potency.

Removing the carbonyl group on the head group led to a full loss of activity for the single substituted compounds, but slightly increased for the double substituted compared to **C6**. This indicates that the carbonyl group on the pyridopyrimidone scaffold plays an important role in the interaction of the inhibitor with the protein surface. The double substituted compounds lacking the carbonyl group most likely have a different orientation in the binding pocket due to their larger size than the single substituted compounds, leading to their activity. The double head group modified

compounds all (single and double substituted) regained or increased their inhibitory activity when the ethyl ester substituted pyrrole ring was introduced.

The exchange of the ester linker against the amide linker led to a full loss of activity in the Alpha assay. Exchanging the oxygen against a nitrogen atom, replaces an H-bond acceptor with an H-bond donor, reversing the interaction needed for inhibition.

Any increase of size to the substituents of the tail group, except for the ester group, led to full loss of activity. Adding a substituent on the nitrogen of the pyrrole also contributed to full loss of inhibition except for the addition of a methyl group, which gave a similar IC_{50} to **C6**, indicating that the NH is not involved in the interaction with the protein surface. The area where the tail group is interacting in the interaction site seems to be narrow and not able to accommodate bigger substituents. The exception to this though is the methyl ester group on the pyrrole ring. Reducing the size to a methyl ketone led to decrease of inhibition for a number of compounds, whereas the extension into the ethyl ester increased the inhibition for compounds containing a methyl group. Exchanging the ketone against an ester adds an H-Bond acceptor which seems to enhance the interaction with the protein surface. Removing the ester also led to full loss of inhibition. This shows that the ester group is an important factor facilitating the interaction with the protein surface. Even though esters are not very stable in plasma and cells, this particular ester group is likely resistant to esterase degradation because of its steric hindrance and will not need to be replaced.

Testing the compounds which gave the most promising alpha IC_{50} values in the cell based biotinylation assay to quantify their influence on the secretion level of FGF2 offered a different view onto these compounds (**Fig. 16**). Compounds containing a bromo substituent had a very strong effect on the secretion but seem to be cytotoxic or hinder cell growth in some cases.

Another compound used as a control (**62**) decreased the secretion significantly but didn't show any activity in the alpha assay. This shows that within cells additional factors might influence the the activity of the compounds.

Two compounds were identified to inhibit the secretion of FGF2 better than **C6**. Examples like compound **67**, which show a more pronounced effect in the cell based assay than in the reconstituted biochemical alpha assay, further confirm that a combinatorial approach to identify inhibitors is needed. Some compounds exhibit no

effect on the secretion of FGF2, while giving a good inhibition level in the alpha assay. These compounds may be unable to penetrate the cell. This requires further investigation. (**Fig. 16** yellow labelled).

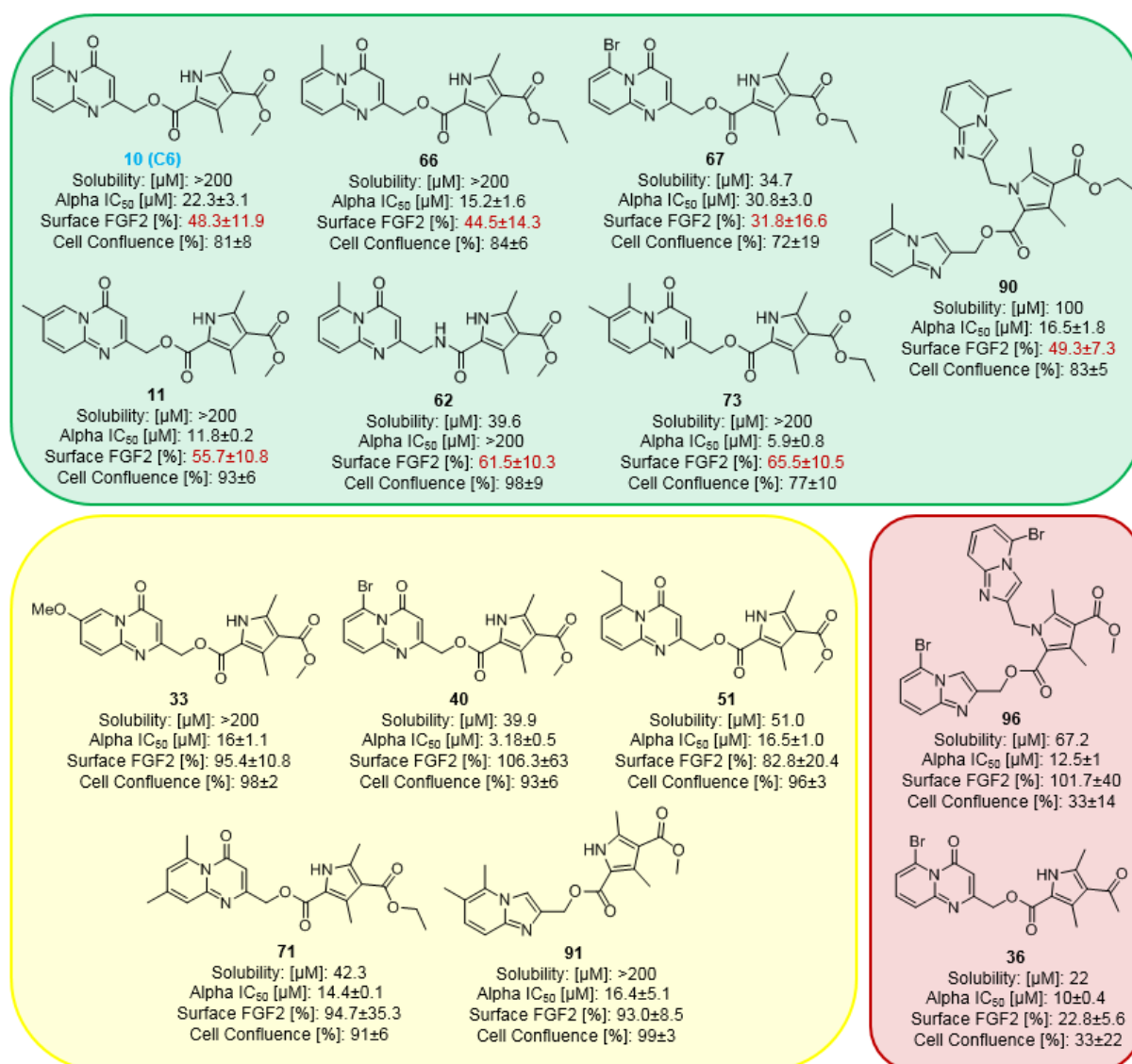


Fig. 16 Overview of biological data obtained for most promising compounds of C6 SAR; **green**: compounds with a better/similar inhibition of FGF2 secretion; **yellow**: compounds with alpha assay activity but no activity in cell-based assay; **red**: compounds that possibly hinder cell growth.

It can be said that the Alpha assay data gives a good indication to evaluate the SAR of **C6**. However, it is not robust enough to solely base decisions on, into which direction the SAR needs to continue. As it is a biochemical assay, it doesn't take into account other factors like cell permeability or toxicity, which play an important role for the development of drug candidates. The fact that compound **62** didn't show any effect in the alpha assay but lowered FGF2 secretion in the biotinylation assay, shows that a more comprehensive approach is needed.

F Conclusion and Outlook

A library of around 130 analogues of **C6** was successfully synthesised and the compounds evaluated for their inhibitory activity on the interaction of Tec Kinase and FGF2 by using the Alpha Assay. Thirteen compounds were identified exhibiting a similar or better IC_{50} than **C6** and further evaluated in the biotinylation assay quantifying their effect on FGF2 secretion. This led to the successful identification of two compounds showing a stronger secretion phenotype for FGF2 secretion than **C6**. Additionally, the well-designed library led to the identification of important structural features on **C6**, that are crucial for its activity as an inhibitor for the interaction of Tec Kinase and FGF2 (**Fig. 15**).

Although the results of the SAR led to the identification of important structural features, a further expansion of the library is necessary to attain an even more insight. As can be seen in **Fig. 17**, additional scaffold changes in the head and tail group as well as the linker region are desirable.

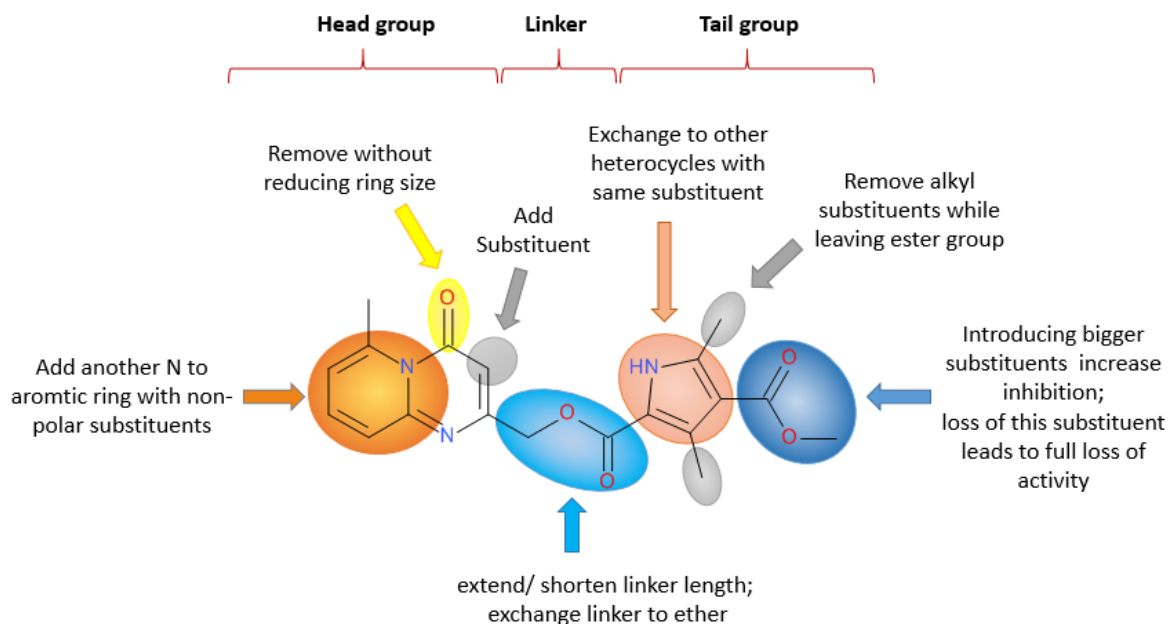


Fig. 17 Overview of additional SAR approaches for **C6**.

Further possible modifications include for example the introduction of an additional heteroatom into the scaffold to help enhance compound solubility. To extend the SAR

even more, the linker region needs to be explored further. An extension or shortening of its length as well as exchanging the ester for an ether linker could give a good insight into the length of the binding groove. Another idea would be to change the attachment site of the linker on either the head or the tail group. While the introduction of larger alkyl substituents on the tail group has been explored, the removal of the alkyl groups still needs to be investigated as well.

Furthermore, all active compounds identified in the alpha assay need to be tested for specificity. For this, the compounds need to be tested against other literature well-known protein-protein-interaction pairs.

Another important next step is the determination of cell toxicity of the identified inhibitors with the Incucyte® proliferation assay¹¹⁵. In general the active compounds ADMET properties (absorption, distribution, metabolism, excretion and toxicity) need to be evaluated to properly assess their potential of being developed into a drug.

The SAR evaluation of the compounds with the alpha assay alone has shown not to be robust enough. All compounds need to be additionally evaluated in a cell based assay to get a more comprehensive picture. A physiologically relevant system to test all compounds in would be the acute myeloid leukaemia cell line MOLM 14, which exhibits a FGF2-dependent chemoresistance towards FLT3 inhibitors¹¹⁸. These cells are also known to overexpress Tec Kinase which makes this system especially relevant to test the Tec Kinase-FGF2 interaction inhibitors with.

Another approach to enhance the inhibitor design would be the identification of the crucial amino acid residues involved in the interaction of FGF2 and Tec Kinase. These residues, so-called 'hot-spots', can give important information on the size of the interaction and so further direct the design efforts of the inhibitor. The identification of these amino acids involved can be achieved through 2-D-NMR analysis.

G Experimental Procedures Biochemistry

1 Alpha® assay

1.1 Protein constructs

1.1.1 His-FGF2Wt

N-terminal (His)₆-tagged FGF2Wt (His-FGF2WT) (stock prepared and kindly provided by Giuseppe La Venuta) is a fusion protein expressed in *E. Coli* according to standard procedures^{153,154}. It was purified on a Nickel affinity column (HiTrap FF, *GE Healthcare*) followed by a heparin affinity column (HiTrap Heparin HP, *GE Healthcare*), before the sample underwent a buffer exchange to the storage buffer of 20mM Tris-HCl, 150mM NaCl, 1mM DTT, 0.1% BSA by PD-10 column. The protein stock was then transformed into a 50% Glycerol solution for storage at -20°C.

1.1.2 GST- ΔN173Tec Kinase

Glutathione S-transferase (GST)-tagged Δ173Tec Kinase (GST-173Tec Kinase) (stock prepared and kindly provided by Giuseppe La Venuta) is a truncated version of human Tec Kinase fused at the N-terminus to a GST-tag. For the expression of this construct the Baculovirus expression system in SF9 insect cells was utilized. After PCR (polymerase chain reaction) amplification of the cDNA, the insert was fused into a pFBDM donor plasmid. Through utilisation of the DH10Bac *E. Coli* strain system (Max Efficiency® DH10Bac™ Competent Cells, Thermo Fisher Scientific) the insert was successfully transformed from the plasmid to the bacmid. This bacmid was then transfected into SF9 cells for expression and purification of the construct. The overexpressed GST-ΔN173Tec Kinase was purified by affinity chromatography on a glutathione affinity column (GSTrap™ FF, *GE Healthcare*). The protein sample was further purified and the buffer exchanged to the storage buffer of 20mM Tris-HCl, 150mM NaCl, 1mM DTT, 0.1% BSA by PD-10 column. This stock was then transformed into a 50% Glycerol stock for storage at -20°C.

¹⁵³ H. M. Müller, J. P. Steringer, S. Wegehingel, S. Bleicken, M. Münster, E. Dimou, S. Unger, G. Weidmann, H. Andreas, A. J. García-Sáez, K. Wild, I. Sinning, W. Nickel, *J. Biol. Chem.*, **2015**, 290, 8925–8937.

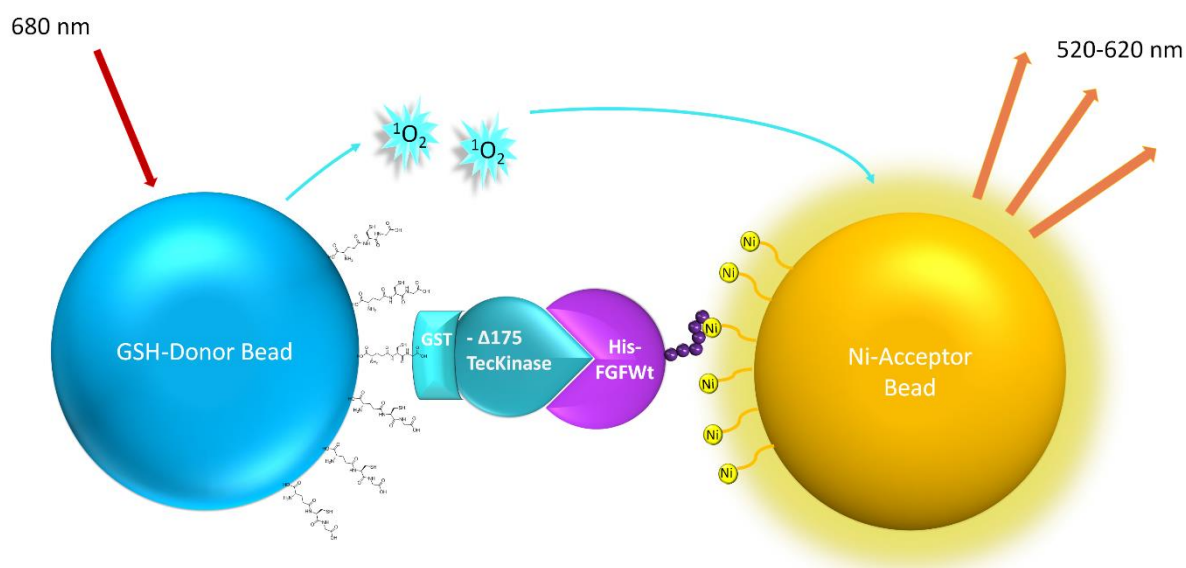
¹⁵⁴ J. P. Steringer, S. Bleicken, H. Andreas, S. Zacherl, M. Laussmann, K. Temmerman, F. X. Contreras, T. A. Bharat, J. Lechner, H. M. Müller, J. A. Briggs, A. J. García-Sáez, W. Nickel, *J. Biol. Chem.*, **2012**, 287, 27659–27669.

1.2 Compound stock solution preparation

All newly synthesised compounds were weighed into 1.5mL Eppendorf tubes on a Sartorius Cubis Analytical Balance and dissolved with the calculated amount needed of DMSO (Chemical grade, Sigma Aldrich) to give 10mM stock solutions. These solutions were heated to 40°C and sonicated to achieve full dissolution. Before using the stock solutions in the assay, they were heated to 40°C for 10 min, sonicated for 5 min before being heated for another 5 min at 40°C.

1.3 Principle of Alpha® assay

AlphaScreen® is a bead-based assay set-up to study biomolecular interactions. The acronym Alpha stands for Amplified luminescent proximity homogeneous assay. The interaction partners bound to beads lead to a luminescent/ fluorescent signal¹⁵⁵ (**Scheme 15**).



Scheme 15 Overview of Alpha® assay for the detection of interaction partners GST-ΔN173Tec Kinase and His-FGF2WT. GST-tagged Tec Kinase is bound through interaction with Glutathione to the donor bead and His-FGF2WT is bound to the Ni²⁺ coated acceptor bead. The interactions of these proteins leads to a luminescent/ fluorescent signal when an excitation with a 680nm laser occurs.

For this principle to work two types of beads are necessary: Donor- and Acceptor beads. Donor beads contain a photosensitizer, phthalocyanine that can excite ambient oxygen into a singlet state when illuminated by a 680nm light source. With the amount of

¹⁵⁵ Perkin Elmer Inc: *USER'S GUIDE TO ALPHA ASSAY PROTEIN:PROTEIN INTERACTIONS*; 2016 [cited Oct 14th 2020 from: <https://www.perkinelmer.com/PDFs/downloads/GDE-AlphaTech.pdf>]

photosensitizer per donor-bead, around 60 000 molecules of singlet oxygen can be generated per second leading to a significant amplification of the signal¹⁵⁶. Due to the approximate 4µs half-life of singlet oxygen, the possible diffusion in solution is limited to around 200nm. The reaction of singlet oxygen with a thioxene derivative on the acceptor bead leads to an energy transmission chain in the beads that ultimately leads to a light emission at 520nm-620nm. Through this proximity dependant energy transfer from one bead to the other and analysis of the intensity of the emitted light, calculation of the dissociation constant of the interaction can be determined. Additionally, inhibition of the interaction partners with e.g. small molecules can be identified and an IC₅₀ determined.

1.4 Alpha® Screen for IC₅₀ determination

The assay was set up in a 384 well-plate format testing the inhibition of the protein-protein interaction between His-FGF2WT and GST-Tec Kinase by the newly synthesised compounds.

	Contr.	200	66,7	22,2	7,41	2,47	0,82	0,27	0,09	0,03	0,01	0,003	200	66,7	22,2	7,41	2,47	0,82	0,27	0,09	0,03	0,01	0,003	BG			
	1	2	3	4	5	6	7	8	9	10	11	12	13	14	15	16	17	18	19	20	21	22	23	24			
A																										A	
B																											B
C																									Tec	C	
D																										D	
E																										E	
F																										F	
G																									F2	G	
H																										H	
I																										I	
J																										J	
K																									Beads	K	
L																										L	
M																										M	
N																										N	
O																										O	
P																										P	

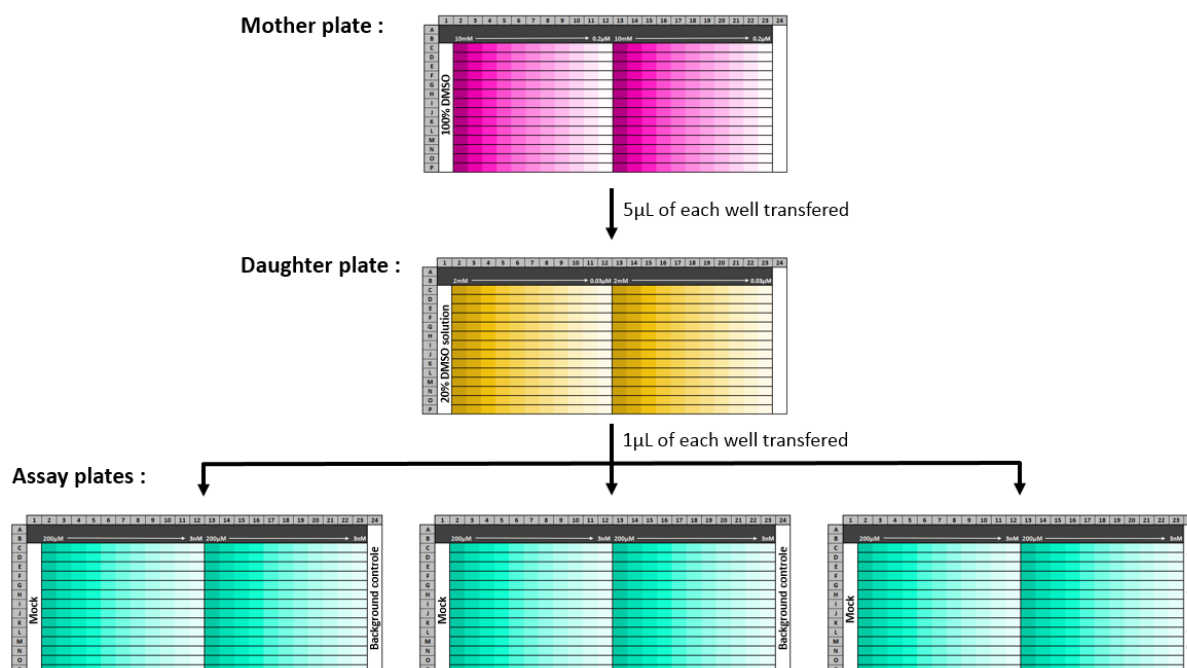
Fig. 18 384-well plate set up capable of testing 26 compounds (two per row of C-P one in light blue wells and one in dark blue wells); negative controls without any compound used to normalize data are in yellow marked wells; background of the single proteins and solely the beads are on the right side marked in column 24.

The compounds were tested in the range from 200µM to 3nM with each well containing 30nM GST-Tec Kinase and 125nM His-FGF2Wt in the presence of a bead mixture of 5µg/mL Nickel chelate acceptor beads (PerkinElmer®, cat n° 6760619C, AlphaScreen® Histidine Detection Kit (Nickel chelate)) and 5µg/mL Glutathione donor beads (PerkinElmer®, cat n° 6765300, AlphaScreen® Glutathione Donor Beads). The final buffer on the plate contains 25mM Tris-HCl (pH 7.4), 150mM NaCl, 1mM DTT,

¹⁵⁶ Peppard, J., et al, *J. Biomol. Screen*, **2003**, 8, 2, 149-156.

0.1% BSA, 0.05% Tween 20 and 2% DMSO. Each compound was tested in 2 replicates each with three technical replicates.

To prepare the compound dilution series, 10 mM compound stock solutions underwent a 10 step 1:3 dilution with DMSO (Sigma Aldrich) performed by PerkinElmer Janus Integrator pipetting robot in a 384 well plate (mother plate). 5 μ L of each dilution step is further diluted in a ratio of 1:5 with water in a new 384 well plate (daughter plate) with the PerkinElmer MultiPROBEII PLUS EX pipetting robot to give 20% DMSO solutions from 2mM to 0.1 μ M. 1 μ L of every well was transferred onto white low volume 384-well assay plates (PerkinElmer® catalog n° 6008280, ProxiPlate™-384 Plus, white, shallow 384-well, pinch bar design) (**Scheme 16**).



Scheme 16 Overview of compound dilution in the mother plate followed by the predilution into the daughter plate followed by the transfer into assay plates.

Once the compounds are on the plate, 4.5 μ L of a mixture of 2.22 fold concentrated GST-Tec Kinase (66.7nM) and His-FGF2Wt (277.8nM) in assay buffer 25mM Tris-HCl (pH 7.4), 150mM NaCl, 1mM DTT, 0.1% BSA, 0.05% Tween 20 were added to the plates by Multidrop™ Combi dispenser (Tube Dispensing Cassette, ThermoFisher Scientific®, article n°24073295) into columns 1-23. Pipetting of control wells was carried out manually. First 1 μ L of assay buffer containing 20% DMSO was added into wells, before 4.5 μ L of 2.22 fold concentrated separate protein solutions were added to their respective wells. Into the bead background wells, 4.5 μ L of assay buffer without DMSO is added. After incubation of the plates at RT for 75 min, 4.5 μ L of a 2.22 fold

concentrated bead mixture of Glutathione and Nickel chelate beads (11.1µg/mL each) are added to each well on the plate. The plates are sealed with adhesive aluminium foil for another incubation of 2 hours at RT. The plate signals were recorded on an Enspire Multimode Plate Reader (Perkin Elmer).

The data was first processed in Microsoft Excel for Windows (Microsoft Office 2016) as follows: all data points were corrected with the average of each protein background (average of protein backgrounds are subtracted by average of bead background) as well as the bead background. The average of the mock values of GST-Tec Kinase and His-FGF2WT (**Scheme 16**, assay plate column 1) was also background corrected. This value was set as 0% inhibition and used to normalize all compound containing wells on the plates.

The data was further analyzed, the graphs plotted and IC50 values for each compound determined in *GraphPad Prism 5 for Windows Version 5.01 Aug 2007* using the non-linear regression function “log(inhibitor) vs. response –variable slope (four parameters)”.

2 Compound Solubility Determination

Compound solubility in assay conditions was determined by measuring the light scattering of the compound solutions from 200µM to 3nM in the alpha assay buffer on a NEPHELOstar Nephelometer (BMG LABTECH).

The light from a laser diode (635nm) with a highly collimated beam passes through the sample. If the laser beam collides with particles, light is scattered and is detected by a photodiode. The light scattered is detected at angles of up to 80 degrees. The relationship between the concentration of the scattering particles and the scattered light intensity in solution is linear.¹⁵⁷

4µL of each compound dilution step was taken from the daughter plate of the alpha screen (**Scheme 16**) and diluted by 36µL of alpha assay buffer without DMSO (25mM Tris-HCl (pH 7.4), 150mM NaCl, 1mM DTT, 0.1% BSA, 0.05% Tween 20) into a 384-well black clear bottom polystyrene Microplate (Corning® Prod n° 3762). The plate was

¹⁵⁷ BMG LABTECH website [cited Oct 16th 2020]:
https://www.bmglabtech.com/fileadmin/06_Support/Download_Documents/Brochures/microplate-reader-nephelostar-plus-brochure.pdf

then covered and incubated at RT for 2.5h to mimic alpha assay incubation time before being measured.

The data was evaluated using Microsoft Excel for Windows (Microsoft Office 2016). The measured data values are plotted against the common logarithm of the concentration. Two linear lines are plotted through the data points connecting all points together. Their intersection point indicates the concentration of precipitation of the compound.

3 Cell surface biotinylation assay to quantify FGF2 secretion

The cell surface biotinylation assay is used to detect and quantify protein populations close to the cell surface. Since FGF2 binds to HSPG's on the cell surface after secretion, this method can be used to analyse the effect of small molecule inhibitors on FGF2 secretion.

CHO cell lines expressing FGF2-GFP Wt and C77/95A (as control cell line) in a doxycycline-dependent manner were used in the experiment. The cells were detached and washed with a trypsin-heparin supplemented PBS buffer (0.5mg/mL) to remove cell surface bound FGF2. Afterwards they were grown in 6-well plates for 2h at 37°C before being treated with the inhibitors (volume ca 1.5mL). The 10mM compound solutions in 100% DMSO were heated for 10min at 37°C, sonicated for 5min before again being heated at 37°C for additional 2-3min to ensure a homogenous compound solution. The cells were incubated (1.5mL) with a final concentration of 25µM of compound in 0.5% DMSO at 37°C. The mock and cell control samples are incubated in 0.5% DMSO. After 24h incubation in the presence of compounds, doxycycline (1µg/mL) was added to induce FGF2-GFP expression for 16h at 37°C. The cell confluence was noted (values normalized to confluence of mock sample) before the cells were washed twice with PBS buffer containing 1mM MgCl₂ and 0.1mM CaCl₂. Afterwards the cells were incubated at 4°C for 30 min with 600µL *incubation buffer* (10mM Triethanolamine (pH 9.0), 150mM NaCl, 2mM CaCl₂) containing 1mg/mL cell impermeable biotinylation reagent (EZ-Link Sulfo-NHS-SS-Biotin², #21331, Pierce) and slowly shaken. Subsequently the cells were washed with 1mL of *quenching buffer* (PBS with 1mM MgCl₂, 0.1mM CaCl₂) containing 100mM glycine at 4°C for 20min to quench surplus biotinylation reagent. To remove any residual biotin the cells were

washed twice with PBS buffer before being treated with 300 μ L *lysis buffer* (50mM Tris-HCl pH 7.5, 62.5mM EDTA pH 8.0, 0.4% deoxycholate with 1% Nonidet P-40 protease inhibitor (Roche applied Science) at 37°C for 10 min. The cells were transferred to a 1.5ml Eppendorf tube, they were sonicated for 3 min and further incubated for 15min at RT. All samples were vortexed every 5mins to solubilize proteins. To remove the solid cell debris, the samples were centrifuged at 13 000rpm at 4°C for 10min. 15 μ L of the supernatant was removed and mixed with 15 μ L of 4xSDS sample buffer for the total input sample. The rest of the supernatant (ca. 270 μ L) was mixed with 20 μ L streptavidin beads (UltraLink immobilized streptavidin, #53114, Pierce), pre-washed with twice 300 μ L *lysis buffer* (centrifuged at 3000g for 1 min between each wash step) and incubated for 1h at RT. The beads were centrifuged down (3000g at 4°C 1min) and washed once with *wash buffer I* (50mM Tris-HCl pH 7.5, 500mM NaCl, 62.5mM EDTA pH 8.0, 0.4% deoxycholate with 1% Nonidet P-40 protease inhibitor (Roche Applied Science)) and twice with *wash buffer II* (50mM Tris-HCl pH 7.5, 500mM NaCl, 62.5mM EDTA pH 8.0, 0.4% deoxycholate with 0.1% Nonidet P-40 protease inhibitor (Roche Applied Science)) (centrifuged at 3000g for 1 min between each wash step). To elute the bead bound material, the beads were incubated at 95°C for 10 min in 40 μ L SDS sample buffer.

Total input samples (“cells”, 10 μ L of 30 μ L sample; 1.5%) and surface sample (10 μ L of 40 μ L elution, 25%) were both resolved with SDS-gel and transferred to Western blot membranes. FGF2-GFP was detected by primary polyclonal anti-FGF2 antibody (rabbit anti FGF2 full length, Pineda) coupled to fluorescent secondary antibody (goat anti rabbit IRDye® 800CW, #926-32211, Li-Cor Biosciences). GAPDH was visualized with monoclonal anti-GAPDH antibody (Lifetech-Ambion) coupled to fluorescent secondary antibody (goat anti-mouse IgG (H+L), Alexa Fluor® 680 conjugate, #A-21057, Life Technologies). FGF2-GFP and GAPDH band intensities were evaluated by using LI-COR Odyssey imaging system.

For each compound, a minimum of four independent experiments were conducted, except for compound **11** with three replicates. The FGF2 surface signal was normalized to the corresponding FGF2 signal of the total cell lysate to give the secreted FGF2-GFP fraction. The average of the mock treated FGF2-GFP secretion fraction was set to 100% and the secretion levels for compounds determined by normalizing to the mock.

H Experimental Procedures Chemistry

1 Chemicals and Analytical Methods

1.1 Chemicals

All chemicals used during syntheses in this thesis were bought commercially from Sigma, TCI Belgium, ABCR, Fluorochem, or Enamine and used without further purification. The solvents were used without further distillation and were purchased from Sigma or VWR.

1.2 NMR

NMR spectra were measured on a 400MHz Bruker Ultra Shield™ spectrometer at room temperature. Samples were measured in deuterated solvents purchased from DEUTERO GmbH. Chemical shifts (δ) were calibrated to the solvent peak as published in G.M Fulmer *et al.*¹⁵⁸ and are given in ppm. Signal multiplets are described with the following descriptors: doublet (d), triplet (t), quartet (q), qu (quintet), hept (heptet) and multiplet (m). Assignments of peaks in ¹H and ¹³C spectra for each compound was determined by COSY, HSQC, HMBC and APT spectra and formatted as follows: δ (multiplicity, coupling values (when present), number of protons, assignment).

1.3 Biotage

Purification of compounds was performed on a Biotage Isolera Four Flash Chromatography system with either 10g, 25g, 50g or 100g Biotage KP-Sil cartridges with their corresponding snaplets (1g, 3g, 10g) for dry-loading of crude materials. Purification was performed with either heptane/EtOAc, cyclohexane/EtOAc or DCM/MeOH with appropriate gradients, determined by TLC.

1.4 TLC

Thin-layer chromatography (TLC) was run on Merck aluminium plates coated with Merck 60 F254 silica. Analysis of the plates was done by UV (254nm) or staining with acidic ethanolic KMnO₄ solution, acidic anisaldehyde solution, ethanolic phosphomolybdic acid or ninhydrin solution before heating to 200-300°C.

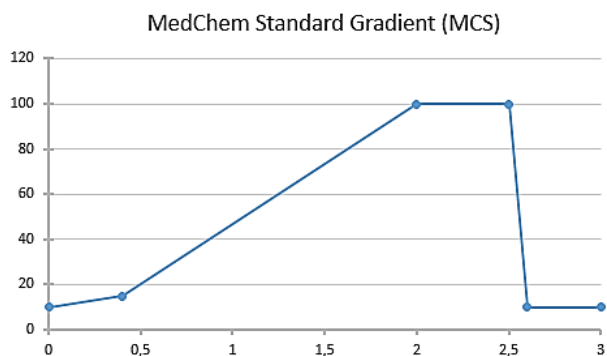
¹⁵⁸ G. R. Fulmer, A. J. M. Miller, N. H. Sherden, H. E. Gottlieb, A. Nudelman, B. M. Stoltz, J. E. Bercaw, K. I. Goldberg, *Organometallics* **2010**, *29*, 2176–2179.

1.5 HPLC

For preparative HPLC an Agilent Infinity 1260 HPLC system was utilized with a C18-column (XBridge Prep C18 5 μ m OBD 19 x 150 mm) and a flow rate of 25ml/ min. An ACN/H₂O gradient with 0.1% TFA was used for purification.

1.6 UHPLC-MS

Compound analysis and reaction controls were performed on an Agilent Infinity 1290 UHPLC-MS system. The analysis was run on an Acquity UHPLC BEH C18 column (1.7 μ m, 2.5 x 50mm) at 40°C and with ACN/H₂O as solvents containing 0.1% TFA. The recorded mass spectra were determined by single quadrupole electrospray ionization. Gradients used during analysis are as follows:



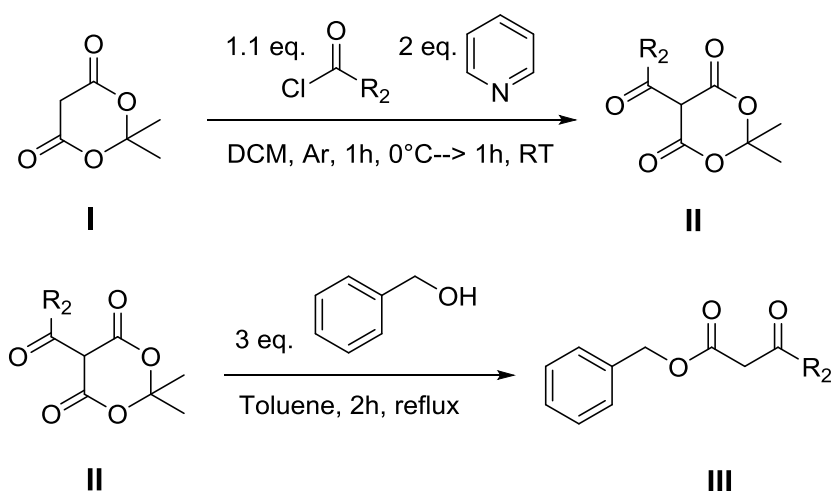
2 Syntheses

2.1 General procedures

2.1.1 General procedure A (Suzuki Cross Coupling Reaction)

An aryl halide (1eq), the boronic acid (1.5eq), K_3PO_4 or KF (3eq), Pd(OAc) and PCy_3 were weighed into a Radleys tube. The tube was evacuated and flushed three times with Ar before degassed toluene and water were added. The solution was heated to $100^\circ C$ while stirring for the indicated amount of time. Monitoring of the reaction progress was done by TLC or UHPLC-MS. The reaction was cooled to RT and the solution filtered through a pad of Celite before water was added to the filtrate and the aqueous solution extracted three times with DCM. The combined organic phases were dried with anh. $NaSO_4$, filtered and the solvent evaporated *in vacuo*. Purification of the product was done by silica gel chromatography with the indicated solvent system. The product was analyzed by NMR and UHPLC-MS.

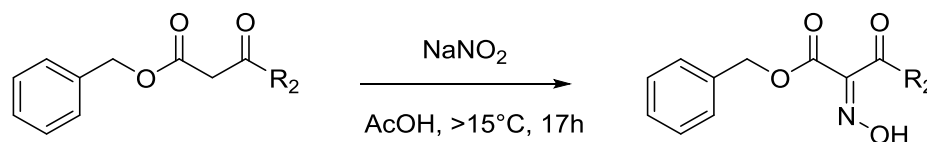
2.1.2 General Procedure B (Pyrrole Synthesis Step I+II)



2,2-dimethyl-1,3-dioxane-4,6-dione (I) (1eq) was dissolved in anhydrous DCM under Argon and the solution cooled to $0^\circ C$ before pyridine (2eq) was added slowly. The indicated acid chloride (1.1eq) was added dropwise to the reaction mixture. After 30 min, the ice bath was removed and the solution stirred for another 30 min. The solvent was removed *in vacuo* and the residue (II) suspended in toluene before benzyl alcohol (3eq) was added. The reaction mixture was heated to $70^\circ C$. Monitoring of the reaction was done by TLC or UHPLC-MS. After the reaction was complete the solution was

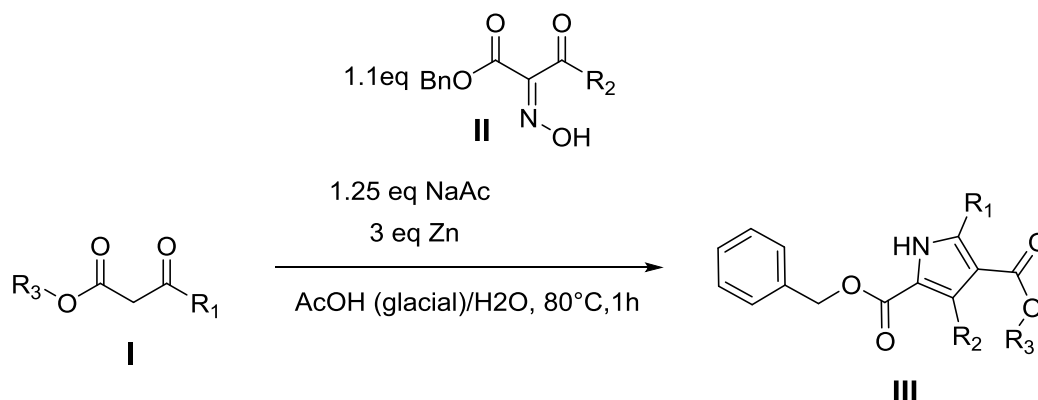
cooled to RT and the solvent evaporated. Purification of the crude was performed by silica chromatography and the product (III) analyzed by NMR and UHPLC-MS.

2.1.3 General Procedure C (Pyrrole Synthesis Step III)



The educt (1eq) was dissolved in a glacial acetic acid/water mixture (9:1) and the solution cooled to 0°C before NaNO₂ (1.5eq) dissolved in water was added dropwise while stirring. The reaction was stirred at 0°C for 1h before cooling was removed and stirring continued overnight at RT. The reaction mixture was diluted with water and the aqueous phase was extracted 3x with DCM. The combined organic phases were washed with sat. NaHCO₃ solution, water and brine, before being dried with anh. Na₂SO₄, followed by filtration and removal of the solvent *in vacuo*. The crude products were analyzed with NMR and used without further purification.

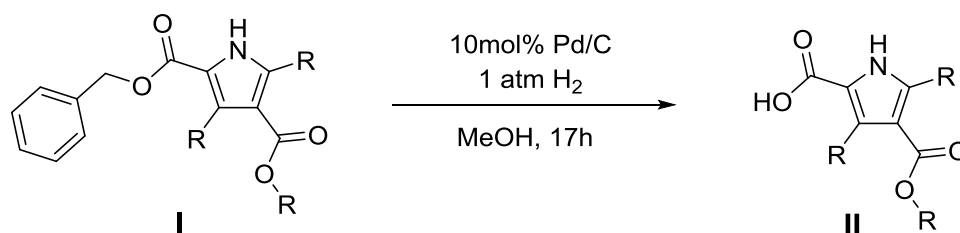
2.1.4 General Procedure D (Pyrrole Synthesis Step IV: Ring closure)



Reagent (I) (1eq) was dissolved in 4mL glacial acetic acid before sodium acetate (1.25eq) dissolved in 3mL H₂O was added. The reaction mixture was heated to 75°C while stirring. Reagent (II) (1.1eq) was dissolved in glacial acetic acid/ water (1:1) and this solution was added portionwise to the reaction mixture in turn with Zn (3eq). The reaction solution was stirred for 1h at 75°C, before the hot solution was filtered and the filtrate added to ice water. The cold aq. phase was extracted with three times DCM. The combined organic phases were washed with sat. NaHCO₃ solution, water and

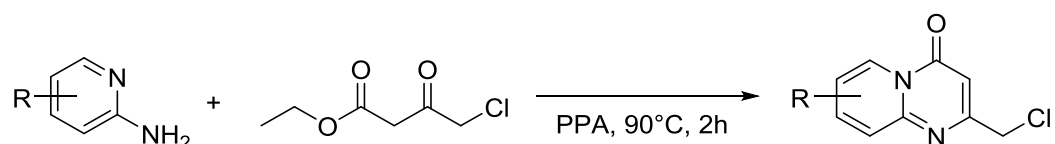
brine, before being dried with $\text{anh. Na}_2\text{SO}_4$, filtered and the solvent removed *in vacuo*. The crude was purified with silica column chromatography and the product analyzed with NMR and UHPLC-MS.

2.1.5 General Procedure E (Pyrrole Synthesis Step V: Removal of benzyl protecting group by hydrogenation)



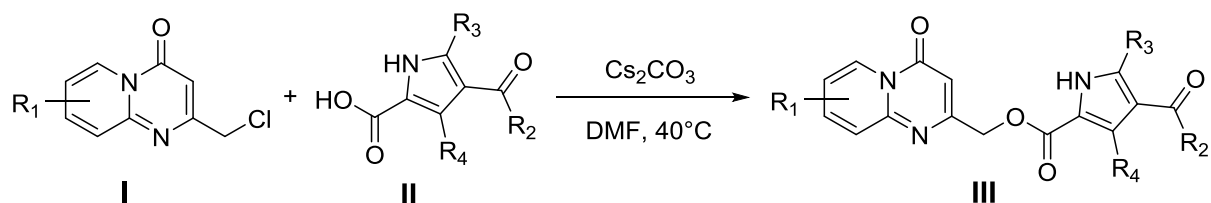
I (1eq) was dissolved in MeOH before Pd/C (10mol%) catalyst was added. The flask was put under H_2 -atmosphere and stirred at RT overnight. After the reaction was complete, monitored by TLC, the reaction solution was filtered through a pad of Celite and the solvent evaporated. The crude product was analyzed by NMR and UHPLC-MS and used without any further purification in the following reaction step.

2.1.6 General procedure F (Pyridopyrimidone head group synthesis)



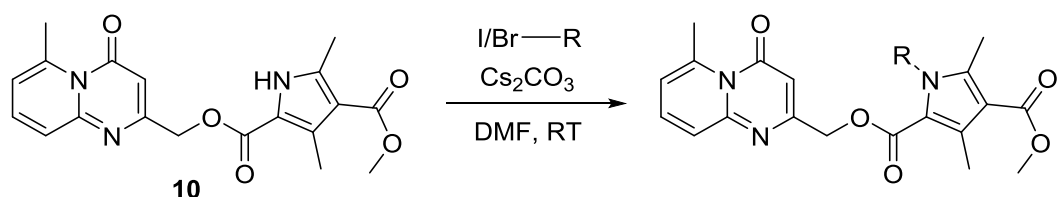
2-amino-pyridine (1eq) and ethyl 4-chloro-3-oxobutanoate (1.1eq) were put into a Radley tube before PPA was added and the mixture slowly heated to 90°C while stirring. The reaction was stirred for 2-3h during which a colour change of the reaction mixture from light yellow to dark brown occurred. The reaction was cooled and quenched with water. The aqueous phase was extracted three times with DCM. The combined organic phases were washed with sat. NaHCO_3 solution, water and brine, before being dried with $\text{anh. Na}_2\text{SO}_4$, filtered and the solvent removed *in vacuo*. Purification of the product was performed by column chromatography on silica. The isolated product was analyzed with UHPLC-MS, NMR and HR-MS.

2.1.7 General procedure G (Alkylation of pyrrole carboxylic acid)



Compound (I), pyrrole-compound (II) and Cs_2CO_3 were dissolved in DMF before heating to 40°C . The reaction progression was monitored by UHPLC-MS. After the reaction was finished, the solvent was removed *in vacuo* and the residue dissolved in water. The aqueous phase was extracted three times with DCM and the combined organic phases dried with anh. NaSO_4 , followed by filtration and removal of the solvent *in vacuo*. The product was purified by silica column chromatography with the indicated solvent system determined by TLC. Analysis of the product (III) was done by NMR and UHPLC-MS.

2.1.8 General procedure H (Pyrrole N-alkylation)



10 (1eq) and Cs_2CO_3 (3eq) were dissolved in 4mL DMF, before the alkyl/benzyl halide (1.5eq) was added. The reaction was stirred at RT and monitored by UHPLC-MS until the reaction was complete. Solvent was removed *in vacuo* and the residue dissolved in 15mL water. The aqueous phase was extracted three times with 20mL DCM. The combined organic phases were dried with anh. NaSO_4 , filtered and the solvent evaporated *in vacuo*. The product was purified by column chromatography on SiO_2 and the isolated product was analyzed by NMR and UHPLC-MS.

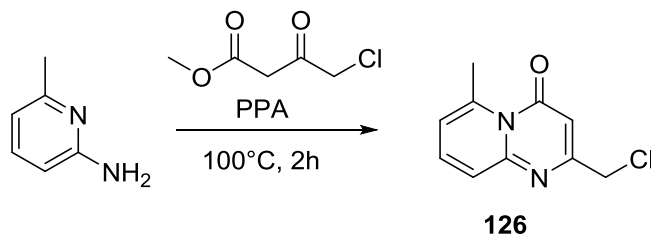
2.2 Syntheses of head group modified compounds

2.2.1 Substituent modification on head group

2.2.1.1 Syntheses of modified 2-(chloromethyl)-4H-pyrido[1,2-a]-4-pyrimidones

All reactions described in this section follow **General Procedure F**.

2-(chloromethyl)-6-methyl-4H-pyrido[1,2-a]pyrimidin-4-one (126)



350mg of 2-Amino-6-methylpyridine (3.23mmol, 1eq), 415 μ L methyl 4-chloro-3-oxobutanoate (4.07mmol; 1eq) and 5g of PPA were heated to 95°C for 2h with stirring. After work up and purification with 25g SiO₂ with a gradient of 15-100% of Heptane/EtOAc, the product was isolated as a white solid in 56% yield.

R_f (TLC, hept/EtOAc 1:1) = 0.34

¹H-NMR (400 MHz, CDCl₃):

δ = 7.45 (dd, *J* = 8.8, 7.0 Hz, 1H, 8-H_{arom}), 7.37 (d, *J* = 8.8 Hz, 1H, 9-H_{arom}), 6.66 (d, *J* = 6.7 Hz, 1H, 7-H_{arom}), 6.42 (s, 1H, C=OCH), 4.42 (s, 2H, CH₂Cl), 3.02 (s, 3H, 6-CH₃).

¹³C-NMR (400 MHz, CDCl₃):

δ = 162.33 (1C, C=OCH), 160.73 (1C, C_{q, arom}), 153.76 (1C, C_{q, arom}), 144.21 (1C, C_{q, arom}), 135.78 (1C, 8-CH_{arom}), 125.16 (1C, 9-CH_{arom}), 118.56 (1C, 7-CH_{arom}), 105.13 (1C, 3-CH_{arom}), 45.33 (1C, CH₂Cl), 24.77 (1C, CH₃).

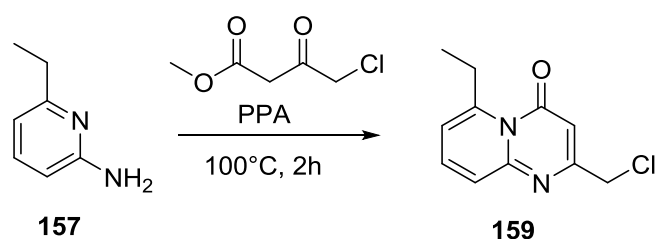
UHPLC-MS

R_t (MCS): 0.398 min

m/z: [M+H]⁺ (calc.) = 209.0

[M+H]⁺ (meas.) = 209.0

2-(chloromethyl)-6-ethyl-4H-pyrido[1,2-a]pyrimidin-4-one (159)



30mg of 2-amino-6-ethyl pyridine (0.25mmol, 1eq), 47 μ L methyl 4-chloro-3-oxobutanoate (0.37mmol, 1.5eq) and 2g of PPA were heated to 95°C for 2h. After aq. work up and purification with 10g SiO₂ with a gradient of cyclohexane/EtOAc 5% \rightarrow 50%, the product was isolated as a white solid in 59% yield (24.3mg, 0.11mmol).

R_f (TLC, hept/EtOAc 1:1) = 0.48

¹H-NMR (400 MHz, CDCl₃):

δ = 7.50 (dd, J = 8.9, 6.9 Hz, 1H, 8-H_{arom}), 7.40 (dd, J = 8.9, 1.3 Hz, 1H, 9-H_{arom}), 6.76 (d, J = 6.9 Hz, 1H, 7-H_{arom}), 6.48 (s, 1H, CHC=O), 4.44 (s, 2H, CH₂Cl), 3.50 (q, J = 7.3 Hz, 2H, CH₂CH₃), 1.28 (t, J = 7.3 Hz, 3H, CH₂CH₃).

¹³C-NMR (100 MHz, CDCl₃):

δ = 161.93 (1C, C=O), 160.38 (1C, C_{q, arom}), 153.80 (1C, C_{q, arom}), 150.00 (1C, C_{q, arom}), 135.94 (1C, 8-CH_{arom}), 125.22 (1C, 9-CH_{arom}), 117.37 (1C, 7-CH_{arom}), 105.28 (1C, CHC=O), 45.25 (1C, CH₂Cl), 29.91 (1C, CH₂CH₃), 15.29 (1C, CH₂CH₃).

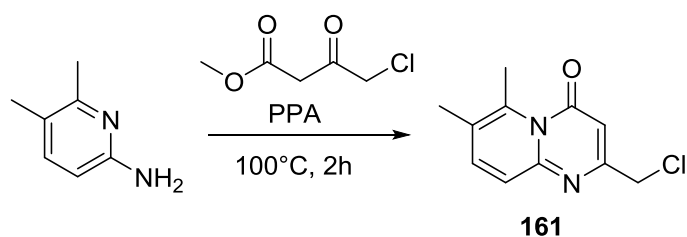
UHPLC-MS

R_t (MCS): 0.473 min

m/z: [M+H]⁺ (calc.) = 223.1

[M+H]⁺ (meas.) = 223.0

2-(chloromethyl)-6,7-dimethyl-4H-pyrido[1,2-a]pyrimidin-4-one (161)



200mg of 2-amino-5,6-dimethyl-pyridine (1.56mmol, 1eq), 219 μ L methyl 4-chloro-3-oxobutanoate (1.71mmol, 1.1eq) and 5g of PPA were heated to 95°C for 2h. After aq. work up and purification with 25g SiO₂ with a gradient of heptane/EtOAc 10% \rightarrow 60%, the product **161** was isolated as a light brown solid in 60% yield (207mg, 0.93mmol).

R_f (TLC, hept/EtOAc 6:4) = 0.19.

¹H-NMR (400 MHz, CDCl₃):

δ = 7.41 (d, J = 9.0 Hz, 1H, CH_{arom}), 7.30 (d, J = 9.0 Hz, 1H, CH_{arom}), 6.43 (s, 1H, COCH), 4.42 (s, 2H, CH₂), 2.81 (s, 3H, CH₃), 2.30 (s, 3H, CH₃).

¹³C-NMR (100 MHz, CDCl₃):

δ = 162.56 (1C, C=OCH), 160.40 (1C, C_{q, arom}), 152.77 (1C, C_{q, arom}), 140.58 (1C, C_{q, arom}), 139.66 (1C, 8-CH_{arom}), 125.23 (1C, C_{q, arom}), 123.72 (1C, 9-CH_{arom}), 104.76 (1C, 3-CH_{arom}), 45.39 (1C, C=OCH), 19.85 (1C, 6-CH₃), 19.19 (1C, 7-CH₃).

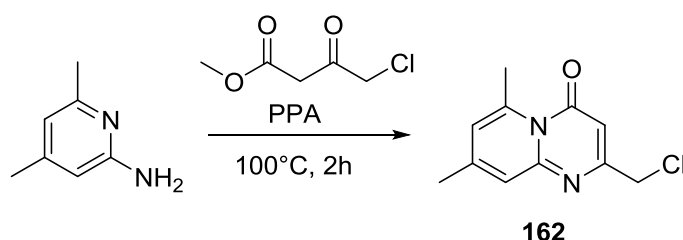
UHPLC-MS

R_t (MCS): 0.994 min

m/z: [M+H]⁺ (calc.) = 223.1

[M+H]⁺ (meas.) = 223.0

2-(chloromethyl)-6,8-dimethyl-4H-pyrido[1,2-a]pyrimidin-4-one (162)



150mg of 2-amino-4,6-dimethyl-pyridine (1.23mmol, 1eq), 182 μ L methyl 4-chloro-3-oxobutanoate (1.35mmol, 1.1eq) and 4g of PPA were heated to 95°C for 2h. After aq. work up and purification with 10g SiO₂ with a gradient of heptane/EtOAc 10% \rightarrow 80%, the product was isolated as a light brown solid in 18% yield (50.4mg, 0.23mmol).

R_f (TLC, hept/EtOAc 1:1) = 0.08.

¹H-NMR (400 MHz, CDCl₃):

δ = 7.20 (s, 1H, 9-H_{arom}), 6.53 (s, 1H, 7-H_{arom}), 6.37 (s, 1H, CHC=O), 4.41 (s, 2H, CH₂Cl), 3.01 (s, 3H, 8-CH₃), 2.34 (s, 3H, 6-CH₃).

¹³C-NMR (100 MHz, CDCl₃):

δ = 162.35 (1C, C=O), 160.82 (1C, C_{q, arom}), 153.74 (1C, C_{q, arom}), 147.94 (1C, C_{q, arom}), 143.42 (1C, C_{q, arom}), 123.21 (1C, 9-CH_{arom}), 121.50 (1C, 7-CH_{arom}), 104.21 (1C, CHC=O), 45.32 (1C, CH₂Cl), 24.66 (1C, 8-CH₃), 21.11 (1C, 6-CH₃).

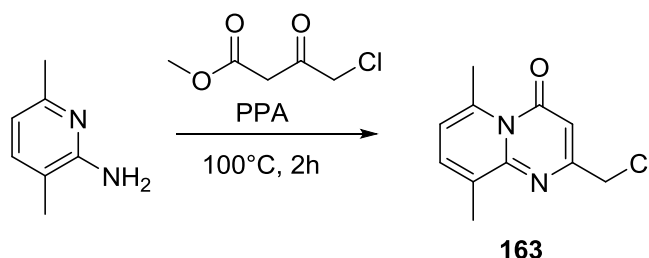
UHPLC-MS

R_t (MCS): 0.283 min

m/z: [M+H]⁺ (calc.) = 223.1

[M+H]⁺ (meas.) = 223.2

2-(chloromethyl)-6,9-dimethyl-4H-pyrido[1,2-a]pyrimidin-4-one (163)



200mg of 2-amino-3,6-dimethyl-pyridine (1.64mmol, 1eq), 231 μ L methyl 4-chloro-3-oxobutanoate (1.80mmol, 1.1eq) and 5g of PPA were heated to 100°C for 2h. After aq. work up and purification with 10g SiO₂ with a gradient of heptane/EtOAc 10% \rightarrow 80%, the product was isolated as a light brown solid in 80% yield (291mg, 1.31mmol).

R_f (TLC, hept/EtOAc 3:2) = 0.40.

¹H-NMR (400 MHz, CDCl₃):

δ = 7.31 (d, J = 7.1 Hz, 1H, H_{arom}), 6.57 (d, J = 7.1 Hz, 1H, H_{arom}), 6.46 (s, 1H, C=OCH), 4.45 (s, 2H, CH₂Cl), 2.97 (s, 3H, CH₃), 2.43 (s, 3H, CH₃).

^{13}C -NMR (100 MHz, CDCl_3):

δ = 162.95 (1C, C=O), 160.13 (1C, $\text{C}_{\text{q,arom}}$), 152.94 (1C, $\text{C}_{\text{q,arom}}$), 141.63 (1C, $\text{C}_{\text{q,arom}}$), 134.48 (1C, 8- CH_{arom}), 133.03 (1C, $\text{C}_{\text{q,arom}}$), 117.91 (1C, 7- CH_{arom}), 104.91 (1C, $\underline{\text{C}}\text{HC=O}$), 45.62 (1C, CH_2Cl), 24.63 (1C, 6- CH_3), 18.75 (1C, 9- CH_3).

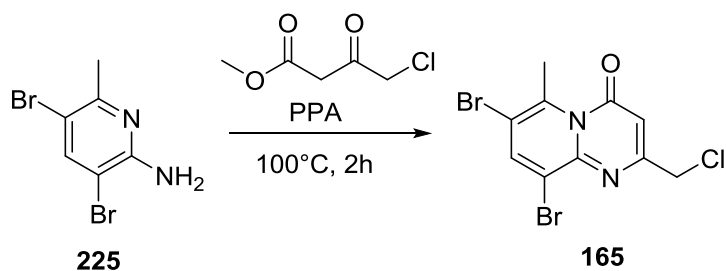
UHPLC-MS

R_t (MCS): 1.672 min

m/z: $[\text{M}+\text{H}]^+$ (calc.) = 223.1

$[\text{M}+\text{H}]^+$ (meas.) = 223.0

[7,9-dibromo-2-\(chloromethyl\)-6-methyl-4H-pyrido\[1,2-a\]pyrimidin-4-one \(165\)](#)



150mg of **225** (0.56mmol, 1eq), 83 μL methyl 4-chloro-3-oxobutanoate (0.62mmol, 1.1eq) and 4g of PPA were heated to 100°C for 2h. After aq. work up and purification with 10g SiO_2 with a gradient of heptane/EtOAc 10% \rightarrow 80%, the product was isolated as a light brown solid in 15% yield (30mg, 0.08mmol).

R_f (TLC, hept/EtOAc 1:1) = 0.45.

^1H -NMR (400 MHz, CDCl_3):

δ = 8.05 (s, 1H, 5- H_{arom}), 6.60 (s, 1H, 3- H_{arom}), 4.51 (s, 2H, CH_2), 2.92 (s, 3H, CH_3).

^{13}C -NMR analysis not possible due to compound instability.

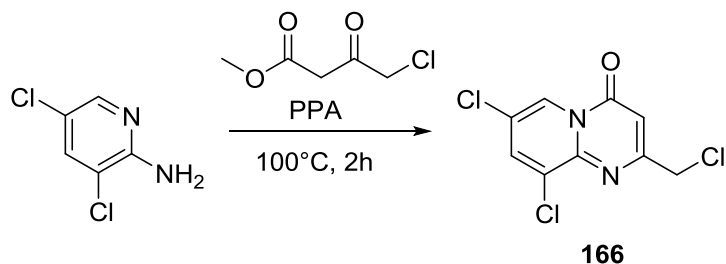
UHPLC-MS

R_t (MCS): 1.557 min

m/z: $[\text{M}+\text{H}]^+$ (calc.) = 364.9, 366.9

$[\text{M}+\text{H}]^+$ (meas.) = 364.9, 366.9

7,9-dichloro-2-(chloromethyl)-4H-pyrido[1,2-a]pyrimidin-4-one (166)



400mg of 2-amino-3,5-dichloro-pyridine (2.45mmol, 1eq), 347 μ L methyl 4-chloro-3-oxobutanoate (2.70mmol, 1.1eq) and 5g of PPA were heated to 100°C for 2h. After aq. work up and purification with 10g SiO₂ with a gradient of DCM/MeOH 1% \rightarrow 5% the product was isolated as a white solid in 16% yield (101.6mg, 0.39mmol).

R_f (TLC, DCM7/MeOH 2%) = 0.10.

¹H-NMR (400 MHz, MeOD-*d*₄):

δ = 8.54 (d, J = 2.0 Hz, 1H, 6-H_{arom}), 8.20 (d, J = 2.1 Hz, 1H, 8-H_{arom}), 6.88 (s, 1H, 3-H_{arom}), 5.11 (s, 2H, CH₂Cl).

¹³C-NMR (400 MHz, MeOD-*d*₄):

δ = 170.37(1C, C=O), 150.43 (1C, C_{q, arom}), 147.98 (1C, C_{q, arom}), 138.47 (1C, 8-CH_{arom}), 130.59 (1C, C_{q, arom}), 128.42 (1C, 6-CH_{arom}), 121.71 (1C, C_{q, arom}), 117.88 (1C, C_{q, arom}), 41.38 (1C, CH₂Cl).

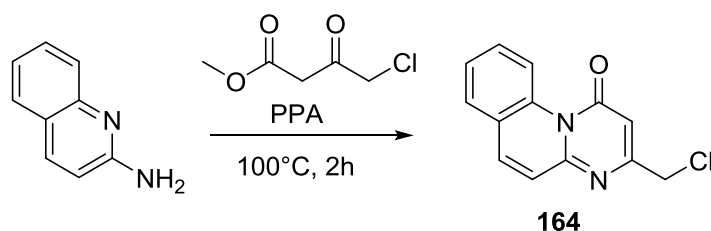
UHPLC-MS

R_t (MCS): 0.673min

m/z: [M+H]⁺ (calc.) = 263.0, 265.0.

[M+H]⁺ (meas.) = 263.0, 265.0.

3-(chloromethyl)-1H-pyrimido[1,2-a]quinolin-1-one (164)



150mg of 2-aminoquinoline (1.04mmol, 1eq), 154 μ L methyl 4-chloro-3-oxobutanoate (1.14mmol, 1.1eq) and 3g of PPA were heated to 100°C for 2h. After aq. work up and purification with 10g SiO₂ with a gradient of heptane/EtOAc 10% \rightarrow 60%, the product was isolated as light brown solid in 38% yield (98mg, 0.40mmol).

R_f (TLC, hept/EtOAc 1:1) = 0.47.

¹H-NMR (400 MHz, CDCl₃):

δ = 9.84 (d, J = 8.9 Hz, 1H, H_{arom}), 7.81 (d, J = 9.3 Hz, 1H, H_{arom}), 7.74-7.62 (m, 2H, H_{arom}), 7.56 (t, J = 7.4 Hz, 1H, H_{arom}), 7.32 (d, J = 9.3 Hz, 1H, H_{arom}), 6.72 (s, 1H, C=OCH), 4.49 (s, 2H, CH₂Cl).

¹³C-NMR (100 MHz, CDCl₃):

δ = 163.16 (1C, C=OCH), 158.67 (1C, C_{q,arom}), 151.69 (1C, C_{q,arom}), 137.91 (1C, CH_{arom}), 135.32 (1C, C_{q,arom}), 130.37 (1C, CH_{arom}), 128.51 (1C, CH_{arom}), 127.50 (1C, CH_{arom}), 125.06 (1C, C_{q,arom}), 123.70 (1C, CH_{arom}), 122.32 (1C, CH_{arom}), 108.89 (1C, C=OCH), 44.58 (1C, CH₂Cl).

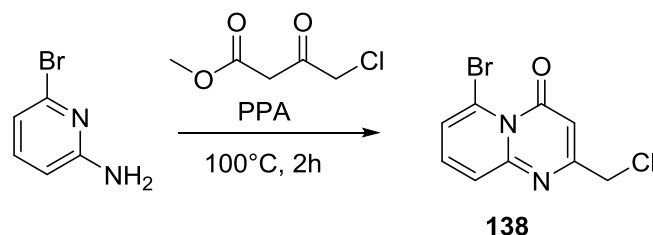
UHPLC-MS

R_t (MCS): 1.266 min

m/z: [M+H]⁺ (calc.) = 244.0

[M+H]⁺ (meas.) = 245.0

6-bromo-2-(chloromethyl)-4H-pyrido[1,2-a]pyrimidin-4-one (138) (AM06-10)



700mg of 2-amino-6-bromo-pyridine (4.05mmol, 1eq), 572μL methyl 4-chloro-3-oxobutanoate (4.45mmol, 1.1eq) and 4g of PPA were heated to 95°C for 2h. After aq. work up and purification with 25g SiO₂ with a gradient of cyclohexane/EtOAc 15% → 100%, the product **138** was isolated as a white solid in 91% yield (770mg, 3.69mmol).

R_f (TLC, hept/EtOAc 1:1) = 0.43

¹H-NMR (400 MHz, CD₃OD):

δ = 7.65 (dd, *J* = 8.8, 7.3 Hz, 1H, 8-H_{arom}), 7.56 (d, *J* = 8.4 Hz, 1H, 7-H_{arom}), 7.52 (d, *J* = 7.2 Hz, 1H, 9-H_{arom}), 6.56 (s, 1H, C=OCH), 4.56 (s, 2H, CH₂).

¹³C-NMR (100 MHz, CD₃OD):

δ = 161.13 (1C, C=O), 154.96 (1C, C_q, arom), 153.94 (1C, C_q, arom), 138.71 (1C, 8-CH_{arom}), 127.14 (1C, 7-CH_{arom}), 125.77 (1C, 9-CH_{arom}), 119.68 (1C, C_q, arom), 105.27 (1C, C=OCH), 45.00 (1C, CH₂Cl).

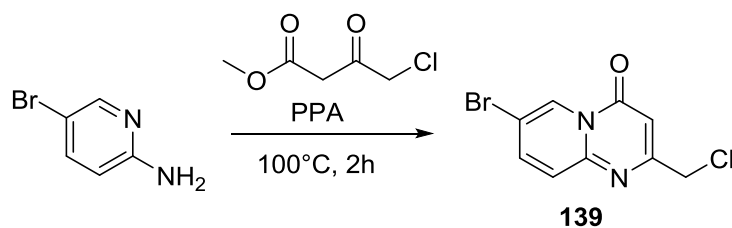
UHPLC-MS

R_t (MCS): 1.193 min

m/z: [M+H]⁺ (calc.) = 272.9; 274.9

[M+H]⁺ (meas.) = 273.0, 275.0

7-bromo-2-(chloromethyl)-4H-pyrido[1,2-a]pyrimidin-4-one (139)



500mg of 2-amino-5-bromo-pyridine (1.89mmol, 1eq), 430 μ L methyl 4-chloro-3-oxobutanoate (3.18mmol, 1.1eq) and 5g of PPA were heated to 100°C for 2h. After aq. work up and purification with 25g SiO₂ with a gradient of DCM/MeOH 0% \rightarrow 3%, the product **139** was isolated as a light brown solid in 87% yield (689mg, 2.52mmol).

R_f (TLC, DCM/MeOH 2%) = 0.62.

¹H-NMR (400 MHz, CDCl₃):

δ = 9.17 (d, *J* = 2.1 Hz, 1H, 6-H_{arom}), 7.80 (dd, *J* = 9.4, 2.2 Hz, 1H, 8-H_{arom}), 7.53 (d, *J* = 9.4 Hz, 1H, 9-H_{arom}), 6.68 (s, 1H, C=OCH), 4.51 (s, 1H, CH₂Cl)

¹³C-NMR (100 MHz, CDCl₃):

δ = 162.54 (1C, C=O), 157.22 (1C, C_{q,arom}), 149.69 (1C, C_{q,arom}), 140.25 (1C, 8-CH_{arom}), 127.62 (1C, 9-CH_{arom}), 127.38 (1C, 6-CH_{arom}), 111.20 (1C, C_{q,arom}), 103.60 (1C, CHC=O), 45.72 (1C, CH₂Cl).

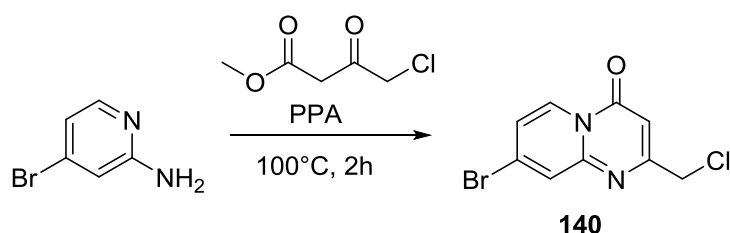
UHPLC-MS

R_t (MCS): 0.846 min

m/z: [M+H]⁺ (calc.) = 272.9; 274.9

[M+H]⁺ (meas.) = 273.0, 275.0

[8-bromo-2-\(chloromethyl\)-4H-pyrido\[1,2-a\]pyrimidin-4-one \(140\)](#)



505 mg 2-amino-4-bromo-pyridine (2.92mmol, 1eq), 412.5 μ L methyl 4-chloro-3-oxobutanoate (3.21mmol, 1.1eq) and 5g of PPA were heated to 100°C for 2h. After aq. work up and purification with 10g SiO₂ with a solvent gradient of cyclohex/EtOAc 10% \rightarrow 30%, the product was isolated as a white solid in 31% yield (248.9mg, 0.91mmol).

R_f (TLC, cyclohex/EtOAc 1:1) = 0.59

$^1\text{H-NMR}$ (400 MHz, CDCl_3):

δ = 8.87 (d, J = 7.6 Hz, 1H, 6- H_{arom}), 7.85 (d, J = 2.1 Hz, 1H, 9- H_{arom}), 7.23 (dd, J = 7.6, 2.1 Hz, 1H, 7- H_{arom}), 6.64 (s, 1H, $\text{C}=\text{OCH}$), 4.50 (s, 2H, CH_2Cl).

$^{13}\text{C-NMR}$ (100 MHz, CDCl_3):

δ = 163.08 (1C, $\text{C}=\text{O}$), 157.88 (1C, $\text{C}_{\text{q,arom}}$), 150.82 (1C, $\text{C}_{\text{q,arom}}$), 132.96 (1C, $\text{C}_{\text{q,arom}}$), 128.20 (1C, CH_{arom}), 127.93 (1C, CH_{arom}), 119.87 (1C, CH_{arom}), 103.40 (1C, $\text{C}=\text{OCH}$), 45.68 (1C, CH_2Cl).

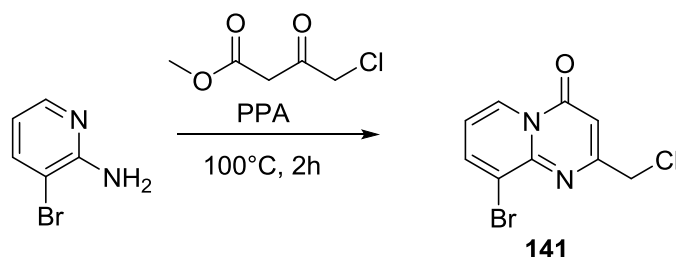
UHPLC-MS

R_t (MCS): 1.329 min

m/z : $[\text{M}+\text{H}]^+$ (calc.) = 272.9, 274.9

$[\text{M}+\text{H}]^+$ (meas.) = 273.0, 275.0

9-bromo-2-(chloromethyl)-4H-pyrido[1,2-a]pyrimidin-4-one (141)



500 mg of 2-amino-3-bromo-pyridine (2.89mmol, 1eq), 408 μL methyl 4-chloro-3-oxobutanoate (3.18mmol, 1.1eq) and 5g of PPA were heated to 100°C for 2h. After aq. work up and purification with 10g SiO_2 with a solvent gradient of cyclohex/EtOAc 5% \rightarrow 35%, the product was isolated as a light yellow solid in 46% yield (362.7mg, 1.33mmol).

R_f (TLC, cyclohex/EtOAc 3:2) = 0.38

$^1\text{H-NMR}$ (400 MHz, CDCl_3):

δ = 9.03 (dd, J = 7.2, 1.4 Hz, 1H, 6- H_{arom}), 8.11 (dd, J = 7.3, 1.5 Hz, 1H, 8- H_{arom}), 7.01 (t, J = 7.2 Hz, 1H, 7- H_{arom}), 6.74 (s, 1H, $\text{C}=\text{OCH}$), 4.60 (s, 2H, CH_2Cl).

^{13}C -NMR (100 MHz, CDCl_3):

δ = 162.83 (1C, C=O), 158.38 (1C, $\text{C}_{\text{q,arom}}$), 148.26 (1C, $\text{C}_{\text{q,arom}}$), 139.84 (1C, 8- CH_{arom}), 127.30 (1C, 6- CH_{arom}), 121.33 (1C, $\text{C}_{\text{q,arom}}$), 115.07 (1C, 7- CH_{arom}), 103.47 (1C, cHC=O), 45.73 (1C, CH_2Cl).

UHPLC-MS

R_t (MCS): 1.429 min

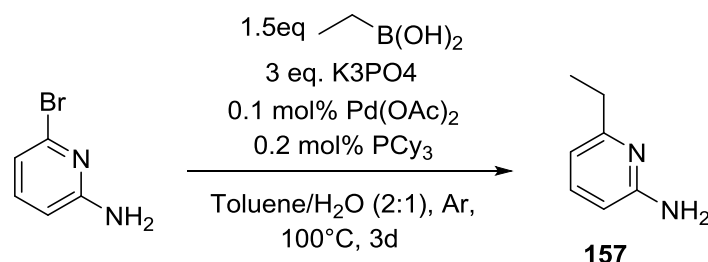
m/z: $[\text{M}+\text{H}]^+$ (calc.) = 272.9, 274.9

$[\text{M}+\text{H}]^+$ (meas.) = 273.1, 275.0

2.2.1.2 Suzuki-Ring modification from Bromopyridine precursors

The following reactions were conducted according to General Procedure **A**.

6-Ethylpyridin-2-amine (157)



200mg 2-amino-6-bromo-pyridine (1.16mmol, 1eq) were stirred with 140.8mg ethyl boronic acid (1.73mmol, 1.5eq), 736mg K_3PO_4 (3.46mmol, 3 eq), 26mg $\text{Pd}(\text{Ac})_2$ (0.12mmol, 10mol%) and 65mg PCy_3 (0.23mmol, 20mol%) in 6mL of a degassed toluene/water mixture (2:1) at 95°C . The reaction was stirred for 3 days and the product purified through column chromatography on 25g SiO_2 with a gradient of cyclohexane/EtOAc of 5% --> 30% --> 100%. The product was isolated as a clear oil in 18%yield (25.5mg, 0.21mmol) (Note: nearly 111mg of SM were recovered)

R_f (TLC, cyclohex/EtOAc 1:1) = 0.24

^1H -NMR (400 MHz, CDCl_3):

δ = 7.44 – 7.38 (m, 1H, 4- H_{arom}), 6.49 (d, J = 7.3 Hz, 1H, 5- H_{arom}), 6.36 (d, J = 8.3 Hz, 1H, 3- H_{arom}), 2.67 (q, J = 7.6 Hz, 2H, CH_2CH_3), 4.38 (s, 3H, NH_3) 1.26 (t, J = 7.6 Hz, 3H, CH_2CH_3).

^{13}C -NMR (400 MHz, CDCl_3):

δ = 159.97 (1C, $\text{C}_{\text{q, arom}}$), 157.64 (1C, $\text{C}_{\text{q, arom}}$), 139.81 (1C, CH_{arom}), 111.26 (1C, CH_{arom}), 107.24 (1C, CH_{arom}), 29.61 (1C, $\underline{\text{C}}\text{H}_2\text{CH}_3$), 13.82 (1C, $\text{CH}_2\underline{\text{C}}\text{H}_3$).

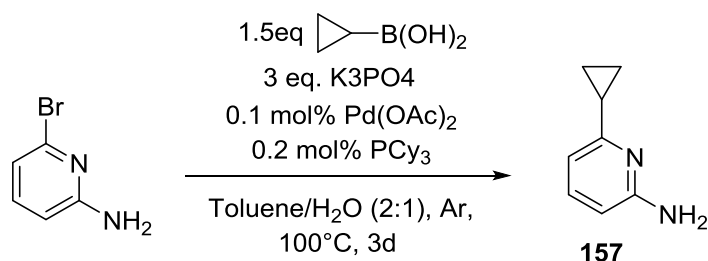
UHPLC-MS

R_{t} (MCS): 0.173 min

m/z: $[\text{M}+\text{H}]^+$ (calc.) = 123.1

$[\text{M}+\text{H}]^+$ (meas.) = 123.2

[6-cyclopropyl-pyridin-2-amine \(157\)](#)



200mg 2-amino-6-bromo-pyridine (1.16mmol, 1eq) were stirred with 149mg cyclopropyl boronic acid (1.73mmol, 1.5eq), 736mg K₃PO₄ (3.46mmol, 3 eq), 13mg Pd(Ac)₂ (0.16mmol, 10mol%) and 32.4mg PCy₃ (0.12mmol, 20mol%) with a degassed solvent mixture of toluene/water (5:1) at 95°C. The reaction was stirred for 48h and the product purified through column chromatography on 25g SiO₂ with a gradient of cyclohexane/EtOAc of 5% --> 25% --> 100%. The product was isolated as a clear oil in 49% yield (75.6mg, 0.56mmol).

R_{f} (TLC, cyclohex/EtOAc 1:1) = 0.52

^1H -NMR (400 MHz, CDCl_3):

δ = 7.31 – 7.26 (m, 1H, 4- H_{arom}), 6.46 (d, J = 7.4 Hz, 1H, 5- H_{arom}), 6.25 (d, J = 8.1 Hz, 1H, 3- H_{arom}), 4.36 (s, 2H, NH₂), 1.88 (tt, J = 7.9, 5.2 Hz, $\underline{\text{C}}\text{H}(\text{CH}_2)_2$), 0.94 – 0.85 (m, 1H, $\text{CH}(\underline{\text{C}}\text{H}_2)_2$).

^{13}C -NMR (101 MHz, CDCl_3):

δ = 161.52 (1C, $\text{C}_{\text{q, arom}}$), 158.10 (1C, $\text{C}_{\text{q, arom}}$), 137.86 (1C, 4- CH_{arom}), 111.00 (1C, 5- CH_{arom}), 105.29 (1C, 3- CH_{arom}), 16.98 (1C, $\underline{\text{C}}\text{H}(\text{CH}_2)_2$), 9.16 (2C, $\text{CH}(\underline{\text{C}}\text{H}_2)_2$).

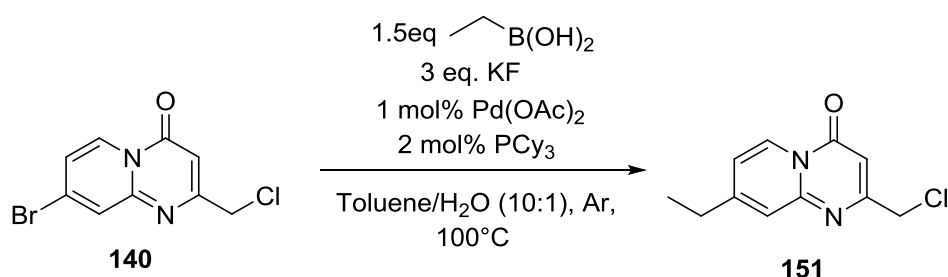
UHPLC-MS

R_t (MCS): 1.205 min

m/z: [M+H]⁺ (calc.) =

[M+H]⁺ (meas.) = 215.2

[2-\(chloromethyl\)-8-ethyl-4H-pyrido\[1,2-a\]pyrimidin-4-one \(151\)](#)



75mg of **140** (0.27mmol, 1eq) were stirred with 30.4mg ethyl boronic acid (0.41mmol, 1.5eq), 47.8mg K₃PO₄ (0.82mmol, 3eq), 0.6mg Pd(Ac)₂ (2.74μmol, 1mol%) and 1.5mg PCy₃ (5.48μmol, 2mol%) in 3mL of degassed toluene/water mixture (10:1) at 95°C. The reaction was stirred for 3 days and the product purified through column chromatography on 25g SiO₂ with a gradient of cyclohexane/EtOAc of 10% --> 40% --> 100%. The product was isolated as a clear oil in 63% yield (38.5mg, 172.90μmol).

R_f (TLC, cyclohex/EtOAc 1:1) = 0.33

¹H-NMR (400 MHz, CDCl₃):

δ = 8.95 (d, *J* = 7.3 Hz, 1H, 6-H_{arom}), 7.45 (s, 1H, 9-H_{arom}), 7.03 (dd, *J* = 7.3, 1.8 Hz, 1H, 7-H_{arom}), 6.57 (s, 1H, C=OCH), 4.50 (s, 2H, CH₂Cl), 2.79 (q, *J* = 7.5 Hz, 2H, CH₂-CH₃), 1.34 (t, *J* = 7.5 Hz, 3H, CH₂-CH₃).

¹³C-NMR (101 MHz, CDCl₃):

δ = 162.59 (1C, C=O), 158.35 (1C, C_{q, arom}), 154.94 (1C, C_{q, arom}), 151.42 (1C, C_{q, arom}), 126.87 (1C, CH_{arom}), 122.85 (1C, CH_{arom}), 117.66 (1C, CH_{arom}), 102.05 (1C, C=OCH), 45.93 (1C, CH₂Cl), 28.54 (1C, CH₂CH₃), 13.35 (1C, CH₂CH₃).

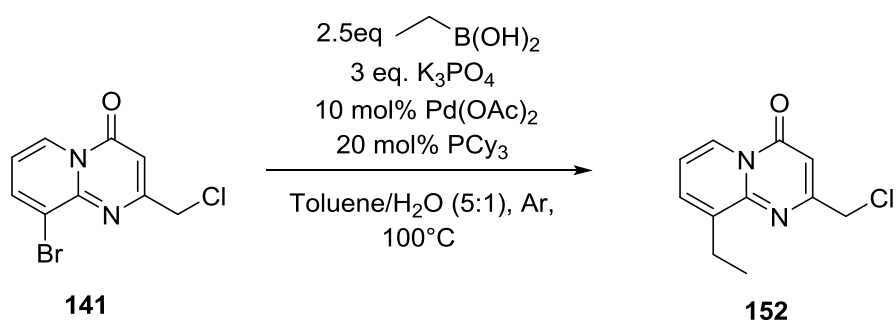
UHPLC-MS

R_t (MCS): 0.564 min

m/z: [M+H]⁺ (calc.) = 223.1

[M+H]⁺ (meas.) = 223.0

[2-\(chloromethyl\)-9-ethyl-4H-pyrido\[1,2-a\]pyrimidin-4-one \(152\)](#)



70mg of **141** (0.26mmol, 1eq) were stirred with 47.3mg ethyl boronic acid (0.64mmol, 2.5eq), 163.0mg K₃PO₄ (0.77mol, 3eq), 5.7mg Pd(Ac)₂ (2.74μmol, 10mol%) and 14.4mg PCy₃ (5.48μmol, 20mol%) in 3mL of degassed toluene and 600mL of degassed water mixture (5:1) at 95°C. The reaction was stirred for 3 days and the product purified through column chromatography on 25g SiO₂ with a gradient of cyclohexane/EtOAc of 5% --> 25% --> 100%. The product was isolated as a clear oil in 22% yield (12.7mg, 57.03μmol).

R_f (TLC, cyclohex/EtOAc 1:1) = 0.58

¹H-NMR (400 MHz, CDCl₃):

δ = 8.95 (d, *J* = 7.1 Hz, 1H, 6-H_{arom}), 7.61 (d, *J* = 6.9 Hz, 1H, 8-H_{arom}), 7.10 (t, *J* = 7.0 Hz, 1H, 7-H_{arom}), 6.65 (s, 1H, C=OCH), 4.54 (s, 2H, CH₂Cl) 3.05 (q, *J* = 7.5 Hz, 2H, CH₂CH₃), 1.33 (t, *J* = 7.5 Hz, 3H, CH₂CH₃).

¹³C-NMR (101 MHz, CDCl₃):

δ = 161.74 (1C, C=O), 159.02 (1C, C_{q, arom}), 150.27 (1C, C_{q, arom}), 140.57 (1C, C_{q, arom}), 133.77 (1C, CH_{arom}), 125.30 (1C, CH_{arom}), 115.45 (1C, CH_{arom}), 102.51 (1C, C=OCH), 46.18 (1C, CH₂Cl) 24.61 (1C, CH₂CH₃), 13.48 (1C, CH₂CH₃).

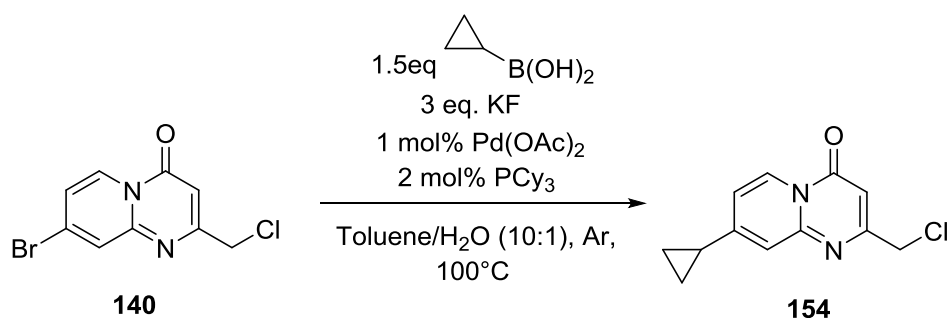
UHPLC-MS

R_t (MCS): 1.291 min

m/z: [M+H]⁺ (calc.) = 223.1

[M+H]⁺ (meas.) = 223.0

[2-\(chloromethyl\)-8-cyclopropyl-4H-pyrido\[1,2-a\]pyrimidin-4-one \(154\)](#)



75mg **140** (0.27mmol, 1eq) were stirred with 35.3mg cyclopropyl boronic acid (0.41mmol, 1.5eq), 47.8mg K₃PO₄ (0.82mmol, 3eq), 0.6mg Pd(Ac)₂ (2.74μmol, 1mol%) and 1.5mg PCy₃ (5.48μmol, 2mol%) in 3mL of degassed toluene/water mixture (10:1) at 95°C. The reaction was stirred for 3 days and the product purified through column chromatography on 25g SiO₂ with a gradient of cyclohexane/EtOAc of 10% --> 40% --> 100%. The product was identified as a clear oil in 74% yield (48.2mg, 205.38μmol).

R_f (TLC, cyclohex/EtOAc 1:1) = 0.36

¹H-NMR (400 MHz, CDCl₃):

δ = 8.91 (d, *J* = 7.7 Hz, 1H, 6-H_{arom}), 7.29 (d, *J* = 2.0 Hz, 1H, 9-H_{arom}), 6.84 (dd, *J* = 7.6, 2.2 Hz, 1H, 7-H_{arom}), 6.52 (s, 1H, CHC=O), 4.49 (s, 2H, CH₂Cl), 2.07 – 1.94 (m, 1H, CH(CH₂)₂), 1.32 – 1.17 (m, 2H, CH(CH₂)₂), 1.04 – 0.88 (m, 2H, CH(CH₂)₂).

¹³C-NMR (101 MHz, CDCl₃):

δ = 162.43 (1C, C=O), 158.19 (1C, C_{q, arom}), 156.66 (1C, C_{q, arom}), 151.04 (1C, C_{q, arom}), 127.00 (1C, 6-CH_{arom}), 119.84 (1C, 9-CH_{arom}), 115.07 (1C, 7-CH_{arom}), 101.51 (1C, CHC=O), 45.76 (1C, CH₂Cl), 15.90 (1C, CH(CH₂)₂), 11.74 (2C, CH(CH₂)₂).

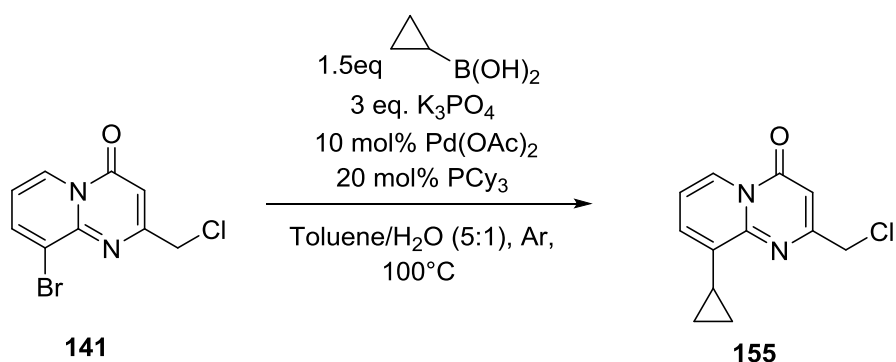
UHPLC-MS

R_t (MCS): 0.546 min

m/z: [M+H]⁺ (calc.) = 235.1

[M+H]⁺ (meas.) = 235.0

[2-\(chloromethyl\)-9-ethyl-4H-pyrido\[1,2-a\]pyrimidin-4-one \(155\)](#)



75mg of **141** (0.27mmol, 1eq) were stirred with 35.3mg cyclopropyl boronic acid (0.41mmol, 1.5eq), 174.6mg K₃PO₄ (0.82mmol, 3eq), 0.6mg Pd(Ac)₂ (2.74μmol, 1mol%) and 1.5mg PCy₃ (5.48μmol, 2mol%) in 3mL of degassed toluene and 600μL of degassed water mixture (5:1) at 95°C. The reaction was stirred for 3 days and the product purified through column chromatography on 25g SiO₂ with a gradient of cyclohexane/EtOAc of 5% --> 25% --> 100%. The product was identified as a clear oil in 85% yield (54.4mg, 231.80μmol).

R_f (TLC, cyclohex/EtOAc 1:1) = 0.64

¹H-NMR (400 MHz, CDCl₃):

δ = 8.89 (dd, *J* = 7.1, 1.5 Hz, 1H, 6-H_{arom}), 7.19 (dd, *J* = 7.1, 1.3 Hz, 1H, 8-H_{arom}), 7.05 (t, *J* = 7.1 Hz, 1H, 7-H_{arom}), 6.66 (s, 1H, C=OCH), 4.56 (s, 2H, CH₂Cl), 2.89 (tt, *J* = 8.5, 5.3 Hz, 1H, CH(CH₂)₂), 1.21 – 1.12 (m, 2H, CH(CH₂)₂), 0.86 – 0.76 (m, 2H, CH(CH₂)₂).

¹³C-NMR (101 MHz, CDCl₃):

δ = 161.78 (1C, C=O), 158.96 (1C, C_{q, arom}), 150.76 (1C, C_{q, arom}), 141.05 (1C, C_{q, arom}), 128.95 (1C, CH_{arom}), 124.39 (1C, CH_{arom}), 115.37 (1C, CH_{arom}), 102.42 (1C, C=OCH), 46.18 (1C, CH₂Cl), 10.83 (1C, CH(CH₂)₂), 10.20 (2C, CH(CH₂)₂).

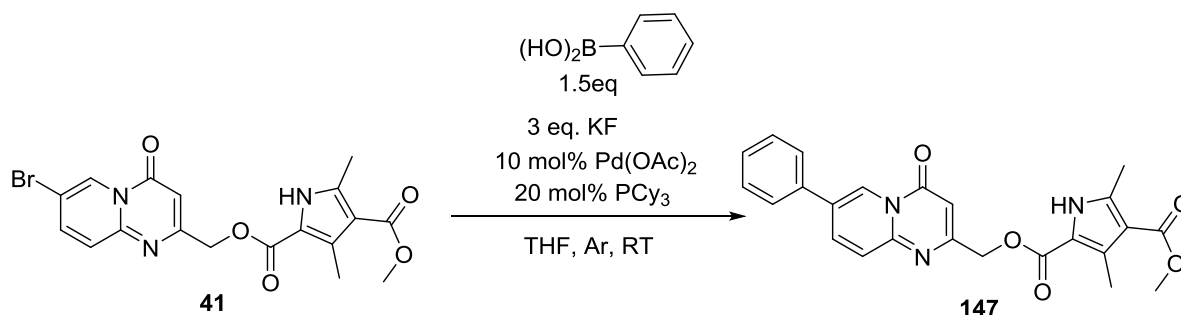
UHPLC-MS

R_t (MCS): 1.247 min

m/z: [M+H]⁺ (calc.) = 235.1

[M+H]⁺ (meas.) = 235.0

[2-\(chloromethyl\)-9-ethyl-4H-pyrido\[1,2-a\]pyrimidin-4-one \(155\)](#)



30mg of **41** (69.1 μmol, 1eq) were stirred with 12.6mg phenyl boronic acid (104 μmol, 1.5eq), 174.6mg KF (207 μmol, 3eq), 1.6mg Pd(Ac)₂ (6.91 μmol, 10mol%) and 3.9mg PCy₃ (13.8 μmol, 20mol%) in 2mL of degassed THF at RT. The reaction was stirred for 2 days and the product purified through HPLC chromatography in ACN/H₂O(+0.1% TFA) with a gradient of 10%-100% over 20 min. The product was identified as a white solid in 25% yield (9.6mg, 17.6 μmol).

R_f (TLC, cyclohex/EtOAc 1:1) =

¹H-NMR (400 MHz, DMSO-d₆):

δ = 12.09 (s, 1H), 9.14 (d, *J* = 1.7 Hz, 1H), 8.39 (dd, *J* = 9.2, 2.1 Hz, 1H), 7.83 (d, *J* = 7.4 Hz, 3H), 7.80 (d, *J* = 9.3 Hz, 1H), 7.56 (t, *J* = 7.5 Hz, 3H), 7.49 (t, *J* = 7.3 Hz, 1H), 6.56 (s, 1H), 5.29 (s, 2H), 3.73 (s, 3H), 2.53 (s, 3H), 2.46 (s, 3H).

¹³C-NMR (101 MHz, DMSO-d₆):

δ = 164.95, 162.42, 159.74, 157.21, 149.80, 144.94, 140.15, 137.16, 130.94, 129.40, 128.86, 128.56, 126.80, 126.03, 123.46, 116.73, 112.53, 99.47, 64.33, 50.59, 13.54, 11.86.

UHPLC-MS

R_t (MCS): 1.678min

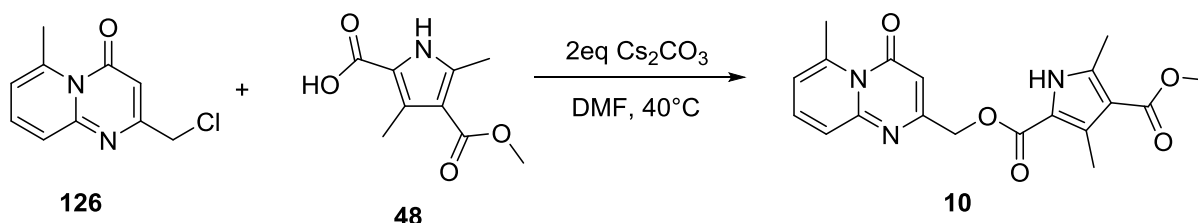
m/z: [M+H]⁺ (calc.) = 432.2

[M+H]⁺ (meas.) = 432.2

2.2.1.3 Syntheses of head group modified methyl ester-pyrrole compounds

All reaction in this section follow **General Procedure G**.

4-methyl 2-((6-methyl-4-oxo-4H-pyrido[1,2-a]pyrimidin-2-yl)methyl) 3,5-dimethyl-1H-pyrrole-2,4-dicarboxylate (10)



223mg of **126** (1.07mmol, 1eq) and 317mg of **48** (1.61mmol, 1.5eq) were stirred with 697mg Cs₂CO₃ (2.14mmol, 2eq) in 5mL DMF at 40°C. The reaction mixture was worked up after 4h and the product purified by column chromatography with 10g SiO₂ and a linear gradient of heptane/EtOAc 35% --> 100%. The product was isolated as a white solid in 23% yield (91mg, 0.25mmol).

R_f (TLC, cyclohex/EtOAc 1:4) = 0.31.

¹H-NMR (400 MHz, CDCl₃):

δ = 12.07 (s, 1H, NH), 7.68 (dd, *J* = 8.9, 7.0 Hz, 1H, 8-H_{arom}), 7.38 (d, *J* = 8.5 Hz, 1H, 9-H_{arom}), 6.93 (d, *J* = 6.9 Hz, 1H, 7-H_{arom}), 6.28 (s, 1H, C=OCH), 5.17 (s, 2H, CH₂OC=O), 3.72 (s, 3H, OCH₃), 2.93 (s, 3H, CH₃), 2.51 (s, 3H, CH₃), 2.44 (s, 3H, CH₃).

¹³C-NMR (101 MHz, CDCl₃):

δ = 164.96 (1C, C=OOCH₃), 161.22 (1C, C=OCH), 160.88 (1C, CH₂OC=O), 159.77 (1C, C_q, arom), 153.19 (1C, C_q, arom), 143.42 (1C, C_q, arom), 140.15 (1C, C_q, arom), 136.74 (1C, 8-CH_{arom}), 130.85 (1C, C_q, arom), 124.48 (1C, 9-CH_{arom}), 118.67 (1C, 7-CH_{arom}), 116.76 (1C, C_q, arom), 112.50 (1C, C_q, arom), 101.76 (1C, C=OCH), 63.87 (1C,

$\underline{\text{C}}\text{H}_2\text{OC}=\text{O}$), 50.61 (1C, $\text{C}=\text{OO}\underline{\text{C}}\text{H}_3$), 24.01 (1C, CH_3), 13.56 (1C, CH_3), 11.87 (1C, CH_3).

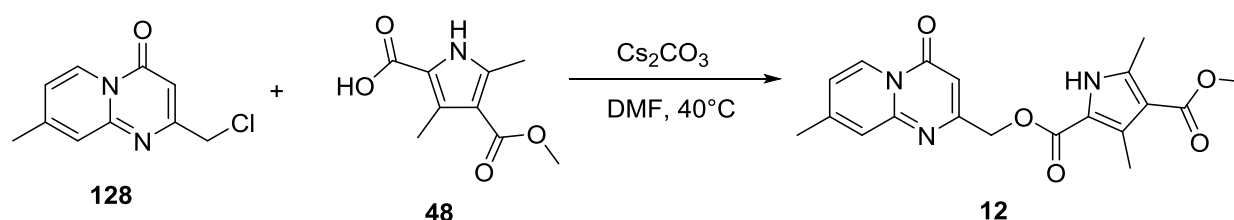
UHPLC-MS

R_t (MCS): 1.477 min

m/z: $[\text{M}+\text{H}]^+$ (calc.) = 370.1

$[\text{M}+\text{H}]^+$ (meas.) = 370.2

[4-methyl 2-\(\(8-methyl-4-oxo-4H-pyrido\[1,2-a\]pyrimidin-2-yl\)methyl\) 3,5-dimethyl-1H-pyrrole-2,4-dicarboxylate \(12\)](#)



40mg **128** (191.7 μmol , 1eq) and 45mg of **48** (230.1 μmol , 1.2eq) were stirred with 697mg Cs_2CO_3 (325.8 μmol , 1.2eq) in 5mL DMF at 40°C . The reaction mixture was worked up after 15h and the crude purified by column chromatography with 10g SiO_2 and a linear gradient of DCM/MeOH 2% --> 15%. The product was isolated as a white solid in a yield of 41 % (29mg, 0.08mmol).

R_f (TLC, cyclohex/EtOAc 1:1) = 0.16.

$^1\text{H-NMR}$ (400 MHz, Methylene Chloride- d_2 MeOD 5:1):

δ = 8.88 (d, J = 7.3 Hz, 1H, 6- H_{arom}), 7.44 (s, 1H, 9- H_{arom}), 7.09 (dd, J = 7.3, 1.9 Hz, 1H, 7- H_{arom}), 6.46 (s, 1H, $\text{C}=\text{OCH}$), 5.24 (s, 2H, $\text{CH}_2\text{OC}=\text{O}$), 3.77 (s, 3H, OCH_3), 2.56 (s, 3H, CH_3), 2.50 (s, 3H, CH_3), 2.48 (s, 3H, CH_3).

$^{13}\text{C-NMR}$ (101 MHz, Methylene Chloride- d_2 MeOD 5:1):

δ = 166.86 (1C, $\underline{\text{C}}=\text{OOCH}_3$), 163.65 (1C, $\underline{\text{C}}=\text{OCH}$), 160.88 (1C, $\text{CH}_2\text{OC}=\text{O}$), 159.09 (1C, C_q , arom), 151.84 (1C, C_q , arom), 150.99 (1C, C_q , arom), 140.97 (1C, C_q , arom), 133.24 (1C, C_q , arom), 127.10 (1C, 6- H_{arom}), 124.09 (1C, 9- H_{arom}), 119.58 (1C, 7- H_{arom}), 117.53 (1C, C_q , arom), 113.72 (1C, C_q , arom), 100.22 (1C, $\text{C}=\text{O}\underline{\text{C}}\text{H}$), 65.02 (1C, $\underline{\text{C}}\text{H}_2\text{OC}=\text{O}$), 51.11 (1C, $\text{C}=\text{OO}\underline{\text{C}}\text{H}_3$), 21.77 (1C, CH_3), 14.12 (1C, CH_3), 12.23 (1C, CH_3).

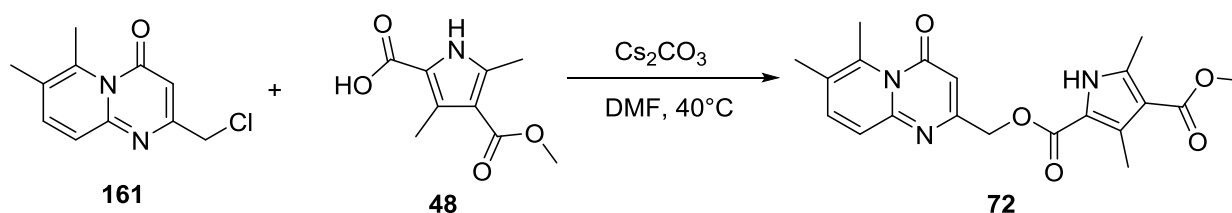
UHPLC-MS

R_t (MCS): 1.350 min

m/z: [M+H]⁺ (calc.) = 370.1

[M+H]⁺ (meas.) = 370.2

2-((6,7-dimethyl-4-oxo-4H-pyrido[1,2-a]pyrimidin-2-yl)methyl) 4-methyl 3,5-dimethyl-1H-pyrrole-2,4-dicarboxylate (72)



50mg XX (0.23mmol, 1eq) and 62mg XX (0.31mmol, 1.5eq) were stirred with 219mg Cs₂CO₃ (0.46mmol, 2eq) in 3mL DMF at 40°C. The reaction mixture was worked up after 3.5h and the crude purified by column chromatography with 10g SiO₂ and a linear gradient of heptane/EtOAc 30% --> 100%. The product was isolated as a white solid in 46% yield (40mg, 0.10mmol).

R_f (TLC, Hept/EtOAc 2:8) = 0.28

¹H-NMR (400 MHz, CDCl₃):

δ = 9.20 (s, 1H, NH), 7.41 (d, J = 9.0 Hz, 1H, 8-H_{arom}), 7.28 (d, J = 9.1 Hz, 1H, 9-H_{arom}), 6.32 (s, 1H, C=OCH), 5.22 (s, 2H, CH₂OCO), 3.83 (s, 3H, OCH₃), 2.81 (s, 3H, 6-CH₃), 2.61 (s, 3H, CH₃), 2.52 (s, 3H, CH₃), 2.31 (s, 3H, 7-CH₃).

¹³C-NMR (101 MHz, CDCl₃):

δ = 165.89 (1C, C=O), 162.53 (1C, C=OCH), 160.63 (1C, CH₂OCO), 160.53 (1C, C_q, arom), 152.83 (1C, C_q, arom), 140.65 (1C, C_q, arom), 139.78 (1C, C_q, arom), 139.67 (1C, 8-CH_{arom}), 132.52 (1C, C_q, arom), 125.12 (1C, C_q, arom), 123.57 (1C, 9-CH_{arom}), 117.24 (1C, C_q, arom), 113.93 (1C, C_q, arom), 102.83 (1C, C=OCH), 64.65 (1C, CH₂OCO), 50.92 (1C, OCH₃), 19.90 (1C, 6-CH₃), 19.22 (1C, 7-CH₃), 14.54 (1C, CH₃), 12.30 (1C, CH₃).

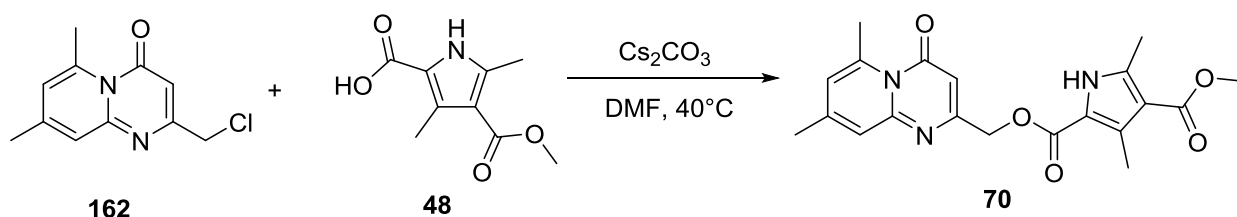
UHPLC-MS

R_t (MCS): 1.670 min

m/z: [M+H]⁺ (calc.) = 384.2

[M+H]⁺ (meas.) = 384.2

[2-\(\(6,8-dimethyl-4-oxo-4H-pyrido\[1,2-a\]pyrimidin-2-yl\)methyl\) 4-methyl 3,5-dimethyl-1H-pyrrole-2,4-dicarboxylate \(70\)](#)



22mg **162** (97μmol, 1eq) and 29mg **48** (146μmol, 1.5eq) were stirred with 95mg Cs₂CO₃ (0.67mmol, 3eq) in 3mL DMF at 40°C. The reaction mixture was worked up after 3h and the crude purified by column chromatography with 10g SiO₂ and a linear gradient of DCM/MeOH 0% --> 4%. The product was isolated as a white solid in 75% yield (28mg, 73μmol).

R_f (TLC, DCM/MeOH 95:5) = 0.43

¹H-NMR (400 MHz, DMSO-d₆):

δ = 12.05 (s, 1H, NH), 7.21 (s, 1H, 9-H_{arom}), 6.82 (s, 1H, 7-H_{arom}), 6.19 (s, 1H, C=OCH), 5.14 (s, 2H, CH₂OC=O), 3.73 (s, 3H, OCH₃), 2.90 (s, 3H, 6-CH₃), 2.51 (s, 3H, CH₃), 2.44 (s, 3H, CH₃), 2.32 (s, 3H, 8-CH₃).

¹³C-NMR (101 MHz, DMSO-d₆):

δ = 164.97 (1C, C=OOCH₃), 161.21 (1C, C=OCH), 161.13 (1C, CH₂OC=O), 159.80 (1C, C_q, arom), 153.18 (1C, C_q, arom), 148.16 (1C, C_q, arom), 142.51 (1C, C_q, arom), 140.13 (1C, C_q, arom), 130.80 (1C, C_q, arom), 122.53 (1C, 9-CH_{arom}), 121.21 (1C, 7-CH_{arom}), 116.79 (1C, C_q, arom), 112.49 (1C, C_q, arom), 100.84 (1C, C=OCH), 63.91 (1C, CH₂OC=O), 50.60 (1C, C=OOCH₃), 23.84 (1C, 6-CH₃), 20.32 (1C, 8-CH₃), 13.54 (1C, CH₃), 11.86 (1C, CH₃).

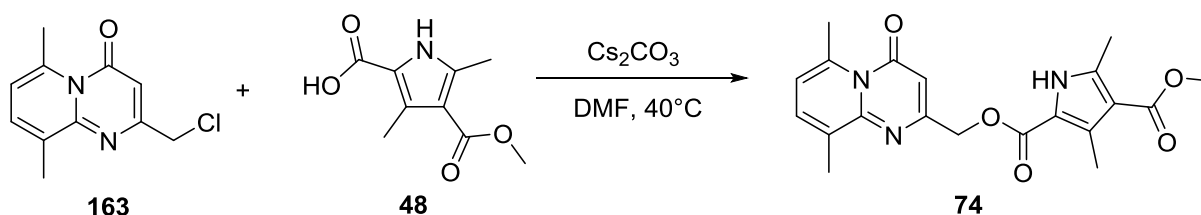
UHPLC-MS

R_t (MCS): 1.465 min

m/z: [M+H]⁺ (calc.) = 384.2

[M+H]⁺ (meas.) = 384.2

2-((6,9-dimethyl-4-oxo-4H-pyrido[1,2-a]pyrimidin-2-yl)methyl) 4-methyl 3,5-dimethyl-1H-pyrrole-2,4-dicarboxylate (74)



50mg of **163** (0.23mmol, 1eq) and 66mg of **48** (0.34mmol, 1.5eq) were stirred with 219mg Cs₂CO₃ (674μmol, 3eq) in 3mL DMF at 40°C. The reaction mixture was worked up after 3.5h and the crude purified by column chromatography with 10g SiO₂ and a linear gradient of hept/EtOAc 10% --> 100%. The product was isolated as a white solid in 64% yield (55mg, 143μmol).

R_f (TLC, hept/EtOAc 1:1) = 0.38.

¹H-NMR (400 MHz, CDCl₃):

δ = 9.02 (s, 1H, NH), 7.31 (d, J = 7.0 Hz, 1H, 8-H_{arom}), 6.57 (d, J = 7.1 Hz, 1H, 7-H_{arom}), 6.33 (s, 1H, C=OCH), 5.26 (s, 2H, CH₂OCO), 3.84 (s, 3H, OCH₃), 2.97 (s, 3H, 6-CH₃), 2.63 (s, 3H, CH₃), 2.53 (s, 3H, CH₃), 2.41 (s, 3H, 9-CH₃).

¹³C-NMR (101 MHz, CDCl₃):

δ = 165.90 (1C, C=OOCH₃), 162.89 (1C, OCO), 160.73 (1C, C_q, arom), 160.29, 153.09 (1C, C_q, arom), 141.68 (1C, C_q, arom), 139.67 (1C, C_q, arom), 134.44 (1C, 8-CH_{arom}), 132.97 (1C, C_q, arom), 132.28 (1C, C_q, arom), 117.81 (1C, 7-CH_{arom}), 117.41 (1C, C_q, arom), 113.93 (1C, C_q, arom), 102.79 (1C, C=OCH), 64.85 (1C, CH₂OC=O), 50.95 (1C, OCH₃), 24.71 (1C, 6-CH₃), 18.75 (1C, 6-CH₃), 14.58 (1C, CH₃), 12.33 (1C, CH₃)

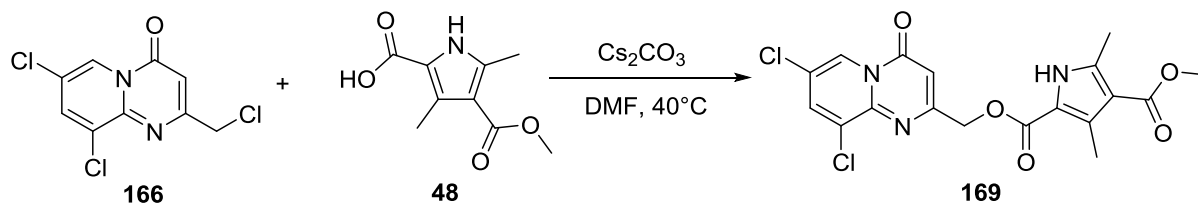
UHPLC-MS

R_t (MCS): 1.922 min

m/z: [M+H]⁺ (calc.) = 384.2

[M+H]⁺ (meas.) = 384.2

2-((7,9-dichloro-4-oxo-4H-pyrido[1,2-a]pyrimidin-2-yl)methyl) 4-methyl 3,5-dimethyl-1H-pyrrole-2,4-dicarboxylate (169)



50mg of **163** (0.19mmol, 1eq) and 56mg of **48** (0.29mmol, 1.5eq) were stirred with 185mg Cs₂CO₃ (0.57mmol, 3eq) in 3mL DMF at 40°C. The reaction mixture was worked up after 17h and the crude purified by column chromatography with 25g SiO₂ and a linear gradient of DCM/MeOH 1% --> 8%. The product was isolated as a white solid in 6% yield (4.9mg, 0.01mmol).

R_f (TLC, DCM/MeOH 6%) = 0.29.

¹H-NMR (400 MHz, CD₃OD):

δ = 8.50 (d, J = 1.9 Hz, 1H, 6-H_{arom}), 8.19 (d, J = 1.9 Hz, 1H, 8-H_{arom}), 6.87 (s, 1H, 3-H_{arom}), 5.62 (s, 2H, CH₂), 3.79 (s, 3H, OCH₃), 2.54 (s, 3H, CH₃), 2.45 (s, 3H, CH₃).

¹³C-NMR (101 MHz, CD₃OD):

δ = 170.50 (1C, C=OCH), 167.37 (1C, C=OOCH₃), 160.66 (1C, CH₂OC=O), 150.25 (1C, C_q, arom), 147.39 (1C, C_q, arom), 142.13 (1C, C_q, arom), 138.33, 134.11 (1C, C_q, arom), 130.41 (1C, C_q, arom), 128.51, 121.78 (1C, C_q, arom), 117.28 (1C, C=OCH), 114.29 (1C, C_q, arom), 61.18 (CH₂OC=O), 51.16 (1C, C=OOCH₃), 13.84 (1C, CH₃), 12.31 (1C, CH₃).

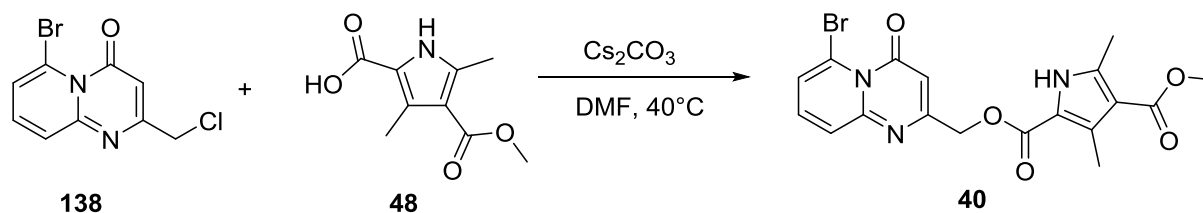
UHPLC-MS

R_t (MCS): 1.641min

m/z: [M+H]⁺ (calc.) = 424.0

[M+H]⁺ (meas.) = 424.0

[2-\(\(6-bromo-4-oxo-4H-pyrido\[1,2-a\]pyrimidin-2-yl\)methyl\) 4-methyl 3,5-dimethyl-1H-pyrrole-2,4-dicarboxylate \(40\)](#)



100mg of **138** (0.37mmol, 1eq) and 79mg of **48** (0.40mmol, 1.1eq) were stirred with 131mg Cs_2CO_3 (0.40mmol, 1.1eq) in 4mL DMF at 40°C. The reaction mixture was worked up after 17h stirring. The product was isolated in a yield of 93% (144.7mg, 0.33mmol).UHPLC-MS and $^1\text{H-NMR}$ and not further purified. The product was isolated as a brown solid in 93% yield (144.7mg, 0.33mmol).

R_f (TLC, DCM/MeOH 98:2) = 0.27.

$^1\text{H-NMR}$ (400 MHz, CDCl_3):

δ = 12.06 (s, 1H, NH), 7.62 (dd, J = 8.7, 7.2 Hz, 1H, 8- H_{arom}), 7.55 – 7.46 (m, 2H, 7- H_{arom} , 9- H_{arom}), 6.45 (s, 1H, $\text{C}=\text{OCH}$), 5.21 (s, 2H, $\text{CH}_2\text{OC}=\text{O}$), 3.73 (s, 3H, OCH_3), 2.51 (s, 3H, CH_3), 2.45 (s, 3H, CH_3).

$^{13}\text{C-NMR}$ (101 MHz, CDCl_3):

δ = 164.95 (1C, $\text{C}=\text{O}$), 160.58 (1C, $\text{CH}_2\text{OC}=\text{O}$), 159.68 ($\text{C}=\text{OCH}$), 159.10 (1C, $\text{C}_{\text{q, arom}}$), 153.11 (1C, $\text{C}_{\text{q, arom}}$), 140.16 (1C, $\text{C}_{\text{q, arom}}$), 136.69 (1C, 8- CH_{arom}), 130.97 (1C, $\text{C}_{\text{q, arom}}$), 125.94 (1C, 9- CH_{arom}), 124.87 (1C, 7- CH_{arom}), 117.47 (1C, $\text{C}_{\text{q, arom}}$), 116.68 (1C, $\text{C}_{\text{q, arom}}$), 101.63 (1C, $\text{C}=\text{OCH}$), 63.80 (1C, $\text{CH}_2\text{OC}=\text{O}$), 50.60 (1C, OCH_3), 13.54 (1C, CH_3), 11.85 (1C, CH_3).

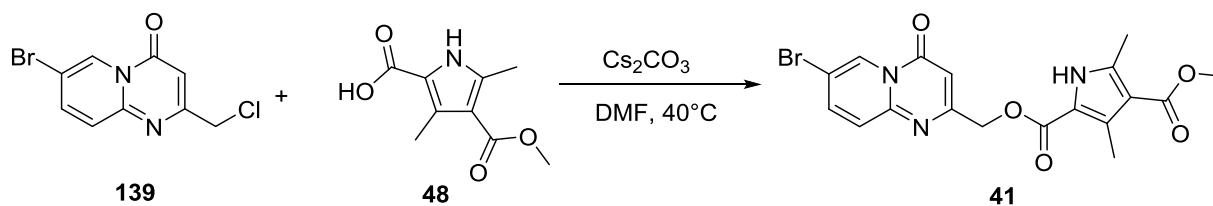
UHPLC-MS

R_t (MCS): 1.548 min

m/z: $[\text{M}+\text{H}]^+$ (calc.) = 433.0, 435.0

$[\text{M}+\text{H}]^+$ (meas.) = 434.0, 436.0

[2-\(\(6-bromo-4-oxo-4H-pyrido\[1,2-a\]pyrimidin-2-yl\)methyl\) 4-methyl 3,5-dimethyl-1H-pyrrole-2,4-dicarboxylate \(41\)](#)



100mg of **139** (0.37mmol, 1eq) and 79mg of **48** (0.40mmol, 1.1eq) were stirred with 131mg Cs₂CO₃ (0.40mmol, 1.1eq) in 4mL DMF at 40°C. The reaction mixture was worked up after 16h stirring. The purity of the crude was analysed by UHPLC-MS and ¹H-NMR and not further purified. The product was isolated as a brown solid in 77% yield (122.3mg, 0.28mmol).

R_f (TLC, hept/EtOAc 1:1) = 0.31.

¹H-NMR (400 MHz, DMSO-d₆):

δ = 12.06 (s, 1H, NH), 9.01 (d, *J* = 1.8 Hz, 1H, 6-H_{arom}), 8.10 (dd, *J* = 9.4, 2.0 Hz, 1H, 8-H_{arom}), 7.63 (d, *J* = 9.5 Hz, 1H, 9-H_{arom}), 6.57 (s, 1H, C=OCH), 5.25 (s, 2H, CH₂OC=O), 3.73 (s, 3H, OCH₃), 2.51 (s, 3H, CH₃), 2.45 (s, 3H, CH₃).

¹³C-NMR (101 MHz, DMSO-d₆):

δ = 165.00 (1C, C=O), 162.61 (1C, C=OCH), 159.73 (1C, CH₂OC=O), 156.38 (1C, C_q, arom), 149.46 (1C, C_q, arom), 140.55 (1C, 8-CH_{arom}), 140.23 (1C, C_q, arom), 131.05 (1C, C_q, arom), 127.28 (1C, 6-CH_{arom}), 126.98 (1C, 9-CH_{arom}), 116.72 (1C, C_q, arom), 112.56 (1C, C_q, arom), 110.62 (1C, C_q, arom), 100.12 (1C, C=OCH), 64.25 (1C, CH₂OC=O), 50.66 (1C, OCH₃), 13.59 (1C, CH₃), 11.90 (1C, CH₃).

UHPLC-MS

R_t (MCS): 1.604 min

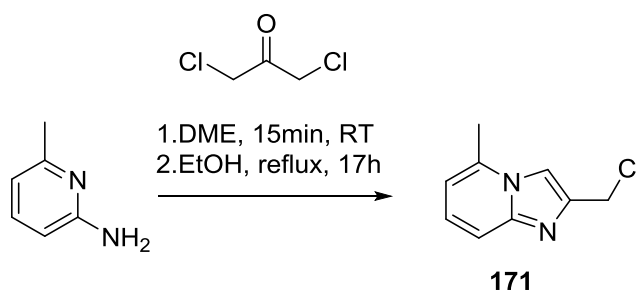
m/z: [M+H]⁺ (calc.) = 433.0, 435.0

[M+H]⁺ (meas.) = 434.0, 436.0

2.2.2 Structural modification of head group

2.2.2.1 Syntheses of imidazo-pyridines

2-(chloromethyl)-5-methyl-imidazo[1,2-a]pyridine (171)



160mg of 2-amino-6-methyl pyridine (1.48mmol, 1eq) was dissolved in 10mL DME before 376mg of 1,3-dichloropropan-2-one (2.96mmol, 2eq) were added. The reaction was stirred at RT for 15 min during which the clear solution turned cloudy. Afterwords the DME was evaporated and the residue dissolved in 10mL EtOH. The reaction mixture was refluxed and the reaction progress monitored by UHPLC-MS. After 14h the reaction was finished and worked-up aqueously. The solvent was removed *in vacuo* and the residue dissolved in 20mL of sat. aq.NaHCO₃ solution. The aqueous phase was extracted with 3x 30 mL DCM. The combined organic phases were dried with anh. NaSO₄, filtered and the solvent evaporated *in vacuo*. The product was purified by column chromatography with 25g SiO₂ and a linear gradient of hept/EtOAc 35% →100%. The product was isolated as a white product in 35% yield (83mg, 0.42mmol).

R_f (TLC, hept/EtOAc 1:1) = 0.23.

¹H-NMR (400 MHz, CDCl₃):

δ = 7.52 (app. t, *J* = 4.3 Hz, 2H, 3-H_{arom}, 8-H_{arom}), 7.20 (dd, *J* = 9.1, 6.9 Hz, 1H, 7-H_{arom}), 6.66 (d, *J* = 6.8 Hz, 1H, 6-H_{arom}), 4.81 (s, 1H, CH₂Cl), 2.59 (s, 3H, CH₃).

¹³C-NMR (101 MHz, CDCl₃):

δ = 145.43 (1C, C_q, arom), 142.41 (1C, C_q, arom), 135.00 (1C, C_q, arom), 126.29 (1C, 7-CH_{arom}), 114.85 (1C, 8-CH_{arom}), 112.44 (1C, 6-CH_{arom}), 108.33 (1C, 3-CH_{arom}), 39.41 (1C, CH₂Cl), 18.81 (1C, 5-CH₃).

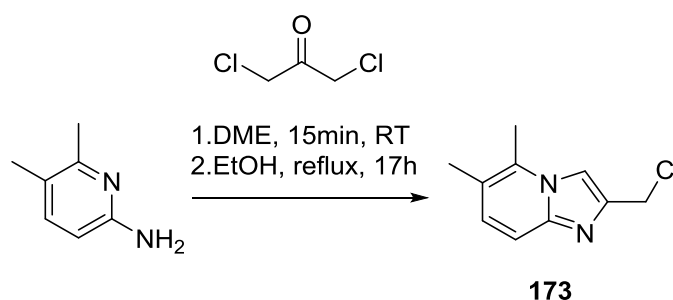
UHPLC-MS

R_t (MCS): 0.274 min

m/z: [M+H]⁺ (calc.) = 181.1

[M+H]⁺ (meas.) = 181.0

2-(chloromethyl)-5,6-dimethyl-imidazo[1,2-a]pyridine (173)



150mg of 2-amino-5,6-dimethyl-pyridine (1.23mmol, 1eq) was dissolved in 10mL DME before 312mg of 1,3-dichloropropan-2-one (2.46mmol, 2eq) were added. The reaction was stirred at RT for 15 min during which the clear solution turned cloudy. Afterwards the DME was evaporated and the residue dissolved in 10mL EtOH. The reaction mixture was refluxed and the reaction progress monitored by UHPLC-MS. After 14h the reaction was finished and worked-up aqueously. The solvent was removed *in vacuo* and the residue dissolved in 20mL of a sat. aq. NaHCO₃ solution. The aqueous phase was extracted with 3x 30mL DCM. The combined organic phases were dried with anh. NaSO₄, filtered and the solvent evaporated *in vacuo*. The product was purified by column chromatography with 25g SiO₂ and a linear gradient of hept/EtOAc 35% →100%. The product was isolated as a white solid in 44% yield (117mg, 0.65mmol).

R_f (TLC, hept/EtOAc 1:1) = 0.25.

¹H-NMR (400 MHz, CDCl₃):

δ = 7.50 (app. d, *J* = 10.3 Hz, 2H, 3-H_{arom}, 8-H_{arom}), 7.16 (d, *J* = 9.1 Hz, 1H, 7-H_{arom}), 4.82 (s, 2H, CH₂Cl), 2.54 (s, 3H, 5-CH₃), 2.36 (s, 3H, 6-CH₃).

^{13}C -NMR (101 MHz, CDCl_3):

δ = 143.55 (1C, $\text{C}_{\text{q, arom}}$), 140.82 (1C, $\text{C}_{\text{q, arom}}$), 132.10 (1C, $\text{C}_{\text{q, arom}}$), 131.36 (1C, 7- CH_{arom}), 120.65 (1C, $\text{C}_{\text{q, arom}}$), 113.49 (1C, 8- CH_{arom}), 108.66 (1C, 3- CH_{arom}), 38.57 (1C, CH_2Cl), 18.00 (1C, 6- CH_3), 15.33 (1C, 5- CH_3).

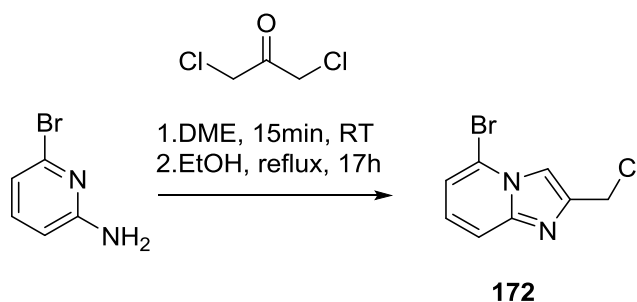
UHPLC-MS

R_t (MCS): 0.481 min

m/z: $[\text{M}+\text{H}]^+$ (calc.) = 195.1

$[\text{M}+\text{H}]^+$ (meas.) = 195.0

5-bromo-2-(chloromethyl)imidazo[1,2-a]pyridine (172)



150mg of a mino pyridine (0.87mmol, 1eq) was dissolved in 10mL DME before 220mg of 1,3-dichloropropan-2-one (1.73mmol, 2eq) were added. The reaction was stirred at RT for 15 min during which the clear solution turned cloudy. Afterwards the DME was evaporated and the residue dissolved in 10mL EtOH. The reaction mixture was refluxed and the reaction progress monitored by UHPLC-MS. After 14h the reaction was finished and worked-up aqueously. The solvent was removed *in vacuo* and the residue dissolved in 20mL of a sat. aq. NaHCO_3 solution. The aqueous phase was extracted with 3x 30mL DCM. The combined organic phases were dried with anh. NaSO_4 , filtered and the solvent evaporated *in vacuo*. The product was purified by column chromatography with 25g SiO_2 and a linear gradient of Hept/EtOAc 35% \rightarrow 100%. The product was isolated as white solid in 90% yield (192mg, 0.78mmol).

R_f (TLC, hept/EtOAc 1:1) = 0.41

$^1\text{H-NMR}$ (400 MHz, CDCl_3):

$\delta = 7.85$ (s, 1H, 3- H_{arom}), 7.68 – 7.56 (m, 1H, 8- H_{arom}), 7.21 – 7.12 (m, 1H, 7- H_{arom}), 7.12 – 7.04 (m, 1H, 6- H_{arom}), 4.79 (s, 1H, CH_2Cl).

$^{13}\text{C-NMR}$ (101 MHz, CDCl_3):

$\delta = 145.65$ (1C, C_q , arom), 142.83 (1C, C_q , arom), 125.96 (1C, 7- CH_{arom}), 116.88 (1C, 6- CH_{arom}), 116.35 (1C, 8- CH_{arom}), 114.49 (1C, C_q , arom), 112.27 (1C, 3- CH_{arom}), 39.25 (1C, CH_2Cl).

UHPLC-MS

R_t (MCS): 0.356 min

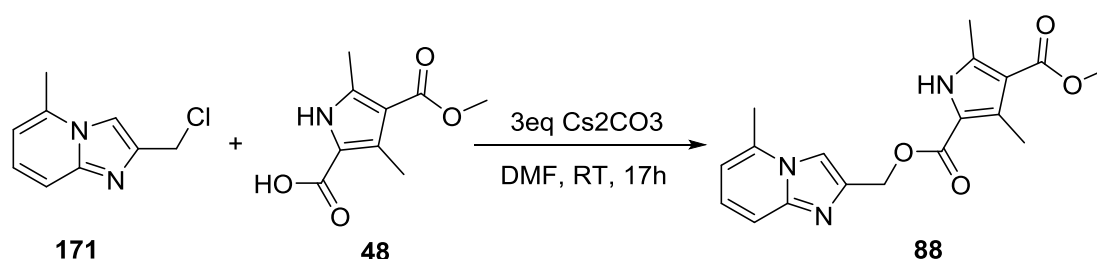
m/z: $[\text{M}+\text{H}]^+$ (calc.) = 244.9, 246.9

$[\text{M}+\text{H}]^+$ (meas.) = 245.0, 247.0

2.2.3 Syntheses of head group modified final compounds

All following syntheses follow **General Procedure G**.

4-methyl 2-((5-methylimidazo[1,2-a]pyridin-2-yl)methyl) 3,5-dimethyl-1H-pyrrole-2,4-dicarboxylate (**88**)



50mg of **171** (SM) (0.28mmol, 1eq), 82mg of **48** (0.42mmol, 1.5eq) and 271mg Cs_2CO_3 (0.83mmol, 3eq) were dissolved in 4mL DMF and stirred at RT for 17h. The product was purified by column chromatography on 10g SiO_2 with a linear gradient of hept/EtOAc 50% \rightarrow 100%. The product was isolated as a white solid in 28% yield (26mg, 0.08mmol).

R_f (TLC, DCM/MeOH 98:2) = 0.28

$^1\text{H-NMR}$ (400 MHz, $\text{DMSO-}d_6$):

δ = 11.93 (s, 1H, NH), 7.87 (s, 1H, 3- H_{arom}), 7.44 (d, J = 9.0 Hz, 1H, 8- H_{arom}), 7.24 (dd, J = 9.1, 6.8 Hz, 1H, 7- H_{arom}), 6.79 (d, J = 6.8 Hz, 1H, 6- H_{arom}), 5.39 (s, 2H, CH_2OCO), 3.70 (s, 3H, OCH_3), 2.59 (s, 3H, 5- CH_3), 2.46 (s, 3H, 3'- CH_3), 2.40 (s, 3H, 5'- CH_3).

$^{13}\text{C-NMR}$ (101 MHz, $\text{DMSO-}d_6$):

δ = 165.05 (1C, C=O), 160.35 (1C, CH_2OCO), 144.76 (1C, $\text{C}_{\text{q, arom}}$), 141.33 (1C, $\text{C}_{\text{q, arom}}$), 139.79 (1C, $\text{C}_{\text{q, arom}}$), 135.41 (1C, $\text{C}_{\text{q, arom}}$), 130.15 (1C, $\text{C}_{\text{q, arom}}$), 125.23 (1C, 7- CH_{arom}), 117.24 (1C, $\text{C}_{\text{q, arom}}$), 114.17 (1C, 8- CH_{arom}), 112.27 (1C, $\text{C}_{\text{q, arom}}$), 111.30 (1C, 6- CH_{arom}), 109.44 (1C, 3- CH_{arom}), 59.79 (1C, CH_2OCO), 50.58 (1C, OCH_3), 18.27 (1C, 5- CH_3), 13.52 (1C, 5'- CH_3), 11.88 (1C, 3'- CH_3).

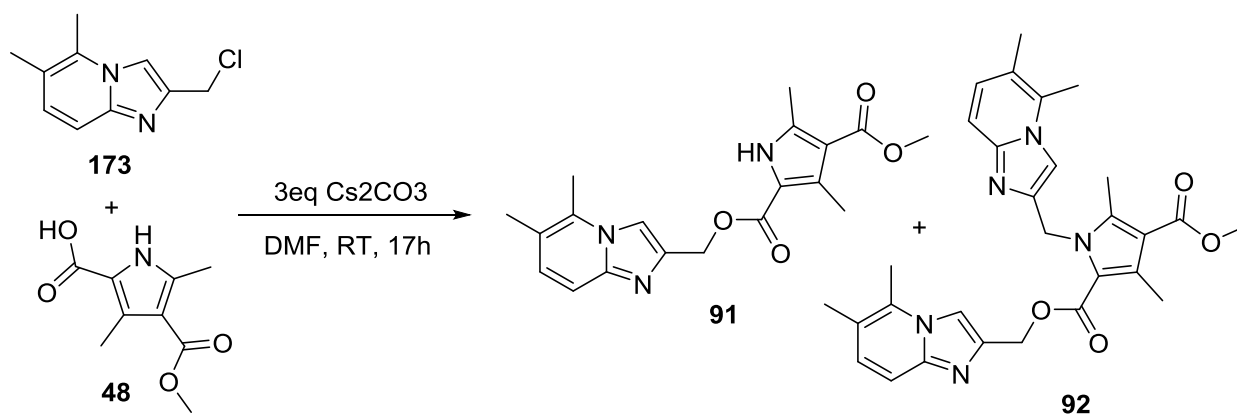
UHPLC-MS

R_t (MCS): 1.451 min

m/z : $[\text{M}+\text{H}]^+$ (calc.) = 342.1

$[\text{M}+\text{H}]^+$ (meas.) = 342.2

[2-\(\(5,6-dimethylimidazo\[1,2-a\]pyridin-2-yl\)methyl\) 4-methyl 3,5-dimethyl-1H-pyrrole-2,4-dicarboxylate \(91\)](#)



50mg of **173** (SM) (0.26mmol, 1eq), 76mg of **48** (0.39mmol, 1.5eq) and 251mg Cs_2CO_3 (0.77mmol, 3 eq) were dissolved in 4mL DMF and stirred at RT for 17h. The product was purified by column chromatography on 10g SiO_2 with a linear gradient of hept/EtOAc 50% \rightarrow 100%. The product **91** was isolated as a white solid in 28% yield

(26mg, 0.08mmol) and the double modified side product **92** as a white solid in 56% yield (37mg, 0.07mmol).

Product 91:

R_f (TLC, DCM/MeOH 98:2) = 0.30

¹H-NMR (400 MHz, DMSO-*d*₆):

δ = 11.93 (s, 1H, NH), 7.85 (s, 1H, 3-H_{arom}), 7.36 (d, *J* = 9.1 Hz, 1H, 8-H_{arom}), 7.16 (d, *J* = 9.2 Hz, 1H, 7-H_{arom}), 5.37 (s, 2H, CH₂OC=O), 3.70 (s, 3H, OCH₃), 2.52 (s, 3H, 5-CH₃), 2.45 (s, 3H, 3'-CH₃), 2.39 (s, 3H, 5'-CH₃), 2.30 (s, 3H, 6-CH₃).

¹³C-NMR (101 MHz, DMSO-*d*₆):

δ = 165.10 (1C, C=OOCH₃), 160.40 (1C, CH₂OC=O), 143.99 (1C, C_{q, arom}), 141.15 (1C, C_{q, arom}), 139.80 (1C, C_{q, arom}), 131.94 (1C, C_{q, arom}), 130.16 (1C, C_{q, arom}), 128.87 (1C, 7-CH_{arom}), 118.16 (1C, C_{q, arom}), 117.29 (1C, C_{q, arom}), 113.63 (1C, 8-CH_{arom}), 112.30 (1C, C_{q, arom}), 109.58 (1C, 3-CH_{arom}), 59.86 (1C, CH₂OC=O), 50.61 (1C, C=OOCH₃), 17.29 (1C, 6-CH₃), 15.04 (1C, 5-CH₃), 13.54 (1C, 5'-CH₃), 11.89 (1C, 3'-CH₃).

UHPLC-MS

R_t (MCS): 1.543 min

m/z: [M+H]⁺ (calc.) = 356.2

[M+H]⁺ (meas.) = 356.2

Side product 92:

R_f (TLC, DCM/MeOH 98:2) = 0.11

¹H-NMR (400 MHz, CD₃OD):

δ = 7.55 (s, 1H, 3-H_{arom}), 7.24 (d, *J* = 9.2 Hz, 1H, 8-H_{arom}), 7.19 (d, *J* = 9.3 Hz, 2H, 7-H_{arom}, 8''-H_{arom}), 7.11 (d, *J* = 9.1 Hz, 1H, 7''-H_{arom}), 6.97 (s, 1H, 3''-H_{arom}), 5.68 (s, 2H, NCH₂), 5.38 (s, 2H, CH₂OC=O), 3.80 (s, 3H, C=OOCH₃), 2.55 (s, 3H, 3'-CH₃), 2.54 (s, 3H, 5'-CH₃), 2.39 (s, 3H, 5-CH₃), 2.33 (s, 3H, 6-CH₃), 2.25 (s, 6H, 5''-CH₃, 6''-CH₃).

¹³C-NMR (101 MHz, CD₃OD):

δ = 167.43 (1C, $\underline{C}=\text{OOCH}_3$), 162.52 (1C, $\text{CH}_2\text{OC}=\underline{\text{O}}$), 145.45 (1C, C_q , arom), 145.31 (1C, C_q , arom), 143.78 (1C, C_q , arom), 143.42 (1C, C_q , arom), 141.08 (1C, C_q , arom), 133.52 (1C, C_q , arom), 133.38 (1C, C_q , arom), 131.97 (1C, C_q , arom), 131.51 (1C, 7- CH_{arom}), 131.19 (1C, 7''- CH_{arom}), 121.28 (1C, C_q , arom), 120.81 (1C, C_q , arom), 120.54 (1C, C_q , arom), 114.08 (1C, 8- CH_{arom}), 113.81 (1C, 8''- CH_{arom}), 113.32 (1C, C_q , arom), 111.03 (1C, 3- CH_{arom}), 108.37 (1C, 3''- CH_{arom}), 60.32 (1C, $\underline{\text{C}}\text{H}_2\text{OC}=\text{O}$), 51.31 (1C, $\text{C}=\text{OO}\underline{\text{C}}\text{H}_3$), 44.95 (1C, NCH_2), 17.69 (2C, 6- CH_3 , 6''- CH_3) 15.06 (1C, 5- CH_3), 14.91 (1C, 5''- CH_3), 13.07 (1C, 3'- CH_3), 12.14 (1C, 5'- CH_3).

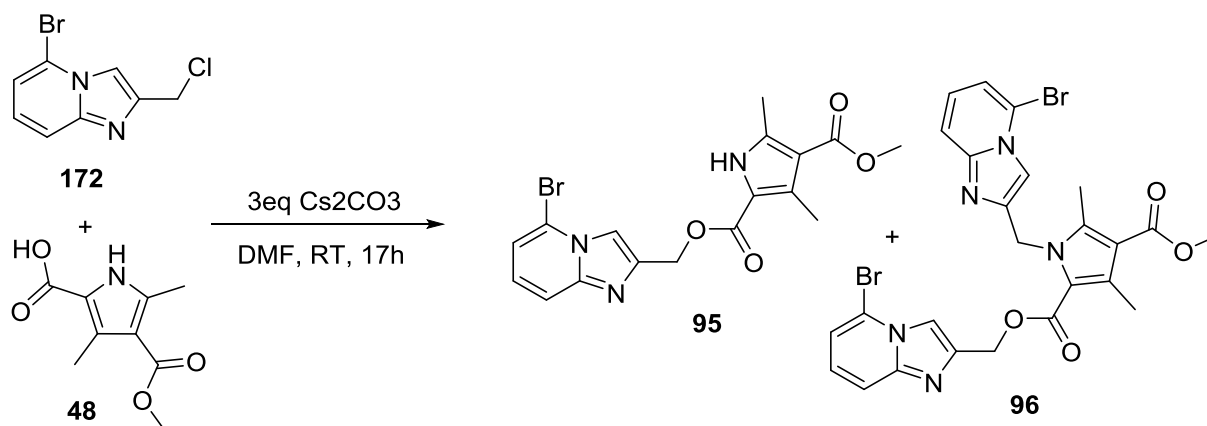
UHPLC-MS

R_t (MCS): 1.450 min

m/z: $[\text{M}+\text{H}]^+$ (calc.) = 514.2

$[\text{M}+\text{H}]^+$ (meas.) = 514.2

[2-\(\(5-bromoimidazo\[1,2-a\]pyridin-2-yl\)methyl\) 4-methyl 3,5-dimethyl-1H-pyrrole-2,4-dicarboxylate \(95\)](#)



50mg of **172** (SM) (0.20mmol, 1eq), 60mg of **48** (0.31mmol, 1.5eq) and 199mg Cs_2CO_3 (0.61mmol, 3 eq) were dissolved in 4mL DMF and stirred at RT for 17h. The product was purified by column chromatography on 10g SiO_2 with a linear gradient of hept/EtOAc 50 \rightarrow 100%. The product **95** was isolated as a white solid in 30% yield (25mg, 0.06mmol) and the double modified side product **96** as a white solid in 54% yield (33.6mg, 0.05mmol).

Product 95:

R_f (TLC, DCM/MeOH 98:2) = 0.23

¹H-NMR (400 MHz, DMSO-*d*₆):

δ = 11.95 (s, 1H, NH), 8.05 (s, 1H, 3-H_{arom}), 7.63 (d, *J* = 8.9 Hz, 1H, 8-H_{arom}), 7.32 (dd, *J* = 7.2, 0.9 Hz, 1H, 6-H_{arom}), 7.25 (dd, *J* = 8.9, 7.3 Hz, 1H, 7-H_{arom}), 5.41 (s, 2H, CH₂), 3.70 (s, 3H, OCH₃), 2.46 (s, 3H, 3'-CH₃), 2.40 (s, 3H, 5'-CH₃).

¹³C-NMR (101 MHz, DMSO-*d*₆):

δ = 165.03 (1C, C=O), 160.27 (1C, CH₂OC=O), 144.91 (1C, C_{q, arom}), 141.82 (1C, C_{q, arom}), 139.88 (1C, C_{q, arom}), 130.28 (1C, C_{q, arom}), 125.81 (1C, 7-CH_{arom}), 117.13 (1C, C_{q, arom}), 116.48 (1C, 6-CH_{arom}), 115.92 (1C, 8-CH_{arom}), 114.11 (1C, C_{q, arom}), 112.50 (1C, 3-CH_{arom}), 112.32 (1C, C_{q, arom}), 59.55 (1C, CH₂OC=O), 50.60 (1C, OCH₃), 13.54 (1C, 5'-CH₃), 11.87 (1C, 3'-CH₃).

UHPLC-MS

R_t (MCS): 1.530 min

m/z: [M+H]⁺ (calc.) = 406.0, 408.0

[M+H]⁺ (meas.) = 406.0, 408.0

Side product 96:

R_f (TLC, DCM/MeOH 98:2) = 0.12

¹H-NMR (400 MHz, CDCl₃):

δ = 7.81 (s, 1H, 3-H_{arom}), 7.61 (d, *J* = 8.9 Hz, 1H, 8-H_{arom}), 7.57 (d, *J* = 8.9 Hz, 1H, 8''-H_{arom}), 7.39 (s, 1H, 3''-H_{arom}), 7.17 – 6.99 (m, 4H, 6/6''-H_{arom}, 7/7''-H_{arom}), 5.76 (s, 2H, s, 2H, NCH₂), 5.50 (s, 2H, s, 2H, CH₂), 3.82 (s, 3H, OMe), 2.64 (s, 3H, 3'-CH₃), 2.61 (s, 3H, 5'-CH₃).

¹³C-NMR (101 MHz, CDCl₃):

δ = 166.07(1C, C=O), 161.64 (1C, C=O), 145.36 (1C, C_{q, arom}), 145.09 (1C, C_{q, arom}), 143.33 (1C, C_{q, arom}), 142.47 (1C, C_{q, arom}), 141.52 (1C, C_{q, arom}), 132.94 (1C, C_{q, arom}), 125.77(1C, 7-CH_{arom}), 125.73(1C, 7''-CH_{arom}), 119.40 (1C, C_{q, arom}), 116.79 (6-CH_{arom},

116.72 (1C, 6''-CH_{arom}), 116.24 (1C, 8-CH_{arom}), 115.86 (1C, 8''-CH_{arom}), 114.58 (1C, C_{q, arom}), 114.54 (1C, C_{q, arom}), 113.54 (1C, C_{q, arom}), 112.67 (1C, 3-CH_{arom}), 111.38 (1C, 3''-CH_{arom}), 60.06 (1C, C_{H2}OC=O), 51.01 (1C, OCH₃), 43.96 (1C, C_{H2}N), 13.27(1C, 5'-CH₃), 12.42 (1C, 3'-CH₃).

UHPLC-MS

R_t (MCS): 1.546 min

m/z: [M+H]⁺ (calc.) = 614.0, 616.0

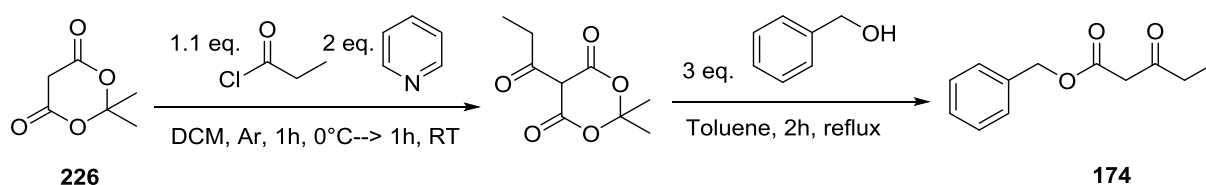
[M+H]⁺ (meas.) = 614.0, 616.0

2.3 Pyrrole-Ring Modification

2.3.1 Substituent-Modification of pyrrole ring

2.3.1.1 Reagent Syntheses

Benzyl 3-oxopentanoate (174)



2g of **226** (13.88mmol, 1eq), 1.39 mL propionyl chloride (15.26mmol, 1,1eq) and 2.24mL pyridine (27.75mmol, 2eq) were stirred 15mL DCM, before the solvent was removed *in vacuo* and the residue refluxed in 10mL toluene with 4.33mL benzyl alcohol (41.63mmol, 3eq). The product was purified with 100g SiO₂ and a linear gradient of heptane /EtOAc 5% → 30%. The product was isolated as a clear liquid in 66% yield (1.88g, 9.13mmol). The purity of the product was determined to be 91% by ¹H-NMR.

R_f (TLC, hept/EtOAc 7:3) = 0.5

¹H-NMR (400 MHz, CDCl₃):

δ = 7.40 – 7.31 (m, 5H, H_{arom}), 5.17 (s, 2H, PhCH₂), 3.49 (s, 2H, C=OCH₂C=O), 2.54 (q, J = 7.3 Hz, 2H, CH₂CH₃), 1.07 (t, J = 7.3 Hz, 3H, CH₂CH₃).

^{13}C -NMR (101 MHz, CDCl_3):

δ = 203.19 (1C, C=O), 167.23 (1C, $\text{OC}=\text{OCH}_2$), 135.43 (1C, $\text{C}_{\text{q, arom}}$), 128.73 (2C, CH_{arom}), 128.56 (1C, CH_{arom}), 128.47 (2C, CH_{arom}), 67.22 (1C, $\text{PhCH}_2\text{OC}=\text{O}$), 49.05 (1C, $\text{OC}=\text{OCH}_2$), 36.46 (1C, CH_2CH_3), 7.65 (1C, CH_2CH_3).

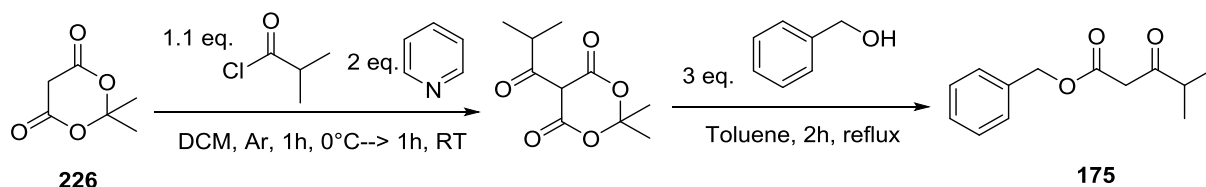
UHPLC-MS

R_t (MCS): 1.752 min

m/z: $[\text{M}+\text{H}]^+$ (calc.) = 207.1

$[\text{M}+\text{H}]^+$ (meas.) = 207.2

Benzyl 4-methyl-3-oxopentanoate (226)



1.5g of **226** (10.41mmol, 1eq), 1.20 mL isobutyryl chloride (11.44mmol, 1,1eq), 1.68mL pyridine (20.82mmol, 2eq), were stirred in 15mL DCM, before the solvent was removed *in vacuo* and the residue refluxed in 10mL toluene with 3.57mL benzyl alcohol (31.22mmol, 3eq). The product was purified with 50g SiO_2 and a linear gradient of heptane /EtOAc 10% → 30%. The product was isolated as a clear liquid in 49% yield (1.13g, 5.12mmol). The purity of the product was determined to be 94% by ^1H -NMR.

R_f (TLC, hept/EtOAc 4:1) = 0.66.

^1H -NMR (400 MHz, CDCl_3):

δ = 7.40 – 7.32 (m, 5H, H_{arom}), 5.18 (s, 2H, PhCH_2), 3.55 (s, 2H, $\text{C}=\text{OCH}_2\text{C}=\text{O}$), 2.70 (hept, J = 7.0 Hz, 1H, $\text{CH}(\text{CH}_3)_2$), 1.12 (d, J = 6.9 Hz, 6H, $\text{CH}(\text{CH}_3)_2$).

^{13}C -NMR (101 MHz, CDCl_3):

δ = 206.46 (1C, C=O), 167.38 (1C, $\text{OC}=\text{O}$), 135.52 (1C, $\text{C}_{\text{q, arom}}$), 128.74 (2C, CH_{arom}), 128.55 (1C, CH_{arom}), 128.48 (2C, CH_{arom}), 67.22 (1C, PhCH_2), 47.18 (1C, $\text{C}=\text{OCH}_2\text{C}=\text{O}$), 41.38 (1C, $\text{CH}(\text{CH}_3)_2$), 18.04 (2C, $\text{CH}(\text{CH}_3)_2$).

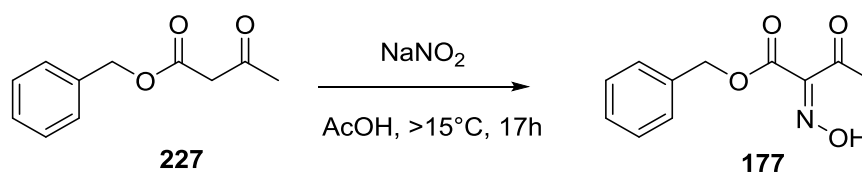
UHPLC-MS

R_t (MCS): 2.017 min

m/z: [M+H]⁺ (calc.) = 221.1

[M+H]⁺ (meas.) = 221.2

Benzyl (E)-2-(hydroxyimino)-3-oxobutanoate (177)



500mg of benzyl 3-oxobutanoate (2.60mmol, 1eq) was dissolved in 1mL glacial acetic acid/water mixture (10:1) before 269mg NaNO₂ (3.90mmol, 1.5eq) dissolved in 1mL water was added. The product was isolated as a yellow oil in 97% yield (563.2mg, 2.55mmol) and 91% purity (determined by ¹H-NMR). The crude was used in the following reaction step without further purification.

R_f (TLC, hept/EtOAc 1:1) = 0.61.

¹H-NMR (400 MHz, CDCl₃):

δ = 9.12 (s, 1H, NOH), 7.43 – 7.32 (m, 5H, H_{arom}), 5.35 (s, 2H, PhCH₂), 2.40 (s, 3H, CH₃).

¹³C-NMR (101 MHz, CDCl₃):

δ = 193.53 (1C, C=O), 161.38 (1C, BnOC=O), 151.15 (1C, C=NOH), 134.67 (1C, C_{q, arom}), 128.77 (2C, CH_{arom}), 128.74 (1C, CH_{arom}), 128.45 (2C, CH_{arom}), 67.94 (1C, PhCH₂), 25.56 (1C, CH₃).

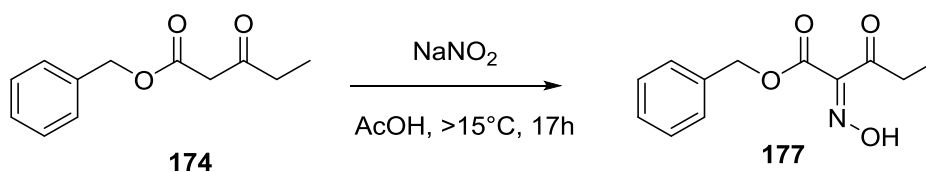
UHPLC-MS

R_t (MCS): 1.670 min

m/z: [M+Na]⁺ (calc.) = 244.1

[M+Na]⁺ (meas.) = 244.0

Benzyl (E)-2-(hydroxyimino)-3-oxopentanoate (177)



172.9mg of **174** (0.83mmol, 1eq) dissolved in 1.5mL glacial acetic acid/water mixture (10:1) was stirred with 86.76mg NaNO_2 (1.26mmol, 1.5eq) dissolved in 1mL water. The product was isolated as a yellow oil in 92% yield (181mg, 0.77mmol) and a purity of 86% (determined by $^1\text{H-NMR}$). The compound was used without further purification in the following reaction steps.

$^1\text{H-NMR}$ (400 MHz, CDCl_3):

δ = 9.08 (s, 1H NOH), 7.43 – 7.32 (m, 5H), 5.35 (s, 2H, PhCH_2), 2.80 (q, J = 7.3 Hz, 2H, CH_2CH_3), 1.12 (t, J = 7.3 Hz, 3H, CH_2CH_3).

$^{13}\text{C-NMR}$ (101 MHz, CDCl_3):

δ = 196.29 (1C, C=O), 161.55 (1C, OC=O), 150.57 (1C, C=NOH), 134.71 (1C, $\text{C}_{\text{q, arom}}$), 128.77 (2C, CH_{arom}), 128.72 (1C, CH_{arom}), 128.45 (2C, CH_{arom}), 67.90 (1C, PhCH_2), 31.35 (1C, CH_2CH_3), 7.55 (1C, CH_2CH_3).

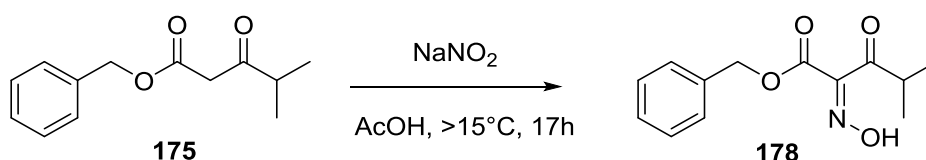
UHPLC-MS

R_t (MCS): 1.713 min

m/z: $[\text{M}+\text{H}]^+$ (calc.) = 236.1

$[\text{M}+\text{H}]^+$ (meas.) = 236.0

Benzyl (E)-2-(hydroxyimino)-4-methyl-3-oxopentanoate (178)



1.36g of **175** (6.18mmol, 1eq) dissolved in 5mL glacial acetic acid/water mixture (10:1) and 639mg NaNO_2 (9.27mmol, 1.5eq) dissolved in 1mL water were stirred. The product was isolated with 100% yield (1.54g, 6.18mmol). The purity of the crude was

determined by $^1\text{H-NMR}$ and UHPLC-MS and product used in the following reaction step without further purification.

R_f (TLC, cyclohex/EtOAc 1:1) = 0.65.

$^1\text{H-NMR}$ (400 MHz, CDCl_3):

δ = 9.23 (s, 1H, NOH), 7.41 – 7.32 (m, 5H, H_{arom}), 5.35 (s, 2H, PhCH_2), 3.39 (hept, J = 6.9 Hz, 1H, $\text{CH}(\text{CH}_3)_2$), 1.14 (d, J = 6.9 Hz, 6H, $\text{CH}(\text{CH}_3)_2$).

$^{13}\text{C-NMR}$ (101 MHz, CDCl_3):

δ = 199.72 (1C, C=O), 161.74 (1C, OC=O), 149.79 (1C, C=NOH), 134.78 (1C, $\text{C}_{\text{q, arom}}$), 128.74 (2C, $\text{Ph-CH}_{\text{arom}}$), 128.68 (1C, $\text{Ph-CH}_{\text{arom}}$), 128.42 (2C, $\text{Ph-CH}_{\text{arom}}$), 67.85 (1C, PhCH_2), 35.76 (1C, $\text{CH}(\text{CH}_3)_2$), 18.43 (2C, $\text{CH}(\text{CH}_3)_2$).

UHPLC-MS

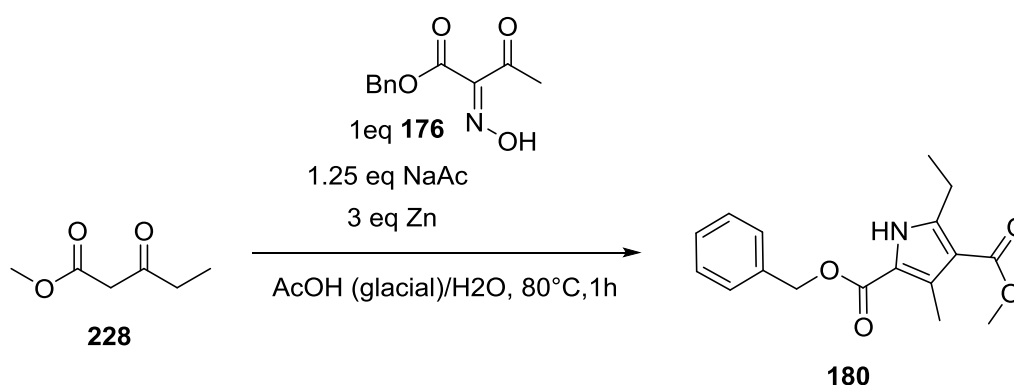
R_t (MCS): 1.757 min

m/z: $[\text{M}+\text{Na}]^+$ (calc.) = 272.1

$[\text{M}+\text{Na}]^+$ (meas.) = 272.2

2.3.1.2 Pyrrole ring syntheses

2-benzyl 4-methyl 5-ethyl-3-methyl-1H-pyrrole-2,4-dicarboxylate (**180**)



518mg of methyl 3-oxopentanoate (3.98mmol, 1.1eq) and 371mg (4.52mmol, 1.25eq) dissolved in 5mL glacial acetic acid, 800mg of **176** (3.62mmol, 1eq) dissolved in 2mL of a 1:1 mixture of glacial acetic acid/water and 710mg Zn (10.85mmol, 3eq) were used to synthesise **180**. After purification on 50g SiO_2 with a linear gradient of hept/EtOAc 5% → 20%, the product was isolated as a clear oil in 26% yield (289mg 0.96mmol).

R_f (TLC, hept/EtOAc 4:1) = 0,32

¹H-NMR (400 MHz, CDCl₃):

δ = 8.85 (s, 1H, NH), 7.47 – 7.33 (m, 5H, Ph-H_{arom}), 5.32 (s, 2H, Ph-CH₂), 3.82 (s, 3H, OMe), 2.94 (q, J = 7.5 Hz, 2H, CH₂CH₃), 2.57 (s, 3H, CH₃), 1.24 (t, J = 7.5 Hz, 3H, CH₂CH₃).

¹³C-NMR (101 MHz, CDCl₃):

δ = 165.83 (1C, C=OOCH₃), 161.34 (1C, BnOC=O), 144.81 (1C, C_{q, arom}), 136.22 (1C, C_{q, arom}), 131.65 (1C, C_{q, arom}), 128.78 (2C, CH_{arom}), 128.43 (1C, CH_{arom}), 128.37 (2C, CH_{arom}), 117.78 (1C, C_{q, arom}), 112.96 (1C, C_{q, arom}), 66.18 (1C, PhCH₂), 50.90 (1C, C=OOCH₃), 21.58 (1C, CH₂CH₃), 13.05 (1C, CH₂CH₃), 12.23 (1C, CH₃).

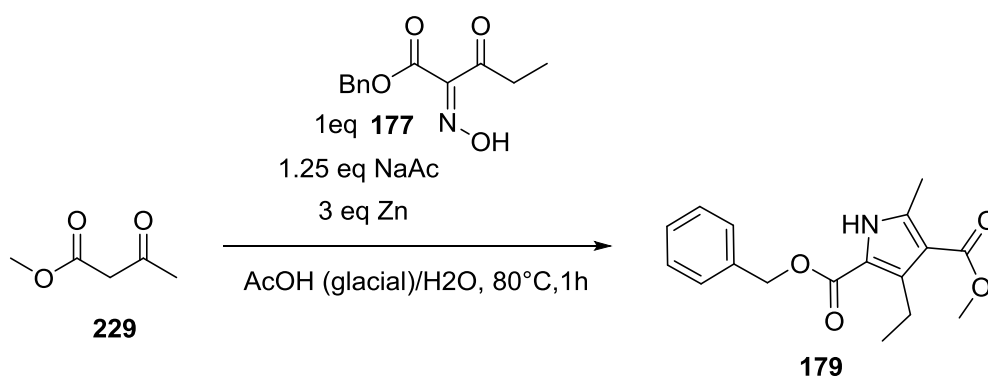
UHPLC-MS

R_t (MCS): 2.078 min

m/z: [M+H]⁺ (calc.) = 302.1

[M+H]⁺ (meas.) = 302.2

2-benzyl 4-methyl 3-ethyl-5-methyl-1H-pyrrole-2,4-dicarboxylate (179)



271mg of XX (2.34mmol, 1.1eq) and 218mg NaOAc (2.66mmol, 1.25eq) dissolved in 3mL glacial acetic acid, 500mg of XX (oxime) (2.13mmol, 1eq) dissolved in 1mL of a 1:1 mixture of glacial acetic acid/water and 417mg Zn (6.38mmol, 3eq) were used to synthesise XX. After purification on 25g SiO₂ with a linear gradient of hept/EtOAc 5% → 15%, the product was isolated as a clear liquid in 54% yield (343.mg 1.14mmol).

R_f (TLC, hept/EtOAc 4:1) = 0.27.

¹H-NMR (400 MHz, CDCl₃):

δ = 9.31 (s, 1H, NH), 7.47 – 7.30 (m, 5H, Ph-H_{arom}), 5.32 (s, 2H, PhCH₂), 3.82 (s, 3H, OCH₃), 3.09 (q, *J* = 7.4 Hz, 2H, CH₂CH₃), 2.49 (s, 3H, CH₃), 1.14 (t, *J* = 7.4 Hz, 3H, CH₂CH₃).

¹³C-NMR (101 MHz, CDCl₃):

δ = 165.69 (1C, C=OOCH₃), 161.32 (1C, CH₂OC=O), 139.54 (1C, C_{q, arom}), 138.31 (1C, C_{q, arom}), 136.15 (1C, C_{q, arom}), 128.73 (2C, CH_{arom}), 128.40 (1C, CH_{arom}), 128.26 (2C, CH_{arom}), 117.17 (1C, C_{q, arom}), 112.83 (1C, C_{q, arom}), 66.23 (1C, CH₂OC=O), 50.83 (1C, C=OOCH₃), 19.23 (1C, CH₂CH₃), 15.67 (1C, CH₂CH₃), 14.46 (1C, CH₃).

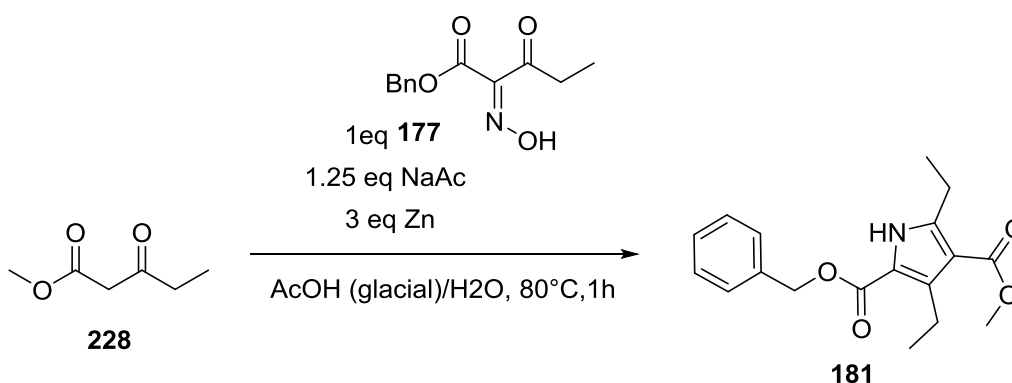
UHPLC-MS

R_t (MCS): 2.049 min

m/z: [M+H]⁺ (calc.) = 302.1

[M+H]⁺ (meas.) = 302.2

2-benzyl 4-methyl 3,5-diethyl-1H-pyrrole-2,4-dicarboxylate (181)



326mg of **228** (2.50mmol, 1.1eq) and 233mg NaOAc (2.85mmol, 1.25eq) dissolved in 3mL glacial acetic acid, 535mg of **177** (2.28mmol, 1eq) dissolved in 1mL of a 1:1 mixture of glacial acetic acid/water and 446mg Zn (6.83mmol, 3eq). The crude was purified on 25g SiO₂ with a linear gradient of Hept/EtOAc 3% → 18%. The product was isolated in 38% yield (272mg, 0.86mmol).

R_f (TLC, hept/EtOAc 4:1) = 0.41

¹H-NMR (400 MHz, CDCl₃):

δ = 8.96 (s, 1H, NH), 7.48 – 7.30 (m, 5H, Ph-H_{arom}), 5.32 (s, 2H, PhCH₂), 3.82 (s, 3H, OCH₃), 3.09 (q, *J* = 7.4 Hz, 2H, 3-CH₂CH₃), 2.94 (q, *J* = 7.5 Hz, 2H, 5-CH₂CH₃), 1.24 (t, *J* = 7.5 Hz, 3H, 5-CH₂CH₃), 1.14 (t, *J* = 7.4 Hz, 3H, 3-CH₂CH₃).

¹³C-NMR (101 MHz, CDCl₃):

δ = 165.58 (1C, C=OOCH₃), 161.26 (1C, CH₂OC=O), 144.91 (1C, C_{q, arom}), 138.24 (1C, C_{q, arom}), 136.18 (1C, C_{q, arom}), 128.75 (2C, CH_{arom}), 128.41 (1C, CH_{arom}), 128.32 (2C, CH_{arom}), 117.17 (1C, C_{q, arom}), 112.02 (1C, C_{q, arom}), 66.23 (1C, CH₂OC=O), 50.89 (1C, C=OOCH₃), 21.64 (1C, 3-CH₂CH₃), 19.26 (1C, 5-CH₂CH₃), 15.68 (1C, 3-CH₂CH₃), 13.06 (1C, 5-CH₂CH₃).

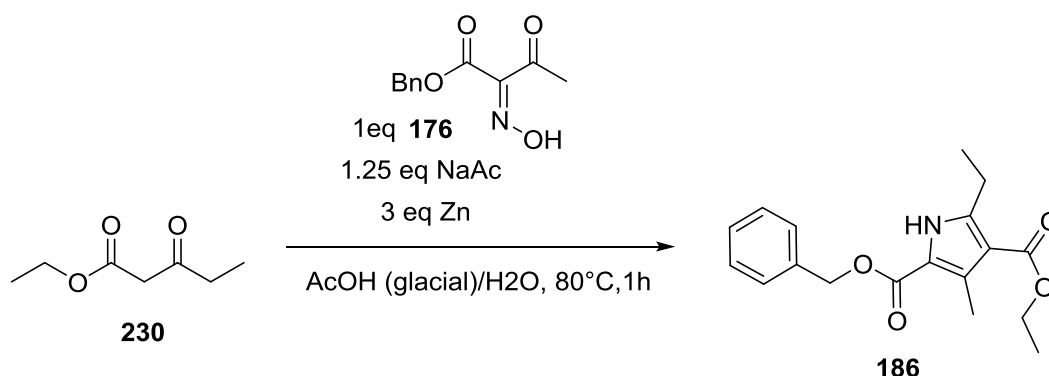
UHPLC-MS

R_t (MCS): 2.131 min

m/z: [M+H]⁺ (calc.) = 316.2

[M+H]⁺ (meas.) = 316.2

2-benzyl 4-ethyl 5-ethyl-3-methyl-1H-pyrrole-2,4-dicarboxylate (186)



574mg of **230** (3.98mmol, 1.1eq) and 371mg NaOAc (4.52mmol, 1.25eq) dissolved in 4mL glacial acetic acid, 800mg of **176** (3.62mmol, 1eq) dissolved in 1mL of a 1:1 mixture of glacial acetic acid/water and 709mg Zn (10.84mmol, 3eq) were used to synthesise **186**. After purification on 50g SiO₂ with a linear gradient of hept/EtOAc 3% → 20%, the product was isolated in 12% yield (370mg, 0.43mmol).

R_f (TLC, hept/EtOAc 4:1) = 0.39.

¹H-NMR (400 MHz, CDCl₃):

δ = 8.91 (s, 1H, NH), 7.45 – 7.33 (m, 5H, Ph-H_{arom}), 5.32 (s, 2H, PhCH₂), 4.29 (q, *J* = 7.1 Hz, 2H, OCH₂CH₃), 2.94 (q, *J* = 7.5 Hz, 2H, 5-CH₂CH₃), 2.58 (s, 3H, 3-CH₃), 1.35 (t, *J* = 7.1 Hz, 3H, OCH₂CH₃), 1.24 (t, *J* = 7.5 Hz, 3H, 5-CH₂CH₃).

¹³C-NMR (101 MHz, CDCl₃):

δ = 165.37 (1C, C=OOCH₃), 161.47 (1C, CH₂OC=O), 144.83 (1C, C_q, arom), 136.21 (1C, C_q, arom), 128.75 (2C, CH_{arom}), 128.53 (1C, CH_{arom}), 128.31 (2C, CH_{arom}), 117.71 (1C, C_q, arom), 113.09 (1C, C_q, arom), 66.14 (1C, CH₂OC=O), 59.67 (1C, C=OOCH₂CH₃), 21.62 (1C, 5-CH₂CH₃), 14.51 (1C, C=OOCH₂CH₃), 13.18 (1C, 5-CH₂CH₃), 12.25 (1C, 3-CH₃).

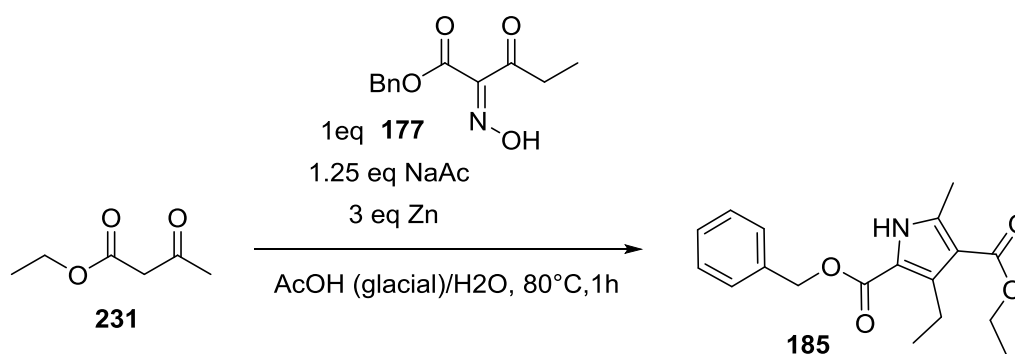
UHPLC-MS

R_t (MCS): 2.033 min

m/z: [M+H]⁺ (calc.) = 316.2

[M+H]⁺ (meas.) = 316.2

[2-benzyl 4-ethyl 3-ethyl-5-methyl-1H-pyrrole-2,4-dicarboxylate \(185\)](#)



487mg of **231** (3.74mmol, 1.1eq) and 349mg NaOAc (4.25mmol, 1.25eq) dissolved in 3mL glacial acetic acid, 800mg of **177** (3.40mmol, 1eq) dissolved in 1mL of a 1:1 mixture of glacial acetic acid/water and 667mg Zn (10.20mmol, 3eq) were used to synthesise **185**. After purification on 50g SiO₂ with a linear gradient of hept/EtOAc 4% → 20%, the product was isolated in 38% yield (384mg, 1.22mmol).

R_f (TLC, hept/EtOAc 4:1) = 0.28.

$^1\text{H-NMR}$ (400 MHz, CDCl_3):

δ = 8.88 (s, 1H, NH), 7.45 – 7.31 (m, 5H, Ph- H_{arom}), 5.31 (s, 2H, Ph CH_2), 4.29 (q, J = 7.1 Hz, 2H, OCH_2CH_3), 3.09 (q, J = 7.4 Hz, 2H, 3- CH_2CH_3), 2.50 (s, 3H, 5- CH_3), 1.35 (t, J = 7.1 Hz, 3H, OCH_2CH_3), 1.15 (t, J = 7.4 Hz, 3H, 3- CH_2CH_3).

$^{13}\text{C-NMR}$ (101 MHz, CDCl_3):

δ = 165.28 (1C, $\text{C}=\text{OOCH}_2\text{CH}_3$), 161.05 (1C, $\text{CH}_2\text{OC}=\text{O}$), 139.26 (1C, $\text{C}_{\text{q, arom}}$), 138.23 (1C, $\text{C}_{\text{q, arom}}$), 136.18 (1C, $\text{C}_{\text{q, arom}}$), 128.76 (2C, Ph- CH_{arom}), 128.44 (1C, Ph- CH_{arom}), 128.37 (2C, Ph- CH_{arom}), 117.05 (1C, $\text{C}_{\text{q, arom}}$), 113.06 (1C, $\text{C}_{\text{q, arom}}$), 66.21 (1C, $\text{CH}_2\text{OC}=\text{O}$), 59.70 (1C, $\text{C}=\text{OOCH}_2\text{CH}_3$), 19.24 (1C, 3- CH_2CH_3), 15.68 (1C, 3- CH_2CH_3), 14.59 (1C, $\text{C}=\text{OOCH}_2\text{CH}_3$), 14.48 (1C, 5- CH_3).

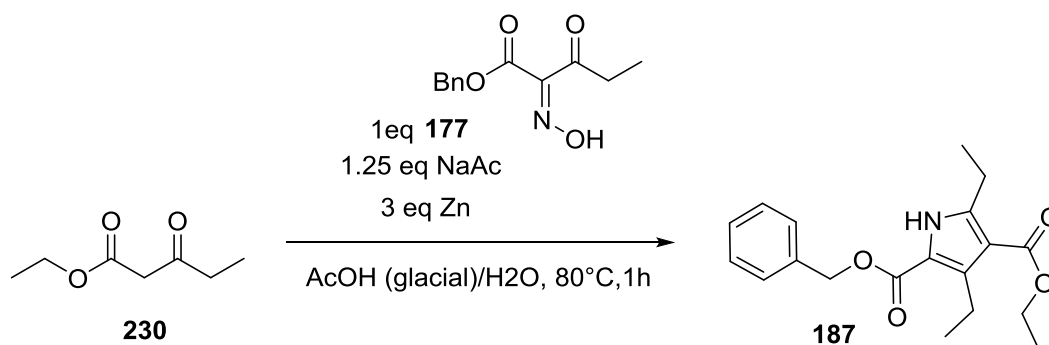
UHPLC-MS:

R_t (MCS): 2.127 min

m/z : $[\text{M}+\text{H}]^+$ (calc.) = 316.2

$[\text{M}+\text{H}]^+$ (meas.) = 316.2

[2-benzyl 4-ethyl 3,5-diethyl-1H-pyrrole-2,4-dicarboxylate \(**187**\)](#)



539mg of **230** (3.74mmol, 1.1eq) and 349mg NaOAc (4.25mmol, 1.25eq) dissolved in 3mL glacial acetic acid, 800mg of **177** (3.40mmol, 1eq) dissolved in 1mL of a 1:1 mixture of glacial acetic acid/water and 667mg Zn (10.20mmol, 3eq) were used to synthesise **187**. After purification on 50g SiO_2 with a linear gradient of hept/EtOAc 4% \rightarrow 15%, the product was isolated in 27% yield (307mg, 0.93mmol).

R_f (TLC, hept/EtOAc 4:1) = 0.34.

$^1\text{H-NMR}$ (400 MHz, CDCl_3):

δ = 8.93 (s, 1H, NH), 7.44 – 7.34 (m, 5H, Ph- H_{arom}), 4.29 (q, J = 7.1 Hz, 2H, OCH_2CH_3), 3.09 (q, J = 7.4 Hz, 2H, 3- CH_2CH_3), 2.94 (q, J = 7.5 Hz, 2H, 5- CH_2CH_3), 1.35 (t, J = 7.1 Hz, 3H, OCH_2CH_3), 1.25 (t, J = 7.6 Hz, 3H, 5- CH_2CH_3), 1.15 (t, J = 7.4 Hz, 3H, 3- CH_2CH_3).

$^{13}\text{C-NMR}$ (101 MHz, CDCl_3):

δ = 165.14 (1C, $\text{C}=\text{OOCH}_2\text{CH}_3$), 161.26 (1C, $\text{CH}_2\text{OC}=\text{O}$), 144.86 (1C, $\text{C}_{\text{q, arom}}$), 138.22 (1C, $\text{C}_{\text{q, arom}}$), 136.20 (1C, $\text{C}_{\text{q, arom}}$), 128.75 (2C, Ph- CH_{arom}), 128.41 (1C, Ph- CH_{arom}), 128.32 (2C, Ph- CH_{arom}), 117.09 (1C, $\text{C}_{\text{q, arom}}$), 112.24 (1C, $\text{C}_{\text{q, arom}}$), 66.21 (1C, $\text{CH}_2\text{OC}=\text{O}$), 59.68 (1C, $\text{C}=\text{OOCH}_2\text{CH}_3$), 21.66 (1C, 5- CH_2CH_3), 19.28 (1C, 3- CH_2CH_3), 15.68 (1C, 3- CH_2CH_3), 14.43 (1C, $\text{C}=\text{OOCH}_2\text{CH}_3$), 13.08 (1C, 5- CH_2CH_3).

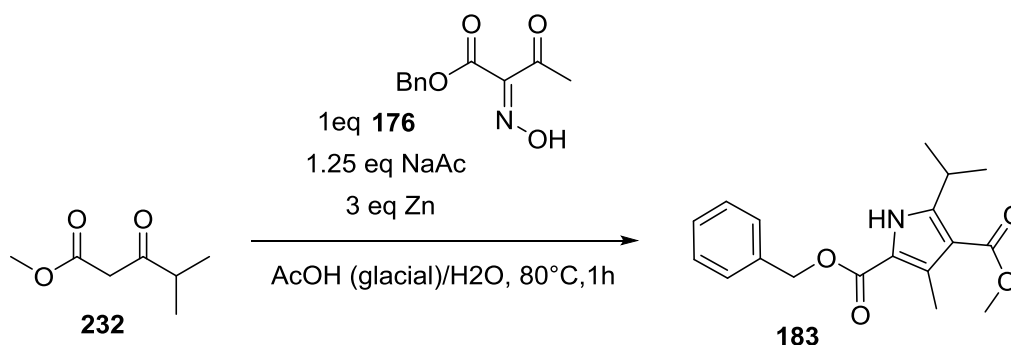
UHPLC-MS

R_t (MCS): 2.217 min

m/z: $[\text{M}+\text{H}]^+$ (calc.) = 330.2

$[\text{M}+\text{H}]^+$ (meas.) = 330.2

2-benzyl 4-methyl 5-isopropyl-3-methyl-1H-pyrrole-2,4-dicarboxylate (183)



574mg of **232** (3.98mmol, 1.1eq) and 371mg NaOAc (4.52mmol, 1.25eq) dissolved in 3mL glacial acetic acid, 800mg of **176** (3.62mmol, 1eq) dissolved in 1mL of a 1:1 mixture of glacial acetic acid/water and 709mg Zn (10.85mmol, 3eq) were used to synthesise **183**. After purification on 25g SiO_2 with a linear gradient of hept/EtOAc 3% \rightarrow 20%, the product was isolated as a white solid in 8% yield (94.2mg, 0.30mmol).

R_f (TLC, hept/EtOAc 4:1) = 0.41.

$^1\text{H-NMR}$ (400 MHz, CDCl_3):

δ = 8.84 (s, 1H, NH), 7.48 – 7.32 (m, 5H, Ph- H_{arom}), 5.33 (s, 2H, Ph CH_2), 3.82 (s, 3H, OCH_3), 3.79 – 3.70 (m, 1H, 5- $\text{CH}(\text{CH}_3)_2$), 2.56 (s, 3H, 3- CH_3), 1.26 (d, J = 7.0 Hz, 6H, 5- $\text{CH}(\text{CH}_3)_2$).

$^{13}\text{C-NMR}$ (101 MHz, CDCl_3):

δ = 165.81 (1C, $\text{C}=\text{OOCH}_3$), 161.60 (1C, $\text{CH}_2\text{OC}=\text{O}$), 148.83 (1C, $\text{C}_{\text{q, arom}}$), 136.26 (1C, $\text{C}_{\text{q, arom}}$), 131.34 (1C, $\text{C}_{\text{q, arom}}$), 128.76 (2C, CH_{arom}), 128.39 (1C, CH_{arom}), 128.29 (2C, CH_{arom}), 117.78 (1C, $\text{C}_{\text{q, arom}}$), 112.50 (1C, $\text{C}_{\text{q, arom}}$), 66.19 (1C, $\text{CH}_2\text{OC}=\text{O}$), 50.90 (1C, $\text{C}=\text{OOCH}_3$), 26.59 (1C, 5- $\text{CH}(\text{CH}_3)_2$), 21.77 (2C, 5- $\text{CH}(\text{CH}_3)_2$), 12.32 (1C, 3- CH_3).

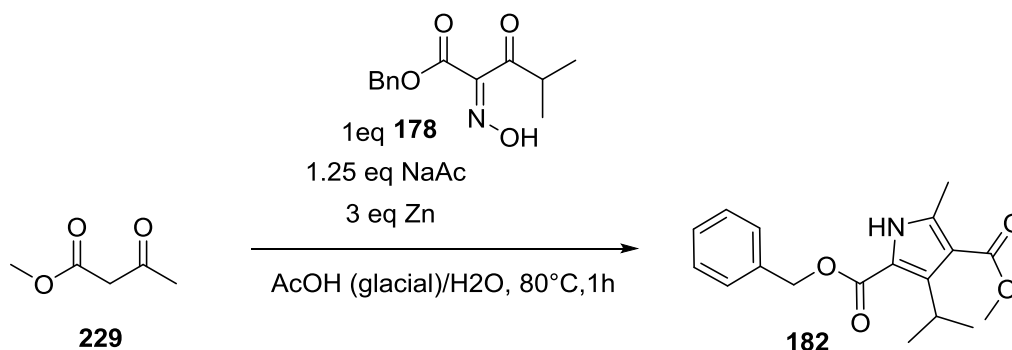
UHPLC-MS

R_t (MCS): 2.144 min

m/z: $[\text{M}+\text{H}]^+$ (calc.) = 316.2

$[\text{M}+\text{H}]^+$ (meas.) = 316.2

2-benzyl 4-methyl 3-isopropyl-5-methyl-1H-pyrrole-2,4-dicarboxylate (182)



205mg of **229** (1.77mmol, 1.1eq) and 165mg NaOAc (2.01mmol, 1.25eq) dissolved in 3mL glacial acetic acid, 400mg of **178** (1.60mmol, 1eq) dissolved in 1mL of a 1:1 mixture of glacial acetic acid/water and 315mg Zn (4.81mmol, 3eq) were used to synthesise **182**. After purification on 25g SiO_2 with a linear gradient of hept/EtOAc 3% \rightarrow 15%, the product was isolated as a white solid in 35% yield (175.5mg, 0.56mmol).

R_f (TLC, hept/EtOAc 4:1) = 0.29

$^1\text{H-NMR}$ (400 MHz, CDCl_3):

$\delta = 8.90$ (s, 1H, NH), 7.45 – 7.31 (m, 5H, Ph- H_{arom}), 5.30 (s, 2H, Ph CH_2), 4.20 – 3.96 (m, 1H, 3- $\text{CH}(\text{CH}_3)_2$), 3.82 (s, 3H, OCH_3), 2.44 (s, 3H, 5- CH_3), 1.32 (d, $J = 7.1$ Hz, 6H, 3- $\text{CH}(\text{CH}_3)_2$).

$^{13}\text{C-NMR}$ (101 MHz, CDCl_3):

$\delta = 165.96$ (1C, $\text{C}=\text{OOCH}_3$), 160.56 (1C, $\text{CH}_2\text{OC}=\text{O}$), 142.14 (1C, $\text{C}_{\text{q, arom}}$), 138.55 (1C, $\text{C}_{\text{q, arom}}$), 136.08 (1C, $\text{C}_{\text{q, arom}}$), 128.78 (2C, Ph- CH_{arom}), 128.58 (1C, Ph- CH_{arom}), 128.50 (2C, Ph- CH_{arom}), 116.76 (1C, $\text{C}_{\text{q, arom}}$), 113.27 (1C, $\text{C}_{\text{q, arom}}$), 66.29 (1C, $\text{CH}_2\text{OC}=\text{O}$), 51.00 (1C, $\text{C}=\text{OOCH}_3$), 25.03 (1C, 3- $\text{CH}(\text{CH}_3)_2$), 21.06 (2C, 3- $\text{CH}(\text{CH}_3)_2$), 14.68 (1C, 5- CH_3).

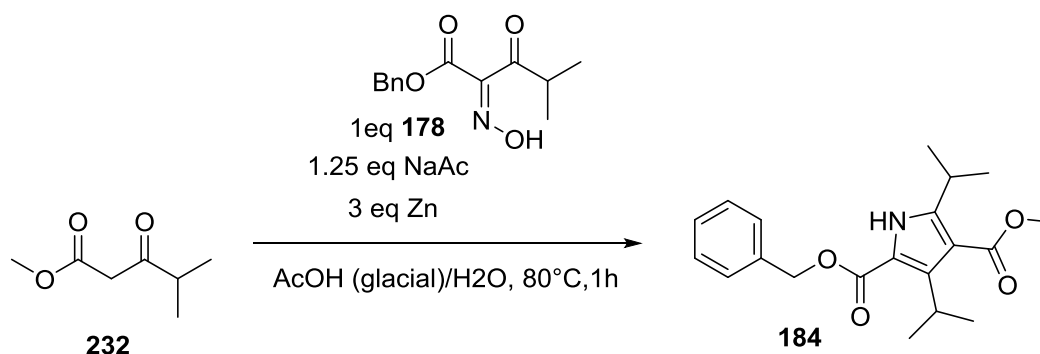
UHPLC-MS

R_t (MCS): 2.123 min

m/z : $[\text{M}+\text{H}]^+$ (calc.) = 316.2

$[\text{M}+\text{H}]^+$ (meas.) = 316.2

2-benzyl 4-methyl 3,5-diisopropyl-1H-pyrrole-2,4-dicarboxylate (**184**)



207mg of **232** (1.43mmol, 1.1eq) and 134mg NaOAc (1.63mmol, 1.25eq) dissolved in 3mL glacial acetic acid, 325mg of **178** (1.30mmol, 1eq) dissolved in 1mL of a 1:1 mixture of glacial acetic acid/water and 256mg Zn (3.91mmol, 3eq) were used to synthesise **184**. After purification on 25g SiO_2 with a linear gradient of hept/EtOAc 3% \rightarrow 20%, the product was isolated as a white solid in 28% yield (127mg, 0.37mmol).

R_f (TLC, hept/EtOAc 1:1) = 0.89.

$^1\text{H-NMR}$ (400 MHz, CDCl_3):

δ = 8.82 (s, 1H, NH), 7.44 – 7.34 (m, 5H, Ph- H_{arom}), 5.32 (s, 2H, Ph CH_2), 4.00 (dq, J = 14.3, 7.1 Hz, 1H, 3- $\text{CH}(\text{CH}_3)_2$), 3.82 (s, 1H), 3.64 – 3.54 (m, 1H, 5- $\text{CH}(\text{CH}_3)_2$), 1.31 (d, J = 7.1 Hz, 6H, 3- $\text{CH}(\text{CH}_3)_2$), 1.25 (d, J = 7.0 Hz, 6H, 5- $\text{CH}(\text{CH}_3)_2$).

$^{13}\text{C-NMR}$ (101 MHz, CDCl_3):

δ = 166.14 (1C, $\text{C}=\text{OOCH}_3$), 160.91 (1C, $\text{CH}_2\text{OC}=\text{O}$), 147.40 (1C, $\text{C}_{\text{q, arom}}$), 141.40 (1C, $\text{C}_{\text{q, arom}}$), 136.20 (1C, $\text{C}_{\text{q, arom}}$), 128.76, 128.45, 128.43, 116.76 (1C, $\text{C}_{\text{q, arom}}$), 112.29 (1C, $\text{C}_{\text{q, arom}}$), 66.28 (1C, $\text{CH}_2\text{OC}=\text{O}$), 51.06 (1C, $\text{C}=\text{OOCH}_3$), 26.64 (1C, 5- $\text{CH}(\text{CH}_3)_2$), 25.21 (1C, 3- $\text{CH}(\text{CH}_3)_2$), 21.95 (1C, 3- $\text{CH}(\text{CH}_3)_2$), 21.23 (1C, 5- $\text{CH}(\text{CH}_3)_2$).

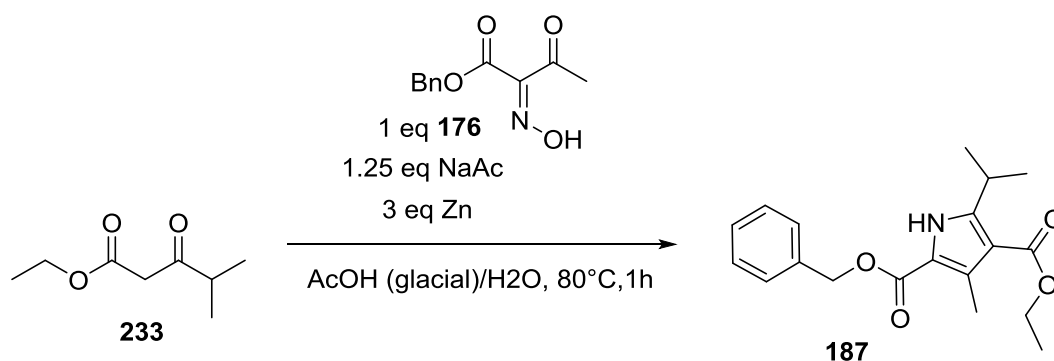
UHPLC-MS

R_t (MCS): 2.100 min

m/z: $[\text{M}+\text{H}]^+$ (calc.) = 344.2

$[\text{M}+\text{H}]^+$ (meas.) = 344.2

2-benzyl 4-ethyl 5-isopropyl-3-methyl-1H-pyrrole-2,4-dicarboxylate (**187**)



629mg of **233** (3.98mmol, 1.1eq) and 371mg NaOAc (4.52mmol, 1.25eq) dissolved in 3mL glacial acetic acid, 800mg of **176** (3.62mmol, 1eq) dissolved in 1mL of a 1:1 mixture of glacial acetic acid/water and 709mg Zn (10.85mmol, 3eq) were used to synthesise **187**. After purification on 50g SiO_2 with a linear gradient of hept/EtOAc 4% \rightarrow 20%, the product was isolated as a white solid in 8% yield (93.4mg, 0.28mmol).

R_f (TLC, hept/EtOAc 4:1) = 0.43

$^1\text{H-NMR}$ (400 MHz, CDCl_3):

$\delta = 8.83$ (s, 1H, NH), 7.45 – 7.32 (m, 5H, Ph- H_{arom}), 5.33 (s, 2H, Ph CH_2), 4.29 (q, $J = 7.1$ Hz, 2H, OCH_2CH_3), 3.85 – 3.67 (m, 1H, 5- $\text{CH}(\text{CH}_3)_2$), 2.57 (s, 3H, 3- CH_3), 1.35 (t, $J = 7.1$ Hz, 3H, OCH_2CH_3), 1.26 (d, $J = 7.0$ Hz, 6H, 5- $\text{CH}(\text{CH}_3)_2$).

$^{13}\text{C-NMR}$ (101 MHz, CDCl_3):

$\delta = 165.36$ (1C, $\text{C}=\text{OOCH}_2\text{CH}_3$), 161.63 (1C, $\text{CH}_2\text{OC}=\text{O}$), 148.69 (1C, $\text{C}_{\text{q, arom}}$), 136.28 (1C, $\text{C}_{\text{q, arom}}$), 131.41 (1C, $\text{C}_{\text{q, arom}}$), 128.76 (2C, Ph- CH_{arom}), 128.38 (1C, Ph- CH_{arom}), 128.27 (2C, Ph- CH_{arom}), 117.72 (1C, $\text{C}_{\text{q, arom}}$), 112.71 (1C, $\text{C}_{\text{q, arom}}$), 66.17 (1C, $\text{CH}_2\text{OC}=\text{O}$), 59.72 (1C, $\text{C}=\text{OOCH}_2\text{CH}_3$), 26.62 (1C, 5- $\text{CH}(\text{CH}_3)_2$), 21.75 (1C, 5- $\text{CH}(\text{CH}_3)_2$), 14.49 (1C, $\text{C}=\text{OOCH}_2\text{CH}_3$), 12.33 (1C, 3- CH_3).

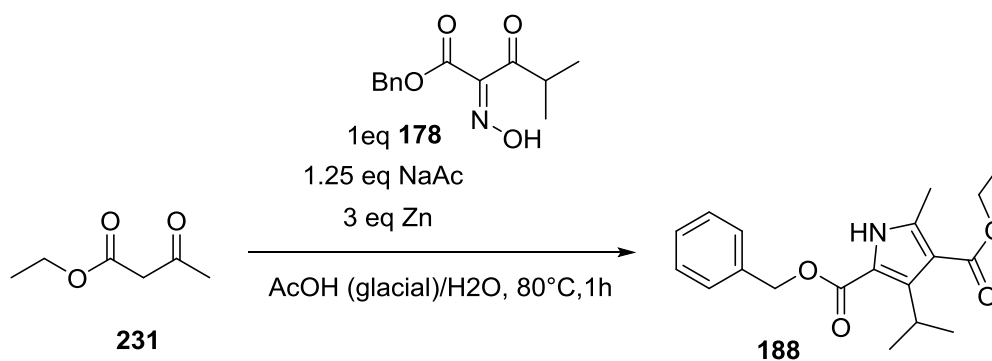
UHPLC-MS

R_t (MCS): 2.216 min

m/z : $[\text{M}+\text{H}]^+$ (calc.) = 330.2

$[\text{M}+\text{H}]^+$ (meas.) = 330.2

2-benzyl 4-ethyl 3-isopropyl-5-methyl-1H-pyrrole-2,4-dicarboxylate (**188**)



230mg of **231** (1.77mmol, 1.1eq) and 165mg NaOAc (2.01mmol, 1.25eq) dissolved in 3mL glacial acetic acid, 400mg of **178** (1.60mmol, 1eq) dissolved in 1mL of a 1:1 mixture of glacial acetic acid/water and 315mg Zn (4.81mmol, 3eq). were used to synthesise **188**. After purification on 25g SiO_2 with a linear gradient of hept/EtOAc 3% \rightarrow 15%, the product was isolated as a white solid in 37% yield (194mg, 0.59mmol).

R_f (TLC, hept/EtOAc 4:1) = 0.30.

$^1\text{H-NMR}$ (400 MHz, CDCl_3):

δ = 8.84 (s, 1H, NH), 7.47 – 7.31 (m, 5H, Ph- H_{arom}), 5.30 (s, 2H, Ph CH_2), 4.30 (q, J = 7.1 Hz, 2H, OCH_2CH_3), 4.15 – 3.99 (m, 1H, 3- $\text{CH}(\text{CH}_3)_2$), 2.45 (s, 3H, 5- CH_3), 1.41 – 1.29 (m, 9H, OCH_2CH_3 , 3- $\text{CH}(\text{CH}_3)_2$).

$^{13}\text{C-NMR}$ (101 MHz, CDCl_3):

δ = 165.55 (1C, $\text{C}=\text{OOCH}_2\text{CH}_3$), 160.54 (1C, $\text{CH}_2\text{OC}=\text{O}$), 142.08 (1C, $\text{C}_{\text{q, arom}}$), 138.41 (1C, $\text{C}_{\text{q, arom}}$), 136.12 (1C, $\text{C}_{\text{q, arom}}$), 128.78 (2C, Ph- CH_{arom}), 128.58 (1C, Ph- CH_{arom}), 128.50 (2C, Ph- CH_{arom}), 116.69 (1C, $\text{C}_{\text{q, arom}}$), 113.59 (1C, $\text{C}_{\text{q, arom}}$), 66.27 (1C, $\text{CH}_2\text{OC}=\text{O}$), 59.97 (1C, $\text{C}=\text{OOCH}_2\text{CH}_3$), 25.06 (1C, 3- $\text{CH}(\text{CH}_3)_2$), 21.09 (2C, 3- $\text{CH}(\text{CH}_3)_2$), 14.75 (1C, 5- CH_3), 14.49 (1C, $\text{C}=\text{OOCH}_2\text{CH}_3$).

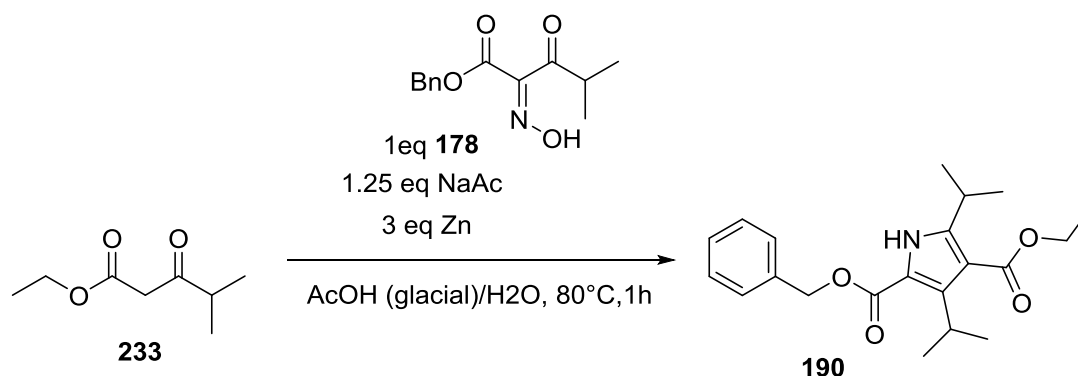
UHPLC-MS

R_t (MCS): 2.194 min

m/z : $[\text{M}+\text{H}]^+$ (calc.) = 330.2

$[\text{M}+\text{H}]^+$ (meas.) = 330.2

[2-benzyl 4-ethyl 3,5-diisopropyl-1H-pyrrole-2,4-dicarboxylate \(**190**\)](#)



227mg of **233** (1.43mmol, 1.1eq) and 134mg NaOAc (1.63mmol, 1.25eq) dissolved in 3mL glacial acetic acid, 325mg of **178** (1.30mmol, 1eq) dissolved in 1mL of a 1:1 mixture of glacial acetic acid/water and 256mg Zn (3.91mmol, 3eq) were used to synthesise **190**. After purification on 25g SiO_2 with a linear gradient of hept/EtOAc 3% \rightarrow 20%, the product was isolated as a white solid in 20% yield (94mg, 0.26mmol).

R_f (TLC, hept/EtOAc 1:1) = 0.81.

$^1\text{H-NMR}$ (400 MHz, CDCl_3):

δ = 8.80 (s, 1H, NH), 7.44 – 7.33 (m, 5H, Ph- H_{arom}), 5.33 (s, 2H, Ph CH_2), 4.30 (q, J = 7.1 Hz, 2H, OCH_2CH_3), 4.08 – 3.93 (m, 1H, 3- $\text{CH}(\text{CH}_3)_2$), 3.67 – 3.52 (m, 1H, 5- $\text{CH}(\text{CH}_3)_2$), 1.37 (t, J = 7.1 Hz, 3H, OCH_2CH_3), 1.32 (d, J = 7.1 Hz, 6H, 3- $\text{CH}(\text{CH}_3)_2$), 1.25 (d, J = 7.0 Hz, 6H, 5- $\text{CH}(\text{CH}_3)_2$).

$^{13}\text{C-NMR}$ (101 MHz, CDCl_3):

δ = 165.73 (1C, $\text{C}=\text{OOCH}_2\text{CH}_3$), 160.93 (1C, $\text{CH}_2\text{OC}=\text{O}$), 147.23 (1C, $\text{C}_{\text{q, arom}}$), 141.37 (1C, $\text{C}_{\text{q, arom}}$), 136.22 (1C, $\text{C}_{\text{q, arom}}$), 128.75 (2C, Ph- CH_{arom}), 128.43 (3C, Ph- CH_{arom}), 116.67 (1C, $\text{C}_{\text{q, arom}}$), 112.64 (1C, $\text{C}_{\text{q, arom}}$), 66.25 (1C, $\text{CH}_2\text{OC}=\text{O}$), 60.08 (1C, $\text{C}=\text{OOCH}_2\text{CH}_3$), 26.67 (1C, 5- $\text{CH}(\text{CH}_3)_2$), 25.23 (2C, 3- $\text{CH}(\text{CH}_3)_2$), 21.94 (1C, 5- $\text{CH}(\text{CH}_3)_2$), 21.25 (2C, 3- $\text{CH}(\text{CH}_3)_2$), 14.40 (1C, $\text{C}=\text{OOCH}_2\text{CH}_3$).

UHPLC-MS

R_t (MCS): 2.156 min

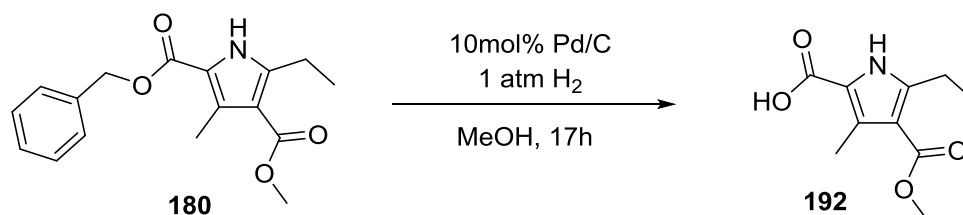
m/z: $[\text{M}+\text{H}]^+$ (calc.) = 358.2

$[\text{M}+\text{H}]^+$ (meas.) = 358.2

2.3.1.3 Benzyl ester deprotection of pyrrole

All following reactions were conducted after General Procedure E.

5-ethyl-4-(methoxycarbonyl)-3-methyl-1H-pyrrole-2-carboxylic acid (**192**)



117 mg of **180** (0.39mmol, 1eq) were dissolved in 10mL MeOH before 10mol% Pd/C was added and the flask put under H_2 -atmosphere. After the work-up, the product was isolated as a clear oil in 87% yield (72mg, 0.34mmol) and used without further purification.

R_f (TLC, hept/EtOAc 1:1) = 0.17.

$^1\text{H-NMR}$ (400 MHz, DMSO-d_6):

$\delta = 11.71$ (s, 1H, NH), 3.70 (s, 3H, OCH_3), 2.81 (q, $J = 7.4$ Hz, 2H, 5- CH_2CH_3), 2.44 (s, 3H, 3- CH_3), 1.09 (t, $J = 7.4$ Hz, 3H, 5- CH_2CH_3).

$^{13}\text{C-NMR}$ (101 MHz, DMSO-d_6):

$\delta = 165.07$ (1C, $\text{C}=\text{OOCH}_3$), 162.49 (1C, COOH), 144.63 (1C, $\text{C}_{\text{q, arom}}$), 142.05 (1C, $\text{C}_{\text{q, arom}}$), 118.76 (1C, $\text{C}_{\text{q, arom}}$), 111.03 (1C, $\text{C}_{\text{q, arom}}$), 50.45 (1C, $\text{C}=\text{OOCH}_3$), 20.30 (1C, 5- CH_2CH_3), 14.51 (1C, 5- CH_2CH_3), 11.83 (1C, 3- CH_3).

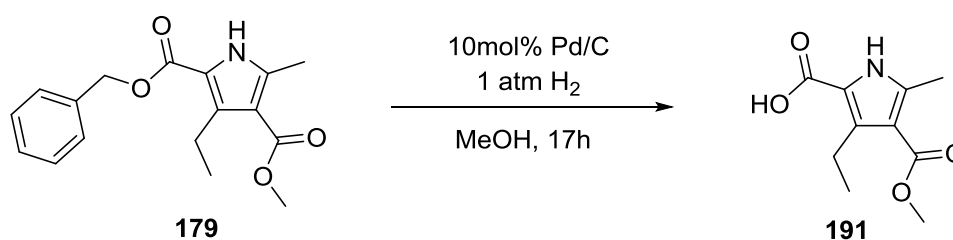
UHPLC-MS

R_t (MCS): 1.595 min

m/z: $[\text{M}+\text{H}]^+$ (calc.) = 226.1

$[\text{M}+\text{H}]^+$ (meas.) = 226.0

3-ethyl-4-(methoxycarbonyl)-5-methyl-1H-pyrrole-2-carboxylic acid (**191**)



321mg of **179** (1.07mmol, 1eq) were dissolved in 15mL MeOH before 10mol% Pd/C was added and the flask put under H_2 -atmosphere. After the work-up, the product was isolated as a clear oil in 92% yield (208mg, 0.99mmol) and used without further purification.

R_f (TLC, hept/EtOAc 1:1) = 0.36.

$^1\text{H-NMR}$ (400 MHz, CD_3OD):

$\delta = 3.79$ (s, 3H, $\text{C}=\text{OOCH}_3$), 3.08 (q, $J = 7.4$ Hz, 2H, 3- CH_2CH_3), 2.45 (s, 3H, 5- CH_3), 1.11 (t, $J = 7.4$ Hz, 3H, 3- CH_2CH_3).

^{13}C -NMR (101 MHz, CD_3OD):

$\delta = 167.60$ (1C, $\underline{\text{C}}=\text{OOCH}_3$), 164.31 (1C, $\text{C}=\text{OOH}$), 140.83 (1C, $\text{C}_{\text{q, arom}}$), 138.91 (1C, $\text{C}_{\text{q, arom}}$), 118.94 (1C, $\text{C}_{\text{q, arom}}$), 112.66 (1C, $\text{C}_{\text{q, arom}}$), 51.03 (1C, $\text{C}=\text{OO}\underline{\text{C}}\text{H}_3$), 19.69 (1C, $3\text{-}\underline{\text{C}}\text{H}_2\text{CH}_3$), 16.04 (1C, $3\text{-}\text{CH}_2\underline{\text{C}}\text{H}_3$), 13.85 (1C, $5\text{-}\text{CH}_3$).

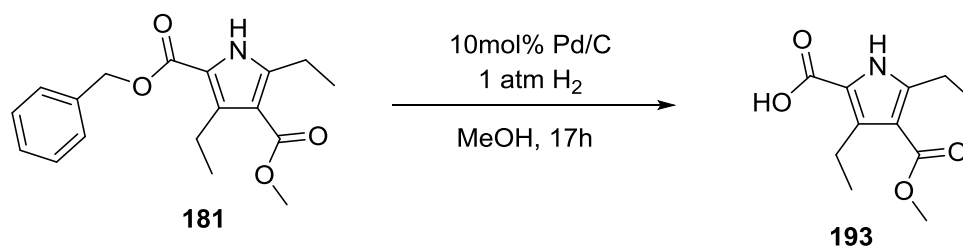
UHPLC-MS

R_{t} (MCS): 1.454 min

m/z: $[\text{M}+\text{H}]^+$ (calc.) = 212.1

$[\text{M}+\text{H}]^+$ (meas.) = 212.0

3,5-diethyl-4-(methoxycarbonyl)-1H-pyrrole-2-carboxylic acid (**193**)



265 mg of **181** (0.84mmol, 1eq) were dissolved in 15mL MeOH before 10mol% Pd/C was added and the flask put under H_2 -atmosphere. After the work-up, the product was isolated as a clear oil in 97% yield (183mg, 0.81mmol) and used without further purification.

R_{f} (TLC, hept/EtOAc 1:1) = 0.34

^1H -NMR (400 MHz, DMSO-d_6):

$\delta = 11.71$ (s, 1H, NH), 3.71 (s, 3H, OCH_3), 2.98 (q, $J = 7.0$ Hz, 2H, $3\text{-}\underline{\text{C}}\text{H}_2\text{CH}_3$), 2.81 (q, $J = 7.3$ Hz, 1H, $5\text{-}\underline{\text{C}}\text{H}_2\text{CH}_3$), 1.10 (t, $J = 7.4$ Hz, 1H, $5\text{-}\text{CH}_2\underline{\text{C}}\text{H}_3$), 1.04 (t, $J = 7.2$ Hz, 1H, $3\text{-}\text{CH}_2\underline{\text{C}}\text{H}_3$).

^{13}C -NMR (101 MHz, DMSO-d_6):

$\delta = 164.87$ (1C, $\underline{\text{C}}=\text{OOCH}_3$), 162.30 (1C, $\text{C}=\text{OOH}$), 144.61 (1C, $\text{C}_{\text{q, arom}}$), 135.53 (1C, $\text{C}_{\text{q, arom}}$), 117.96 (1C, $\text{C}_{\text{q, arom}}$), 110.13 (1C, $\text{C}_{\text{q, arom}}$), 50.47 (1C, $\text{C}=\text{OO}\underline{\text{C}}\text{H}_3$), 20.37 (1C, $5\text{-}\underline{\text{C}}\text{H}_2\text{CH}_3$), 18.29 (1C, $3\text{-}\underline{\text{C}}\text{H}_2\text{CH}_3$), 15.82 (1C, $5\text{-}\text{CH}_2\underline{\text{C}}\text{H}_3$), 14.51 (1C, $3\text{-}\text{CH}_2\underline{\text{C}}\text{H}_3$).

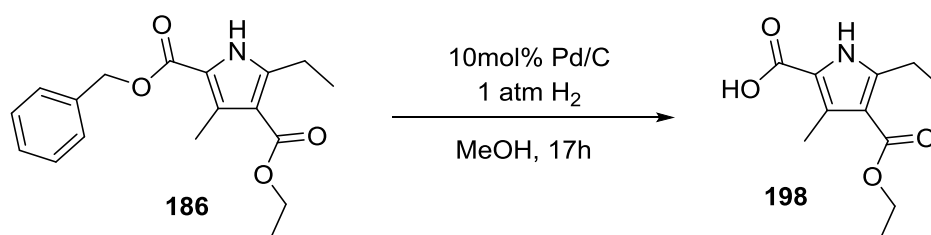
UHPLC-MS

R_t (MCS): 1.579 min

m/z: [M+H]⁺ (calc.) = 226.1

[M+H]⁺ (meas.) = 226.2

4-(ethoxycarbonyl)-5-ethyl-3-methyl-1H-pyrrole-2-carboxylic acid (198)



363 mg of **186** (1.15mmol, 1eq) were dissolved in 15mL MeOH before 10mol% Pd/C was added and the flask put under H₂-atmosphere. After the work-up, the product was isolated as a yellow oil in 78% yield (201mg, 0.89mmol) and used without further purification.

R_f (TLC, hept/EtOAc 1:1) = 0.23

¹H-NMR (400 MHz, DMSO-d₆):

δ = 11.71 (s, 1H, NH), 4.17 (q, *J* = 7.1 Hz, 2H, OCH₂CH₃), 2.82 (q, *J* = 7.4 Hz, 2H, 5-CH₂CH₃), 2.44 (s, 3H, 3-CH₃), 1.26 (t, *J* = 7.1 Hz, 3H, OCH₂CH₃), 1.10 (t, *J* = 7.4 Hz, 3H, 5-CH₂CH₃).

¹³C-NMR (101 MHz, DMSO-d₆):

δ = 164.54 (1C, C=OOCH₂CH₃), 162.34 (1C, C=OOH), 144.68 (1C, C_q, arom), 128.92 (1C, C_q, arom), 118.31 (1C, C_q, arom), 111.24 (1C, C_q, arom), 58.83 (1C, C=OOCH₂CH₃), 20.35 (1C, 5-CH₂CH₃), 14.49 (1C, C=OOCH₂CH₃), 14.24 (1C, 5-CH₂CH₃), 11.76 (1C, 3-CH₃).

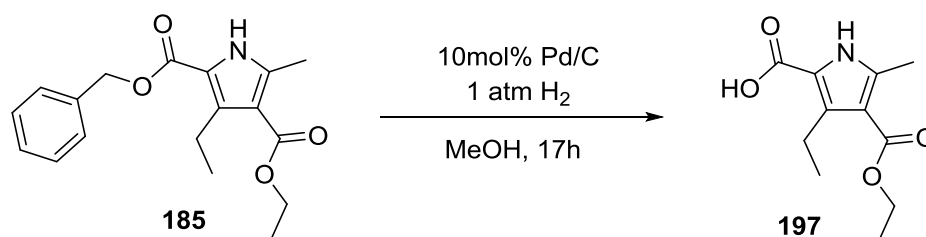
UHPLC-MS

R_t (MCS): 1.595 min

m/z: [M+H]⁺ (calc.) = 226.1

[M+H]⁺ (meas.) = 226.0

4-(ethoxycarbonyl)-3-ethyl-5-methyl-1H-pyrrole-2-carboxylic acid (197)



290 mg of **185** (0.92mmol, 1eq) were dissolved in 15mL MeOH before 10mol% Pd/C was added and the flask put under H₂-atmosphere. After the work-up, the product was isolated as a yellow oil in 102% yield (211mg, 0.94mmol) and used without further purification.

R_f (TLC, hept/EtOAc 1:1) = 0.21

¹H-NMR (400 MHz, CD₃OD):

δ = 4.26 (q, *J* = 7.1 Hz, 2H, OCH₂CH₃), 3.09 (q, *J* = 7.0 Hz, 2H, 3-CH₂CH₃), 2.45 (s, 3H, 5-CH₃), 1.36 (t, *J* = 7.2 Hz, 3H, OCH₂CH₃), 1.12 (t, *J* = 7.3 Hz, 3H, 3-CH₂CH₃).

¹³C-NMR (101 MHz, CD₃OD):

δ = 167.20 (1C, C=OOCH₂CH₃), 164.35 (1C, C=OOH), 140.79 (1C, C_{q, arom}), 138.77 (1C, C_{q, arom}), 118.95 (1C, C_{q, arom}), 112.82 (1C, C_{q, arom}), 60.52 (1C, C=OOCH₂CH₃), 19.72 (1C, 3-CH₂CH₃), 16.08 (1C, 3-CH₂CH₃), 14.72 (1C, C=OOCH₂CH₃), 13.90 (1C, 5-CH₃).

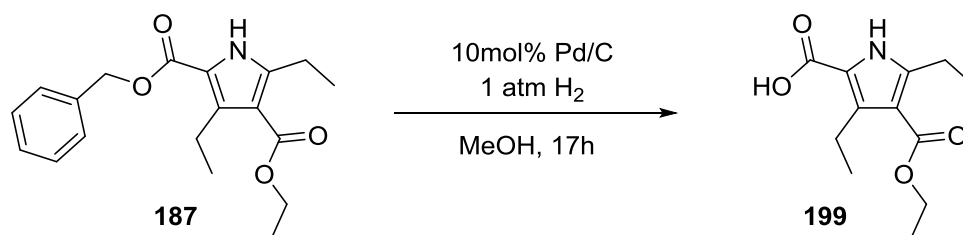
UHPLC-MS

R_t (MCS): 1.591 min

m/z: [M+H]⁺ (calc.) = 226.1

[M+H]⁺ (meas.) = 226.2

4-(ethoxycarbonyl)-3,5-diethyl-1H-pyrrole-2-carboxylic acid (199)



304 mg of **187** (0.92mmol, 1eq) were dissolved in 15mL MeOH before 10mol% Pd/C was added and the flask put under H₂-atmosphere. After the work-up, the product was isolated as a yellow oil in 100% yield (220mg, 0.92mmol) and used without further purification.

R_f (TLC, hept/EtOAc 1:1) = 0.23.

¹H-NMR (400 MHz, CD₃OD):

δ = 4.26 (q, *J* = 7.1 Hz, 2H, OCH₂CH₃), 3.09 (q, *J* = 7.3 Hz, 2H, 3-CH₂CH₃), 2.90 (q, *J* = 7.5 Hz, 2H, 5-CH₂CH₃), 1.36 (t, *J* = 7.1 Hz, 3H, OCH₂CH₃), 1.20 (t, *J* = 7.5 Hz, 3H, 5-CH₂CH₃), 1.12 (t, *J* = 7.4 Hz, 3H, 3-CH₂CH₃).

¹³C-NMR (101 MHz, CD₃OD):

δ = 166.98 (C=OOCH₂CH₃), 164.43 (C=OOH), 146.64 (1C, C_q, arom), 138.77 (1C, C_q, arom), 119.03 (1C, C_q, arom), 111.93 (1C, C_q, arom), 60.53 (C=OOCH₂CH₃), 22.02 (1C, 5-CH₂CH₃), 19.75 (1C, 3-CH₂CH₃), 16.08 (1C, 3-CH₂CH₃), 14.69 (C=OOCH₂CH₃), 14.66 (1C, 5-CH₂CH₃).

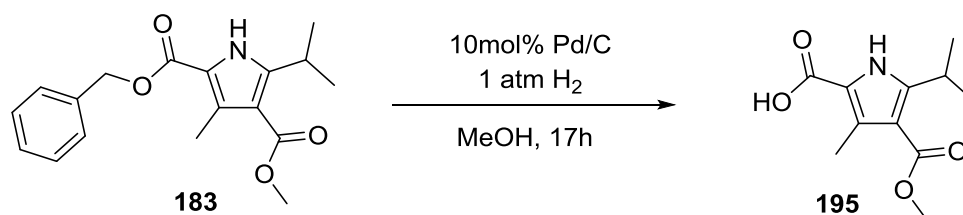
UHPLC-MS

R_t (MCS): 1.693 min

m/z: [M+H]⁺ (calc.) = 240.1

[M+H]⁺ (meas.) = 240.2

5-isopropyl-4-(methoxycarbonyl)-3-methyl-1H-pyrrole-2-carboxylic acid (195)



107 mg of **183** (0.34mmol, 1eq) were dissolved in 10mL MeOH before 10mol% Pd/C was added and the flask put under H₂-atmosphere. After the work-up, the product was isolated as a yellow oil in 99% yield (76mg, 0.34mmol) and used without further purification.

R_f (TLC, hept/EtOAc 1:1) = 0.14.

¹H-NMR (400 MHz, CD₃OD):

δ = 3.79 (s, 3H, OCH₃), 3.78 – 3.71 (m, 1H, CH(CH₃)₂), 2.51 (s, 3H, 3-CH₃), 1.27 (d, J = 7.1 Hz, 6H, CH(CH₃)₂).

¹³C-NMR (101 MHz, CD₃OD):

δ = 167.74 (1C, C=OOC₃H₇), 164.86 (1C, C=OOH), 150.15 (1C, C_q, arom), 131.51 (1C, C_q, arom), 120.15 (1C, C_q, arom), 112.55 (1C, C_q, arom), 51.09 (1C, C=OOC₃H₇), 27.67 (1C, 5-CH(CH₃)₂), 21.84 (2C, 5-CH(CH₃)₂), 12.30 (1C, 3-CH₃).

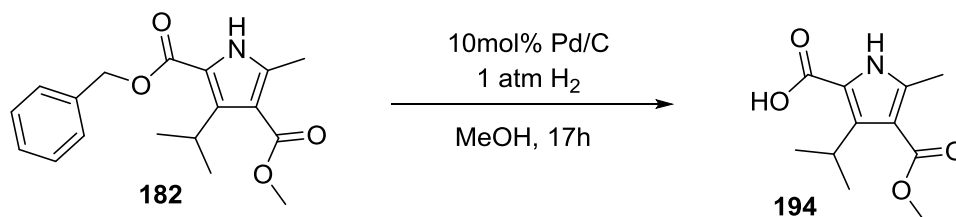
UHPLC-MS

R_t (MCS): 1.584 min

m/z: [M+H]⁺ (calc.) = 226.1

[M+H]⁺ (meas.) = 226.2

3-isopropyl-4-(methoxycarbonyl)-5-methyl-1H-pyrrole-2-carboxylic acid (194)



169 mg of **182** (0.53mmol, 1eq) were dissolved in 10mL MeOH before 10mol% Pd/C was added and the flask put under H₂-atmosphere. After the work-up, the product was isolated as yellow oil in 99% yield (120mg, 0.53mmol) and used without further purification.

R_f (TLC, hept/EtOAc 1:1) = 0.34.

¹H-NMR (400 MHz, CDCl₃):

δ = 9.03 (s, 1H, NH), 4.19 – 3.96 (m, 1H, 3-CH(CH₃)₂), 3.84 (s, 3H, OCH₃), 2.48 (s, 3H, 5-CH₃), 1.34 (d, *J*=7.1 Hz, 6H, 3-CH(CH₃)₂)

¹³C-NMR (101 MHz, CDCl₃):

δ = 166.01 (1C, C=OOCH₃), 165.85 (1C, C=OOH), 143.97 (1C, C_{q, arom}), 139.59 (1C, C_{q, arom}), 116.17 (1C, C_{q, arom}), 113.81 (1C, C_{q, arom}), 51.11 (1C, C=OOCH₃), 25.08 (1C, 3-CH(CH₃)₂), 20.97 (2C, 3-CH(CH₃)₂), 14.82 (1C, 5-CH₃).

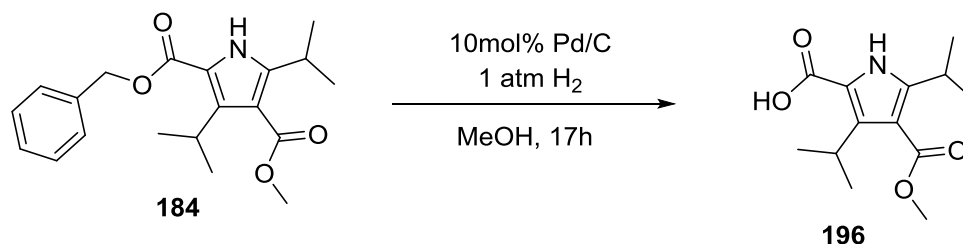
UHPLC-MS

R_t (MCS): 1.571 min

m/z: [M+H]⁺ (calc.) = 226.1

[M+H]⁺ (meas.) = 226.2

3,5-diisopropyl-4-(methoxycarbonyl)-1H-pyrrole-2-carboxylic acid (196)



122 mg of **184** (0.35mmol, 1eq) were dissolved in 10mL MeOH before 10mol% Pd/C was added and the flask put under H₂-atmosphere. After the work-up, the product was isolated as a yellow oil in 90% yield (81mg, 0.32mmol) and used without further purification.

R_f (TLC, hept/EtOAc 1:1) = 0.37

¹H-NMR (400 MHz, CDCl₃):

δ = 8.92 (s, 1H, NH), 4.09 – 3.93 (m, 1H, 3-CH(CH₃)₂), 3.84 (s, 3H, OCH₃), 3.72 – 3.52 (m, 1H, 5-CH(CH₃)₂), 1.34 (d, *J* = 6.3 Hz, 6H, 3-CH(CH₃)₂), 1.28 (d, *J* = 6.2 Hz, 6H, 5-CH(CH₃)₂).

¹³C-NMR (101 MHz, CDCl₃):

δ = 166.07 (1C, C=OOCH₃), 165.99 (1C, C=OOH), 148.36 (1C, C_q, arom), 143.49 (1C, C_q, arom), 116.09 (1C, C_q, arom), 112.81 (1C, C_q, arom), 51.16 (1C, C=OOCH₃), 26.72 (1C, 5-CH(CH₃)₂), 25.23 (1C, 3-CH(CH₃)₂), 21.90 (2C, 5-CH(CH₃)₂), 21.10 (2C, 3-CH(CH₃)₂).

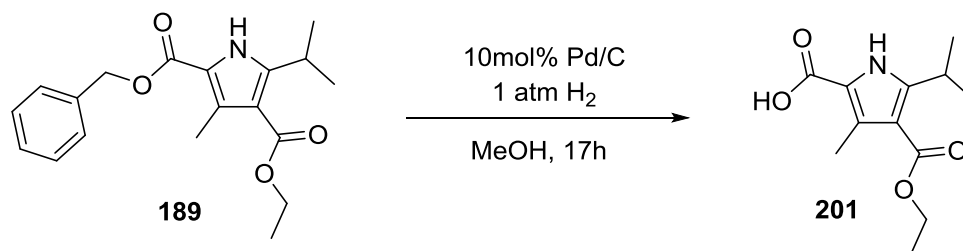
UHPLC-MS

R_t (MCS): 1.649 min

m/z: [M+H]⁺ (calc.) = 254.1

[M+H]⁺ (meas.) = 254.2

4-(ethoxycarbonyl)-5-isopropyl-3-methyl-1H-pyrrole-2-carboxylic acid (201)



163 mg of **189** (0.49mmol, 1eq) were dissolved in 10mL MeOH before 10mol% Pd/C was added and the flask put under H₂-atmosphere. After the work-up, the product was isolated as a yellow oil in 102% yield (121mg, 0.50mmol) and used without further purification.

R_f (TLC, hept/EtOAc 1:1) = 0.16.

¹H-NMR (400 MHz, CDCl₃):

δ = 8.89 (s, 1H, NH), 4.31 (q, *J* = 7.1 Hz, 2H, OCH₂CH₃), 3.86 – 3.69 (m, 1H, CH(CH₃)₂), 2.59 (s, 3H, 3-CH₃) 1.37 (t, *J* = 7.1 Hz, 3H, OCH₂CH₃), 1.29 (d, *J* = 6.9 Hz, 6H, CH(CH₃)₂).

¹³C-NMR (101 MHz, CDCl₃):

δ = 166.40 (1C, C=OOCH₂CH₃), 165.21 (1C, C=OOH), 149.62 (1C, C_q, arom), 133.73 (1C, C_q, arom), 116.98 (1C, C_q, arom), 113.23 (1C, C_q, arom), 59.84 (1C, C=OOCH₂CH₃), 26.69 (1C, 5-CH(CH₃)₂), 21.71 (2C, 5-CH(CH₃)₂), 14.51 (1C, C=OOCH₂CH₃), 12.27 (1C, 3-CH₃).

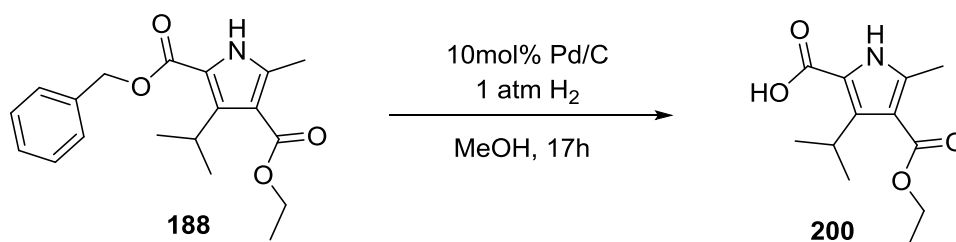
UHPLC-MS

R_t (MCS): 1.695 min

m/z: [M+H]⁺ (calc.) = 240.1

[M+H]⁺ (meas.) = 240.2

4-(ethoxycarbonyl)-3-isopropyl-5-methyl-1H-pyrrole-2-carboxylic acid (200)



185 mg of **188** (0.56mmol, 1eq) were dissolved in 10mL MeOH before 10mol% Pd/C was added and the flask put under H₂-atmosphere. After the work-up, the product was isolated as a yellow oil in 100% yield (135mg, 0.56mmol) and used without further purification.

R_f (TLC, hept/EtOAc 1:1) = 0.34.

¹H-NMR (400 MHz, CD₃OD):

δ = 4.26 (q, *J* = 7.1 Hz, 2H, OCH₂CH₃), 4.11 (hept, *J* = 7.1 Hz, 1H, 3-CH(CH₃)₂), 2.41 (s, 3H, 5-CH₃), 1.36 (t, *J* = 7.1 Hz, 2H), 1.31 (d, *J* = 7.1 Hz, 6H, 3-CH(CH₃)₂).

¹³C-NMR (101 MHz, CD₃OD):

δ = 167.49 (1C, C=OOCH₂CH₃), 164.21 (1C, C=OOH), 142.18 (1C, C_q, arom), 140.09 (1C, C_q, arom), 118.68 (1C, C_q, arom), 113.38 (1C, C_q, arom), 60.73 (1C, C=OOCH₂CH₃), 25.85 (1C, CH(CH₃)₂), 21.41 (2C, CH(CH₃)₂), 14.73 (1C, 5-CH₃), 14.06 (1C, C=OOCH₂CH₃).

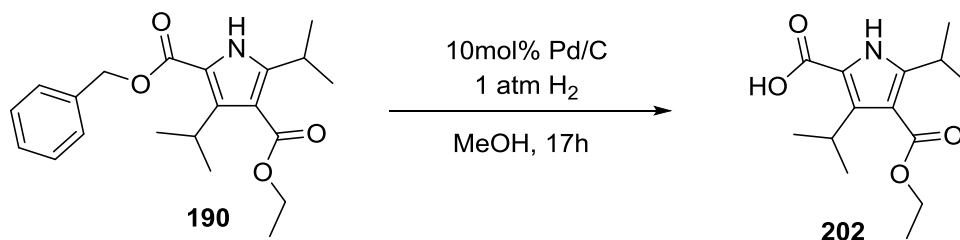
UHPLC-MS

R_t (MCS): 1.689 min

m/z: [M+H]⁺ (calc.) = 240.1

[M+H]⁺ (meas.) = 240.2

4-(ethoxycarbonyl)-3,5-diisopropyl-1H-pyrrole-2-carboxylic acid (**202**)



89mg of **190** (0.25mmol, 1eq) were dissolved in 10mL MeOH before 10mol% Pd/C was added and the flask put under H₂-atmosphere. After the work-up, the product was isolated as a yellow oil in 97% yield (64mg, 0.24mmol) and used without further purification.

R_f (TLC, hept/EtOAc 1:1) = 0.37

¹H-NMR (400 MHz, CDCl₃):

δ = 8.89 (s, 1H, NH), 4.31 (q, *J* = 7.1 Hz, 2H, OCH₂CH₃), 4.10 – 3.94 (m, 1H, 3-CH(CH₃)₂), 3.70 – 3.51 (m, 1H, 5-CH(CH₃)₂), 1.41 – 1.32 (m, 9H, OCH₂CH₃, 3-CH(CH₃)₂), 1.28 (d, *J* = 7.0 Hz, 6H, 5-CH(CH₃)₂).

¹³C-NMR (101 MHz, CDCl₃):

δ = 166.01 (1C, C=OOCH₂CH₃), 165.57 (1C, COOH), 148.19 (1C, C_q, arom), 143.44 (1C, C_q, arom), 115.99 (1C, C_q, arom), 113.17 (1C, C_q, arom), 60.19 (1C, C=OOCH₂CH₃), 26.74 (1C, 5-CH(CH₃)₂), 25.25 (1C, 3-CH(CH₃)₂), 21.89 (2C, 3-CH(CH₃)₂), 21.13 (2C, 5-CH(CH₃)₂), 14.40 (1C, C=OOCH₂CH₃).

UHPLC-MS

R_t (MCS): 1.736 min

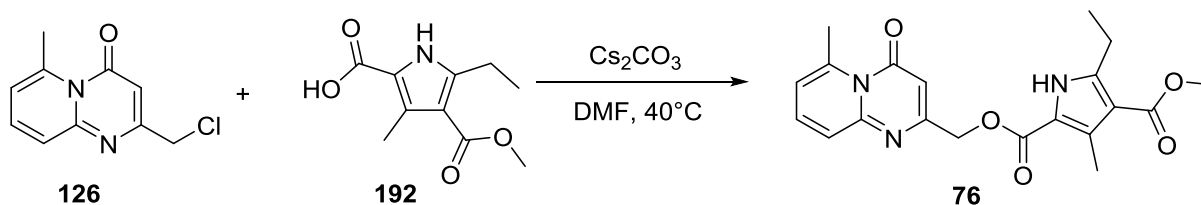
m/z: [M+H]⁺ (calc.) = 268.2

[M+H]⁺ (meas.) = 268.2

2.3.1.4 Pyrrole substituent modified final compounds

All following reactions follow the **General Procedure G**.

4-methyl 2-((6-methyl-4-oxo-4H-pyrido[1,2-a]pyrimidin-2-yl)methyl) 5-ethyl-3-methyl-1H-pyrrole-2,4-dicarboxylate (76)



102mg of **126** (0.49mmol, 1.5eq), 69mg of **192** (0.33mmol, 1eq) and 319mg Cs_2CO_3 (0.98mmol, 3eq) were stirred in 8mL DMF at 40°C for 16h. After the work-up, the crude was purified through column chromatography with 25g SiO_2 and a linear gradient of hept/EtOAc 30%-->100%. The product was isolated as a white solid in 41% yield (51mg, 0.13mmol).

R_f (TLC, DCM/MeH 2%) = 0.27.

$^1\text{H-NMR}$ (400 MHz, DMSO-d_6):

δ = 12.03 (s, 1H, NH), 7.68 (dd, J = 8.9, 7.0 Hz, 1H, 8- H_{arom}), 7.38 (d, J = 8.8 Hz, 1H, 9- H_{arom}), 6.93 (d, J = 6.9 Hz, 1H, 7- H_{arom}), 6.29 (s, 1H, C=OCH), 5.17 (s, 2H, $\text{CH}_2\text{OC=O}$), 3.73 (s, 3H, C=OOCH₃), 2.93 (s, 3H, 6-CH₃), 2.87 (q, J = 7.4 Hz, 2H, 5'-CH₂CH₃), 2.51 (s, 3H, 3'-CH₃), 1.14 (t, J = 7.4 Hz, 3H, 5'-CH₂CH₃).

$^{13}\text{C-NMR}$ (101 MHz, DMSO-d_6):

δ = 164.79 (1C, C=OOCH₃), 161.20 (1C, C=OCH), 160.85 (1C, CH₂OC=O), 159.82 (1C, C_q, arom), 153.17 (1C, C_q, arom), 145.92 (1C, C_q, arom), 143.39 (1C, C_q, arom), 136.70 (1C, 8-CH_{arom}), 130.71 (1C, C_q, arom), 124.46 (1C, 9-CH_{arom}), 118.65 (1C, 7-CH_{arom}), 116.82 (1C, C_q, arom), 111.65 (1C, C_q, arom), 101.79 (1C, C=OCH), 63.90 (1C, CH₂OC=O), 50.60 (1C, C=OOCH₃), 23.97 (1C, 6-CH₃), 20.35 (1C, 5'-CH₂CH₃), 14.45 (1C, 5'-CH₂CH₃), 11.89 (1C, 3'-CH₃).

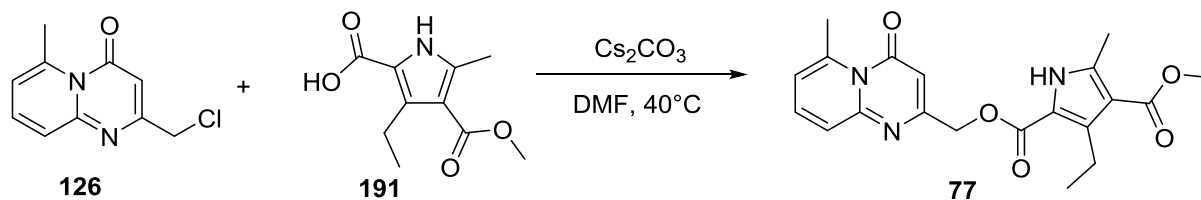
UHPLC-MS

R_t (MCS): 1.702 min

m/z : $[\text{M}+\text{H}]^+$ (calc.) = 384.2

$[\text{M}+\text{H}]^+$ (meas.) = 384.2

4-methyl 2-((6-methyl-4-oxo-4H-pyrido[1,2-a]pyrimidin-2-yl)methyl) 3-ethyl-5-methyl-1H-pyrrole-2,4-dicarboxylate (77)



74mg of **126** (0.36mmol, 1.5eq), 50mg of **191** (0.24mmol, 1eq) and 232mg Cs_2CO_3 (0.71mmol, 3eq) were stirred in 4mL DMF at 40°C for 16h. After the work-up, the crude was purified through column chromatography with 10g SiO_2 and a linear gradient of hept/EtOAc 40%-->100%. The product was isolated as white solid in 35% yield (32mg, 0.08mmol).

R_f (TLC, hept/EtOAc 1:1) = 0.14.

$^1\text{H-NMR}$ (400 MHz, DMSO-d_6):

δ = 12.05 (s, 1H, NH), 7.68 (dd, J = 8.9, 7.0 Hz, 1H, 8- H_{arom}), 7.38 (d, J = 8.9 Hz, 1H, 9- H_{arom}), 6.93 (d, J = 6.9 Hz, 1H, 7- H_{arom}), 6.29 (s, 1H, $\text{C}=\text{OCH}$), 5.18 (s, 2H, $\text{CH}_2\text{OC}=\text{O}$), 3.73 (s, 3H, $\text{C}=\text{OOCH}_3$), 3.04 (q, J = 7.3 Hz, 2H, 3'- CH_2CH_3), 2.93 (s, 3H, 6- CH_3), 2.44 (s, 3H, 5'- CH_3), 1.08 (t, J = 7.3 Hz, 3H, 3'- CH_2CH_3).

$^{13}\text{C-NMR}$ (101 MHz, DMSO-d_6):

δ = 164.74 (1C, $\text{C}=\text{OOCH}_3$), 161.23 (1C, $\text{C}=\text{OCH}$), 160.87 (1C, $\text{CH}_2\text{OC}=\text{O}$), 159.56 (1C, C_q , arom), 153.20 (1C, C_q , arom), 143.43 (1C, C_q , arom), 140.16 (1C, C_q , arom), 137.61 (1C, C_q , arom), 136.75 (1C, 8- CH_{arom}), 124.48 (1C, 9- CH_{arom}), 118.68 (1C, 7- CH_{arom}), 116.10 (1C, C_q , arom), 111.59 (1C, C_q , arom), 101.73 (1C, $\text{C}=\text{OCH}$), 63.90 (1C, $\text{CH}_2\text{OC}=\text{O}$), 50.62 (1C, $\text{C}=\text{OOCH}_3$), 24.02 (1C, 6- CH_3), 18.44 (1C, 3'- CH_2CH_3), 15.67 (1C, 3'- CH_2CH_3), 11.89 (1C, 5'- CH_3).

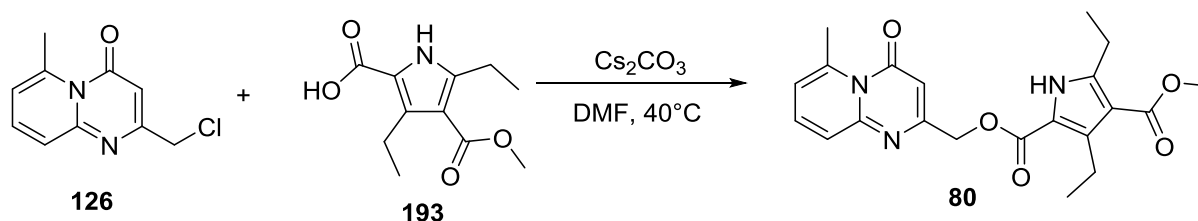
UHPLC-MS

R_t (MCS): 1.699 min

m/z: $[\text{M}+\text{H}]^+$ (calc.) = 384.2

$[\text{M}+\text{H}]^+$ (meas.) = 384.2

4-methyl 2-((6-methyl-4-oxo-4H-pyrido[1,2-a]pyrimidin-2-yl)methyl) 3,5-diethyl-1H-pyrrole-2,4-dicarboxylate (80)



69mg of **126** (0.33mmol, 1.5eq), 50mg of **193** (0.22mmol, 1eq) and 217mg Cs_2CO_3 (0.67mmol, 3eq) were stirred in 4mL DMF at 40°C for 16h. After the work-up, the crude was purified through column chromatography with 10g SiO_2 and a linear gradient of hept/EtOAc 40%-->100%. The product was isolated as a white solid in 55% yield (46mg, 0.11mmol).

R_f (TLC, hept/EtOAc 1:1) = 0.15.

$^1\text{H-NMR}$ (400 MHz, DMSO-d_6):

δ = 12.01 (s, 1H, NH), 7.67 (dd, J = 8.9, 7.0 Hz, 1H, 8- H_{arom}), 7.38 (d, J = 8.6 Hz, 1H, 9- H_{arom}), 6.92 (d, J = 6.9 Hz, 1H, 7- H_{arom}), 6.29 (s, 1H, C=OCH), 5.17 (s, 2H, $\text{CH}_2\text{OC=O}$), 3.74 (s, 3H, C=OOCH₃), 3.03 (q, J = 7.3 Hz, 2H, 3'- CH_2CH_3), 2.93 (s, 3H, 6- CH_3), 2.86 (q, J = 7.4 Hz, 2H, 5'- CH_2CH_3), 1.14 (t, J = 7.4 Hz, 3H, 5'- CH_2CH_3), 1.08 (t, J = 7.3 Hz, 3H, 3'- CH_2CH_3).

$^{13}\text{C-NMR}$ (101 MHz, DMSO-d_6):

δ = 164.65 (1C, C=OOCH₃), 161.27 (1C, C=OCH), 160.97 (1C, $\text{CH}_2\text{OC=O}$), 159.65 (1C, $\text{C}_{\text{q, arom}}$), 153.23 (1C, $\text{C}_{\text{q, arom}}$), 145.94 (1C, $\text{C}_{\text{q, arom}}$), 143.45 (1C, $\text{C}_{\text{q, arom}}$), 137.49 (1C, $\text{C}_{\text{q, arom}}$), 136.79 (1C, 8- CH_{arom}), 124.50 (1C, 9- CH_{arom}), 118.73 (1C, 7- CH_{arom}), 116.21 (1C, $\text{C}_{\text{q, arom}}$), 110.77 (1C, $\text{C}_{\text{q, arom}}$), 101.80 (1C, C=OCH), 63.97 (1C, $\text{CH}_2\text{OC=O}$), 50.69 (1C, C=OOCH₃), 24.04 (1C, 6- CH_3), 20.48 (1C, 5'- CH_2CH_3), 18.53 (1C, 3'- CH_2CH_3), 15.70 (1C, 3'- CH_2CH_3), 14.53 (1C, 5'- CH_2CH_3).

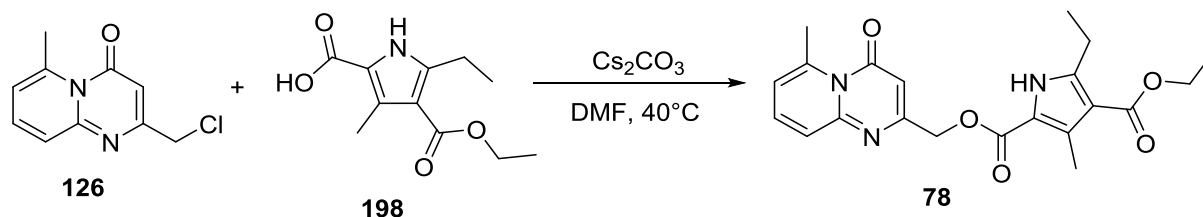
UHPLC-MS

R_t (MCS): 1.779 min

m/z : $[\text{M}+\text{H}]^+$ (calc.) = 398.2

$[\text{M}+\text{H}]^+$ (meas.) = 398.2

4-ethyl 2-((6-methyl-4-oxo-4H-pyrido[1,2-a]pyrimidin-2-yl)methyl) 5-ethyl-3-methyl-1H-pyrrole-2,4-dicarboxylate (78)



56mg of **126** (0.27mmol, 1.5eq), 50mg of **198** (0.22mmol, 1eq) and 217mg Cs_2CO_3 (0.67mmol, 3eq) were stirred in mL DMF at 40°C for 16h. After the work-up the crude was purified through column chromatography with 25g SiO_2 and a linear gradient of hept/EtOAc 40%-->100%. The product was isolated as a white solid in 62% yield (55mg, 0.14mmol).

R_f (TLC, hept/EtOAc 3:7) = 0.35.

$^1\text{H-NMR}$ (400 MHz, DMSO-d_6):

δ = 12.00 (s, 1H, NH), 7.68 (dd, J = 8.9, 7.0 Hz, 1H, 8- H_{arom}), 7.39 (d, J = 8.6 Hz, 1H, 9- H_{arom}), 6.93 (d, J = 6.9 Hz, 1H, 7- H_{arom}), 6.29 (s, 1H, C=OCH), 5.17 (s, 2H, $\text{CH}_2\text{OC=O}$), 4.20 (q, J = 7.1 Hz, 2H, C=OOCH $\underline{\text{C}}\text{H}_2\text{CH}_3$), 2.93 (s, 3H, 6- CH_3), 2.87 (q, J = 7.4 Hz, 2H, 5'- CH_2CH_3), 2.52 (s, 3H, 3'- CH_3), 1.28 (t, J = 7.1 Hz, 3H, C=OOCH $\underline{\text{C}}\text{H}_2\text{CH}_3$), 1.14 (t, J = 7.4 Hz, 3H, 5'- CH_2CH_3).

$^{13}\text{C-NMR}$ (101 MHz, DMSO-d_6):

δ = 164.32 (1C, $\underline{\text{C}}=\text{OOCH}_3$), 161.22 (1C, $\underline{\text{C}}=\text{OCH}$), 160.88 (1C, $\text{CH}_2\text{OC}\underline{\text{C}}=\text{O}$), 159.84 (1C, $\text{C}_{\text{q,arom}}$), 153.19 (1C, $\text{C}_{\text{q,arom}}$), 145.84 (1C, $\text{C}_{\text{q,arom}}$), 143.41 (1C, $\text{C}_{\text{q,arom}}$), 136.73 (1C, 8- CH_{arom}), 130.83 (1C, $\text{C}_{\text{q,arom}}$), 124.48 (1C, 9- CH_{arom}), 118.67 (1C, 7- CH_{arom}), 116.77 (1C, $\text{C}_{\text{q,arom}}$), 111.81 (1C, $\text{C}_{\text{q,arom}}$), 101.80 (1C, C=O $\underline{\text{C}}\text{H}$), 63.90 (1C, $\underline{\text{C}}\text{H}_2\text{OC=O}$), 59.03 (1C, C=OO $\underline{\text{C}}\text{H}_2\text{CH}_3$), 23.97 (1C, 6- CH_3), 20.41 (1C, 5'- $\underline{\text{C}}\text{H}_2\text{CH}_3$), 14.46 (1C, 5'- CH_2CH_3), 14.20 (1C, C=OO $\underline{\text{C}}\text{H}_2\text{CH}_3$), 11.87 (1C, 3'- CH_3).

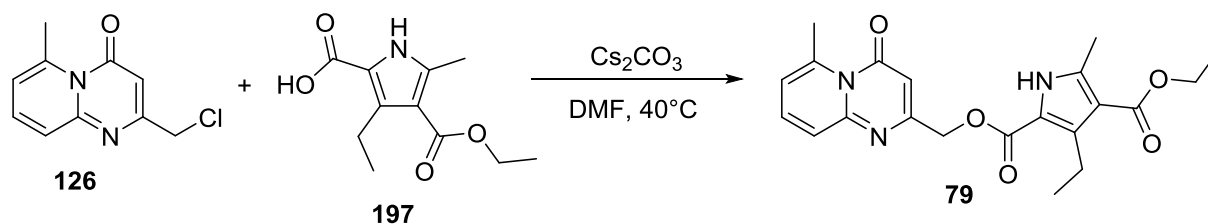
UHPLC-MS

R_t (MCS): 1.796 min

m/z: $[\text{M}+\text{H}]^+$ (calc.) = 398.2

$[\text{M}+\text{H}]^+$ (meas.) = 398.2

[4-ethyl 2-\(\(6-methyl-4-oxo-4H-pyrido\[1,2-a\]pyrimidin-2-yl\)methyl\) 3-ethyl-5-methyl-1H-pyrrole-2,4-dicarboxylate \(79\)](#)



56mg of **126** (0.27mmol, 1.5eq), 50mg of **197** (0.22mmol, 1eq) and 217mg Cs₂CO₃ (0.67mmol, 3eq) were stirred in 4.5mL DMF at 40°C for 16h. After the work-up, the crude was purified through column chromatography with 10g SiO₂ and a linear gradient of hept/EtOAc 30%-->100%. The product was isolated as a white solid in 63% yield (56, 0.14mmol).

R_f (TLC, hept/EtOAc 7:3) = 0.35.

¹H-NMR (400 MHz, CDCl₃):

δ = 9.26 (s, 1H, NH), 7.54 – 7.39 (m, 2H, 8-H_{arom}, 9-H_{arom}), 6.69 (d, *J* = 6.5 Hz, 1H, 7-H_{arom}), 6.32 (s, 1H, C=OCH), 5.22 (s, 2H, CH₂OC=O), 4.30 (q, *J* = 7.1 Hz, 2H, C=OOCH₂CH₃), 3.13 (q, *J* = 7.4 Hz, 2H, 3'-CH₂CH₃), 3.04 (s, 3H, 6-CH₃), 2.54 (s, 3H, 5'-CH₃), 1.37 (t, *J* = 7.1 Hz, 3H, C=OOCH₂CH₃), 1.20 (t, *J* = 7.4 Hz, 3H, 3'-CH₂CH₃).

¹³C-NMR (101 MHz, CDCl₃):

δ = 165.22 (1C, C=OOCH₃), 161.59 (1C, C=OCH), 160.11 (1C, CH₂OC=O), 160.06 (1C, C_{q,arom}), 153.46 (1C, C_{q,arom}), 144.78 (1C, C_{q,arom}), 140.08 (1C, C_{q,arom}), 139.38 (1C, C_{q,arom}), 136.73 (1C, 8-CH_{arom}), 124.35 (1C, 9-CH_{arom}), 119.17 (1C, 7-CH_{arom}), 116.27 (1C, C_{q,arom}), 113.21 (1C, C_{q,arom}), 103.16 (1C, C=OCH), 63.94 (1C, CH₂OC=O), 59.71 (1C, C=OOCH₂CH₃), 24.85 (1C, 6-CH₃), 19.30 (1C, 3'-CH₂CH₃), 15.67 (1C, 3'-CH₂CH₃), 14.59 (1C, 5'-CH₃), 14.48 (1C, C=OOCH₂CH₃).

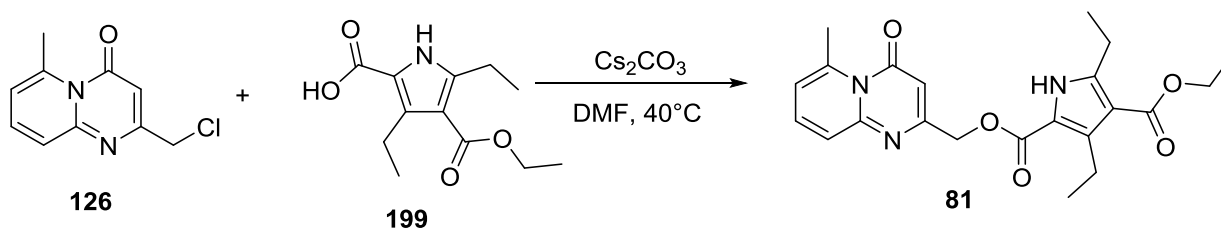
UHPLC-MS

R_t (MCS): 1.778 min

m/z: [M+H]⁺ (calc.) = 398.2

[M+H]⁺ (meas.) = 398.2

4-ethyl 2-((6-methyl-4-oxo-4H-pyrido[1,2-a]pyrimidin-2-yl)methyl) 3,5-diethyl-1H-pyrrole-2,4-dicarboxylate (81)



52mg of **126** (0.25mmol, 1.2eq), 50mg of **199** (0.21mmol, 1eq) and 204mg Cs_2CO_3 (0.63mmol, 3eq) were stirred in 4.5mL DMF at 40°C for 16h. After the work-up, the crude was purified through column chromatography with 10g SiO_2 and a linear gradient of hept/EtOAc 30% -->100%. The product was isolated as a white solid in 61% yield (52mg, 0.13mmol).

R_f (TLC, hept/EtOAc 1:1) = 0.42.

$^1\text{H-NMR}$ (400 MHz, CDCl_3):

δ = 9.16 (s, 1H, NH), 7.46 (dd, J = 16.8, 9.9 Hz, 2H, 8- H_{arom} , 9- H_{arom}), 6.69 (d, J = 6.5 Hz, 1H, 7- H_{arom}), 6.33 (s, 1H, C=OCH), 5.23 (s, 2H, $\text{CH}_2\text{OC}=\text{O}$), 4.30 (q, J = 7.1 Hz, 2H, C=OOCH $\underline{\text{C}}\text{H}_2\text{CH}_3$), 3.14 (q, J = 7.4 Hz, 3H, 3'-CH $\underline{\text{C}}\text{H}_2\text{CH}_3$), 3.04 (s, 3H, 6- CH_3), 2.98 (q, J = 7.5 Hz, 2H, 5'-CH $\underline{\text{C}}\text{H}_2\text{CH}_3$), 1.37 (t, J = 7.1 Hz, 3H, C=OOCH $\underline{\text{C}}\text{H}_2\text{CH}_3$), 1.27 (t, J = 7.5 Hz, 3H, 5'-CH $\underline{\text{C}}\text{H}_2\text{CH}_3$), 1.20 (t, J = 7.4 Hz, 3H, 3'-CH $\underline{\text{C}}\text{H}_2\text{CH}_3$).

$^{13}\text{C-NMR}$ (101 MHz, CDCl_3):

δ = 165.07 (1C, $\underline{\text{C}}=\text{OOCH}_3$), 161.66 (1C, $\underline{\text{C}}=\text{OCH}$), 160.29 (1C, $\text{CH}_2\text{OC}=\underline{\text{O}}$), 160.26 (1C, $\text{C}_{\text{q,arom}}$), 153.51 (1C, $\text{C}_{\text{q,arom}}$), 145.59 (1C, $\text{C}_{\text{q,arom}}$), 144.68 (1C, $\text{C}_{\text{q,arom}}$), 139.29 (1C, $\text{C}_{\text{q,arom}}$), 136.63 (1C, 8- CH_{arom}), 124.44 (1C, 9- CH_{arom}), 118.99 (1C, 7- CH_{arom}), 116.38 (1C, $\text{C}_{\text{q,arom}}$), 112.43 (1C, $\text{C}_{\text{q,arom}}$), 103.15 (1C, C=O $\underline{\text{C}}\text{H}$), 64.11 (1C, $\underline{\text{C}}\text{H}_2\text{OC}=\text{O}$), 59.71 (1C, C=OO $\underline{\text{C}}\text{H}_2\text{CH}_3$), 24.83 (1C, 6- CH_3), 21.68 (1C, 5'- $\underline{\text{C}}\text{H}_2\text{CH}_3$), 19.35 (1C, 3'- $\underline{\text{C}}\text{H}_2\text{CH}_3$), 15.69 (1C, 3'-CH $\underline{\text{C}}\text{H}_2\text{CH}_3$), 14.43 (1C, C=OOCH $\underline{\text{C}}\text{H}_2\text{CH}_3$), 13.19 (1C, 5'-CH $\underline{\text{C}}\text{H}_2\text{CH}_3$).

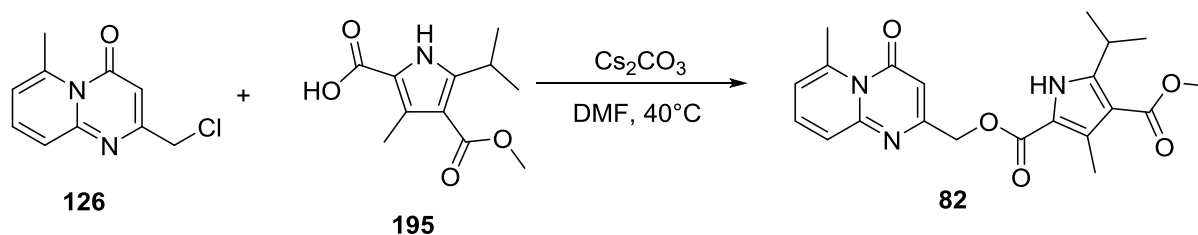
UHPLC-MS

R_t (MCS): 1.856 min

m/z: $[\text{M}+\text{H}]^+$ (calc.) = 412.2

$[\text{M}+\text{H}]^+$ (meas.) = 412.2

4-methyl 2-((6-methyl-4-oxo-4H-pyrido[1,2-a]pyrimidin-2-yl)methyl) 5-isopropyl-3-methyl-1H-pyrrole-2,4-dicarboxylate (82)



56mg of **126** (0.27mmol, 1.5eq), 50mg of **195** (0.22mmol, 1eq) and 217mg Cs₂CO₃ (0.67mmol, 3eq) were stirred in 4.5mL DMF at 40°C for 16h. After the work-up, the crude was purified through column chromatography with 25g SiO₂ and a linear gradient of hept/EtOAc 40%-->100%. The product was isolated as a white solid in 77% yield (68mg, 0.17mmol).

R_f (TLC, hept/EtOAc 7:3) = 0.48.

¹H-NMR (400 MHz, CDCl₃):

δ = 8.98 (s, 1H, NH), 7.46 (dd, *J* = 8.9, 6.9 Hz, 1H, 8-H_{arom}), 7.36 (d, *J* = 8.9 Hz, 1H, 9-H_{arom}), 6.67 (d, *J* = 6.8 Hz, 1H, 7-H_{arom}), 6.33 (s, 1H, C=OCH), 5.24 (s, 2H, CH₂OC=O), 3.84 (s, 3H, C=OOCH₃), 3.83 – 3.70 (m, 1H, 5'-CH(CH₃)₂), 3.04 (s, 3H, 6-CH₃), 2.62 (s, 3H, 3'-CH₃), 1.29 (d, *J* = 7.0 Hz, 6H, 5'-CH(CH₃)₂).

¹³C-NMR (101 MHz, CDCl₃):

δ = 165.73 (1C, C=OOCH₃), 162.30 (1C, C=OCH), 161.04 (1C, CH₂OC=O), 160.87 (1C, C_{q,arom}), 153.84 (1C, C_{q,arom}), 149.34 (1C, C_{q,arom}), 144.31 (1C, C_{q,arom}), 135.77 (1C, 8-CH_{arom}), 132.18 (1C, C_{q,arom}), 125.06 (1C, 9-CH_{arom}), 118.45 (1C, 7-CH_{arom}), 117.26 (1C, C_{q,arom}), 112.71 (1C, C_{q,arom}), 103.16 (1C, C=OCH), 64.74 (1C, CH₂OC=O), 50.95 (1C, C=OOCH₃), 26.65 (1C, 5'-CH(CH₃)₂), 24.85 (1C, 6-CH₃), 21.78 (2C, 5'-CH(CH₃)₂), 12.45 (1C, 3'-CH₃).

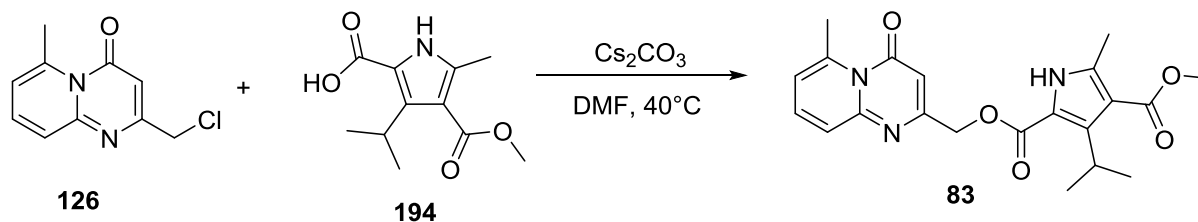
UHPLC-MS

R_t (MCS): 1.772 min

m/z: [M+H]⁺ (calc.) = 398.2

[M+H]⁺ (meas.) = 398.2

4-methyl 2-((6-methyl-4-oxo-4H-pyrido[1,2-a]pyrimidin-2-yl)methyl) 3-isopropyl-5-methyl-1H-pyrrole-2,4-dicarboxylate (83)



69mg of **126** (0.33mmol, 1.5eq), 50mg of **194** (0.22mmol, 1eq) and 217mg Cs_2CO_3 (0.67mmol, 3eq) were stirred in mL DMF at 40°C for 16h. After the work-up the crude was purified through column chromatography with 10g SiO_2 and a linear gradient of hept/EtOAc 40%-->100%. The product was isolated as a white solid in 41% yield (36mg, 0.09mmol).

R_f (TLC, hept/EtOAc 2:3) = 0.21.

$^1\text{H-NMR}$ (400 MHz, CD_3OD):

δ = 7.66 (dd, J = 8.9, 7.0 Hz, 1H, 8- H_{arom}), 7.42 (d, J = 8.9 Hz, 1H, 9- H_{arom}), 6.91 (d, J = 6.9 Hz, 1H, 7- H_{arom}), 6.33 (s, 1H, C=OCH), 5.21 (s, 2H, $\text{CH}_2\text{OC}=\text{O}$), 4.11 (hept, J = 7.1 Hz, 1H, 3'- $\text{CH}(\text{CH}_3)_2$), 3.80 (s, 3H, C=OOCH₃), 3.01 (s, 3H, 6- CH_3), 2.45 (s, 3H, 5'- CH_3), 1.31 (d, J = 7.1 Hz, 6H, 3'- $\text{CH}(\text{CH}_3)_2$).

$^{13}\text{C-NMR}$ (101 MHz, CD_3OD):

δ = 167.61 (1C, C=OOCH₃), 164.06 (1C, C=OCH), 162.98 (1C, $\text{CH}_2\text{OC}=\text{O}$), 161.10 (1C, $\text{C}_{\text{q,arom}}$), 155.25 (1C, $\text{C}_{\text{q,arom}}$), 145.56 (1C, $\text{C}_{\text{q,arom}}$), 143.97 (1C, $\text{C}_{\text{q,arom}}$), 141.15 (1C, $\text{C}_{\text{q,arom}}$), 138.14 (1C, 8- CH_{arom}), 125.28 (1C, 9- CH_{arom}), 120.44 (1C, 7- CH_{arom}), 117.30 (1C, $\text{C}_{\text{q,arom}}$), 113.66 (1C, $\text{C}_{\text{q,arom}}$), 103.37 (1C, C=OCH), 65.00 (1C, $\text{CH}_2\text{OC}=\text{O}$), 51.24 (1C, C=OOCH₃), 26.01 (1C, 3'- $\text{CH}(\text{CH}_3)_2$), 24.78 (1C, 6- CH_3), 21.25 (2C, 3'- $\text{CH}(\text{CH}_3)_2$), 14.00 (1C, 5'- CH_3).

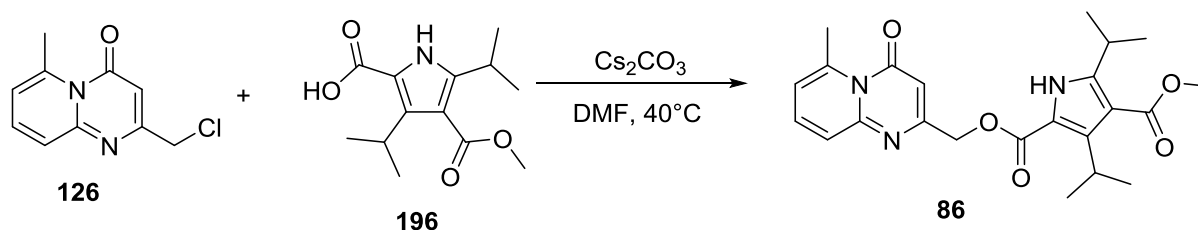
UHPLC-MS

R_t (MCS): 1.778 min

m/z : $[\text{M}+\text{H}]^+$ (calc.) = 398.2

$[\text{M}+\text{H}]^+$ (meas.) = 398.2

4-methyl 2-((6-methyl-4-oxo-4H-pyrido[1,2-a]pyrimidin-2-yl)methyl) 3,5-diisopropyl-1H-pyrrole-2,4-dicarboxylate (86)



25mg of **126** (0.12mmol, 1.5eq), 20mg of **196** (0.08mmol, 1eq) and 77mg Cs_2CO_3 (0.24mmol, 3eq) were stirred in 2mL DMF at 40°C for 5h. After the work-up the crude was purified through column chromatography with 10g SiO_2 and a linear gradient of hept/EtOAc 40%-->100%. The product was isolated as a white solid in 76% yield (25mg, 0.06mmol).

R_f (TLC, hept/EtOAc 1:1) = 0.29.

$^1\text{H-NMR}$ (400 MHz, DMSO-d_6):

δ = 8.94 (s, 1H), 7.56 – 7.43 (m, 1H, 8- H_{arom}), 7.43 – 7.30 (m, 1H, 9- H_{arom}), 6.68 (d, J = 6.3 Hz, 1H, 7- H_{arom}), 6.31 (s, 1H, $\text{C}=\text{OCH}$), 5.24 (s, 2H, $\text{CH}_2\text{OC}=\text{O}$), 4.02 (hept, J = 7.2 Hz, 1H, 3'- $\text{CH}(\text{CH}_3)_2$), 3.84 (s, 3H, $\text{C}=\text{OOCH}_3$), 3.62 (hept, J = 6.9 Hz, 1H, 5'- $\text{CH}(\text{CH}_3)_2$), 3.04 (s, 3H, 6- CH_3), 1.34 (d, J = 7.1 Hz, 6H, 3'- $\text{CH}(\text{CH}_3)_2$), 1.29 (d, J = 7.0 Hz, 6H, 5'- $\text{CH}(\text{CH}_3)_2$).

$^{13}\text{C-NMR}$ (101 MHz, DMSO-d_6):

δ = 166.09 (1C, $\text{C}=\text{OOCH}_3$), 164.73 (1C, $\text{C}=\text{OCH}$), 162.27 (1C, $\text{CH}_2\text{OC}=\text{O}$), 160.04 (1C, $\text{C}_{\text{q,arom}}$), 153.71 (1C, $\text{C}_{\text{q,arom}}$), 148.03 (1C, $\text{C}_{\text{q,arom}}$), 145.44 (1C, $\text{C}_{\text{q,arom}}$), 142.39 (1C, $\text{C}_{\text{q,arom}}$), 136.02 (1C, 8- CH_{arom}), 126.06 (1C, 9- CH_{arom}), 120.63 (1C, 7- CH_{arom}), 118.75 (1C, $\text{C}_{\text{q,arom}}$), 112.48 (1C, $\text{C}_{\text{q,arom}}$), 103.22 (1C, $\text{C}=\text{OCH}$), 51.13 (1C, OCH_3), 26.72 (1C, 3'- $\text{CH}(\text{CH}_3)_2$), 25.29 (1C, 6- CH_3), 24.87 (2C, 5'- $\text{CH}(\text{CH}_3)_2$), 21.98 (2C, 5'- $\text{CH}(\text{CH}_3)_2$), 21.21 (2C, 3'- $\text{CH}(\text{CH}_3)_2$).

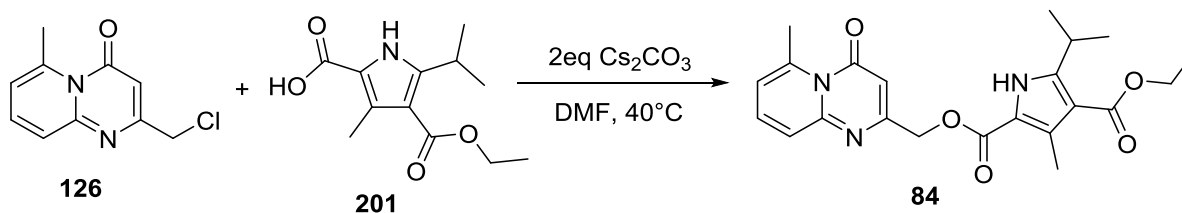
UHPLC-MS

R_t (MCS): 1.778 min

m/z: $[\text{M}+\text{H}]^+$ (calc.) = 426.2

$[\text{M}+\text{H}]^+$ (meas.) = 426.2

4-ethyl 2-((6-methyl-4-oxo-4H-pyrido[1,2-a]pyrimidin-2-yl)methyl) 5-isopropyl-3-methyl-1H-pyrrole-2,4-dicarboxylate (84)



52mg of **126** (0.25mmol, 1.2eq), 50mg of **201** (0.21mmol, 1eq) and 204mg Cs₂CO₃ (0.63mmol, 3eq) were stirred in 4.5mL DMF at 40°C for 16h. After the work-up the crude was purified through column chromatography with 10g SiO₂ and a linear gradient of hept/EtOAc 30%-->100%. The product was isolated as a white product in 75% yield (64mg, 0.16mmol).

R_f (TLC, hept/EtOAc 7:3) = 0.41.

¹H-NMR (400 MHz, CDCl₃):

δ = 8.95 (s, 1H, NH), 7.45 (dd, *J* = 8.9, 6.8 Hz, 1H, 8-H_{arom}), 7.36 (d, *J* = 8.3 Hz, 1H, 9-H_{arom}), 6.67 (d, *J* = 6.8 Hz, 1H, 7-H_{arom}), 6.33 (s, 1H, C=OCH), 5.24 (s, 2H, CH₂OC=O), 4.31 (q, *J* = 7.1 Hz, 2H, C=OOCH₂CH₃), 3.87 – 3.70 (m, 1H, 5'-CH(CH₃)₂), 3.04 (s, 3H, 6-CH₃), 2.62 (s, 3H, 3'-CH₃), 1.37 (t, *J* = 7.1 Hz, 3H, C=OOCH₂CH₃), 1.29 (d, *J* = 7.0 Hz, 6H, 5'-CH(CH₃)₂).

¹³C-NMR (101 MHz, CDCl₃):

δ = 165.28 (1C, C=OOCH₃), 162.31 (1C, C=OCH), 161.08 (1C, CH₂OC=O), 160.90 (1C, C_{q,arom}), 153.85 (1C, C_{q,arom}), 149.20 (1C, C_{q,arom}), 144.31 (1C, C_{q,arom}), 135.76 (1C, 8-CH_{arom}), 132.25 (1C, C_{q,arom}), 125.08 (1C, 9-CH_{arom}), 118.44 (1C, 7-CH_{arom}), 117.20 (1C, C_{q,arom}), 112.94 (1C, C_{q,arom}), 103.16 (1C, C=OCH), 64.75 (1C, CH₂OC=O), 59.79 (1C, C=OOCH₂CH₃), 26.68 (1C, 5'-CH(CH₃)₂), 24.78 (1C, 6-CH₃), 21.77 (2C, 5'-CH(CH₃)₂), 14.51 (1C, C=OOCH₂CH₃), 12.49 (1C, 3'-CH₃).

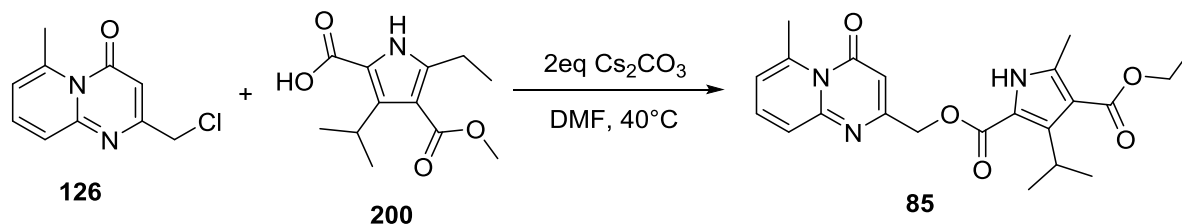
UHPLC-MS

R_t (MCS): 1.856 min

m/z: [M+H]⁺ (calc.) = 412.2

[M+H]⁺ (meas.) = 412.2

4-ethyl 2-((6-methyl-4-oxo-4H-pyrido[1,2-a]pyrimidin-2-yl)methyl) 3-isopropyl-5-methyl-1H-pyrrole-2,4-dicarboxylate (85)



65mg of **126** (0.31mmol, 1.5eq), 50mg of **200** (0.21mmol, 1eq) and 204mg Cs₂CO₃ (0.63mmol, 3eq) were stirred in 4mL DMF at 40°C for 15h. After the work-up, the crude was purified through column chromatography with 10g SiO₂ and a linear gradient of hept/EtOAc 40%-->100%. The product was isolated as a white solid in 87% yield (73mg, 0.18mmol).

R_f (TLC, hept/EtOAc 3:7) = 0.28.

¹H-NMR (400 MHz, CD₃OD):

δ = 7.66 (dd, *J* = 8.9, 7.0 Hz, 1H, 8-H_{arom}), 7.42 (d, *J* = 8.9 Hz, 1H, 9-H_{arom}), 6.91 (d, *J* = 7.0 Hz, 1H, 7-H_{arom}), 6.33 (s, 1H, C=OCH), 5.21 (s, 2H, CH₂OC=O), 4.27 (q, *J* = 7.1 Hz, 2H, C=OOCH₂CH₃), 4.11 (hept, *J* = 7.2 Hz, 1H, 3'-CH(CH₃)₂), 3.00 (d, *J* = 6.6 Hz, 1H, 6-CH₃), 2.46 (s, 3H, 5'-CH₃), 1.37 (t, *J* = 7.1 Hz, 3H, C=OOCH₂CH₃), 1.32 (d, *J* = 7.1 Hz, 6H, 3'-CH(CH₃)₂).

¹³C-NMR (101 MHz, CD₃OD):

δ = 167.23 (1C, C=OOCH₃), 164.06 (1C, C=OCH), 162.97 (1C, CH₂OC=O), 161.12 (1C, C_{q,arom}), 155.24 (1C, C_{q,arom}), 145.55 (1C, C_{q,arom}), 143.91 (1C, C_{q,arom}), 141.15 (1C, C_{q,arom}), 138.14 (1C, 8-CH_{arom}), 125.28 (1C, 9-CH_{arom}), 120.45 (1C, 7-CH_{arom}), 117.23 (1C, C_{q,arom}), 113.91 (1C, C_{q,arom}), 103.37 (1C, C=OCH), 64.98 (1C, CH₂OC=O), 60.91 (1C, C=OOCH₂CH₃), 26.02 (1C, 3'-CH(CH₃)₂), 24.79 (1C, 6-CH₃), 21.29 (2C, 3'-CH(CH₃)₂), 14.72 (1C, C=OOCH₂CH₃), 14.13 (1C, 5'-CH₃).

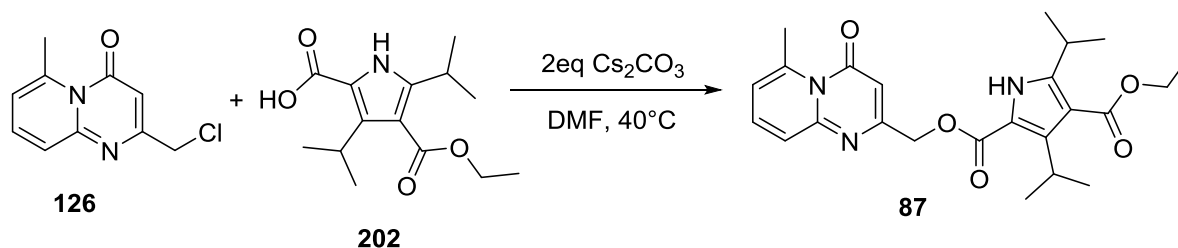
UHPLC-MS

R_t (MCS): 1.859 min

m/z: [M+H]⁺ (calc.) = 412.2

[M+H]⁺ (meas.) = 412.2

[4-ethyl 2-\(\(6-methyl-4-oxo-4H-pyrido\[1,2-a\]pyrimidin-2-yl\)methyl\) 3,5-diisopropyl-1H-pyrrole-2,4-dicarboxylate \(87\)](#)



86mg of **126** (0.41mmol, 1.5eq), 73mg of **202** (0.27mmol, 1eq) and 268mg Cs₂CO₃ (0.82mmol, 3eq) were stirred in 5mL DMF at 40°C for 16h. After the work-up, the crude was purified through column chromatography with 10g SiO₂ and a linear gradient of hept/EtOAc 35%-->100%. The product was isolated as a white solid in 55% yield (56mg, 0.13mmol).

R_f (TLC, hept/EtOAc 1:1) = 0.20.

¹H-NMR (400 MHz, CD₃OD):

δ = 7.67 (dd, *J* = 8.9, 7.0 Hz, 1H, 8-H_{arom}), 7.44 (d, *J* = 8.9 Hz, 1H, 9-H_{arom}), 6.92 (d, *J* = 6.9 Hz, 1H, 7-H_{arom}), 6.32 (s, 1H, C=OCH), 5.23 (s, 2H, CH₂OC=O), 4.28 (q, *J* = 7.1 Hz, 2H, C=OOCH₂CH₃), 4.00 (hept, *J* = 7.2 Hz, 1H, 3'-CH(CH₃)₂), 3.61 (hept, *J* = 7.0 Hz, 1H, 5'-CH(CH₃)₂), 3.02 (s, 3H, 6-CH₃), 1.37 (t, *J* = 7.1 Hz, 3H, C=OOCH₂CH₃), 1.31 (d, *J* = 7.2 Hz, 12H, 3'-CH(CH₃)₂, 5'-CH(CH₃)₂).

¹³C-NMR (101 MHz, CD₃OD):

δ = 167.72 (1C, C=OOCH₂CH₃), 164.02 (1C, C=OCH), 162.78 (1C, CH₂OC=O), 161.32 (1C, C_{q,arom}), 155.32 (1C, C_{q,arom}), 149.34 (1C, C_{q,arom}), 145.62 (1C, C_{q,arom}), 142.65 (1C, C_{q,arom}), 138.23 (1C, 8-CH_{arom}), 125.22 (1C, 9-CH_{arom}), 120.50 (1C, 7-CH_{arom}), 117.56 (1C, C_{q,arom}), 113.46 (1C, C_{q,arom}), 103.61 (1C, C=OCH), 65.10 (1C, CH₂OC=O), 61.21 (1C, C=OOCH₂CH₃), 27.89 (1C, 5'-CH(CH₃)₂), 26.02 (1C, 3'-CH(CH₃)₂), 24.78 (1C, 6-CH₃), 22.01 (2C, 5'-CH(CH₃)₂), 21.29 (2C, 3'-CH(CH₃)₂), 14.62 (1C, C=OOCH₂CH₃).

UHPLC-MS

R_t (MCS): 1.871 min

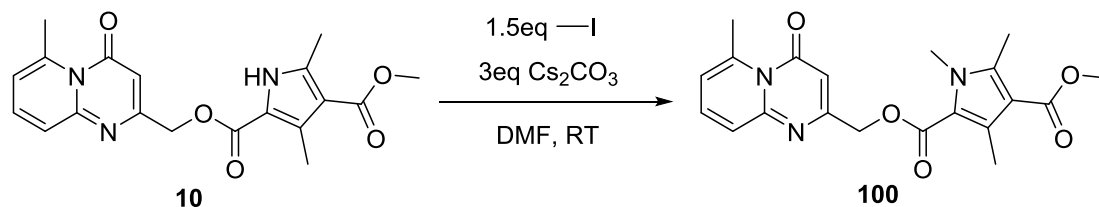
m/z: [M+H]⁺ (calc.) = 440.2

[M+H]⁺ (meas.) = 440.2

2.3.2 N-modified pyrrole compounds

All following reaction steps follow **General Procedure H**.

4-methyl 2-((6-methyl-4-oxo-4H-pyridof[1,2-a]pyrimidin-2-yl)methyl) 1,3,5-trimethyl-1H-pyrrole-2,4-dicarboxylate (100)



21mg of **10** (56.9 μ mol, 1eq) and 56mg Cs₂CO₃ (170.6 μ mol, 3eq) were dissolved in 2mL DMF before 12mg methyl iodide (85.3 μ mol, 1.5eq) was added and the reaction stirred for 17h. The crude product was purified on 10g SiO₂ with a linear gradient of cyclohexane/ EtOAc 30% \rightarrow 100%. The product was isolated as a white solid in 76% yield (17mg, 43.3 μ mol).

R_f (TLC, hept/EtOAc 1:1) = 0.18.

¹H-NMR (400 MHz, CDCl₃):

δ = 7.45 (dd, J = 8.9, 6.8 Hz, 1H, 8-H_{arom}), 7.36 (d, J = 8.4 Hz, 1H, 9-H_{arom}), 6.66 (d, J = 6.7 Hz, 1H, 7-H_{arom}), 6.33 (s, 1H, C=OCH), 5.23 (s, 2H, CH₂OC=O), 3.83 (s, 3H, C=OOCH₃), 3.81 (s, 3H, NCH₃), 3.03 (s, 3H, 6-CH₃), 2.62 (s, 3H, 3'-CH₃), 2.53 (s, 3H, 5'-CH₃).

¹³C-NMR (101 MHz, CDCl₃):

δ = 166.11 (1C, C=OOCH₃), 162.23 (1C, C=OCH), 161.49 (1C, CH₂OC=O), 161.17 (1C, C_q, arom), 153.72 (1C, C_q, arom), 144.32 (1C, C_q, arom), 142.20 (1C, C_q, arom), 135.83 (1C, 8-CH_{arom}), 132.43 (1C, C_q, arom), 124.96 (1C, 9-CH_{arom}), 119.73 (1C, C_q, arom), 118.49 (1C, 7-CH_{arom}), 112.90 (1C, C_q, arom), 103.09 (1C, C=OCH), 64.52 (1C, CH₂OC=O), 50.96 (1C, C=OOCH₃), 33.39 (1C, NCH₃), 24.85 (1C, 6-CH₃), 13.26 (1C, 3'-CH₃), 12.24 (1C, 5'-CH₃).

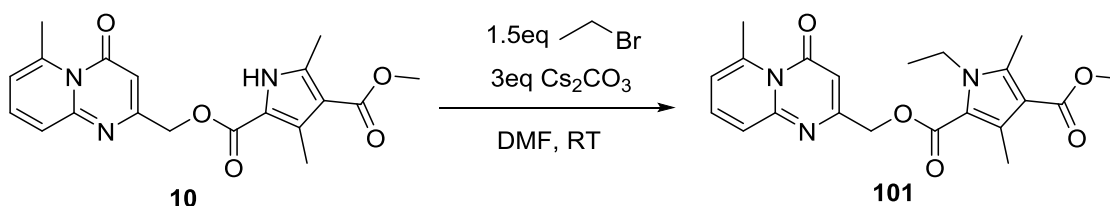
UHPLC-MS

R_t (MCS): 1.538 min

m/z: [M+H]⁺ (calc.) = 384.2

[M+H]⁺ (meas.) = 384.2

4-methyl 2-((6-methyl-4-oxo-4H-pyrido[1,2-a]pyrimidin-2-yl)methyl) 1-ethyl-3,5-dimethyl-1H-pyrrole-2,4-dicarboxylate (101)



15mg of **10** (41.2 μ mol, 1eq) and 40mg Cs₂CO₃ (123.5 μ mol, 3eq) were dissolved in 2mL DMF before 7mg ethyl bromide (61.7 μ mol, 1.5eq) was added and the reaction stirred for 24h. The crude product was purified on 10g SiO₂ with a linear gradient of cyclohexane/ EtOAc of 30% \rightarrow 100%. The product was isolated as a white solid in 69% yield (11mg, 28.4 μ mol).

R_f (TLC, hept/EtOAc 1:1) = 0.28.

¹H-NMR (400 MHz, CDCl₃):

δ = 7.45 (dd, J = 8.9, 6.8 Hz, 1H, 8-H_{arom}), 7.36 (d, J = 8.7 Hz, 1H, 9-H_{arom}), 6.66 (d, J = 6.8 Hz, 1H, 7-H_{arom}), 6.33 (s, 1H, C=OCH), 5.23 (s, 2H, CH₂OC=O), 4.34 (q, J = 7.1 Hz, 2H, NCH₂CH₃), 3.83 (s, 3H, OCH₃), 3.03 (s, 3H, 6-CH₃), 2.62 (s, 3H, 3'-CH₃), 2.54 (s, 3H, 5'-CH₃), 1.29 (t, J = 7.1 Hz, 3H, NCH₂CH₃).

¹³C-NMR (101 MHz, CDCl₃):

δ = 166.16 (1C, C=OOCH₃), 162.16 (1C, C=OCH), 161.19 (1C, CH₂OC=O), 161.10 (1C, C_q, arom), 153.66 (1C, C_q, arom), 144.36 (1C, C_q, arom), 141.41 (1C, C_q, arom), 135.92 (1C, 8-CH_{arom}), 132.66 (1C, C_q, arom), 124.87 (1C, 9-CH_{arom}), 118.72 (1C, 7-CH_{arom}), 118.55 (1C, C_q, arom), 113.12 (1C, C_q, arom), 103.07 (1C, C=OCH), 64.43 (1C, CH₂OC=O), 50.96 (1C, C=OOCH₃), 40.72 (1C, NCH₂CH₃), 24.86 (1C, 6-CH₃), 16.10 (1C, NCH₂CH₃), 13.37 (1C, 3'-CH₃), 11.84 (1C, 5'-CH₃).

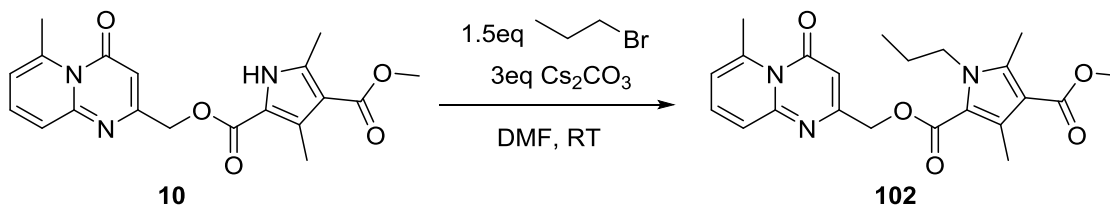
UHPLC-MS

R_t (MCS): 1.607 min

m/z: [M+H]⁺ (calc.) = 398.2

[M+H]⁺ (meas.) = 398.2

4-methyl 2-((6-methyl-4-oxo-4H-pyrido[1,2-a]pyrimidin-2-yl)methyl) 3,5-dimethyl-1-propyl-1H-pyrrole-2,4-dicarboxylate (102)



15mg of **10** (40.3 μ mol, 1eq) and 39mg Cs₂CO₃ (123.5 μ mol, 3eq) were dissolved in 2mL DMF before 7mg propyl bromide (61.7 μ mol, 1.5eq) was added and the reaction stirred for 24h. The crude product was purified on 10g SiO₂ with a linear gradient of cyclohexane/ EtOAc of 30% \rightarrow 100%. The product was isolated as a white solid in 72% yield (12mg, 29.2 μ mol).

R_f (TLC, hept/EtOAc 1:1) = 0.28.

¹H-NMR (400 MHz, CDCl₃):

δ = 7.45 (dd, J = 8.9, 6.8 Hz, 1H, 8-H_{arom}), 7.36 (d, J = 8.7 Hz, 1H, 9-H_{arom}), 6.66 (d, J = 6.7 Hz, 1H, 7-H_{arom}), 6.32 (s, 1H, C=OCH), 5.23 (s, 2H, CH₂OC=O), 4.29 – 4.12 (m, 2H, NCH₂CH₂CH₃), 3.83 (s, 3H, OCH₃), 3.03 (s, 3H, 6-CH₃), 2.62 (s, 3H, 3'-CH₃), 2.53 (s, 3H, 5'-CH₃), 1.75 – 1.60 (m, 2H, NCH₂CH₂CH₃), 0.91 (t, J = 7.4 Hz, 3H, NCH₂CH₂CH₃).

¹³C-NMR (101 MHz, CDCl₃):

δ = 166.19 (1C, C=OOCH₃), 162.14 (1C, C=OCH), 161.24 (1C, CH₂OC=O), 161.09 (1C, C_q, arom), 153.65 (1C, C_q, arom), 144.37 (1C, C_q, arom), 141.70 (1C, C_q, arom), 135.89 (1C, 8-CH_{arom}), 132.65 (1C, C_q, arom), 124.65 (1C, 9-CH_{arom}), 118.96 (1C, C_q, arom), 118.56 (1C, 7-CH_{arom}), 113.05 (1C, C_q, arom), 103.05 (1C, C=OCH), 64.39 (1C, CH₂OC=O), 50.96 (1C, C=OOCH₃), 47.15 (1C, NCH₂CH₂CH₃), 24.86 (1C, 6-CH₃), 24.31 (1C, NCH₂CH₂CH₃), 13.37 (1C, 3'-CH₃), 12.12 (1C, NCH₂CH₂CH₃), 11.84 (1C, 5'-CH₃).

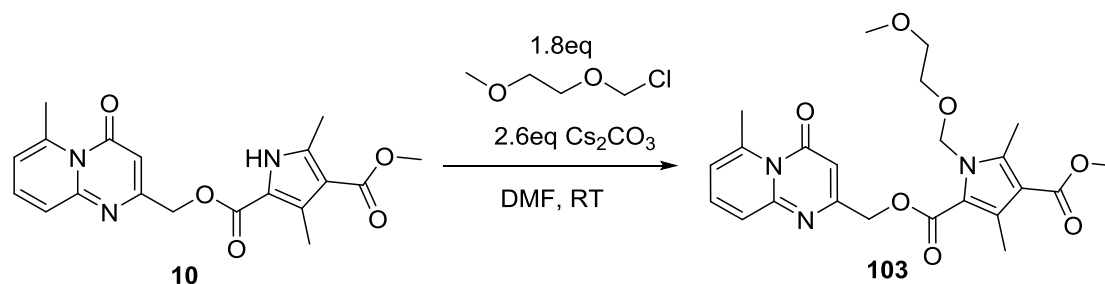
UHPLC-MS

R_t (MCS): 1.674 min

m/z: [M+H]⁺ (calc.) = 412.2

[M+H]⁺ (meas.) = 412.2

4-methyl-2-((6-methyl-4-oxo-4H-pyrido[1,2-a]pyrimidin-2-yl)methyl)-1-((2-methoxyethoxy)methyl)-3,5-dimethyl-1H-pyrrole-2,4-dicarboxylate (103)



21mg of **10** (56.0 μ mol, 1eq) and 46mg Cs₂CO₃ (142.1 μ mol, 2.6eq) were dissolved in 3mL DMF before 13mg MEMCl (101.5 μ mol, 1.8eq) was added and the reaction stirred for 24h. The crude product was purified on 10g SiO₂ with a linear gradient of cyclohexane/ EtOAc of 30% \rightarrow 100%. The product was isolated as a white solid in 49% yield (13mg, 28.0 μ mol).

R_f (TLC, hept/EtOAc 1:4) = 0.18.

¹H-NMR (400 MHz, CDCl₃):

δ = 7.52 – 7.44 (m, 1H, 8-H_{arom}), 7.41 (d, J = 8.6 Hz, 1H, 9-H_{arom}), 6.68 (d, J = 6.7 Hz, 1H, 7-H_{arom}), 6.32 (s, 1H, C=OCH), 5.83 (s, 2H, NCH₂OCH₂CH₂OCH₃), 5.25 (s, 2H, CH₂OC=O), 3.84 (s, 3H, OCH₃), 3.61 – 3.57 (m, 2H, NCH₂OCH₂CH₂OCH₃), 3.50 – 3.44 (m, 2H, NCH₂OCH₂CH₂OCH₃), 3.33 (s, 3H, NCH₂OCH₂CH₂OCH₃), 3.04 (s, 3H, 6-CH₃), 2.61 (s, 6H, 3'-CH₃, 5'-CH₃).

¹³C-NMR (101 MHz, CDCl₃):

δ = 165.91 (1C, C=OOCH₃), 161.95 (1C, C=OCH), 161.31 (1C, CH₂OC=O), 161.31 (1C, C_q, arom), 153.60 (1C, C_q, arom), 144.48 (1C, C_q, arom), 143.73 (1C, C_q, arom), 136.27 (1C, 8-CH_{arom}), 133.09 (1C, C_q, arom), 124.63 (1C, 9-CH_{arom}), 119.59 (1C, C_q, arom), 118.72 (1C, 7-CH_{arom}), 114.28 (1C, C_q, arom), 103.07 (1C, C=OCH), 73.96 (1C, NCH₂OCH₂CH₂OCH₃), 71.73 (1C, NCH₂OCH₂CH₂OCH₃), 67.38 (1C, NCH₂OCH₂CH₂OCH₃), 64.39 (1C, CH₂OC=O), 59.12 (1C, NCH₂OCH₂CH₂OCH₃), 51.10 (1C, C=OOCH₃), 24.86 (1C, 6-CH₃), 13.28 (1C, 3'-CH₃), 12.15 (1C, 5'-CH₃).

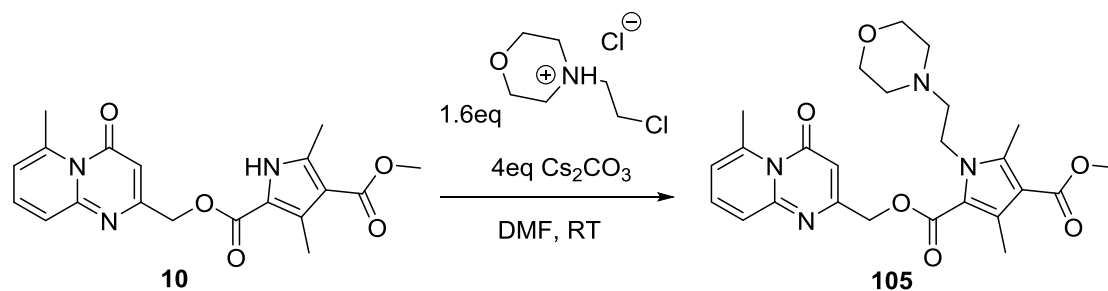
UHPLC-MS

R_t (MCS): 1.537 min

m/z: [M+H]⁺ (calc.) = 458.2

[M+H]⁺ (meas.) = 458.2

[4-methyl 2-\(\(6-methyl-4-oxo-4H-pyrido\[1,2-a\]pyrimidin-2-yl\)methyl\) 3,5-dimethyl-1-\(2-morpholinoethyl\)-1H-pyrrole-2,4-dicarboxylate \(105\)](#)



30mg of **10** (81.2 μ mol, 1eq) and 106mg Cs₂CO₃ (324.9 μ mol, 4eq) were dissolved in 2mL DMF before 23mg XX (121.8 μ mol, 1.6eq) was added and the reaction stirred for 24h. The crude product was purified on 10g SiO₂ with a linear gradient of cyclohexane/EtOAc of 30% \rightarrow 100%. The product was isolated as a white solid in 59% yield (22mg, 47.8 μ mol).

R_f (TLC, hept/EtOAc 1:1) = 0.27.

¹H-NMR (400 MHz, CDCl₃):

δ = 7.50 – 7.40 (m, 1H, 8-H_{arom}), 7.35 (d, J = 8.9 Hz, 1H, 9-H_{arom}), 6.66 (d, J = 6.8 Hz, 1H, 7-H_{arom}), 6.32 (s, 1H, C=OCH), 5.22 (s, 2H, CH₂OC=O), 4.44 (s, 2H, NCH₂), 3.83 (s, 3H, OCH₃), 3.69 (s, 4H, N(CH₂CH₂)O), 3.03 (s, 3H, 6-CH₃), 2.62 (s, 3H, 3'-CH₃), 2.58 (s, 3H, 5'-CH₃), 2.52 (s, 4H, N(CH₂CH₂)O).

¹³C-NMR (101 MHz, CDCl₃):

δ = 166.04 (1C, C=OOCH₃), 162.30 (1C, C=OCH), 161.29 (1C, CH₂OC=O), 160.23 (1C, C_q, arom), 153.81 (1C, C_q, arom), 144.27 (1C, C_q, arom), 142.11 (1C, C_q, arom), 135.71 (1C, 8-CH_{arom}), 132.74 (1C, C_q, arom), 125.11 (1C, 9-CH_{arom}), 119.04 (1C, C_q, arom), 118.41 (1C, 7-CH_{arom}), 113.35 (1C, C_q, arom), 103.15 (1C, C=OCH), 66.96 (1C, N-CH₂N), 64.61 (1C, CH₂OC=O), 54.02 (2C, N(CH₂CH₂)O), 51.03 (1C, C=OOCH₃), 42.94 (2C, N(CH₂CH₂)O), 24.87 (1C, 6-CH₃), 13.41 (1C, 3'-CH₃), 12.19 (1C, 5'-CH₃).

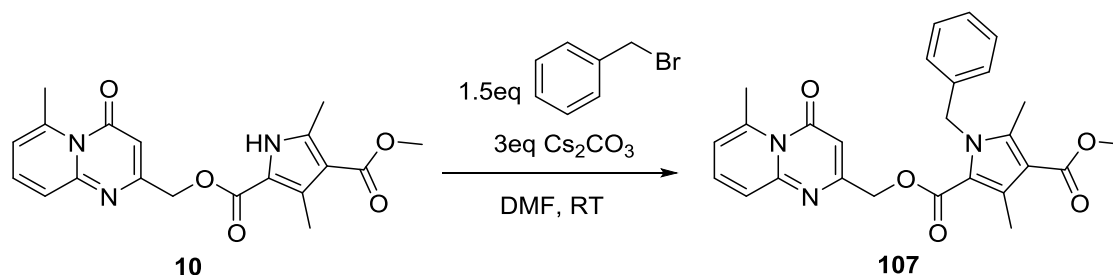
UHPLC-MS

R_t (MCS): 1.354 min

m/z: [M+H]⁺ (calc.) = 483.2

[M+H]⁺ (meas.) = 483.2

4-methyl 2-((6-methyl-4-oxo-4H-pyrido[1,2-a]pyrimidin-2-yl)methyl) 1-benzyl-3,5-dimethyl-1H-pyrrole-2,4-dicarboxylate (107)



20mg of **10** (54.1 μ mol, 1eq) and 53mg Cs₂CO₃ (162.4 μ mol, 3eq) were dissolved in 2.5mL DMF before 14mg benzyl bromide (81.2 μ mol, 1.5eq) was added and the reaction stirred for 2h. The crude product was purified on 10g SiO₂ with a linear gradient of cyclohexane/ EtOAc of 25% \rightarrow 100%. The product was isolated as a white solid in 98% yield (24.2mg, 53.1 μ mol).

R_f (TLC, DCM/MeOH 2%) = 0.59.

¹H-NMR (400 MHz, CDCl₃):

δ = 7.45 – 7.38 (m, 1H, 8-H_{arom}), 7.27 (dd, J = 17.6, 7.6 Hz, 3H, 9-H_{arom}, Ph-H_{arom}), 7.21 (d, J = 7.4 Hz, 1H, Ph-H_{arom}), 6.90 (d, J = 7.4 Hz, 2H, Ph-H_{arom}), 6.64 (d, J = 6.8 Hz, 1H, 7-H_{arom}), 6.22 (s, 1H, C=OCH), 5.62 (s, 2H, CH₂Ph), 5.14 (s, 2H, CH₂OC=O), 3.84 (s, 2H, OCH₃), 3.02 (s, 3H, 6-CH₃), 2.67 (s, 2H, 3'-CH₃), 2.47 (s, 3H, 5'-CH₃).

¹³C-NMR (101 MHz, CDCl₃):

δ = 166.08 (1C, C=OOCH₃), 162.16(1C, C=OCH), 161.17 (1C, CH₂OC=O), 160.95 (1C, C_{q, arom}), 153.58 (1C, C_{q, arom}), 144.24 (1C, C_{q, arom}), 142.53 (1C, C_{q, arom}), 137.51 (1C, C_{q, arom}), 135.70 (1C, 8-CH_{arom}), 132.90 (1C, C_{q, arom}), 128.84, 127.28, 125.76 (5C, Ph-CH), 124.99 (1C, 9-CH_{arom}), 119.59 (1C, C_{q, arom}), 118.42 (1C, 7-CH_{arom}), 113.57 (1C, C_{q, arom}), 103.18 (1C, C=OCH), 64.59 (1C, CH₂OC=O), 51.04 (1C, C=OOCH₃), 48.79 (1C, CH₂Ph), 24.83 (1C, 6-CH₃), 13.40 (1C, 3'-CH₃), 12.19 (1C, 5'-CH₃).a

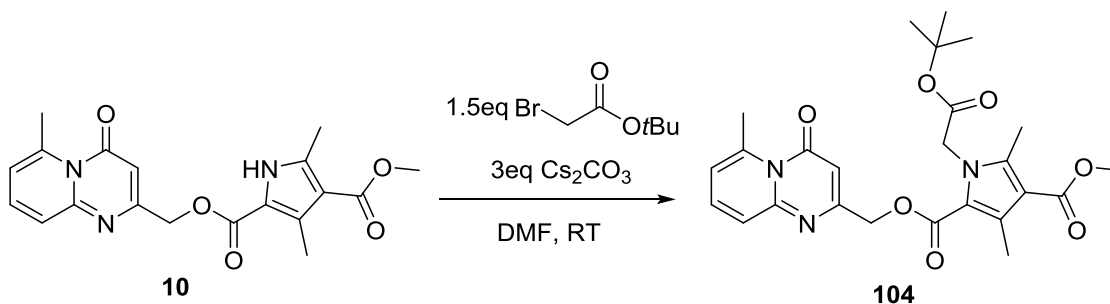
UHPLC-MS

R_t (MCS): 1.704 min

m/z: [M+H]⁺ (calc.) = 460.2

[M+H]⁺ (meas.) = 460.2

4-methyl 2-((6-methyl-4-oxo-4H-pyrido[1,2-a]pyrimidin-2-yl)methyl) 1-(2-(tert-butoxy)-2-oxoethyl)-3,5-dimethyl-1H-pyrrole-2,4-dicarboxylate (104)



30mg of **10** (81.2 μmol , 1eq) and 80mg Cs_2CO_3 (245.3 μmol , 3eq) were dissolved in 2mL DMF before 24mg **XX** (122.6 μmol , 1.5eq) was added and the reaction stirred for 24h. The crude product was purified on 10g SiO_2 with a linear gradient of cyclohexane/EtOAc of 30% \rightarrow 100%. The product was isolated as a white solid in 87% yield (34mg, 71.1 μmol).

R_f (TLC, hept/EtOAc 1:1) = 0.22.

$^1\text{H-NMR}$ (400 MHz, CDCl_3):

δ = 7.50 – 7.42 (m, 1H, 8- H_{arom}), 7.39 (d, J = 8.5 Hz, 1H, 9- H_{arom}), 6.67 (d, J = 6.6 Hz, 1H, 7- H_{arom}), 6.32 (s, 1H, $\text{C}=\text{OCH}$), 5.21 (s, 2H, $\text{CH}_2\text{OC}=\text{O}$), 4.97 (s, 2H, NCH_2), 3.83 (s, 3H, OCH_3), 3.03 (s, 3H, 6- CH_3), 2.64 (s, 3H, 3'- CH_3), 2.49 (s, 3H, 5'- CH_3), 1.44 (s, 9H, $\text{C}(\text{CH}_3)_3$).

$^{13}\text{C-NMR}$ (101 MHz, CDCl_3):

δ = 167.50 (1C, $\text{C}=\text{OOC}(\text{CH}_3)_3$), 165.96 (1C, $\text{C}=\text{OOCH}_3$), 162.16 (1C, $\text{C}=\text{OCH}$), 161.46 (1C, $\text{CH}_2\text{OC}=\text{O}$), 160.96 (1C, C_q , arom), 153.70 (1C, C_q , arom), 144.28 (1C, C_q , arom), 142.45 (1C, C_q , arom), 135.78 (1C, 8- CH_{arom}), 132.73 (1C, C_q , arom), 124.96 (1C, 9- CH_{arom}), 119.40 (1C, C_q , arom), 118.44 (1C, 7- CH_{arom}), 113.47 (1C, C_q , arom), 103.18 (1C, $\text{C}=\text{OCH}$), 82.65 (1C, $\text{C}=\text{OOC}(\text{CH}_3)_3$), 64.61 (1C, $\text{CH}_2\text{OC}=\text{O}$), 51.00 (1C, $\text{C}=\text{OOCH}_3$), 47.90 (1C, NCH_2), 28.12 (3C, $\text{C}=\text{OOC}(\text{CH}_3)_3$), 24.86 (1C, 6- CH_3), 13.35 (1C, 3'- CH_3), 12.00 (1C, 5'- CH_3).

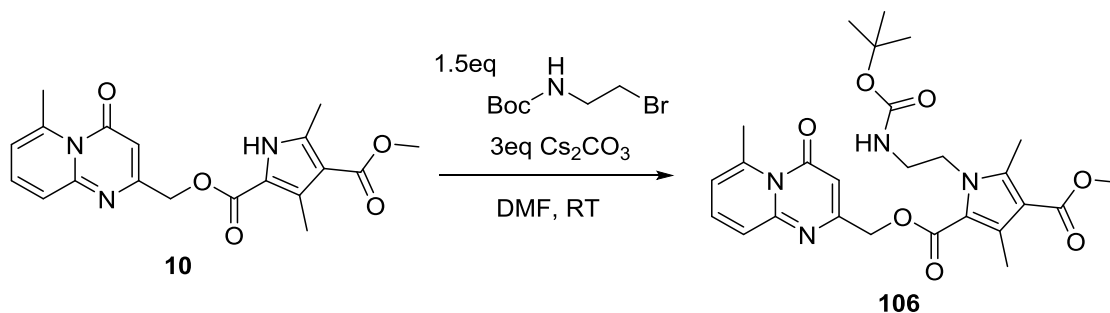
UHPLC-MS

R_t (MCS): 1.667 min

m/z : $[\text{M}+\text{H}]^+$ (calc.) = 484.2

$[\text{M}+\text{H}]^+$ (meas.) = 484.2

4-methyl 2-((6-methyl-4-oxo-4H-pyrido[1,2-a]pyrimidin-2-yl)methyl) 1-(2-((tert-butoxycarbonyl)Amino)ethyl)-3,5-dimethyl-1H-pyrrole-2,4-dicarboxylate (106)



20.4mg of **10** (55μmol, 1eq) and 106mg Cs₂CO₃ (324.9μmol, 6eq) were dissolved in 4mL DMF before 36mg XX (162.4μmol, 3eq) was added and the reaction stirred for 3d at 40°C. The crude product was purified on 10g SiO₂ with a linear gradient of cyclohexane/ EtOAc of 40% →80%. The product was isolated as a white solid in 75% yield (21.3mg, 41.6μmol).

R_f (TLC, cyclohex/EtOAc 2:8) = 0.23.

¹H-NMR (400 MHz, CDCl₃):

δ = 7.53 – 7.38 (m, 2H, 8-H_{arom}, 9-H_{arom}), 6.69 (d, *J* = 6.3 Hz, 1H, 7-H_{arom}), 6.32 (s, 1H, C=OCH), 5.23 (s, 2H, CH₂OC=O), 4.95 (s, 1H, NCH₂CH₂NHBoc), 4.40 (t, *J* = 6.0 Hz, 2H, NCH₂CH₂NHBoc), 3.83 (s, 3H, OCH₃), 3.40 (dd, *J* = 12.2, 6.0 Hz, 2H, NCH₂CH₂NHBoc), 3.04 (s, 3H, 6-CH₃), 2.62 (s, 3H, 3'-CH₃), 2.56 (s, 3H, 5'-CH₃), 1.40 (s, 9H, C(CH₃)₃).

¹³C-NMR (101 MHz, CDCl₃):

δ = 165.99 (1C, C=OOCH₃), 161.16 (1C, C=OCH), 161.29 (2C, CH₂OC=O, C_q, arom), 156.58 (1C, NHC=O), 153.58 (1C, C_q, arom), 144.54 (1C, C_q, arom), 142.80 (1C, C_q, arom), 136.31 (1C, 8-CH_{arom}), 133.35 (1C, C_q, arom), 124.50 (1C, 9-CH_{arom}), 118.86 (2C, C_q, arom, 7-CH_{arom}), 113.43 (1C, C_q, arom), 103.23 (1C, C=OCH), 79.72 (1C, C(CH₃)₃), 64.32 (1C, CH₂OC=O), 51.03 (1C, C=OOCH₃), 45.03 (1C, NCH₂CH₂NH), 42.94 (1C, NCH₂CH₂NH), 28.48 (3C, C(CH₃)₃), 24.86 (1C, 6-CH₃), 13.40 (1C, 3'-CH₃), 12.17 (1C, 5'-CH₃).

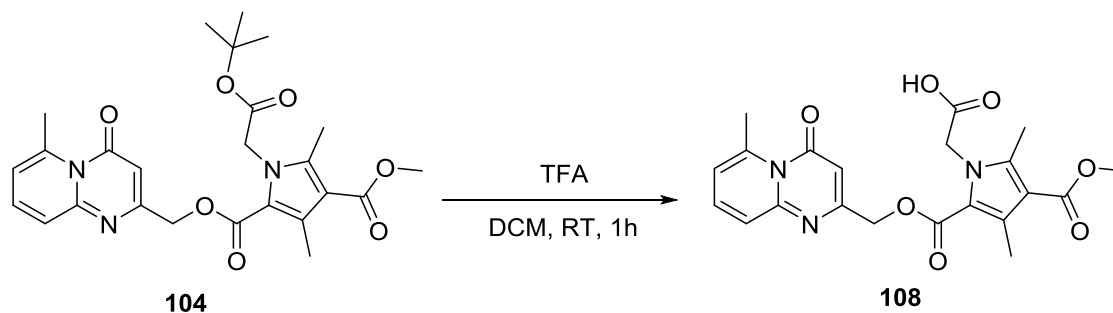
UHPLC-MS

R_t (MCS): 1.646 min

m/z: [M+H]⁺ (calc.) = 513.2

[M+H]⁺ (meas.) = 513.2

[2-\(3-\(methoxycarbonyl\)-2,4-dimethyl-5-\(\(\(6-methyl-4-oxo-4H-pyrido\[1,2-a\]pyrimidin-2-yl\)methoxy\)carbonyl\)-1H-pyrrol-1-yl\)acetic acid \(108\)](#)



15mg of **104** (30 μ mol, 1eq) was dissolved in 1mL DCM before 100mL of TFA is added and the reaction stirred for 1h. The reaction was monitored by UHPLC-MS. The crude product was analysed by UHPLC-MS and NMR and no purification was needed. The product was isolated as a white solid in 98% yield (16mg, 29.4 μ mol).

R_f (TLC, DCM/MeOH 2%) = 0.05.

¹H-NMR (400 MHz, CDCl₃):

δ = 7.99 (s, 2H, 8-H_{arom}, 9-H_{arom}), 7.17 (s, 1H, 7-H_{arom}), 6.34 (s, 1H, C=OCH), 5.34 (s, 2H, CH₂OC=O), 4.97 (s, 2H, NCH₂C=O), 3.83 (s, 3H, OCH₃), 3.11 (s, 3H, 6-CH₃), 2.58 (s, 3H, 3'-CH₃), 2.50 (s, 3H, 5'-CH₃).

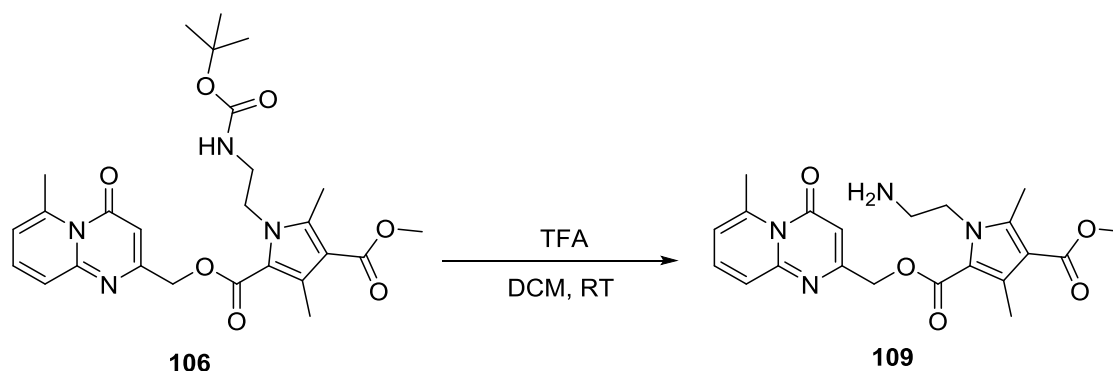
UHPLC-MS

R_t (MCS): 1.387 min

m/z: [M+H]⁺ (calc.) = 428.15

[M+H]⁺ (meas.) = 428.2

[4-methyl 2-\(\(6-methyl-4-oxo-4H-pyrido\[1,2-a\]pyrimidin-2-yl\)methyl\) 1-\(2-Aminoethyl\)-3,5-dimethyl-1H-pyrrole-2,4-dicarboxylate \(109\)](#)



16mg of **106** (33.1 μ mol, 1eq) were dissolved in 600 μ L DCM, before 400 μ L TFA was added. The reaction was monitored UHPLC-MS and was finished after stirring for 1h at RT. The excess of TFA and the solvent were removed *in vacuo* and the crude dried under high vacuum. The product was isolated as a white solid in 68% yield (9.3mg, 22.5 μ mol).

R_f (TLC, cyclohex/EtOAc) = 0.06.

¹H-NMR (400 MHz, CDCl₃):

δ = 7.80 (dd, J = 8.7, 7.2 Hz, 1H, 8-H_{arom}), 7.50 (d, J = 8.7 Hz, 1H, 9-H_{arom}), 7.03 (d, J = 7.1 Hz, 1H, 7-H_{arom}), 6.34 (s, 1H, C=OCH), 5.29 (m, 2H, CH₂OC=O), 4.59 (t, J = 6.4 Hz, 2H, NCH₂CH₂NH₂), 3.81 (s, 3H, OCH₃), 3.27 (s, 2H, NCH₂CH₂NH₂), 3.03 (s, 3H, 6-CH₃), 2.59 (s, 3H, 3'-CH₃), 2.57 (s, 3H, 5'-CH₃).

¹³C-NMR (101 MHz, CDCl₃):

δ = 167.09 (1C, C=OOCH₃), 163.80 (1C, C=OCH), 162.13 (1C, CH₂OC=O), 162.13 (1C, C_q, arom), 155.09 (1C, C_q, arom), 145.72 (1C, C_q, arom), 143.91 (1C, C_q, arom), 138.52 (1C, 8-CH_{arom}), 134.00 (1C, C_q, arom), 125.02 (1C, 9-CH_{arom}), 120.68 (1C, 7-CH_{arom}), 117.44 (1C, C_q, arom), 114.85 (1C, C_q, arom), 103.51 (1C, C=OCH), 65.51 (1C, CH₂OC=O), 51.43 (1C, C=OOCH₃), 43.46 (1C, NCH₂CH₂NH₂), 40.54 (1C, NCH₂CH₂NH₂), 24.75 (1C, 6-CH₃), 13.47 (1C, 3'-CH₃), 12.05 (1C, 5'-CH₃).

UHPLC-MS

R_t (MCS): 1.159 min

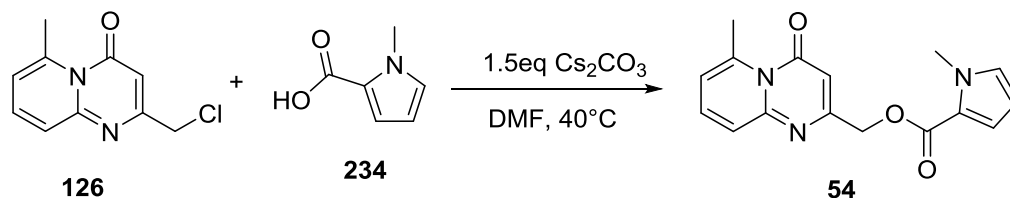
m/z: [M+H]⁺ (calc.) = 413.2

[M+H]⁺ (meas.) = 413.2

2.3.3 Substituent subtraction of pyrrole

All following reactions were conducted according to **General procedure G**.

(6-methyl-4-oxo-4H-pyrido[1,2-a]pyrimidin-2-yl)methyl 1-methyl-1H-pyrrole-2-
carboxylate (54)



200mg of **126** (0.96mmol, 1eq), 132mg of **234** (1.05mmol, 1.1 eq) and 468mg of Cs_2CO_3 (1.44mmol, 1.5eq) were dissolved in 10mL DMF and stirred at 40°C for 24h. The product was isolated as a yellow solid in 93% yield (264mg, 0.89mmol). No further purification was needed as was determined through NMR analysis.

R_f (TLC, Hept/EtOAc 1:1) = 0.2

$^1\text{H-NMR}$ (400 MHz, CDCl_3):

δ = 7.42 (dd, J = 8.9, 6.9 Hz, 1H, 8- H_{arom}), 7.33 (d, J = 8.8 Hz, 1H, 9- H_{arom}), 7.09 (dd, J = 4.0, 1.8 Hz, 1H, 3'- H_{arom}), 6.83 (t, J = 2.0 Hz, 1H, 4'- H_{arom}), 6.63 (d, J = 6.8 Hz, 1H, 7- H_{arom}), 6.36 (s, 1H, C=OCH), 6.14 (dd, J = 4.0, 2.5 Hz, 1H, 5'- H_{arom}), 5.17 (s, 2H, CH_2), 3.93 (s, 1H, NCH₃), 3.02 (s, 3H, 6-CH₃).

$^{13}\text{C-NMR}$ (101 MHz, CDCl_3):

δ = 161.61 (1C, C_q , arom), 160.45, 153.72 (1C, C_q , arom), 144.16 (1C, C_q , arom), 135.55 (1C, 8- CH_{arom}), 130.29 (1C, 4'- CH_{arom}), 125.02 (1C, 9- CH_{arom}), 121.72 (1C, C_q , arom), 118.74 (1C, 3'- CH_{arom}), 118.25 (1C, 7- CH_{arom}), 108.28 (1C, 5'- CH_{arom}), 102.88 (1C, C=OCH), 64.16 (1C, CH_2), 36.94 (1C, NCH₃), 24.79 (1C, 6-CH₃).

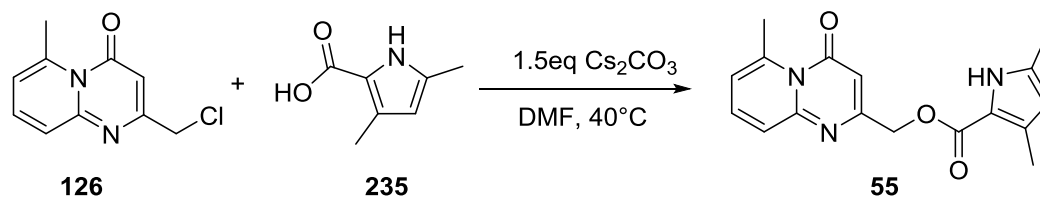
UHPLC-MS

R_t (MCS): 1.374 min

m/z : $[\text{M}+\text{H}]^+$ (calc.) = 298.3

$[\text{M}+\text{H}]^+$ (meas.) = 298.2

[\(6-methyl-4-oxo-4H-pyrido\[1,2-a\]pyrimidin-2-yl\)methyl](#) [3,5-dimethyl-1H-pyrrole-2-carboxylate \(55\)](#)



200mg of **126** (0.96mmol, 1eq), 147mg of **235** (1.05mmol, 1.1 eq) and 468mg of Cs₂CO₃ (1.44mmol, 1.5eq) were dissolved in 10mL DMF and stirred at 40°C for 24h. The product was isolated as a yellow solid in 98% yield (264mg, 0.89mmol). No further purification was needed as was determined through NMR analysis.

R_f (TLC, Hept/EtOAc 1:1) = 0.13

¹H-NMR (400 MHz, CDCl₃):

δ = 9.00 (s, 1H, NH), 7.42 (dd, *J* = 8.9, 6.8 Hz, 1H, 8-H_{arom}), 7.33 (d, *J* = 8.2 Hz, 1H, 9-H_{arom}), 6.64 (d, *J* = 6.8 Hz, 1H, 7-H_{arom}), 6.35 (s, 1H, C=OCH), 5.83 (d, *J* = 2.7 Hz, 1H, 4'-H_{arom}), 5.19 (s, 2H, CH₂), 3.02 (s, 3H, 6-CH₃), 2.36 (s, 3H, 3'-CH₃), 2.25 (s, 3H, 5'-CH₃).

¹³C-NMR (101 MHz, CDCl₃):

δ = 162.34 (1C, C=OCH), 161.66 (1C, OC=O), 160.65 (1C, C_q, arom), 153.71 (1C, C_q, arom), 144.20 (1C, C_q, arom), 135.59 (1C, 8-CH_{arom}), 133.56 (1C, C_q, arom), 130.54 (1C, C_q, arom), 125.01 (1C, 9-CH_{arom}), 118.30 (1C, 7-CH_{arom}), 116.96 (1C, C_q, arom), 111.89 (1C, 4'-CH_{arom}), 103.00 (1C, C=OCH), 64.21 (1C, CH₂), 24.81 (1C, 6-CH₃), 13.23 (1C, 5'-CH₃), 13.18 (1C, 3'-CH₃).

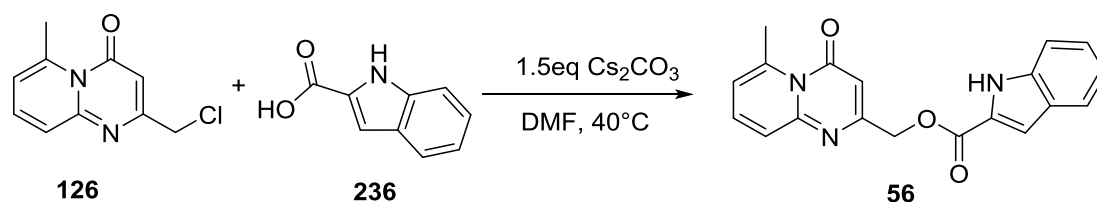
UHPLC-MS

R_t (MCS): 1.490 min

m/z: [M+H]⁺ (calc.) = 312.3

[M+H]⁺ (meas.) = 312.2

[\(6-methyl-4-oxo-4H-pyrido\[1,2-a\]pyrimidin-2-yl\)methyl 1H-indole-2-carboxylate \(**56**\)](#)



200mg of **126** (0.96mmol, 1eq), 170mg of **236** (1.05mmol, 1.1 eq) and 468mg of Cs_2CO_3 (1.44mmol, 1.5eq) were dissolved in 10mL DMF and stirred at 40°C for 24h. The product was isolated as a white solid in 97% yield (264mg, 0.89mmol). No further purification was needed as was determined through NMR analysis.

R_f (TLC, Hept/EtOAc 1:1) = 0.16

$^1\text{H-NMR}$ (400 MHz, DMSO-d_6):

δ = 12.04 (s, 1H, NH), 7.73 – 7.62 (m, 2H, 8- H_{arom} , 3'- H_{arom}), 7.49 (d, J = 8.3 Hz, 1H, 7'- H_{arom}), 7.38 (d, J = 8.7 Hz, 1H, 9- H_{arom}), 7.32 (d, J = 1.4 Hz, 1H, 8'- H_{arom}), 7.29 (t, J = 7.7 Hz, 1H, 6'- H_{arom}), 7.10 (t, J = 7.5 Hz, 1H, 5'- H_{arom}), 6.91 (d, J = 6.9 Hz, 1H, 7- H_{arom}), 6.35 (s, 1H, C=OCH), 5.26 (s, 2H, CH_2), 2.92 (s, 3H, 6- CH_3).

$^{13}\text{C-NMR}$ (101 MHz, DMSO-d_6):

δ = 161.19 (1C, C=OCH), 160.65 (1C, OC=O), 160.46 (1C, Cq, arom), 153.22 (1C, Cq, arom), 143.41 (1C, Cq, arom), 137.65 (1C, Cq, arom), 136.69, 126.73 (1C, Cq, arom), 126.47 (1C, Cq, arom), 124.98 (1C, 9- CH_{arom}), 124.48 (1C, CH_{arom}), 122.21 (1C, CH_{arom}), 120.33 (1C, 3'- CH_{arom}), 118.66 (1C, 7- CH_{arom}), 112.66 (1C, CH_{arom}), 108.73 (1C, CH_{arom}), 101.86 (1C, C=OCH), 64.55 (1C, CH_2), 23.98 (1C, CH_3).

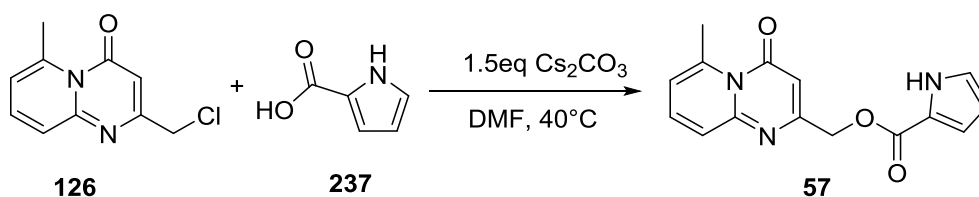
UHPLC-MS

R_t (MCS): 1.577 min

m/z: $[\text{M}+\text{H}]^+$ (calc.) = 334.3

$[\text{M}+\text{H}]^+$ (meas.) = 334.2

(6-methyl-4-oxo-4H-pyrido[1,2-a]pyrimidin-2-yl)methyl-1H-pyrrole-2-carboxylate (57)



200mg of **126** (0.96mmol, 1eq), 117mg of **237** (1.05mmol, 1.1 eq) and 468mg of Cs₂CO₃ (1.44mmol, 1.5eq) were dissolved in 10mL DMF and stirred at 40°C for 24h. The product was isolated as a light brown solid in 93% yield (252mg, 0.89mmol). No further purification was needed as was determined through NMR analysis.

R_f (TLC, Hept/EtOAc 1:1) = 0.1

¹H-NMR (400 MHz, CDCl₃):

δ = 9.45 (s, 1H, NH), 7.43 (dd, *J* = 8.9, 6.8 Hz, 1H, 8-H_{arom}), 7.34 (d, *J* = 9.0 Hz, 1H, 9-H_{arom}), 7.05 (ddd, *J* = 3.8, 2.4, 1.5 Hz, 1H, 4'-H_{arom}), 7.00 (td, *J* = 2.7, 1.5 Hz, 1H, 5'-H_{arom}), 6.65 (d, *J* = 6.7 Hz, 1H, 7-H_{arom}), 6.36 (s, 1H, C=OCH), 6.30 (dt, *J* = 3.7, 2.5 Hz, 1H, 3'-H_{arom}), 5.21 (d, *J* = 0.6 Hz, 2H, CH₂), 3.02 (s, 3H, 6-CH₃).

¹³C-NMR (101 MHz, CDCl₃):

δ = 162.33 (1C, C=OCH), 161.17 (1C, OC=O), 160.40 (1C, C_{q, arom}), 153.79 (1C, C_{q, arom}), 144.24 (1C, C_{q, arom}), 135.65 (1C, 8-CH_{arom}), 125.05 (1C, 9-CH_{arom}), 123.73 (1C, 5'-CH_{arom}), 122.08 (1C, C_{q, arom}), 118.36 (1C, 7-CH_{arom}), 116.35 (1C, 4'-CH_{arom}), 110.86 (1C, 3'-CH_{arom}), 103.09 (1C, C=OCH), 64.58 (1C, CH₂), 24.82 (1C, 6-CH₃).

UHPLC-MS

R_t (MCS): 1.070 min

m/z: [M+H]⁺ (calc.) = 284.3

[M+H]⁺ (meas.) = 284.2

(6-methyl-4-oxo-4H-pyrido[1,2-a]pyrimidin-2-yl)methyl 1-methyl-1H-imidazole-5-
carboxylate (58)



200mg of **126** (0.96 mmol, 1eq), 133mg of **238** (1.05mmol, 1.1 eq) and 468mg of Cs₂CO₃ (1.44mmol, 1.5eq) were dissolved in 10mL DMF and stirred at 40°C for 23h. The product was isolated as a white solid in 96% yield (274mg, 0.92mmol). No further purification was needed as was determined through NMR analysis.

R_f (TLC, H₂O/ACN 94:6) = 0.46.

¹H-NMR (400 MHz, CDCl₃):

δ = 7.87 (d, *J* = 0.9 Hz, 1H, 4'-H_{arom}), 7.59 (s, 1H, 2'-H_{arom}), 7.45 (dd, *J* = 8.9, 6.9 Hz, 1H, 8-H_{arom}), 7.35 (dd, *J* = 8.9, 0.7 Hz, 1H, 9-H_{arom}), 6.66 (d, *J* = 6.7 Hz, 1H, 7-H_{arom}), 6.32 (s, 1H), 5.21 (s, 2H, CH₂), 3.92 (s, 3H, NCH₃), 3.03 (s, 3H, 6-CH₃).

¹³C-NMR (101 MHz, CDCl₃):

δ = 162.25 (1C, C=OCH), 160.73 (1C, OC=O), 159.76 (1C, C_{q, arom}), 153.86 (1C, C_{q, arom}), 144.29 (1C, C_{q, arom}), 143.08 (1C, 2'-CH_{arom}), 138.56 (1C, 4'-CH_{arom}), 135.74 (1C, 8-CH_{arom}), 125.10 (1C, 9-CH_{arom}), 122.59 (1C, C_{q, arom}), 118.43 (1C, 7-CH_{arom}), 103.05 (1C, C=OCH), 64.73 (1C, CH₂), 34.25 (1C, NCH₃), 24.82 (1C, 6-CH₃).

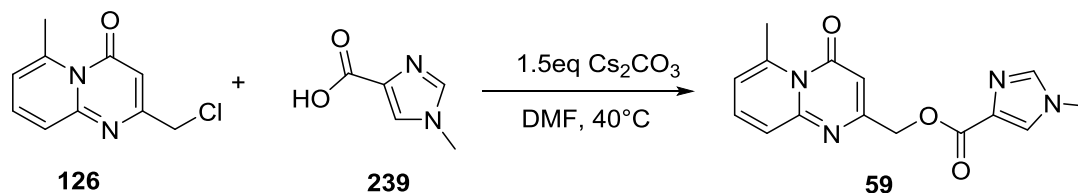
UHPLC-MS

R_t (MCS): 0.194 min

m/z: [M+H]⁺ (calc.) = 299.3

[M+H]⁺ (meas.) = 299.2

(6-methyl-4-oxo-4H-pyrido[1,2-a]pyrimidin-2-yl)methyl 1-methyl-1H-imidazole-4-
carboxylate (59)



200mg of **126** (0.96 mmol, 1eq), 136mg of **239** (1.08mmol, 1.2eq) and 520mg of Cs₂CO₃ (1.60mmol, 1.7eq) were dissolved in 10mL DMF and stirred at 40°C for 24h. The product was isolated as a white solid in 97% yield (277mg, 0.93mmol). No further purification was needed as was determined through NMR analysis.

R_f (TLC, Hept/EtOAc 1:1) =

¹H-NMR (400 MHz, CDCl₃):

δ = 7.67 (d, *J* = 1.3 Hz, 1H, 2'-H_{arom}), 7.50 (d, *J* = 1.1 Hz, 1H, 5'-H_{arom}), 7.42 (dd, *J* = 8.9, 6.8 Hz, 1H, 8-H_{arom}), 7.34 (dd, *J* = 8.9, 0.8 Hz, 1H, 9-H_{arom}), 6.64 (d, *J* = 6.6 Hz, 1H, 7-H_{arom}), 6.37 (s, 1H, C=OCH), 5.25 (d, *J* = 0.7 Hz, 2H, CH₂), 3.77 (s, 3H, NCH₃), 3.02 (s, 3H, 6-CH₃).

¹³C-NMR (101 MHz, CDCl₃):

δ = 162.34 (1C, C=OCH), 162.03 (1C, OC=O), 161.24 (1C, C_{q, arom}), 153.75 (1C, C_{q, arom}), 144.16 (1C, C_{q, arom}), 139.02 (1C, 5'-CH_{arom}), 135.52 (1C, 8-CH_{arom}), 133.47 (1C, C_{q, arom}), 126.90 (1C, 2'-CH_{arom}), 125.12 (1C, 9-CH_{arom}), 118.27 (1C, 7-CH_{arom}), 103.11 (1C, C=OCH), 64.72 (1C, CH₂), 33.99 (1C, NCH₃), 24.81 (1C, 6-CH₃).

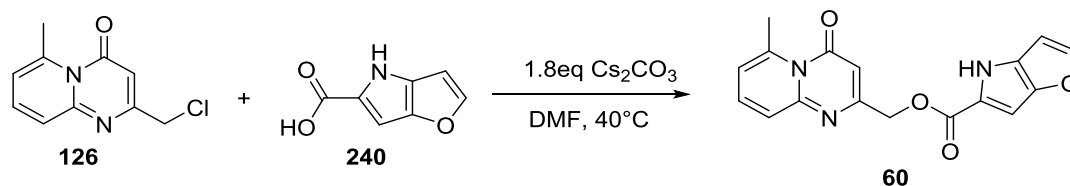
UHPLC-MS

R_t (MCS): 0.333 min

m/z: [M+H]⁺ (calc.) = 299.1

[M+H]⁺ (meas.) = 299.2

(6-methyl-4-oxo-4H-pyrido[1,2-a]pyrimidin-2-yl)methyl 4H-furo[3,2-b]pyrrole-5-
carboxylate (60)



83mg of **126** (0.40mmol, 1eq), 100mg of **240** (0.66mmol, 1.65eq) and 323mg of Cs₂CO₃ (0.72mmol, 1.8eq) were dissolved in 10mL DMF and stirred at 40°C for 4h. After work-up, the crude product was purified with HPLC (H₂O/ACN+0.1%TFA, 10% -> 100%, 15 min gradient). The product was isolated as a white solid in 25% yield (44.4mg, 0.10mmol).

R_f (TLC, Hept/EtOAc 1:1) = 0.156

¹H-NMR (400 MHz, DMSO-d₆):

δ = 11.84 (s, 1H, NH), 7.84 (s, 1H, H_{arom}), 7.67 (t, *J* = 7.6 Hz, 1H, 8-H_{arom}), 7.38 (d, *J* = 8.3 Hz, 1H, 9-H_{arom}), 6.92 (s, 2H, 8-H_{arom}, H_{arom}), 6.65 (s, 1H, 4'-H_{arom}), 6.29 (s, 1H, C=OCH), 5.18 (s, 2H, CH₂), 2.93 (s, 3H, 6-CH₃).

¹³C-NMR (101 MHz, DMSO-d₆):

δ = 161.63 (1C, C=OCH), 161.25 (1C, OC=O), 160.90 (1C, C_q, arom), 153.60 (1C, C_q, arom), 150.35 (1C, CH_{arom}), 147.50 (1C, C_q, arom), 143.89 (1C, C_q, arom), 137.21 (1C, 8-CH_{arom}), 130.49 (1C, C_q, arom), 124.83 (1C, 9-CH_{arom}), 123.05 (1C, C_q, arom), 119.12 (1C, 7-CH_{arom}), 102.17 (1C, C=OCH), 99.92 (1C, CH_{arom}), 97.17 (1C, 4'-CH_{arom}), 64.39 (1C, CH₂), 24.44 (1C, 6-CH₃).

UHPLC-MS

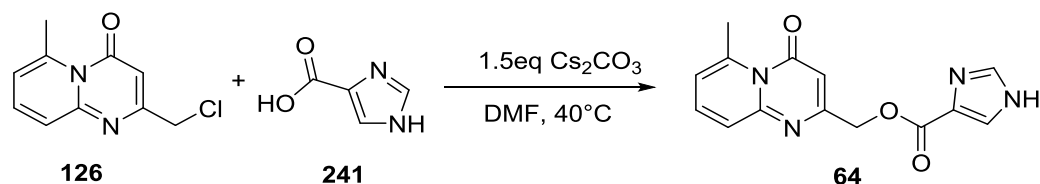
R_t (MCS): 1.395 min

m/z: [M+H]⁺ (calc.) = 324.1

[M+H]⁺ (meas.) = 324.2

(6-methyl-4-oxo-4H-pyrido[1,2-a]pyrimidin-2-yl)methyl 1H-imidazole-4-carboxylate

(64)



118mg of **241** (1.05mmol, 2.2eq) and 486mg of Cs₂CO₃ (mmol, 3eq) were dissolved in 8mL anh. DMF and stirred at 100°C for 15 min before 100mg **10** (0.48mmol, 1eq) dissolved in 2mL DMF was added dropwise to the hot solution. The reaction was stirred for 96h at 90°C. After the reaction was finished the solvent was evaporated and the resulting solid resuspended in 30mL water. The aqueous phase was extracted with three times 30mL water. The combined organic phases were washed with water and brine before being dried with anh. NaSO₄, filtered and the solvent evaporated *in vacuo*. The crude was further purified through column chromatography on 10g SiO₂ with a linear gradient of DCM/MeOH 0% --> 12%. The product was isolated as a white product in 7% yield (10mg, 0.02mmol). The product was analyzed by NMR and UHPLC-MS.

R_f (TLC, DCM/MeOH 97:3) = 0.071

¹H-NMR (400 MHz, CDCl₃):

δ = 7.92 (s, 1H, 5'-CH_{arom}), 7.87 (s, 1H, 2'-CH_{arom}), 7.46 (dd, *J* = 8.9, 6.9 Hz, 1H, 8-CH_{arom}), 7.37 (d, *J* = 8.8 Hz, 1H, 9-CH_{arom}), 6.68 (d, *J* = 6.9 Hz, 1H, 7-CH_{arom}), 6.35 (s, 1H, C=OCH), 5.26 (s, 2H, CH₂), 3.03 (s, 3H, 6-CH₃).

¹³C-NMR (101 MHz, CDCl₃):

δ = 162.36 (1C, C=OCH), 160.83 (1C, OC=O), 160.68 (1C, C_{q, arom}), 153.86 (1C, C_{q, arom}), 144.32 (1C, C_{q, arom}), 137.49 (1C, 5'-CH_{arom}), 135.86 (1C, 8-CH_{arom}), 128.34 (1C, C_{q, arom}), 127.97 (1C, 2'-CH_{arom}), 125.08 (1C, 9-CH_{arom}), 118.58 (1C, 7-CH_{arom}), 103.24 (1C, C=OCH), 65.02 (1C, CH₂), 24.87 (1C, 6-CH₃).

UHPLC-MS

R_t (MCS): 0.255 min

m/z: [M+H]⁺ (calc.) = 285.1

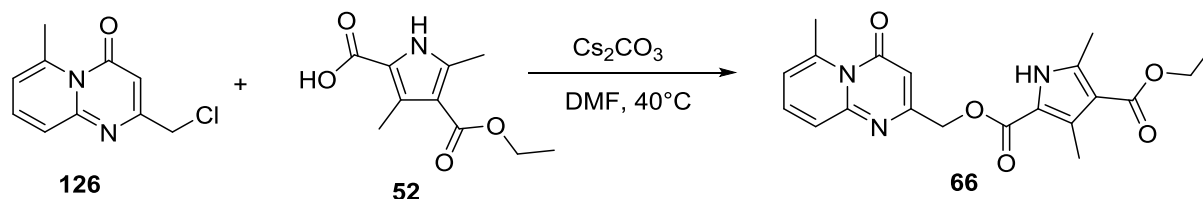
[M+H]⁺ (meas.) = 285.2

2.3.4 Ester group modification of pyrrole ring

2.3.4.1 Head-group modified compounds

All following reactions were conducted according to **General Procedure G**.

4-ethyl 2-((6-methyl-4-oxo-4H-pyrido[1,2-a]pyrimidin-2-yl)methyl) 3,5-dimethyl-1H-pyrrole-2,4-dicarboxylate (66)



30mg **126** (0.14mmol, 1eq) and 33mg **52** (0.16mmol, 1.1eq) were stirred with 52mg Cs_2CO_3 (0.16mmol, 1.1eq) in 4mL DMF at 40°C . The reaction mixture was worked up after 17h and the crude not purified further because analysis by UHPLC-MS and NMR showed no impurities. The product **66** was isolated as a light brown solid in 98% yield (4.3mg, 0.14mmol).

R_f (TLC, cyclohex/EtOAc 1:1) = 0.10.

$^1\text{H-NMR}$ (400 MHz, DMSO-d_6):

δ = 12.05 (s, 1H, NH), 7.68 (dd, J = 8.5, 7.3 Hz, 1H, 8- H_{arom}), 7.39 (d, J = 8.8 Hz, 1H, 9- H_{arom}), 6.93 (d, J = 7.0 Hz, 1H, 7- H_{arom}), 6.28 (s, 1H, C=OCH), 5.17 (s, 2H, $\text{CH}_2\text{OC=O}$), 4.19 (q, J = 7.1 Hz, 2H, OCH_2CH_3), 2.93 (s, 3H, 6- CH_3), 2.51 (s, 3H, CH_3), 2.45 (s, 3H, CH_3), 1.28 (t, J = 7.1 Hz, 3H, OCH_2CH_3).

$^{13}\text{C-NMR}$ (100 MHz, DMSO-d_6):

δ = 164.53 (1C, C=O), 161.25 (1C, C=OCH), 160.92 (1C, $\text{CH}_2\text{OC=O}$), 159.80 (1C, $\text{C}_{\text{q, arom}}$), 153.22 (1C, $\text{C}_{\text{q, arom}}$), 143.44 (1C, $\text{C}_{\text{q, arom}}$), 140.13 (1C, $\text{C}_{\text{q, arom}}$), 136.77 (1C, 8- CH_{arom}), 130.89 (1C, $\text{C}_{\text{q, arom}}$), 124.50 (1C, 9- CH_{arom}), 118.70 (1C, 7- CH_{arom}), 116.72 (1C, $\text{C}_{\text{q, arom}}$), 112.66 (1C, $\text{C}_{\text{q, arom}}$), 101.78 (1C, C=OCH), 63.87 (1C, $\text{CH}_2\text{OC=O}$), 59.03 (1C, OCH_2CH_3), 24.02 (1C, 6- CH_3), 14.31 (1C, OCH_2CH_3), 13.58 (1C, CH_3), 11.87 (1C, CH_3).

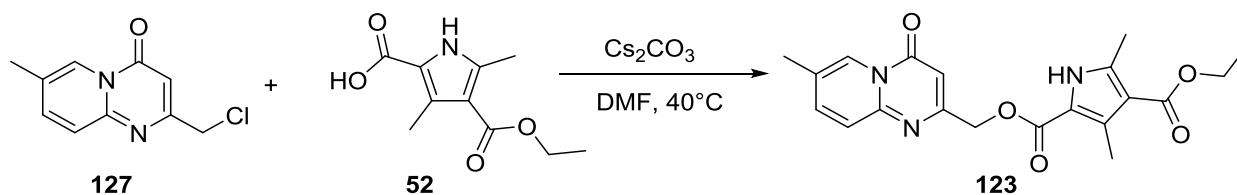
UHPLC-MS

R_t (MCS): 1.497 min

m/z: $[\text{M}+\text{H}]^+$ (calc.) = 384.2

$[\text{M}+\text{H}]^+$ (meas.) = 384.2

[4-ethyl 2-\(\(7-methyl-4-oxo-4H-pyrido\[1,2-a\]pyrimidin-2-yl\)methyl\) 3,5-dimethyl-1H-pyrrole-2,4-dicarboxylate \(123\)](#)



30mg **127** (0.14mmol, 1eq) and 33mg **52** (0.22mmol, 1.5eq) were stirred with 52mg Cs_2CO_3 (0.29mmol, 2eq) in 3mL DMF at 40°C. The reaction was finished after 2h as determined by UHPLC-MS. The reaction mixture was worked up and the crude purified with 10g SiO_2 with a gradient of cyclohexane/EtOAc 20% --> 100%. The product was isolated as a light brown solid in 52% yield (28.5mg, 0.07mmol).

R_f (TLC, cyclohex(EtOAc 1:1)) = 0.11.

$^1\text{H-NMR}$ (400 MHz, DMSO-d_6):

δ = 9.32 (s, 1H, NH), 8.86 (s, 1H, 6- H_{arom}), 7.66 (s, 2H, 8- H_{arom} , 9- H_{arom}), 6.50 (s, 1H, C=OCH), 5.30 (s, 2H, $\text{CH}_2\text{OC=O}$), 4.30 (q, J = 7.1 Hz, 2H, OCH_2CH_3), 2.62 (s, 3H, CH_3), 2.54 (s, 3H, CH_3), 2.45 (s, 3H, 7- CH_3), 1.37 (t, J = 7.1 Hz, 3H, OCH_2CH_3).

$^{13}\text{C-NMR}$ (100 MHz, DMSO-d_6):

δ = 165.46 (1C, C=O), 161.91 (1C, C=OCH), 160.43 (1C, $\text{CH}_2\text{OC=O}$), 157.92 (1C, $\text{C}_{\text{q, arom}}$), 149.99 (1C, $\text{C}_{\text{q, arom}}$), 140.14 (1C, 8- CH_{arom}), 139.87 (1C, $\text{C}_{\text{q, arom}}$), 132.73 (1C, $\text{C}_{\text{q, arom}}$), 126.38 (1C, $\text{C}_{\text{q, arom}}$), 125.36 (1C, 9- CH_{arom}), 125.06 (1C, 6- CH_{arom}), 117.04 (1C, $\text{C}_{\text{q, arom}}$), 114.13 (1C, $\text{C}_{\text{q, arom}}$), 100.59 (1C, C=OCH), 64.77 (1C, $\text{CH}_2\text{OC=O}$), 59.74 (1C, OCH_2CH_3), 18.50 (1C, 7- CH_3), 14.56 (1C, CH_3), 12.32 (1C, CH_3).

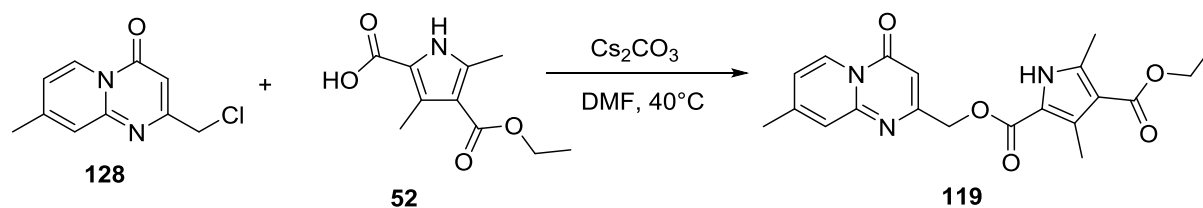
UHPLC-MS

R_t (MCS): 1.486 min

m/z: $[\text{M}+\text{H}]^+$ (calc.) = 384.2

$[\text{M}+\text{H}]^+$ (meas.) = 384.2

[4-ethyl 2-\(\(8-methyl-4-oxo-4H-pyrido\[1,2-a\]pyrimidin-2-yl\)methyl\) 3,5-dimethyl-1H-pyrrole-2,4-dicarboxylate \(119\)](#)



40mg **128** (191.7 μ mol, 1eq) and 48.6mg **52** (230.1 μ mol, 1.2eq) were stirred with 697mg Cs₂CO₃ (325.8 μ mol, 1.2eq) in 5mL DMF at 40°C. The reaction mixture was worked up aqueously after 15h. The product was isolated as a white solid in 66% yield (48.9mg, 127.5 μ mol) without further purification.

R_f (TLC, cyclohex/EtOAc 1:1) = 0.14.

¹H-NMR (400 MHz, DMSO-d₆):

δ = 12.07 (s, 1H, NH), 8.85 (d, J = 7.3 Hz, 1H, 6-H_{arom}), 7.49 (s, 1H, 9-H_{arom}), 7.24 (dd, J = 7.3, 1.8 Hz, 1H, 7-H_{arom}), 6.38 (s, 1H, C=OCH), 5.22 (s, 2H, CH₂OC=O), 4.18 (q, J = 7.1 Hz, 2H, CH₂-CH₃), 2.49 (s, 3H, CH₃), 2.46 (s, 3H, 8-CH₃), 2.44 (s, 3H, CH₃), 1.27 (t, J = 7.1 Hz, 3H, CH₂-CH₃).

¹³C-NMR (100 MHz, DMSO-d₆):

δ = 164.77 (1C, C=O), 163.04 (1C, C=OCH), 159.98 (1C, CH₂OC=O), 157.44 (1C, C_q, arom), 150.84 (1C, C_q, arom), 150.17 (1C, C_q, arom), 140.31 (1C, C_q, arom), 131.13 (1C, C_q, arom), 126.53 (1C, 6-CH_{arom}), 123.69 (1C, 9-CH_{arom}), 119.13 (1C, 7-CH_{arom}), 116.89 (1C, C_q, arom), 112.84 (1C, C_q, arom), 98.54 (1C, C=OCH), 64.51 (1C, CH₂OC=O), 59.28 (1C, OCH₂CH₃), 21.02 (1C, 8-CH₃), 14.47 (1C, OCH₂CH₃), 13.74 (1C, CH₃), 12.03 (1C, CH₃).

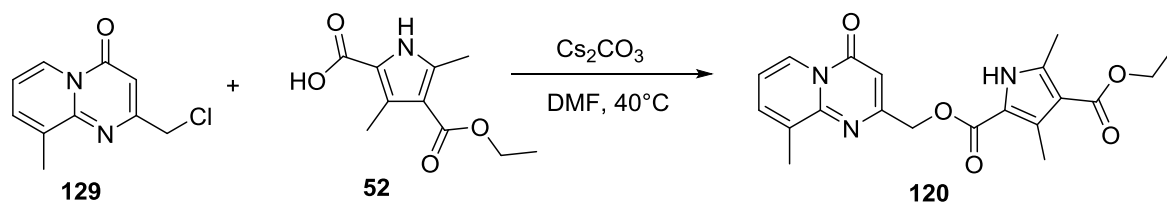
UHPLC-MS

R_t (MCS): 1.464 min

m/z: [M+H]⁺ (calc.) = 384.2

[M+H]⁺ (meas.) = 384.2

[4-ethyl 2-\(\(9-methyl-4-oxo-4H-pyrido\[1,2-a\]pyrimidin-2-yl\)methyl\) 3,5-dimethyl-1H-pyrrole-2,4-dicarboxylate \(120\)](#)



40mg **129** (191.7 μ mol, 1eq) and 48.6mg **52** (230.1 μ mol, 1.2eq) were stirred with 697mg Cs₂CO₃ (325.8 μ mol, 1.2eq) in 5mL DMF at 40°C. The reaction mixture was worked up aqueously after 15h. The product was isolated as white solid in 74% yield (27.9mg, 72.8 μ mol).

R_f (TLC, cyclohext/EtOAc 1:1) = 0.37.

¹H-NMR (400 MHz, DMSO-d₆):

δ = 12.07 (s, 1H, NH), 8.85 (d, J = 6.6 Hz, 1H, 6-H_{arom}), 7.87 (d, J = 7.3 Hz, 1H, 8-H_{arom}), 7.28 (t, J = 7.0 Hz, 1H, 7-H_{arom}), 6.47 (s, 1H, C=OCH), 5.28 (s, 2H, CH₂OC=O), 4.18 (q, J = 7.3 Hz, 2H, CH₂-CH₃), 2.52 (s, 3H, CH₃), 2.47 (s, 3H, 9-CH₃), 2.44 (s, 3H, CH₃), 1.27 (t, J = 7.0 Hz, 3H, CH₂-CH₃).

¹³C-NMR was not determined due to very bad solubility of compound in common organic solvents.

UHPLC-MS

R_t (MCS): 1.582 min

m/z: [M+H]⁺ (calc.) = 384.2

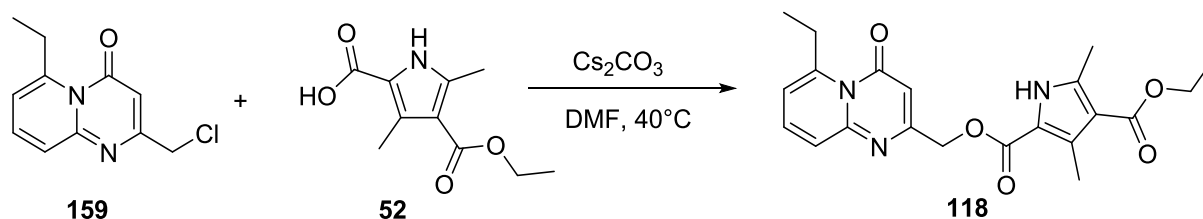
[M+H]⁺ (meas.) = 384.2

HR-MS:

m/z: [M+H]⁺ (calc.) =

[M+H]⁺ (meas.) =

4-ethyl 2-((6-ethyl-4-oxo-4H-pyrido[1,2-a]pyrimidin-2-yl)methyl) 3,5-dimethyl-1H-pyrrole-2,4-dicarboxylate (118)



19.2mg **159** (87.1 μ mol, 1eq) and 28mg **52** (130.7 μ mol, 1.5eq) were stirred with 43mg Cs₂CO₃ (130.7 μ mol, 1.5eq) in 3mL DMF at 40°C. The reaction was finished after 16h. The reaction was worked up aqueously and the crude purified with 10g SiO₂ with a linear gradient of cyclohexane/EtOAc 30% --> 100%.The product was isolated as a light brown solid in 95% yield (33mg, 83 μ mol).

R_f (TLC, cyclohexane/EtOAc 1:1) = 0.30.

¹H-NMR (400 MHz, CDCl₃):

δ = 9.16 (s, 1H, NH), 7.50 (dd, J = 8.8, 7.0 Hz, 1H, 8-H_{arom}), 7.40 (d, J = 8.7 Hz, 1H, 9-H_{arom}), 6.76 (d, J = 6.8 Hz, 1H, 7-H_{arom}), 6.37 (s, 1H, C=OCH), 5.24 (s, 2H, CH₂OC=O), 4.30 (q, J = 7.1 Hz, 2H, OCH₂CH₃), 3.50 (q, J = 7.3 Hz, 2H, CH₂CH₃), 2.63 (s, 3H, CH₃), 2.53 (s, 3H, CH₃), 1.37 (t, J = 7.1 Hz, 3H, OCH₂CH₃), 1.27 (t, J = 7.3 Hz, 3H, CH₂CH₃).

¹³C-NMR (100 MHz, CDCl₃):

δ = 165.48 (1C, C=O), 161.55 (1C, C=OCH), 160.39 (1C, CH₂OC=O), 159.73 (1C, C_q, arom), 153.66 (1C, C_q, arom), 150.26 (1C, C_q, arom), 139.85 (1C, C_q, arom), 136.36 (1C, 8-CH_{arom}), 132.72 (1C, C_q, arom), 124.70 (1C, 9-CH_{arom}), 117.53 (1C, 7-CH_{arom}), 117.04 (1C, C_q, arom), 114.10 (1C, C_q, arom), 103.29 (1C, C=OCH), 64.18 (1C, CH₂OC=O), 59.74 (1C, OCH₂CH₃), 29.95 (1C, 6-CH₂CH₃), 15.29 (1C, 6-CH₂CH₃), 14.57 (2C, CH₃, OCH₂CH₃), 12.30 (1C, CH₃).

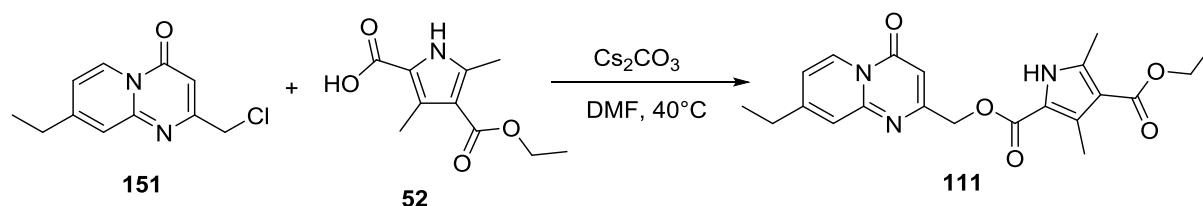
UHPLC-MS

R_t (MCS): 1.546 min

m/z: [M+H]⁺ (calc.) = 398.2

[M+H]⁺ (meas.) = 398.2

4-ethyl 2-((8-ethyl-4-oxo-4H-pyrido[1,2-a]pyrimidin-2-yl)methyl) 3,5-dimethyl-1H-pyrrole-2,4-dicarboxylate (111)



15mg **151** (67.4 μ mol, 1eq) and 17mg **52** (80.8 μ mol, 1.2eq) were stirred with 26mg Cs₂CO₃ (80.8 μ mol, 1.2eq) in 3mL DMF at 40°C. The reaction was finished after 2.5h. The reaction was worked up aqueously and the crude purified with 10g SiO₂ with a linear gradient of DCM/MeOH 3% -->5%. The product was isolated as a white solid in 86% yield (23.1mg, 58.1 μ mol).

R_f (TLC, cyclohexane/EtOAc 3:7) = 0.43.

¹H-NMR (400 MHz, CDCl₃):

δ = 9.77 (s, 1H, NH), 8.93 (d, J = 7.2 Hz, 1H, 6-H_{arom}), 7.46 (s, 1H, 9-H_{arom}), 7.02 (d, J = 7.3 Hz, 1H, 7-H_{arom}), 6.45 (s, 1H, C=OCH), 5.27 (s, 2H, CH₂), 4.28 (q, J = 7.1 Hz, 2H, OCH₂CH₃), 2.78 (q, J = 7.4 Hz, 2H, CH₂CH₃), 2.61 (s, 3H, 3'-CH₃), 2.51 (s, 3H, 5'-CH₃), 1.39 – 1.27 (m, 6H, OCH₂CH₃, CH₂CH₃).

¹³C-NMR (101 MHz, CDCl₃):

δ = 165.52 (1C, C=O), 162.48 (1C, C=OCH), 160.45 (1C, CH₂OCH=O), 158.08 (1C, C_q, arom), 155.31 (1C, C_q, arom), 151.30 (1C, C_q, arom), 140.01 (1C, C_q, arom), 132.70 (1C, C_q, arom), 126.94 (1C, 6-CH_{arom}), 122.45 (1C, 9-CH_{arom}), 117.62 (1C, 7-CH_{arom}), 117.04 (1C, C_q, arom), 113.95 (1C, C_q, arom), 100.04 (1C, C=OCH), 64.73 (1C, CH₂OC=O), 59.67 (1C, OCH₂CH₃), 28.55 (1C, CH₂CH₃), 14.53 (1C, OCH₂CH₃), 14.45 (1C, 5'-CH₃), 13.38 (1C, CH₂CH₃), 12.27 (1C, 3'-CH₃).

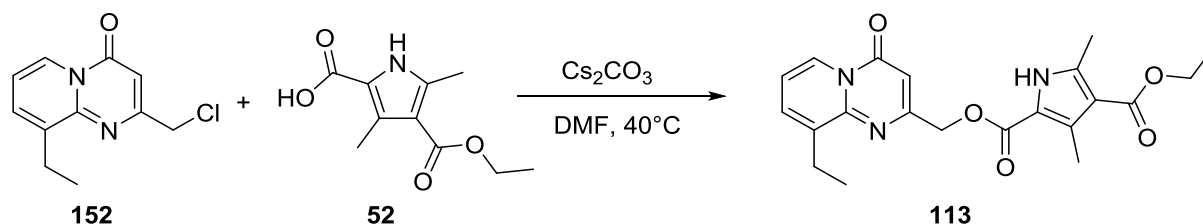
UHPLC-MS

R_t (MCS): 1.553 min

m/z: [M+H]⁺ (calc.) = 398.2

[M+H]⁺ (meas.) = 398.2

[4-ethyl 2-\(\(9-ethyl-4-oxo-4H-pyrido\[1,2-a\]pyrimidin-2-yl\)methyl\) 3,5-dimethyl-1H-pyrrole-2,4-dicarboxylate \(113\)](#)



7.4mg **152** (33.2 μ mol, 1eq) and 8mg **52** (39.9 μ mol, 1.2eq) were stirred with 13mg Cs₂CO₃ (39.9 μ mol, 1.2eq) in 3mL DMF at 40°C. The reaction was finished after 16h. The reaction mixture was worked up aqueously and the crude purified with 10g SiO₂ with a linear gradient of cyclohexane/EtOAc 30% -->100%. The product was isolated as a white solid in 69% yield (9.1mg, 22.9 μ mol).

R_f (TLC, cyclohex/EtOAc 3:7) = 0.67.

¹H-NMR (400 MHz, DMSO-d₆):

δ = 9.00 (s, 1H, NH), 8.95 (d, J = 7.1 Hz, 1H, 6-H_{arom}), 7.60 (d, J = 6.5 Hz, 1H, 8-H_{arom}), 7.08 (t, J = 7.1 Hz, 1H, 7-H_{arom}), 6.51 (s, 1H, C=OCH), 5.34 (s, 2H, CH₂), 4.31 (q, J = 7.1 Hz, 2H, OCH₂CH₃), 3.02 (dd, J = 14.9, 7.4 Hz, 2H, CH₂CH₃), 2.64 (s, 3H, 3'-CH₃), 2.55 (s, 3H, 5'-CH₃), 1.37 (t, J = 7.1 Hz, 3H, OCH₂CH₃), 1.30 (t, J = 7.5 Hz, 3H, CH₂CH₃).

¹³C-NMR (101 MHz, DMSO-d₆):

δ = 165.46 (1C, C=O), 163.74 (1C, C=OCH), 161.93 (1C, CH₂OC=O), 158.89 (1C, C_q, arom), 150.38 (1C, C_q, arom), 140.46 (1C, C_q, arom), 139.65 (1C, C_q, arom), 133.73 (1C, 8-CH_{arom}), 129.88 (1C, C_q, arom), 125.33 (1C, 6-CH_{arom}), 117.33 (1C, C_q, arom), 115.29 (1C, 7-CH_{arom}), 114.17 (1C, C_q, arom), 100.29 (1C, C=OCH), 65.22 (1C, CH₂OC=O), 59.77 (1C, OCH₂CH₃), 29.86 (1C, CH₂CH₃), 14.62 (1C, 5'-CH₃), 14.58 (1C, OCH₂CH₃), 13.52 (1C, CH₂CH₃), 12.37 (1C, 3'-CH₃).

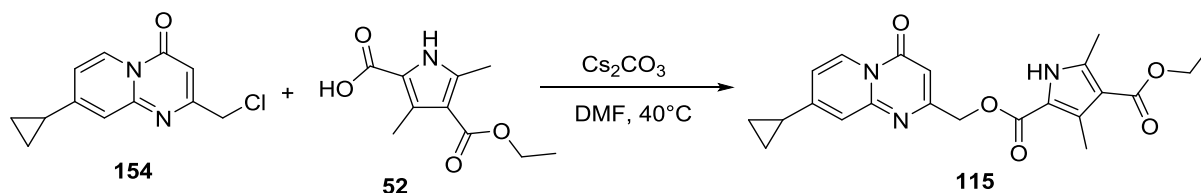
UHPLC-MS

R_t (MCS): 1.656 min

m/z: [M+H]⁺ (calc.) = 398.2

[M+H]⁺ (meas.) = 398.2

4-ethyl 2-((8-cyclopropyl-4-oxo-4H-pyrido[1,2-a]pyrimidin-2-yl)methyl) 3,5-dimethyl-1H-pyrrole-2,4-dicarboxylate (115)



20mg **154** (85.2 μ mol, 1eq), 22mg **52** (102.3 μ mol, 1.2eq) with 33mg Cs₂CO₃ (102.3 μ mol, 1.2eq) in 3mL DMF at 40°C. The reaction was finished after 3h. The reaction was worked up aqueously and the crude purified with 10g SiO₂ with a linear gradient of cyclohexane/EtOAc 30% -->100%.The product was isolated as a white solid in 66% yield (22.9mg, 55.9 μ mol).

R_f (TLC, cyclohexane/EtOAc 3:7) = 0.45.

¹H-NMR (400 MHz, CDCl₃):

δ = 9.37 (s, 1H, NH), 8.91 (d, *J* = 7.4 Hz, 1H, 6-H_{arom}), 7.37 (s, 1H, 9-H_{arom}), 6.84 (d, *J* = 9.0 Hz, 1H, 7-H_{arom}), 6.40 (s, 1H, C=OCH), 5.28 (s, 2H, CH₂OC=O), 4.30 (q, *J* = 7.1 Hz, 2H, OCH₂CH₃), 2.62 (s, 1H, CH₃), 2.54 (s, 1H, CH₃), 2.07 – 1.98 (m, 1H, CH(CH₂)₂), 1.37 (t, *J* = 7.1 Hz, 3H, OCH₂CH₃), 1.29 – 1.23 (m, 2H, CH(CH₂)₂), 1.01 – 0.94 (m, 12H, CH(CH₂)₂).

¹³C-NMR (101 MHz, CDCl₃):

δ = 165.48 (1C, C=O), 163.03 (1C, C=OCH), 160.34 (1C, CH₂OC=O), 157.90 (1C, C_{q, arom}), 156.85 (1C, C_{q, arom}), 150.89 (1C, C_{q, arom}), 139.91 (1C, C_{q, arom}), 132.82 (1C, C_{q, arom}), 127.11 (1C, 6-CH_{arom}), 119.56 (1C, 9-CH_{arom}), 116.99 (1C, C_{q, arom}), 114.93 (1C, 7-CH_{arom}), 114.09 (1C, C_{q, arom}), 99.51 (1C, C=OCH), 64.65 (1C, CH₂OC=O), 59.73 (1C, OCH₂CH₃), 15.97 (1C, CH(CH₂)₂), 14.57 (2C, (1C, CH₃, OCH₂CH₃), 12.30 (1C, CH₃), 11.84 (2C, CH(CH₂)₂).

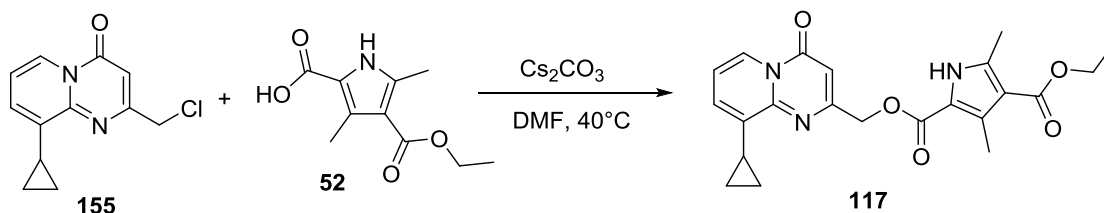
UHPLC-MS

R_t (MCS): 1.545min

m/z: [M+H]⁺ (calc.) = 410.2

[M+H]⁺ (meas.) = 410.2

4-ethyl 2-((9-cyclopropyl-4-oxo-4H-pyrido[1,2-a]pyrimidin-2-yl)methyl) 3,5-dimethyl-1H-pyrrole-2,4-dicarboxylate (117)



25mg **155** (106.5 μmol , 1eq), 27mg **52** (127.8 μmol , 1.2eq) with 42mg Cs_2CO_3 (127.8 μmol , 1.2eq) in 4mL DMF at 40°C . The reaction was finished after 6h. The reaction was worked up aqueously and the crude purified with 10g SiO_2 with a linear gradient of cyclohexane/EtOAc 30% -->100%.The product was isolated as a white solid in 56% yield (24.2mg, 59.7 μmol).

R_f (TLC, cyclohexane/EtOAc 1:1) = 0.43

$^1\text{H-NMR}$ (400 MHz, CDCl_3):

δ = 9.00 (s, 1H, NH), 8.90 (d, J = 8.4 Hz, 1H, 6- H_{arom}), 7.20 (d, J = 7.8 Hz, 1H, 8- H_{arom}), 7.05 (t, J = 7.1 Hz, 1H, 7- H_{arom}), 6.53 (s, 1H, C=OCH), 5.37 (s, 2H, $\text{CH}_2\text{OC}=\text{O}$), 4.31 (q, J = 7.1 Hz, 2H, OCH_2CH_3), 2.90 – 2.79 (m, 1H, $\text{CH}(\text{CH}_2)_2$), 2.64 (s, 3H, CH_3), 2.54 (s, 3H, CH_3), 1.37 (t, J = 7.1 Hz, 3H, OCH_2CH_3), 1.14 (dt, J = 6.4, 4.6 Hz, 2H, $\text{CH}(\text{CH}_2)_2$), 0.80 (dt, J = 6.5, 4.7 Hz, 2H, $\text{CH}(\text{CH}_2)_2$).

$^{13}\text{C-NMR}$ (101 MHz, CDCl_3):

δ = 165.46 (1C, C=O), 163.55 (1C, $\text{C}=\text{OCH}$), 160.68 (1C, $\text{CH}_2\text{OC}=\text{O}$), 158.72 (1C, C_q , arom), 148.12 (1C, C_q , arom), 140.78 (1C, C_q , arom), 139.68 (1C, C_q , arom), 132.44 (1C, C_q , arom), 129.49 (1C, 8- CH_{arom}), 124.57 (1C, 6- CH_{arom}), 117.29 (1C, C_q , arom), 115.36 (1C, 7- CH_{arom}), 114.15 (1C, C_q , arom), 100.33 (1C, C=OCH), 65.12 (1C, $\text{CH}_2\text{OC}=\text{O}$), 59.77 (1C, OCH_2CH_3), 14.62 (1C, CH_3), 14.57 (1C, OCH_2CH_3), 12.39 (1C, CH_3), 11.01 (1C, $\text{CH}(\text{CH}_2)_2$), 9.98 (2C, $\text{CH}(\text{CH}_2)_2$).

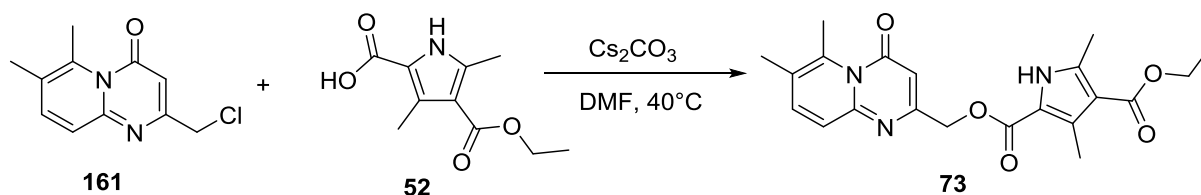
UHPLC-MS

R_t (MCS): 1.679min

m/z: $[\text{M}+\text{H}]^+$ (calc.) = 410.2

$[\text{M}+\text{H}]^+$ (meas.) = 410.2

[2-\(\(6,7-dimethyl-4-oxo-4H-pyrido\[1,2-a\]pyrimidin-2-yl\)methyl\) 4-ethyl 3,5-dimethyl-1H-pyrrole-2,4-dicarboxylate \(73\)](#)



50mg **161** (225 μmol , 1eq) and 71mg **52** (337 μmol , 1.5eq) were stirred with 219mg Cs_2CO_3 (674 μmol , 2eq) in 4mL DMF at 40°C . The reaction mixture was worked up aqueously after 3.5h and the crude purified by column chromatography with 10g SiO_2 and a linear gradient of heptane/EtOAc 20% --> 100%. The product was isolated as a white solid in 77% yield (68.7mg, 173 μmol).

R_f (TLC, hept/EtOAc 2:8) = 0.30

$^1\text{H-NMR}$ (400 MHz, CDCl_3):

δ = 9.23 (s, 1H, NH), 7.41 (d, J = 9.0 Hz, 1H, 8- H_{arom}), 7.28 (d, J = 9.0 Hz, 1H, 7- H_{arom}), 6.33 (s, 1H, C=OCH), 5.21 (s, 2H, CH_2OCO), 4.30 (q, J = 7.1 Hz, 2H, $\text{CH}_2\text{-CH}_3$), 2.81 (s, 3H, 6- CH_3), 2.62 (s, 3H, CH_3), 2.53 (s, 3H, CH_3), 2.31 (s, 3H, 7- CH_3), 1.36 (t, J = 7.1 Hz, 3H, $\text{CH}_2\text{-CH}_3$).

$^{13}\text{C-NMR}$ (100 MHz, CDCl_3):

δ = 165.47 (1C, C=O), 162.52 (1C, $\text{C}=\text{OCH}$), 160.64 (1C, $\text{CH}_2\text{OC}=\text{O}$), 160.56 (1C, C_q , arom), 152.83 (1C, C_q , arom), 140.65 (1C, C_q , arom), 139.73 (1C, 8- CH_{arom}), 139.66 (1C, C_q , arom), 132.54 (1C, C_q , arom), 125.14 (1C, C_q , arom), 123.56 (1C, 9- CH_{arom}), 117.18 (1C, C_q , arom), 114.10 (1C, C_q , arom), 102.84 (1C, C=OCH), 64.64 (1C, $\text{CH}_2\text{OC}=\text{O}$), 59.73 (1C, CH_2CH_3), 19.90 (1C, 6- CH_3), 19.21 (1C, 7- CH_3), 14.56 (2C, CH_3 , CH_2CH_3), 12.32 (1C, CH_3).

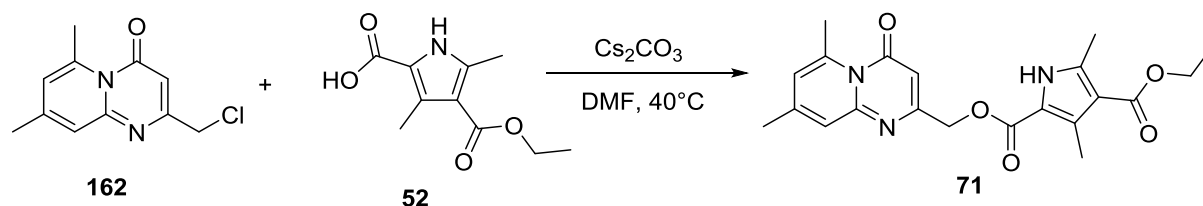
UHPLC-MS

R_t (MCS): 1.762 min

m/z : $[\text{M}+\text{H}]^+$ (calc.) = 398.2

$[\text{M}+\text{H}]^+$ (meas.) = 398.2

[2-\(\(6,8-dimethyl-4-oxo-4H-pyrido\[1,2-a\]pyrimidin-2-yl\)methyl\) 4-ethyl 3,5-dimethyl-1H-pyrrole-2,4-dicarboxylate \(71\)](#)



21mg **162** (95 μ mol, 1eq) and 30mg **52** (143 μ mol, 1.5eq) were stirred with 93mg Cs₂CO₃ (286 μ mol, 3eq) in 3mL DMF at 40°C. The reaction mixture was worked up aqueously after 3h and the crude purified by column chromatography with 10g SiO₂ and a linear gradient of DCM/MeOH 0% --> 5%. The product was isolated as a white solid in 84% yield (32mg, 81 μ mol).

R_f (TLC, DCM/MeOH 95:5) = 0.43.

¹H-NMR (400 MHz, CDCl₃):

δ = 9.38 (s, 1H, NH), 7.26 (s, 1H, 9-H_{arom} under CDCl₃ peak) 6.55 (s, 1H, 7-H_{arom}), 6.25 (s, 1H, C=OCH), 5.20 (s, 2H, CH₂OC=O), 4.29 (q, *J* = 7.1 Hz, 2H, OCH₂CH₃), 3.01 (s, 3H, 6-CH₃), 2.61 (s, 3H, CH₃), 2.53 (s, 3H, CH₃), 2.35 (s, 3H, 8-CH₃), 1.36 (t, *J* = 7.1 Hz, 3H, OCH₂CH₃).

¹³C-NMR (101 MHz, CDCl₃):

δ = 165.48 (1C, C=O), 162.03 (1C, C=OCH), 161.97 (1C, CH₂OC=O), 160.39 (1C, C_q, arom), 153.58 (1C, C_q, arom), 148.38 (1C, C_q, arom), 143.61 (1C, C_q, arom), 139.81 (1C, C_q, arom), 132.66 (1C, C_q, arom), 122.77 (1C, 9-CH_{arom}), 121.57 (1C, 7-CH_{arom}), 117.06 (1C, C_q, arom), 114.05 (1C, C_q, arom), 102.28 (1C, C=OCH), 64.27 (1C, CH₂OC=O), 59.71 (1C, OCH₂CH₃), 24.69 (1C, 6-CH₃), 21.19 (1C, 8-CH₃), 14.57 (1C, OCH₂CH₃), 14.56 (1C, CH₃), 12.29 (1C, CH₃).

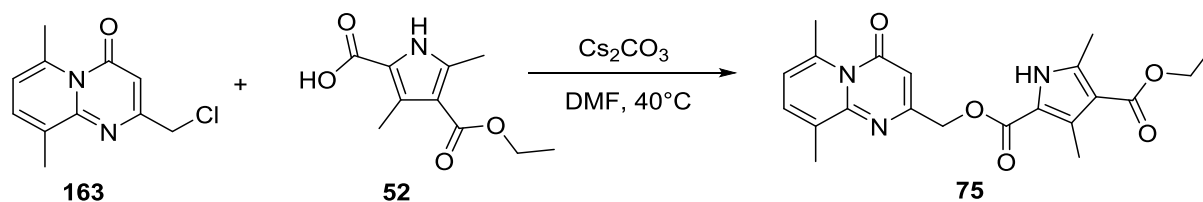
UHPLC-MS

R_t (MCS): 1.512 min

m/z: [M+H]⁺ (calc.) = 398.2

[M+H]⁺ (meas.) = 398.2

[2-\(\(6,9-dimethyl-4-oxo-4H-pyrido\[1,2-a\]pyrimidin-2-yl\)methyl\) 4-ethyl 3,5-dimethyl-1H-pyrrole-2,4-dicarboxylate \(75\)](#)



50mg **163** (225 μ mol, 1eq) and 71mg **52** (337 μ mol, 1.5eq) were stirred with 219mg Cs₂CO₃ (674 μ mol, 3eq) in 3mL DMF at 40°C. The reaction mixture was worked up aqueously after 3.5h and the crude purified by column chromatography with 10g SiO₂ and a linear gradient of hept/EtOAc 10% --> 100%. The product was isolated as a white solid in 38% (33.8mg, 85 μ mol).

R_f (TLC, hept/EtOAc 1:1) = 0.41.

¹H-NMR (400 MHz, CDCl₃):

δ = 9.04 (s, 1H, NH), 7.32 (d, J = 7.1 Hz, 1H, 8-H_{arom}), 6.57 (d, J = 7.1 Hz, 1H, 7-H_{arom}), 6.34 (s, 1H, C=OCH), 5.26 (s, 2H, CH₂-OC=O), 4.30 (q, J = 7.1 Hz, 2H, CH₂-CH₃), 2.97 (s, 3H, 6-CH₃), 2.63 (s, 3H, CH₃), 2.54 (s, 3H, CH₃), 2.41 (s, 3H, 9-CH₃), 1.37 (t, J = 7.1 Hz, 3H, CH₂-CH₃).

¹³C-NMR (101 MHz, CDCl₃):

δ = 165.48 (1C, C=O), 162.90 (1C, C=O), 160.76 (1C, C_{q,arom}), 160.32 (1C, C=O), 153.09 (1C, C_{q,arom}), 141.68 (1C, C_{q,arom}), 139.62 (1C, C_{q,arom}), 134.44 (1C, CH_{arom}), 132.97(1C, C_{q,arom}), 132.32(1C, C_{q,arom}), 117.81(1C, CH_{arom}), 117.35 (1C, C_{q,arom}), 114.10 (1C, C_{q,arom}), 102.79 (1C, C=OCH), 64.84 (1C, CH₂COO), 59.74 (1C, CH₂CH₃), 24.69 (1C, CH₃), 18.74 (1C, CH₃), 14.57 (1C, CH₃), 14.34 (1C, CH₂CH₃), 12.36 (1C, CH₃).

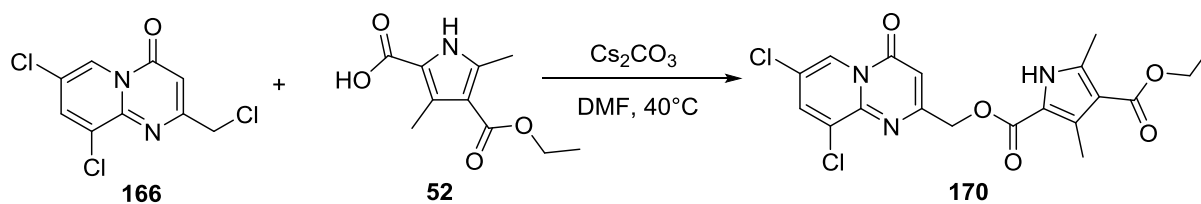
UHPLC-MS

R_t (MCS): 2.016

m/z: [M+H]⁺ (calc.) = 398.2

[M+H]⁺ (meas.) = 398.2

[2-\(\(7,9-dichloro-4-oxo-4H-pyrido\[1,2-a\]pyrimidin-2-yl\)methyl\) 4-ethyl 3,5-dimethyl-1H-pyrrole-2,4-dicarboxylate \(170\)](#)



50mg of **163** (0.19mmol, 1eq) and 60mg of **52** (0.29mmol, 1.5eq) were stirred with 185mg Cs_2CO_3 (0.57mmol, 3eq) in 3mL DMF at 40°C . The reaction mixture was worked up after 17h and the crude purified by column chromatography with 25g SiO_2 and a linear gradient of DCM/MeOH 1% --> 8%. The product was isolated as a white solid in 7% yield (5.9mg, 0.01mmol).

R_f (TLC, DCM/MeOH 6%) = 0.26.

$^1\text{H-NMR}$ (400 MHz, $\text{CD}_3\text{OD_SPE}$):

δ = 8.50 (d, J = 2.0 Hz, 1H), 8.19 (d, J = 2.0 Hz, 1H), 6.87 (s, 1H), 5.62 (s, 2H), 4.26 (q, J = 7.1 Hz, 2H), 2.55 (s, 2H), 2.46 (s, 2H), 1.35 (t, J = 7.1 Hz, 3H).

$^{13}\text{C-NMR}$ (101 MHz, $\text{CD}_3\text{OD_SPE}$):

δ = 170.50 (1C, $\text{C}=\text{OCH}$), 166.97 (1C, $\text{C}=\text{OOEt}$), 160.67 (1C, $\text{CH}_2\text{OC}=\text{O}$), 150.25 (1C, C_q, arom), 147.41 (1C, C_q, arom), 142.09 (1C, C_q, arom), 138.33, 134.13 (1C, C_q, arom), 130.40 (1C, C_q, arom), 128.51, 121.79 (1C, C_q, arom), 117.68 (1C, $\text{C}=\text{OCH}$), 117.27, 114.43 (1C, C_q, arom), 61.18 (1C, $\text{CH}_2\text{OC}=\text{O}$), 60.71 (1C, OCH_2CH_3), 14.75 (1C, OCH_2CH_3), 13.91 (1C, CH_3), 12.36 (1C, CH_3).

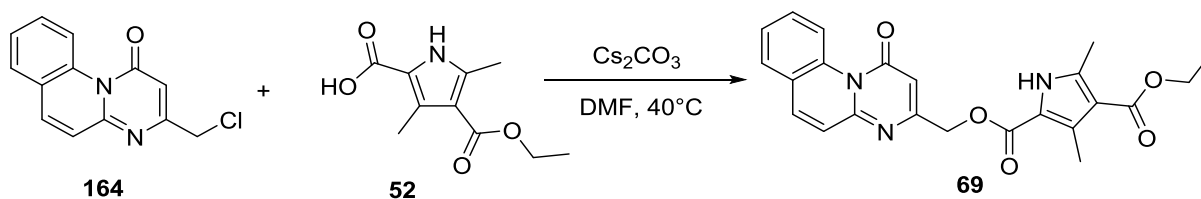
UHPLC-MS

R_t (MCS): 1.736min

m/z: $[\text{M}+\text{H}]^+$ (calc.) = 438.1

$[\text{M}+\text{H}]^+$ (meas.) = 438.0

[4-ethyl 2-\(\(1-oxo-1H-pyrimido\[1,2-a\]quinolin-3-yl\)methyl\) 3,5-dimethyl-1H-pyrrole-2,4-dicarboxylate \(69\)](#)



33.5mg **164** (137 μmol , 1eq) and 43mg **52** (205 μmol , 1.5eq) were stirred with 134mg Cs_2CO_3 (411 μmol , 3eq) in 3mL DMF at 40°C . The reaction mixture was worked up aqueously after 3h and the crude purified by column chromatography with 10g SiO_2 and a linear gradient of DCM/MeOH 0% --> 5%. The product was isolated as a white solid in 28% yield (15.9mg, 38 μmol).

R_f (TLC, DCM/MeOH 98:2) = 0.55.

$^1\text{H-NMR}$ (400 MHz, DMSO-d_6):

δ = 12.06 (s, 1H, NH), 9.75 (d, J = 8.7 Hz, 1H, 7- H_{arom}), 8.16 (d, J = 9.0 Hz, 1H, 12- H_{arom}), 7.97 (d, J = 7.9 Hz, 1H, 8- H_{arom}), 7.74 (t, J = 7.8 Hz, 1H, 10- H_{arom}), 7.66 (t, J = 7.3 Hz, 1H, 9- H_{arom}), 7.38 (d, J = 9.2 Hz, 1H, 13- H_{arom}), 6.62 (s, 1H, C=OCH), 5.25 (s, 2H, $\text{CH}_2\text{OC}=\text{O}$), 4.19 (q, J = 7.3 Hz, 2H, OCH_2CH_3), 2.53 (s, 3H, CH_3), 2.46 (s, 3H, CH_3), 1.28 (t, J = 6.6 Hz, 3H, OCH_2CH_3).

$^{13}\text{C-NMR}$ (101 MHz, DMSO-d_6):

δ = 164.53 (1C, C=O), 162.56 (1C, C=OCH), 159.73 (1C, $\text{CH}_2\text{OC}=\text{O}$), 159.66 (1C, $\text{C}_{\text{q, arom}}$), 151.32 (1C, $\text{C}_{\text{q, arom}}$), 140.17 (1C, $\text{C}_{\text{q, arom}}$), 137.57 (1C, 12- CH_{arom}), 134.78 (1C, $\text{C}_{\text{q, arom}}$), 131.04 (1C, $\text{C}_{\text{q, arom}}$), 129.65 (1C, 10- CH_{arom}), 128.75 (1C, 8- CH_{arom}), 127.15 (1C, 9- CH_{arom}), 124.85 (1C, $\text{C}_{\text{q, arom}}$), 124.12 (1C, 13- CH_{arom}), 121.41 (1C, 7- CH_{arom}), 116.66 (1C, $\text{C}_{\text{q, arom}}$), 112.69 (1C, $\text{C}_{\text{q, arom}}$), 105.77 (1C, C=OCH), 63.61 (1C, $\text{CH}_2\text{OC}=\text{O}$), 59.04 (1C, OCH_2CH_3), 14.31 (1C, OCH_2CH_3), 13.59 (1C, CH_3), 11.88 (1C, CH_3).

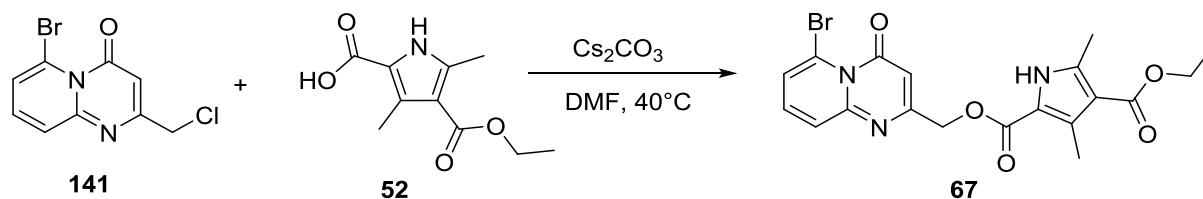
UHPLC-MS

R_t (MCS): 1.766 min

m/z: $[\text{M}+\text{H}]^+$ (calc.) = 420.2

$[\text{M}+\text{H}]^+$ (meas.) = 420.2.

[2-\(\(6-bromo-4-oxo-4H-pyrido\[1,2-a\]pyrimidin-2-yl\)methyl\) 4-ethyl 3,5-dimethyl-1H-pyrrole-2,4-dicarboxylate \(67\)](#)



50mg **141** (0.18mmol, 1eq) and 42mg **52** (0.20mmol, 1.1eq) were stirred with 66mg Cs₂CO₃ (0.20mmol, 1.1eq) in 2mL DMF at 40°C. The reaction mixture was worked up aqueously after 17h. No further purification was needed as was determined through NMR and UHPLC-MS analysis. The product was isolated as a light brown solid in 90% yield (73.7mg, 0.16mmol).

R_f (TLC, cyclohex/EtOAc 1:1) = 0.15.

¹H-NMR (400 MHz, DMSO-d₆):

δ = 12.04 (s, 1H, NH), 7.62 (dd, *J* = 9.0, 7.0 Hz, 1H, 8-H_{arom}), 7.55 – 7.42 (m, 2H, 7-H_{arom}, 9-H_{arom}), 6.45 (s, 1H, C=OCH), 5.20 (s, 2H, CH₂OC=O), 4.19 (q, *J* = 7.1 Hz, 2H, OCH₂CH₃), 2.52 (s, 3H, CH₃), 2.45 (s, 3H, CH₃), 1.28 (t, *J* = 7.1 Hz, 3H, OCH₂CH₃).

¹³C-NMR (100 MHz, DMSO-d₆):

δ = 164.51 (1C, C=O), 160.60 (1C, CH₂OC=O), 159.69 (1C, C=OCH), 159.12 (1C, C_q, arom), 153.11 (1C, C_q, arom), 140.13 (1C, C_q, arom), 136.70 (1C, 8-CH_{arom}), 131.02 (1C, C_q, arom), 125.95 (1C, 7-CH_{arom}), 124.88 (1C, 9-CH_{arom}), 117.50 (1C, C_q, arom), 116.63 (1C, C_q, arom), 112.66 (1C, C_q, arom), 101.63 (1C, C=OCH), 63.81 (1C, CH₂OC=O), 59.03 (1C, OCH₂CH₃), 14.31 (1C, OCH₂CH₃), 13.58 (1C, CH₃), 11.86 (1C, CH₃).

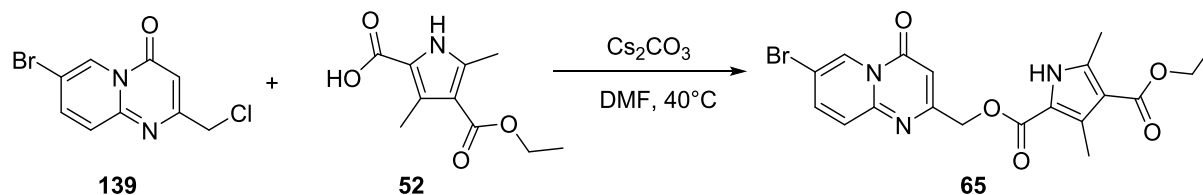
UHPLC-MS

R_t (MCS): 1.610 min

m/z: [M+H]⁺ (calc.) = 447.0, 449.0

[M+H]⁺ (meas.) = 448.0, 450.0

[2-\(\(7-bromo-4-oxo-4H-pyrido\[1,2-a\]pyrimidin-2-yl\)methyl\) 4-ethyl 3,5-dimethyl-1H-pyrrole-2,4-dicarboxylate \(65\)](#)



55mg **139** (0.2mmol, 1eq) and 47mg **52** (0.22mmol, 1.1eq) were stirred with 72mg Cs₂CO₃ (0.22mmol, 1.1eq) in 2mL DMF at 40°C. The reaction mixture was worked up aqueously after 17h. The product was isolated as a light brown solid in 99% yield (89mg, 0.19mmol) with no further purification needed.

R_f (TLC, cyclohex/EtOAc 1:1) = 0.15.

¹H-NMR (400 MHz, DMSO-d₆):

δ = 12.06 (s, 1H, NH), 9.01 (d, *J* = 2.1 Hz, 1H, 6-H_{arom}), 8.11 (dd, *J* = 9.4, 2.3 Hz, 1H, 8-H_{arom}), 7.63 (d, *J* = 9.5 Hz, 1H, 9-H_{arom}), 6.57 (s, 1H, C=OCH), 5.25 (s, 2H, CH₂OC=O), 4.19 (q, *J* = 7.1 Hz, 2H, OCH₂CH₃), 2.52 (s, 3H, CH₃), 2.45 (s, 3H, CH₃), 1.28 (t, *J* = 7.1 Hz, 3H, OCH₂CH₃).

¹³C-NMR (100 MHz, DMSO-d₆):

δ = 164.51 (1C, C=O), 162.58 (1C, C=OCH), 159.70 (1C, CH₂OC=O), 156.35 (1C, C_{q, arom}), 149.43 (1C, C_{q, arom}), 140.51 (1C, 8-CH_{arom}), 140.14 (1C, C_{q, arom}), 131.03 (1C, C_{q, arom}), 127.25 (1C, 9-CH_{arom}), 126.95 (1C, 6-CH_{arom}), 116.64 (1C, C_{q, arom}), 112.67 (1C, C_{q, arom}), 110.58 (1C, C_{q, arom}), 100.08 (1C, C=OCH), 64.22 (1C, CH₂OC=O), 59.02 (1C, OCH₂CH₃), 14.30 (1C, OCH₂CH₃), 13.57 (1C, CH₃), 11.86 (1C, CH₃).

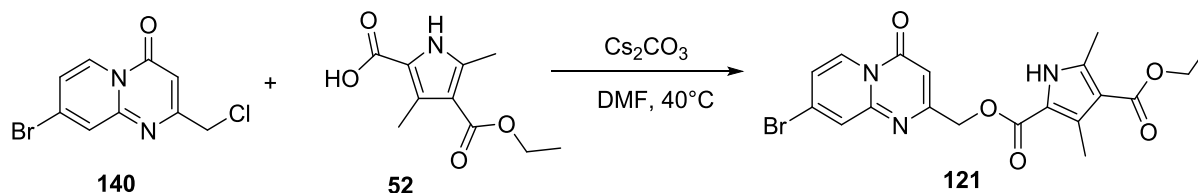
UHPLC-MS

R_t (MCS): 1.607 min

m/z: [M+H]⁺ (calc.) = 447.0, 449.0

[M+H]⁺ (meas.) = 448.0, 450.0

[2-\(\(8-bromo-4-oxo-4H-pyrido\[1,2-a\]pyrimidin-2-yl\)methyl\) 4-ethyl 3,5-dimethyl-1H-pyrrole-2,4-dicarboxylate \(121\)](#)



20mg **140** (73.12 μmol , 1eq) and 23mg **52** (109.68 μmol , 1.5eq) were stirred with 48mg Cs_2CO_3 (146.24 μmol , 2eq) in 3mL DMF at 40°C . The reaction was finished after 1.5h and worked up aqueously. The product was isolated as a light brown solid in 63% yield (20.6mg, 45.95 μmol) with no further purification needed.

R_f (TLC, cyclohex/EtOAc 1:1) = 0.40.

$^1\text{H-NMR}$ (400 MHz, CDCl_3):

δ = 9.08 (s, 1H, NH), 8.86 (d, J = 7.6 Hz, 1H, 6- H_{arom}), 7.85 (s, 1H, 9- H_{arom}), 7.23 (dd, J = 7.6, 1.6 Hz, 1H, 7- H_{arom}), 6.51 (s, 1H, C=OCH), 5.29 (s, 2H, $\text{CH}_2\text{OC}=\text{O}$), 4.30 (q, J = 7.1 Hz, 2H, OCH_2CH_3), 2.63 (s, 3H, CH_3), 2.54 (s, 3H, CH_3), 1.37 (t, J = 7.1 Hz, 4H, OCH_2CH_3).

$^{13}\text{C-NMR}$ (100 MHz, CDCl_3):

δ = 165.41 (1C, C=O), 163.14 (1C, $\text{C}=\text{OCH}$), 160.42 (1C, $\text{CH}_2\text{OC}=\text{O}$), 157.63 (1C, $\text{C}_{\text{q, arom}}$), 150.76 (1C, $\text{C}_{\text{q, arom}}$), 139.94 (1C, $\text{C}_{\text{q, arom}}$), 132.74 (1C, $\text{C}_{\text{q, arom}}$), 128.01 (1C, 6- CH_{arom}), 127.86 (1C, 9- CH_{arom}), 119.89 (2C, $\text{C}_{\text{q, arom}}$, 7- CH_{arom}), 116.97, (1C, $\text{C}_{\text{q, arom}}$) 114.20 (1C, $\text{C}_{\text{q, arom}}$), 101.25 (1C, C=OCH), 64.66 (1C, $\text{CH}_2\text{OC}=\text{O}$), 59.79 (1C, OCH_2CH_3), 14.60 (1C, CH_3), 14.57 (1C, OCH_2CH_3), 12.36 (1C, CH_3).

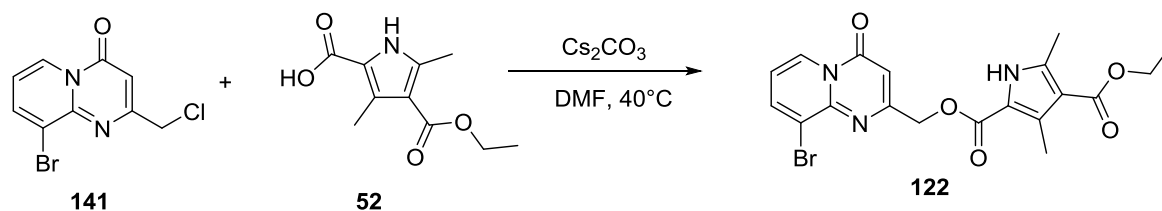
UHPLC-MS

R_t (MCS): 1.599 min

m/z: $[\text{M}+\text{H}]^+$ (calc.) = 448.1, 450.1

$[\text{M}+\text{H}]^+$ (meas.) = 448.0, 450.0

[2-\(\(9-bromo-4-oxo-4H-pyrido\[1,2-a\]pyrimidin-2-yl\)methyl\) 4-ethyl 3,5-dimethyl-1H-pyrrole-2,4-dicarboxylate \(122\)](#)



20mg **141** ($73.12\mu\text{mol}$, 1eq) and 23mg **52** ($109.68\mu\text{mol}$, 1.5eq) was stirred with 48mg Cs_2CO_3 ($146.24\mu\text{mol}$, 2eq) in 3mL DMF at 40°C . The reaction was finished after 1.5h and worked up aqueously. The crude was purified with 10g SiO_2 and a linear gradient of CH/EA 10% \rightarrow 100%. The product was isolated as a white solid in 36% yield (11.9mg , $26.54\mu\text{mol}$).

R_f (TLC, cyclohex/EtOAc 1:1) = 0.39.

$^1\text{H-NMR}$ (400 MHz, DMSO-d_6):

δ = 12.08 (s, 1H, NH), 8.95 (dd, $J = 7.1, 1.1$ Hz, 1H, 6- H_{arom}), 8.41 (dd, $J = 7.3, 1.2$ Hz, 1H, 7- H_{arom}), 7.23 (t, $J = 7.2$ Hz, 1H, 8- H_{arom}), 6.57 (s, 1H, C=OCH), 5.29 (s, 2H, $\text{CH}_2\text{OC=O}$), 4.19 (q, $J = 7.1$ Hz, 2H, OCH_2CH_3), 2.53 (s, 3H, CH_3), 2.46 (s, 3H, CH_3), 1.28 (t, $J = 7.1$ Hz, 3H, OCH_2CH_3).

$^{13}\text{C-NMR}$ (100 MHz, DMSO-d_6):

δ = 164.54 (1C, C=O), 162.44 (1C, $\underline{\text{C}}=\text{OCH}$), 159.76 (1C, $\text{CH}_2\text{OC}\underline{\text{C}}=\text{O}$), 157.43 (1C, $\text{C}_{\text{q, arom}}$), 147.95 (1C, $\text{C}_{\text{q, arom}}$), 140.93 (1C, 8- CH_{arom}), 140.17 (1C, $\text{C}_{\text{q, arom}}$), 131.05 (1C, $\text{C}_{\text{q, arom}}$), 127.36 (1C, 6- CH_{arom}), 119.76 (1C, $\text{C}_{\text{q, arom}}$), 116.71 (1C, $\text{C}_{\text{q, arom}}$), 115.83 (1C, 7- CH_{arom}), 112.68 (1C, $\text{C}_{\text{q, arom}}$), 100.03 (1C, C=O $\underline{\text{C}}\text{H}$), 64.30 (1C, $\underline{\text{C}}\text{H}_2\text{OC=O}$), 59.05 (1C, OCH_2CH_3), 14.32 (1C, $\text{OCH}_2\text{C}\underline{\text{H}}_3$), 13.60 (1C, CH_3), 11.92 (1C, CH_3).

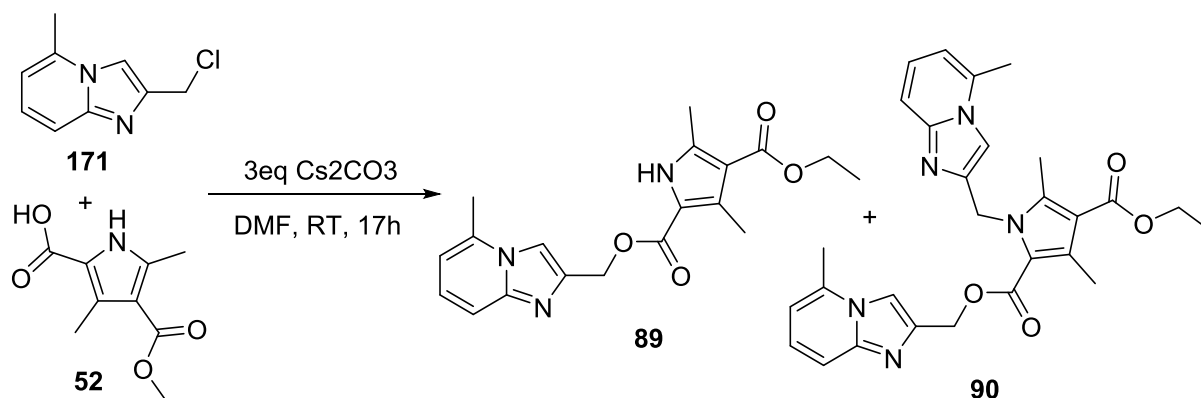
UHPLC-MS

R_t (MCS): 1.578 min

m/z : $[\text{M}+\text{H}]^+$ (calc.) = 448.1, 450.1

$[\text{M}+\text{H}]^+$ (meas.) = 448.0, 450.0

[4-methyl 2-\(\(5-methylimidazo\[1,2-a\]pyridin-2-yl\)methyl\) 3,5-dimethyl-1H-pyrrole-2,4-dicarboxylate \(89\)](#)



50mg of **171** (SM) (0.28mmol, 1eq), 82mg of **52** (0.42mmol, 1.5eq) and 271mg Cs_2CO_3 (0.83mmol, 3 eq) were dissolved in 4mL DMF and stirred at RT for 17h. The crude was purified by column chromatography on 10g SiO_2 with a linear gradient of hept/EtOAc 40 \rightarrow 100%. The product **89** was isolated as a white solid in 22% yield (22mg, 0.06mmol) and the double modified side product **90** in 64% (44mg, 0.09mmol).

Product **89**:

R_f (TLC, hept/EtOAc 1:4) = 0.45.

$^1\text{H-NMR}$ (400 MHz, $\text{DMSO-}d_6$):

δ = 11.93 (s, 1H, NH), 7.87 (s, 1H, 3- H_{arom}), 7.44 (d, J = 9.1 Hz, 1H, 8- H_{arom}), 7.24 (dd, J = 8.8, 7.1 Hz, 1H, 7- H_{arom}), 6.79 (d, J = 6.8 Hz, 1H, 6- H_{arom}), 5.38 (s, 2H, CH_2OCO), 4.16 (q, J = 7.1 Hz, 2H, CH_2CH_3), 2.58 (s, 3H, 5- CH_3), 2.46 (s, 3H, CH_3), 2.40 (s, 3H, CH_3), 1.25 (t, J = 7.1 Hz, 3H, CH_2CH_3).

$^{13}\text{C-NMR}$ (101 MHz, $\text{DMSO-}d_6$):

δ = 164.71 (1C, $\text{C}=\text{O}$), 160.41 (1C, $\text{CH}_2\text{OC}=\text{O}$), 144.88 (1C, $\text{C}_{\text{q, arom}}$), 141.40 (1C, $\text{C}_{\text{q, arom}}$), 139.81 (1C, $\text{C}_{\text{q, arom}}$), 135.49 (1C, $\text{C}_{\text{q, arom}}$), 130.31 (1C, $\text{C}_{\text{q, arom}}$), 125.37 (1C, 7- CH_{arom}), 117.25 (1C, $\text{C}_{\text{q, arom}}$), 114.22 (1C, 8- CH_{arom}), 112.50 (1C, $\text{C}_{\text{q, arom}}$), 111.41 (1C, 6- CH_{arom}), 109.49 (1C, 3- CH_{arom}), 59.85 (1C, $\text{CH}_2\text{OC}=\text{O}$), 59.09 (1C, CH_2CH_3), 18.33 (1C, 5- CH_3), 14.39 (1C, CH_2CH_3), 13.60 (1C, CH_3), 11.93 (1C, CH_3).

UHPLC-MS

R_t (MCS): 1.532 min

m/z : $[\text{M}+\text{H}]^+$ (calc.) = 356.2

$[\text{M}+\text{H}]^+$ (meas.) = 356.2

Side Product **90**:

R_f (TLC, hept/EtOAc 1:4) = 0.07

¹H-NMR (400 MHz, DMSO-*d*₆):

δ = 7.48 (appar. d, *J* = 7.7 Hz, 2H, 3-H_{arom}, 8-H_{arom}), 7.44 (d, *J* = 9.0 Hz, 1H, 8''-H_{arom}), 7.13 (ddd, *J* = 15.5, 9.1, 6.9 Hz, 2H, 7-H_{arom}, 7''-H_{arom}), 7.04 (s, 1H, 3''-H_{arom}), 6.61 (d, *J* = 6.8 Hz, 1H, 6-H_{arom}), 6.55 (d, *J* = 6.9 Hz, 1H, 6''-H_{arom}), 5.76 (s, 2H, CH₂), 5.49 (s, 2H, NCH₂), 4.28 (q, *J* = 7.1 Hz, 2H, OCH₂CH₃), 2.62 (s, 3H, 5'-CH₃), 2.60 (s, 3H, 3'-CH₃), 2.50 (s, 3H, 5-CH₃), 2.41 (s, 3H, 5''-CH₃), 1.34 (t, *J* = 7.1 Hz, 3H, OCH₂CH₃).

¹³C-NMR (101 MHz, DMSO-*d*₆):

δ = 165.73 (1C, C=O), 161.77 (1C, CH₂OC=O), 145.54 (1C, C_{q, arom}), 145.30 (1C, C_{q, arom}), 143.80 (1C, C_{q, arom}), 142.24 (1C, C_{q, arom}), 141.77 (1C, C_{q, arom}), 134.87 (1C, C_{q, arom}), 134.81 (1C, C_{q, arom}), 132.60 (1C, C_{q, arom}), 125.35 (1C, 7-CH_{arom}), 125.29 (1C, 7''-CH_{arom}), 119.59 (1C, C_{q, arom}), 115.01 (1C, 8-CH_{arom}), 114.58 (1C, 8''-CH_{arom}), 113.51 (1C, C_{q, arom}), 111.85 (1C, 6-CH_{arom}), 111.70 (1C, 6'-CH_{arom}), 108.75 (1C, 3-CH_{arom}), 107.30 (1C, 3''-CH_{arom}), 60.56 (1C, CH₂OC=O), 59.81 (1C, CH₂CH₃), 44.39 (1C, NCH₂), 18.85 (1C, 5-CH₃), 18.82 (1C, 5''-CH₃), 14.55 (1C, CH₂CH₃), 13.23 (1C, 3'-CH₃), 12.38 (1C, 5'-CH₃).

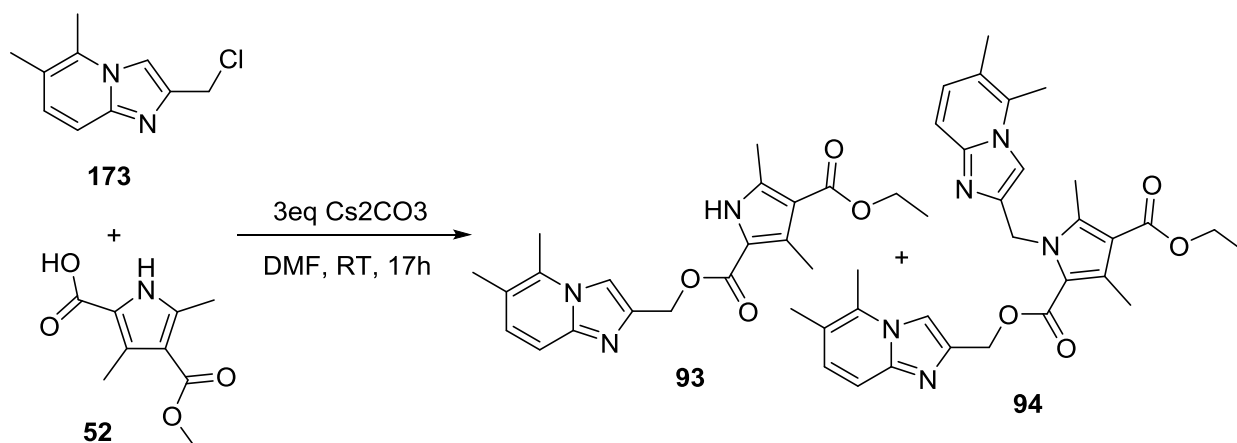
UHPLC-MS

R_t (MCS): 1.532 min

m/z: [M+H]⁺ (calc.) = 500.2

[M+H]⁺ (meas.) = 500.2

[2-\(\(5,6-dimethylimidazo\[1,2-a\]pyridin-2-yl\)methyl\) 4-ethyl 3,5-dimethyl-1H-pyrrole-2,4-dicarboxylate \(**93**\)](#)



31mg of **173** (SM) (0.16mmol, 1eq), 50mg of **52** (0.24mmol, 1.5eq) and 156mg Cs₂CO₃ (0.48mmol, 3 eq) were dissolved in 3mL DMF and stirred at RT for 1.5h. The crude was purified by column chromatography on 10g SiO₂ with a linear gradient of Hept/EtOAc 40→100%. The product **93** was isolated as a light brown solid in 26% yield (15mg, 0.04mmol) and the double modified side product **94** in 44% (19mg, 0.04mmol).

Product **93**:

R_f (TLC, hept/EtOAc 1:4) = 0.51.

¹H-NMR (400 MHz, DMSO-*d*₆):

δ = 11.91 (s, 1H, NH), 7.85 (s, 1H, 3-H_{arom}), 7.36 (d, *J* = 9.1 Hz, 1H, 8-H_{arom}), 7.15 (d, *J* = 9.1 Hz, 1H, 7-H_{arom}), 5.36 (s, 2H, CH₂OC=O), 4.16 (q, *J* = 7.0 Hz, 2H, CH₂CH₃), 2.51 (s, 3H, 5-CH₃), 2.46 (s, 3H, 3'-CH₃), 2.40 (s, 3H, 5'-CH₃), 2.30 (s, 3H, 6-CH₃), 1.25 (t, *J* = 7.1 Hz, 3H, CH₂CH₃).

¹³C-NMR (101 MHz, DMSO-*d*₆):

δ = 164.64 (1C, C=O), 160.39 (1C; CH₂OC=O), 144.02 (1C, C_{q, arom}), 141.21 (1C, C_{q, arom}), 139.73 (1C, C_{q, arom}), 131.91 (1C, C_{q, arom}), 130.19 (1C, C_{q, arom}), 128.82 (1C, 7-CH_{arom}), 118.12 (1C, C_{q, arom}), 117.24 (1C, C_{q, arom}), 113.66 (1C, 8-CH_{arom}), 112.43 (1C, C_{q, arom}), 109.55 (1C, 3-CH_{arom}), 59.89 (1C; CH₂OC=O), 59.02 (1C, CH₂CH₃), 17.30 (1C, 6-CH₃), 15.05 (1C, 5-CH₃), 14.35 (1C, CH₂CH₃), 13.56 (1C, 5'-CH₃), 11.89 (1C, 3'-CH₃).

UHPLC-MS

R_t (MCS): 1.586 min

m/z: [M+H]⁺ (calc.) = 370.2

[M+H]⁺ (meas.) = 370.2

Side Product **94**:

R_f (TLC, hept/EtOAc 1:4) = 0.05.

¹H-NMR (400 MHz, DMSO-*d*₆):

δ = 7.41 (s, 1H, 3-H_{arom}), 7.37 (d, J = 9.2 Hz, 1H, 8-H_{arom}), 7.34 (d, J = 9.1 Hz, 1H, 8''-H_{arom}), 7.04 (d, J = 9.1 Hz, 1H, 7-H_{arom}), 7.00 (d, J = 9.1 Hz, 1H, 7''-H_{arom}), 6.97 (s, 1H, 3''-H_{arom}), 5.72 (s, 2H, CH₂N), 5.46 (s, 2H, CH₂OC=O), 4.28 (q, J = 7.1 Hz, 2H, CH₂CH₃), 2.61 (s, 3H, 3'-CH₃), 2.59 (s, 3H, 5'-CH₃), 2.39 (s, 3H, 5-CH₃), 2.31 (s, 3H, 6-CH₃), 2.30 (s, 3H, 5''-CH₃), 2.26 (s, 3H, 6''-CH₃), 1.34 (t, J = 7.1 Hz, 3H, CH₂CH₃).

¹³C-NMR (101 MHz, DMSO-*d*₆):

δ = 165.76 (1C, C=O), 161.78 (1C, CH₂OC=O), 144.68 (1C, C_q, arom), 144.48 (1C, C_q, arom), 143.65 (1C, C_q, arom), 142.14 (1C, C_q, arom), 141.58 (1C, C_q, arom), 132.45 (1C, C_q, arom), 131.50 (1C, C_q, arom), 131.39 (1C, C_q, arom), 129.08 (1C, 7-CH_{arom}), 128.93 (1C, 7''-CH_{arom}), 119.72 (1C, C_q, arom), 118.73 (1C, C_q, arom), 118.53 (1C, C_q, arom), 114.34 (1C, 8-CH_{arom}), 113.90 (1C, 8''-CH_{arom}), 113.41 (1C, C_q, arom), 108.91 (1C, 3-CH_{arom}), 107.35 (1C, 3''-CH_{arom}), 60.64 (1C, CH₂OC=O), 59.78 (1C, CH₂CH₃), 44.47 (1C, NCH₂), 17.90 (1C, 6-CH₃), 17.88 (1C, 6''-CH₃), 15.28 (1C, 5-CH₃), 15.27 (1C, 5''-CH₃), 14.56 (1C, CH₂CH₃), 13.19 (1C, 5'-CH₃), 12.36 (1C, 3'-CH₃).

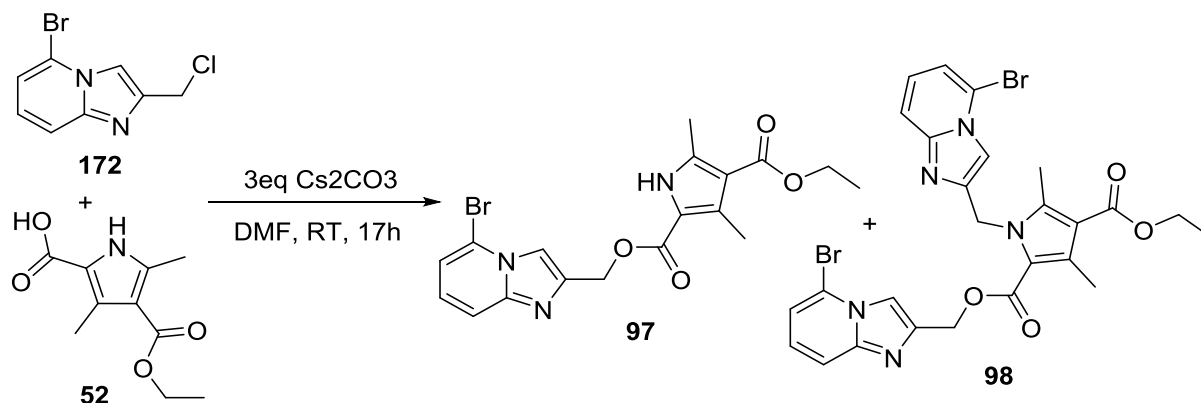
UHPLC-MS

R_t (MCS): 1.507 min

m/z: [M+H]⁺ (calc.) = 528.3

[M+H]⁺ (meas.) = 528.2

[2-\(\(5-bromoimidazo\[1,2-a\]pyridin-2-yl\)methyl\) 4-ethyl 3,5-dimethyl-1H-pyrrole-2,4-dicarboxylate \(97\)](#)



50mg of **172** (SM) (0.20mmol, 1eq), 65mg of **52** (0.31mmol, 1.5eq) and 199mg Cs₂CO₃ (0.61mmol, 3 eq) were dissolved in 4mL DMF and stirred at RT for 17h. The crude was purified by column chromatography on 10g SiO₂ with a linear gradient of hept/EtOAc 40→100%. The product **97** was isolated as a light brown solid in 19% yield (16mg, 0.04mmol) and the double modified side product **98** in 35% (22mg, 0.04mmol).

Product 97:

R_f (TLC, hept/EtOAc 1:4) = 0.55.

¹H-NMR (400 MHz, DMSO-*d*₆):

δ = 11.93 (s, 1H, NH), 8.05 (s, 1H, 3-H_{arom}), 7.63 (d, *J* = 8.8 Hz, 1H, 8-H_{arom}), 7.32 (d, *J* = 7.1 Hz, 1H, 6-H_{arom}), 7.29 – 7.21 (m, 1H, 7-H_{arom}), 5.40 (s, 2H, CH₂OC=O), 4.17 (q, *J* = 7.0 Hz, 2H, CH₂CH₃), 2.47 (s, 3H, CH₃), 2.40 (s, 3H, CH₃), 1.26 (t, *J* = 7.0 Hz, 3H, CH₂CH₃).

¹³C-NMR (101 MHz, DMSO-*d*₆):

δ = 164.58 (1C, C=O), 160.27 (1C, CH₂OC=O), 144.92 (1C, C_{q, arom}), 141.82 (1C, C_{q, arom}), 139.82 (1C, C_{q, arom}), 130.32 (1C, C_{q, arom}), 125.83 (1C, 7-CH_{arom}), 117.07 (1C, C_{q, arom}), 116.49 (1C, 6-CH_{arom}), 115.91 (1C, 8-CH_{arom}), 114.10 (1C, C_{q, arom}), 112.49 (1C, 3-CH_{arom}), 59.53 (1C, CH₂OC=O), 59.00 (1C, OCH₂CH₃), 14.32 (1C, OCH₂CH₃), 13.55 (1C, 5'-CH₃), 11.85 (1C, 3'-CH₃).

UHPLC-MS

R_t (MCS): 1.570 min

m/z: [M+H]⁺ (calc.) = 420.0, 422.0

[M+H]⁺ (meas.) = 420.0, 422.0

Side Product **98**:

R_f (TLC, hept/EtOAc 1:4) = 0.17.

¹H-NMR (400 MHz, CDCl₃):

δ = 7.80 (s, 1H, 3-H_{arom}), 7.58 (d, *J* = 8.9 Hz, 1H, 8-H_{arom}), 7.53 (d, *J* = 8.9 Hz, 1H, 8''-H_{arom}), 7.39 (s, 1H, 3''-H_{arom}), 7.14 – 7.01 (m, 3H, 6-H_{arom}, 7-H_{arom}, 7''-H_{arom}), 6.98 (d, *J* = 7.2 Hz, 1H, 6''-H_{arom}), 5.75 (s, 2H, (NCH₂)), 5.49 (s, 2H, CH₂), 4.29 (q, *J* = 7.1 Hz, 2H, OCH₂CH₃), 2.64 (s, 3H, 5'-CH₃), 2.61 (s, 3H, 3'-CH₃), 1.35 (t, *J* = 7.1 Hz, 3H, OCH₂CH₃).

¹³C-NMR (101 MHz, CDCl₃):

δ = 165.67 (1C, C=O), 161.70 (1C, CH₂OC=O), 145.57 (1C, C_{q, arom}), 145.36 (1C, C_{q, arom}), 143.83 (1C, C_{q, arom}), 142.35 (1C, C_{q, arom}), 141.93 (1C, C_{q, arom}), 132.83 (1C, C_{q, arom}), 125.40 (1C, 7-CH_{arom}), 125.26 (1C, 7''-CH_{arom}), 119.38 (1C, C_{q, arom}), 116.55 (1C, 6-CH_{arom}), 116.40 (1C, 6''-CH_{arom}), 116.39 (1C, 8-CH_{arom}), 116.05 (1C, 8''-CH_{arom}), 114.39 (1C, C_{q, arom}), 113.66 (1C, C_{q, arom}), 112.59 (1C, 3-CH_{arom}), 111.32 (1C, 3''-CH_{arom}), 60.25 (1C, CH₂OC=O), 59.85 (1C, OCH₂CH₃), 44.13 (1C, NCH₂), 14.55 (1C, OCH₂CH₃), 13.27 (1C, 3'-CH₃), 12.39 (1C, 5'-CH₃).

UHPLC-MS

R_t (MCS): 1.584 min

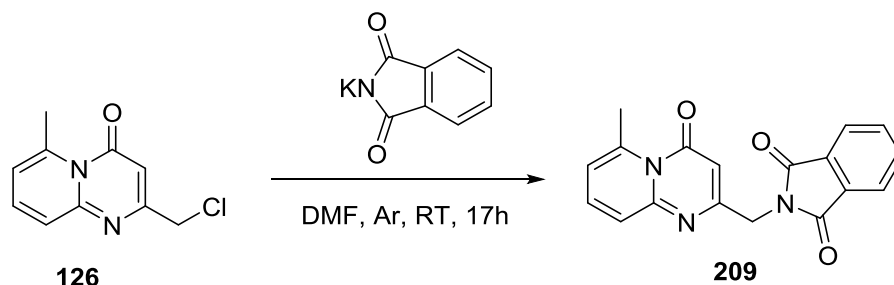
m/z: [M+H]⁺ (calc.) = 628.0, 630.0

[M+H]⁺ (meas.) = 628.0, 630.0

2.4 Amide linker modification

2.4.1 Amine Synthesis

2-((6-methyl-4-oxo-4H-pyrido[1,2-a]pyrimidin-2-yl)methyl)isoindoline-1,3-dione (Gabriel Step I) (209)



1.33g (6.38mmol, 1eq) of **126** was dissolved in 35mL DMF under Ar atmosphere, before 1.31g of potassium phthalimide (7.07mmol, 1.1eq) was added. The reaction was finished after 17h stirring at RT. The solvent was evaporated *in vacuo* and the residue suspended in 80mL water. The aqueous phase was extracted with 3x80mL DCM. The combined organic phases were washed with water, brine and dried over anh. NaSO₄. After filtering the organic phase, the solvent was evaporated *in vacuo*. The product was isolated as a light yellow solid in 88% yield (1.79g, 5.60mmol) and used without further purification.

R_f (TLC, Hept/EtOAc 2:3) = 0.25.

¹H-NMR (400 MHz, CDCl₃):

δ = 7.89 (dd, *J* = 5.4, 3.1 Hz, 2H, H_{arom}), 7.75 (dd, *J* = 5.5, 3.1 Hz, 2H, H_{arom}), 7.39 (dd, *J* = 9.0, 6.8 Hz, 1H, 8-H_{arom}), 7.28 (d, *J* = 8.9 Hz, 1H, 9-H_{arom}), 6.62 (d, *J* = 6.9 Hz, 1H, 7-H_{arom}), 6.08 (s, 1H, C=OCH), 4.80 (s, 2H, CH₂), 2.98 (s, 3H, 6-CH₃).

¹³C-NMR (101 MHz, CDCl₃):

δ = 167.97 (2C, C=O), 162.16 (1C, C=OCH), 160.29 (1C, C_{q, arom}), 153.79 (1C, C_{q, arom}), 144.15 (1C, C_{q, arom}), 135.56 (1C, 8-CH_{arom}), 134.34 (2C, CH_{arom}), 132.17 (2C, C_{q, arom}), 125.32 (1C, 9-CH_{arom}), 123.70 (2C, CH_{arom}), 118.43 (1C, 7-CH_{arom}), 102.93 (1C, C=OCH), 41.85 (1C, CH₂), 24.75 (1C, 6-CH₃).

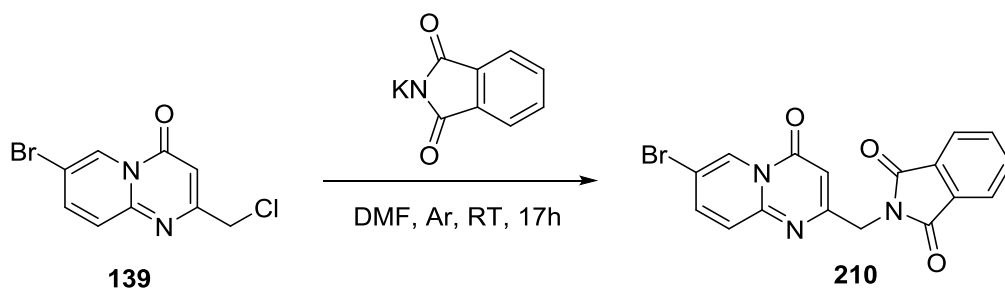
UHPLC-MS

R_t (MCS): 1.248 min

m/z: [M+H]⁺ (calc.) = 320.1.

[M+H]⁺ (meas.) = 320.0

[2-\(\(6-methyl-4-oxo-4H-pyrido\[1,2-a\]pyrimidin-2-yl\)methyl\)isoindoline-1,3-dione](#)
(Gabriel Step I) (**210**)



50mg (0.18mmol, 1eq) of **139** was dissolved in 2mL DMF under Ar atmosphere, before 35mg of potassium phthalimide (0.19mmol, 1.1eq) was added. The reaction was finished after 1.5h stirring at RT. The solvent was evaporated *in vacuo* and the residue suspended in 80mL water. The aqueous phase was extracted with 3x80mL DCM. The combined organic phases were washed with 0.2M NaOH solution, water, brine and dried over anh. NaSO₄. After filtering the organic phase, the solvent was evaporated *in vacuo*. The crude was purified with 10g SiO₂ column chromatography using a DCM/MeOH of 0%--> 3%. The product was isolated as a white solid in 82% yield (57.8g, 0.15mmol).

R_f (TLC, Hept/EtOAc 2:3) = 0.44.

¹H-NMR (400 MHz, CDCl₃):

δ = 9.12 (d, J = 2.1 Hz, 1H), 7.92 (dd, J = 5.4, 3.1 Hz, 2H), 7.78 (dd, J = 5.5, 3.1 Hz, 2H), 7.74 (dd, J = 9.4, 2.2 Hz, 1H), 7.45 (d, J = 9.4 Hz, 1H), 6.33 (s, 1H), 4.89 (s, 2H).

¹³C-NMR (101 MHz, CDCl₃):

δ = 167.92, 162.09, 156.97, 149.70, 139.94, 134.43, 132.12, 127.55, 127.49, 123.77, 110.97, 101.49, 42.31.

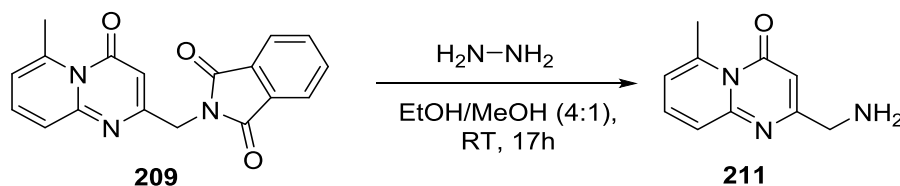
UHPLC-MS

R_t (MCS): 1.505min.

m/z: [M+H]⁺ (calc.) = 384.0, 386.0.

[M+H]⁺ (meas.) = 384.0, 386.0.

2-(Aminomethyl)-6-methyl-4H-pyrido[1,2-a]pyrimidin-4-one (211)



1.75g of **209** (5.48mmol, 1eq) were dissolved in 100mL of a EtOH/MeOH mixture (5:1) before 1.33mL of Hydrazine monohydrate (27.40mmol, 5eq) was added slowly at RT. The solution was stirred for 17h and the reaction progress monitored on TLC. After the reaction was finished, the mixture was filtered and the supernatant was coevaporated twice with toluene under reduced pressure. The product was isolated as a yellow solid in 105% yield (1.17g, 4.65mmol) and a purity of 82% (determined by $^1\text{H-NMR}$).

R_f (TLC, DCM/MeOH 4%) = 0.04.

$^1\text{H-NMR}$ (400 MHz, $\text{DMSO-}d_6$):

δ = 7.59 (dd, J = 8.9, 6.9 Hz, 1H, 8- H_{arom}), 7.30 (d, J = 8.8 Hz, 1H, 9- H_{arom}), 6.83 (dt, J = 6.9, 1.3 Hz, 1H, 7- H_{arom}), 6.31 (s, 1H, C=OCH), 3.86 (s, 2H, CH_2), 3.61 (d, J = 0.9 Hz, 2H), 2.91 (s, 3H, 6- CH_3).

$^{13}\text{C-NMR}$ (101 MHz, $\text{DMSO-}d_6$):

δ = 167.78 (1C, C=OCH), 161.55 (1C, $\text{C}_{\text{q, arom}}$), 152.73 (1C, $\text{C}_{\text{q, arom}}$), 143.05 (1C, $\text{C}_{\text{q, arom}}$), 135.98 (1C, 8- CH_{arom}), 124.42 (1C, 9- CH_{arom}), 118.02 (1C, 7- CH_{arom}), 102.01 (1C, C=OCH), 46.41 (1C, CH_2), 24.02 (1C, 6- CH_3).

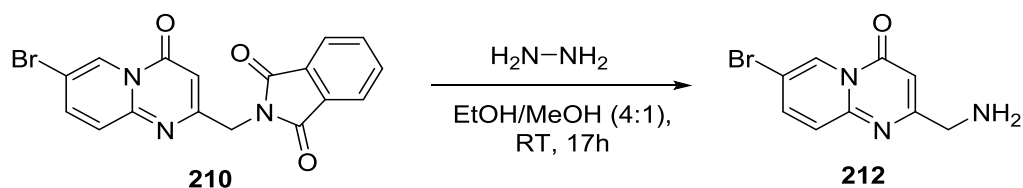
UHPLC-MS

R_t (PSM): 0.428 min

m/z: $[\text{M}+\text{H}]^+$ (calc.) = 190.2

$[\text{M}+\text{H}]^+$ (meas.) = 190.2

2-(Aminomethyl)-7-bromo-4H-pyrido[1,2-a]pyrimidin-4-one (212)



50g of **210** (0.13mmol, 1eq) were dissolved in 5mL of a EtOH before 24 μ L of hydrazine monohydrate (0.32mmol, 2.5eq) was added slowly. The solution was stirred for 1h at 80°C and the reaction progress monitored on TLC. After the reaction was finished, the mixture was filtered and the supernatant was coevaporated twice with toluene under reduced pressure. The crude was purified with 10g SiO₂ column chromatography using a DCM/MeOH of 0%--> 7%. The product was isolated as a white solid in 41% yield (13mg, 0.05mmol).

R_f (TLC, DCM/MeOH 4%) = 0.04.

¹H-NMR (400 MHz, DMSO-*d*₆):

δ = 8.98 (d, J = 2.2 Hz, 1H), 8.03 (d, J = 2.2 Hz, 1H), 7.57 (d, J = 9.5 Hz, 1H), 6.58 (s, 1H), 3.71 (s, 2H).

UHPLC-MS

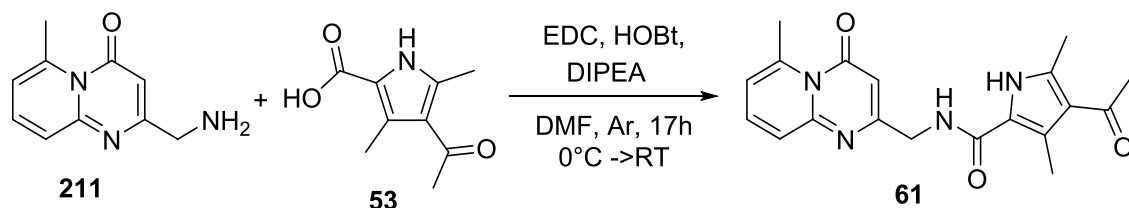
R_t (MCS): min

m/z: [M+H]⁺ (calc.) =

[M+H]⁺ (meas.) =

2.4.2 Peptide coupling

4-acetyl-3,5-dimethyl-N-((6-methyl-4-oxo-4H-pyrido[1,2-a]pyrimidin-2-yl)methyl)-1H-pyrrole-2-carboxamide (61)



100mg of **53** (0.55mmol, 1eq) was dissolved in 3mL DMF under Ar-atmosphere and cooled to 0°C before 137mg EDC·HCl (0.72mmol, 1.3eq), 101mg HOBt (0.66mmol,

1.2eq) and 481 μ L DIPEA (2.76mmol, 5eq). The solution was stirred for 15 min before 125mg of **211** (0.66mmol, 1.2eq) dissolved in 2mL anhydrous DMF was added. The solution was slowly warmed to RT over night. The reaction was monitored by UHPLC-MS and determined to be finished after 16.5h. The solvent of the reaction mixture was evaporated and the residue suspended in 20mL water. The aqueous phase was extracted with EtOAc before the remaining solid in the aqueous phase was filtered off and dried over P₄O₁₀. The product was isolated as a white solid in 15% yield (35mg, 0.08mmol).

R_f (TLC, Water/ACN 96:4) = 0.76.

¹H-NMR (400 MHz, DMSO-*d*₆):

δ = 11.56 (s, 1H, NH), 8.11 (t, *J* = 5.7 Hz, 1H, NHC=O), 7.66 (dd, *J* = 8.4, 7.4 Hz, 1H, 8-H_{arom}), 7.37 (d, *J* = 8.8 Hz, 1H, 9-H_{arom}), 6.90 (d, *J* = 6.8 Hz, 1H, 7-H_{arom}), 6.12 (s, 1H, C=OCH), 4.33 (d, *J* = 5.7 Hz, 2H, CH₂HNC=O), 2.92 (s, 3H, 6-CH₃), 2.49 (s, 3H, 5'-CH₃), 2.45 (s, 3H, 3'-CH₃), 2.35 (s, 3H, C=OCH₃).

¹³C-NMR (101 MHz, DMSO-*d*₆):

δ = 194.42 (1C, C=OCH₃), 163.70 (1C, HNC=O), 161.44 (1C, C=OCH), 161.31 (1C, C_{q, arom}), 152.99 (1C, C_{q, arom}), 143.28 (1C, C_{q, arom}), 136.63 (1C, C_{q, arom}), 136.47 (1C, 8-CH_{arom}), 124.43 (1C, 9-CH_{arom}), 123.97 (1C, C_{q, arom}), 121.46 (1C, C_{q, arom}), 118.44 (1C, 7-CH_{arom}), 101.84 (1C, C=OCH), 43.29 (1C, CH₂NH), 31.17 (1C, C=OCH₃), 24.00 (1C, 6-CH₃), 14.56 (1C, 5'-CH₃), 12.44 (1C, 3'-CH₃).

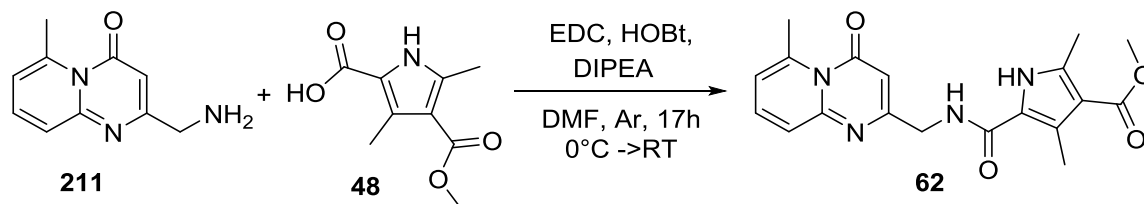
UHPLC-MS

R_t (MCS): 0.850 min

m/z: [M+H]⁺ (calc.) = 353.4

[M+H]⁺ (meas.) = 353.2

[Methyl -2,4-dimethyl-5-\(\(\(6-methyl-4-oxo-4H-pyrido\[1,2-a\]pyrimidin-2-yl\)methyl\)carbamoyl\) -1H-pyrrole-3-carboxylate \(62\)](#)



111mg of **48** (0.56mmol, 1eq) was dissolved in 3mL dry DMF under Ar-atmosphere and cooled to 0°C before 140mg EDC·HCl (0.73mmol, 1.3eq), 103mg HOBT (0.67mmol, 1.2 eq) and 498μL DIPEA (2.81mmol, 5eq) was added. After stirring for 15 min, 128mg (0.67mmol, 1.2eq) **211** was added and the reaction mixture slowly warmed to RT overnight. The reaction progress was monitored by UHPLC-MS. After 18h the reaction was finished and the solvent evaporated. The crude was dissolved in a water/EtOAc mixture, and the remaining solid filtered off. The solid was continued to be washed with water and EtOAc before being dried over P₄O₁₀. The product was isolated as a white solid in 35% yield (72mg, 0.20mmol).

R_f (TLC, Water/ACN 96:4) = 0.80

¹H-NMR (400 MHz, DMSO-*d*₆):

δ = 11.61 (s, 1H, NH), 8.06 (t, *J* = 5.8 Hz, 1H, NHC=O), 7.65 (dd, *J* = 8.8, 7.0 Hz, 1H, 8-H_{arom}), 7.37 (d, *J* = 8.8 Hz, 1H, 9-H_{arom}), 6.90 (d, *J* = 6.9 Hz, 1H, 7-H_{arom}), 6.12 (s, 1H, C=OCH), 4.33 (d, *J* = 5.8 Hz, 2H, CH₂NH), 3.71 (s, 3H, OCH₃), 2.92 (s, 3H, 6-CH₃), 2.47 (s, 3H, 3'-CH₃), 2.41 (s, 3H, 5'-CH₃).

¹³C-NMR (101 MHz, DMSO-*d*₆):

δ = 165.33 (1C, C=OOCH₃), 163.66 (1C, 1C, C=OCH), 161.28 (1C, NHC=O), 161.25 (1C, C_q, arom), 152.98 (1C, C_q, arom), 143.26 (1C, C_q, arom), 137.23 (1C, C_q, arom), 136.43 (1C, 8-CH_{arom}), 124.52 (1C, C_q, arom), 124.42 (1C, 9-CH_{arom}), 121.55 (1C, C_q, arom), 118.41 (1C, 7-CH_{arom}), 111.36 (1C, C_q, arom), 101.85 (1C, 1C, C=OCH), 50.40 (1C, C=OOCH₃), 43.27 (1C, CH₂NH), 23.97 (1C, 6-CH₃), 13.59 (1C, 3'-CH₃), 11.80 (1C, 5'-CH₃).

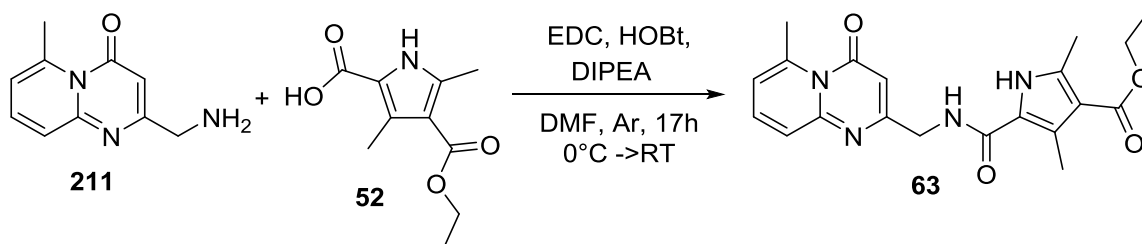
UHPLC-MS

R_t (MCS): 1.261 min

m/z: [M+H]⁺ (calc.) = 369.39

[M+H]⁺ (meas.) = 396.2

[Ethyl-2,4-dimethyl-5-\(\(\(6-methyl-4-oxo-4H-pyrido\[1,2-a\]pyrimidin-2-yl\)-methyl\)-carbamoyl\)-1H-pyrrole-3-carboxylate \(63\)](#)



119mg of **52** (0.56mmol, 1eq) was dissolved in 3mL dry DMF under Ar-atmosphere and cooled to 0°C before 140mg EDC·HCl (0.73mmol, 1.3eq), 103mg HOBT (0.67mmol, 1.2 eq) and 498μL DIPEA (2.81mmol, 5eq) was added. After stirring for 15 min, 128mg (0.67mmol, 1.2eq) **211** was added and the reaction mixture slowly warmed to RT overnight. The reaction progress was monitored by UHPLC-MS. After 18h the reaction was finished and the solvent evaporated. The crude was dissolved in a water/EtOAc mixture, and the remaining solid filtered off. The solid was continued to be washed with water and EtOAc, before being dried over P₄O₁₀. The product was isolated as a white solid in 54% yield (117mg, 0.31mmol).

R_f (TLC, Water/ACN 96:4) = 0.73

¹H-NMR (400 MHz, DMSO-*d*₆):

δ = 11.58 (s, 1H, NH), 8.04 (t, *J* = 5.9 Hz, 1H, NHC=O), 7.66 (dd, *J* = 8.9, 7.0 Hz, 1H, 8-H_{arom}), 7.37 (d, *J* = 8.4 Hz, 1H, 9-H_{arom}), 6.90 (d, *J* = 6.9 Hz, 1H, 7-H_{arom}), 6.12 (s, 1H, C=OCH), 4.33 (d, *J* = 5.8 Hz, 2H, CH₂NH), 4.18 (q, *J* = 7.1 Hz, 2H, OCH₂CH₃), 2.92 (s, 3H, 6-CH₃), 2.48 (s, 3H, 3'-CH₃), 2.41 (s, 3H, 5'-CH₃), 1.27 (t, *J* = 7.1 Hz, 3H, OCH₂CH₃).

¹³C-NMR (101 MHz, DMSO-*d*₆):

δ = 164.88 (1C, C=O), 163.67 (1C, C=OCH), 161.28 (1C, NHC=O), 161.25 (1C, C_q, arom), 152.98 (1C, C_q, arom), 143.26 (1C, C_q, arom), 137.16 (1C, C_q, arom), 136.44 (1C, 8-CH_{arom}), 124.55 (1C, C_q, arom), 124.42 (1C, 9-CH_{arom}), 121.49 (1C, C_q, arom), 118.41 (1C, 7-CH_{arom}), 111.51 (1C, C_q, arom), 101.84 (1C, C=OCH), 58.74 (1C, OCH₂CH₃), 43.26 (1C, CH₂NH), 23.97 (1C, 6-CH₃), 14.34 (1C, OCH₂CH₃), 13.61 (1C, 5'-CH₃), 11.78 (1C, 3'-CH₃).

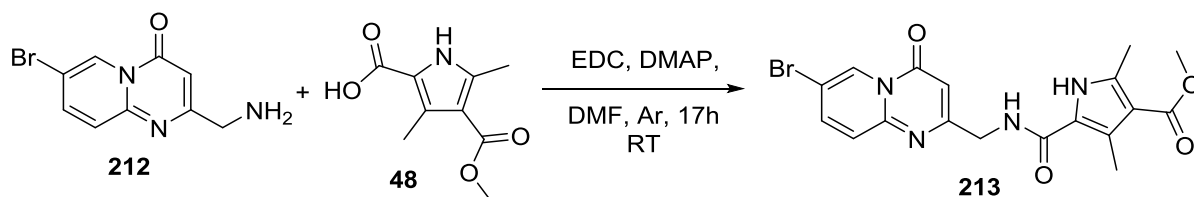
UHPLC-MS

R_t (MCS): 1.396 min

m/z: [M+H]⁺ (calc.) = 383.41

[M+H]⁺ (meas.) = 383.2

[Methyl 5-\(\(\(7-bromo-4-oxo-4H-pyrido\[1,2-a\]pyrimidin-2-yl\)methyl\)carbamoyl\)-2,4-dimethyl-1H-pyrrole-3-carboxylate \(213\)](#)



18mg of **48** (93.3 μ mol, 1eq) was dissolved in 4mL dry DMF under Ar-atmosphere and before 18mg EDC \cdot HCl (93.3 μ mol, 1eq) and 23mg DMAP (185.8 μ mol, 2eq) were added. After stirring for 15 min, 24mg (93 μ mol, 1.2eq) **212** was added and the reaction mixture stirred overnight. The reaction progress was monitored by UHPLC-MS. After 18h the reaction was finished and the solvent evaporated. The crude was purified via HPLC with ACN/H₂O+0.1%TFA with a gradient of 10--> 100% over 20min. The product was isolated as a white solid in 8% yield (4.2mg, 0.01mmol).

R_f (TLC, Water/ACN 96:4) = 0.64

¹H-NMR (400 MHz, CDCl₃):

δ = 9.90 (s, 1H, NH), 9.18 (s, 1H, 6-H_{arom}), 7.92 (d, J = 8.0 Hz, 7H, 8-H_{arom}), 7.74 (d, J = 8.0 Hz, 1H, 9-H_{arom}), 6.52 (s, 1H, C=OCH), 4.65 (s, 2H, CH₂), 3.82 (s, 3H, OCH₃), 2.65 (s, 3H, CH₃), 2.50 (s, 3H, CH₃).

¹³C-NMR could not be measured due to bad solubility in common organic solvents.

UHPLC-MS

R_t (MCS): 1.406 min

m/z: [M+H]⁺ (calc.) = 433.1, 435.1

[M+H]⁺ (meas.) = 433.9, 435.0

I Appendix

1 Literature

- [1] WHO Cancer, <https://www.who.int/news-room/fact-sheets/detail/cancer>; March **2021**.
- [2] N. Turner, R. Grose, *Nat. Rev. Cancer*, **2010**, 10(2), 116-129.
- [3] G. La Venuta, M. Zeitler, J. P. Steringer, H.-M. Müller, W. Nickel, *J. Biol. Chem.*, **2015**, 290(45), 27015-27020.
- [4] P. Walter, *J. Cell Biol.*, **1981**, 91(2), 557-561.
- [5] I. Saraogi, S. O. Shan, *Traffic*, **2011**, 12(5), 535-542.
- [6] J. G. D’Arcangelo, K. R. Stahmer, E.A. Miller, *Biochimica et Biophysica Acta*, **2013**, 1833(11), 2464-2472.
- [7] F. Gu, C. M. Crump, G. Thomas, *Cell Mol. Life Sci.*, **2001**, 58(8), 1067-1084.
- [8] C. Viotti, “Unconventional Protein Secretion: Methods and Protocols, Chapter I: ER to Golgi-dependent Protein secretion: the conventional way”, Editors: A. Pompa, F. De Marchis, **2016**, Springer New York: New York, NY.
- [9] W. Nickel, M. Seedorf, *Annu. Rev. Cell Dev. Biol.*, **2008**, 24, 287-308.
- [10] C. Rabouille, *Trends in Cell. Biol.*, **2017**, 27(3), 230-240.
- [11] K.K. Kandaswamy, G. Pugalenti, E. Hartmann, K.-U. Kalies, S. Moller, P. N. Suganthan, T. Martinez, *Biochem. Biophys. Res. Commun.*, **2010**, 391(3), 1306-1311.
- [12] C.Eder, *Immunobiology*, **2009**, 214, 543-553.
- [13] M. Palotta, W. Nickel, *J. Cell Sci.*, **2020**, 133, jcs250449.
- [14] W. Nickel, *Traffic*, **2011**, 12, 799-805.
- [15] C. Seelenmeyer, S. Wegehangel, I. Tews, M. Künzler, M. Aebi, W. Nickel, *J. Cell Biol.*, **2005**, 171, 373-381.
- [16] F. Rayne, S. Debaisieux, A. Bonhoure, B. Beaumelle, *Cell. Biol. Int.*, **2010**, 34(4), 409-413.
- [17] E. Dimou, W. Nickel, *Curr. Biol.*, **2018**, 28, R406-R410.
- [18] I. Prudovsky, D. Kacer, J. David, V. Shah, S. Jayanthi, I. Huber, R. Dakshinamurthy, O. Ganter, R. Soldi, D. Neivandt, O. Guvench, T. K. Suresh Kumar, *Biochemistry*, **2016**, 55(7), 1159–1167.
- [19] P. W. Denny, S. Gokool, D. G. Russel, M. C. Field, D. F. Smith, *J. Biol. Chem.*, **2000**, 275, 11075-11025.

- [20] A. Rubartelli, F. Cozzolino, M. Talio, R. Sitia, *EMBO J.*, **1990**, 9, 1503-1510.
- [21] J. Lippencott-Schwartz, L. C. Yuan, J. S. Bonifacio, R. D. Klausner, *Cell*, **1989**, 56(5), 801–813.
- [22] S. Debaisieux, F. Rayne, H. Yezid, B. Beaumelle, *Traffic*, **2012**, 13, 355-363.
- [23] M. Zeitler, J. P. Steringer, H.-M. Müller, M. P. Mayer, W. Nickel, *J. Biol. Chem.*, **2015**, 290(36), 21976-21984.
- [24] R. T. Böttcher, C. Niehrs, *Endocrine Rev.*, **2005**, 26(1), 63–77.
- [25] R. Tsuboi, D. B. Rifkin, *J Exp. Med.*, **1990**, 172, 245-251.
- [26] T. J. Stegmann, *BioDrugs*, **1999**, 11(5), 301–8.
- [27] R. Cao, E. Bråkenhielm, R. Pawliuk, D. Wariaro, M. J. Post, E. Wahlberg, P. Leboulch, Cao Y, *Nature Medicine*, **2003**, 9(5), 604–13.
- [28] M. Okada-Ban, J. P. Thiery, J. Jouanneau, *Int J. Biochem Cell Biol*, **2000**, 32(3), 263–267.
- [29] O.A. Ibrahim, F. Zhang, A. V. Eliseenkova, R. J. Linhardt, M. Mohammadi, *Hum. Mol. Genet.*, **2004**; 13, 69-78.
- [30] V. Sørensen, T. Nilsen, A. Wiedlocha, *Bioessays*, **2006**, 28(5), 504–514.
- [31] R. Z. Florkiewicz, A. Sommer, *PNAS*, **1989**, 86, 3978–3981.
- [32] ¹ P.-J. Yu, G. Ferrari, A. C. Galloway, P. Mignatti, G. Pintucci. *J Cell Biochem*, **2007**, 100(5), 1100-1108.
- [33] F. Wang, L. Yang, L. Shi, Q. Li, G. Zhang, J. Wu, J. zheng, B. Jiao, *Oncotarget*, **2015**, 6(25), 21468-21478.
- [34] D. M Ornitz, N. Itoh, *Wiley Interdiscip Rev Dev Biol.*, **2015**, 4(3), 215–266.
- [35] J. P. Steringer, W. Nickel, *Semin. Cell Dev. Biol.*, **2018**, 83(3), 3-7.
- [36] H. Ago, Y. Kitagawa, A. Fujishima, Y. Matsuura, Y. Katsube, *J Biochem*, **1991**, 110(3), 360-363.
- [37] J.S. Kastrup, E. S. Eriksson, H. Dalboge, H. Flodgaard, *Acta Crystallogr D Biol Crystallogr*, **1997**, 53, 160-168.
- [38] O. A. Ibrahim, F. Zhan, S. C. Hrstka, M. Mohammadi, R. J. Linhardt, *Biochemistry (Mosc)*, **2004**; 43, 4724-4730.
- [39] M. A. Karajannis, L. Vincent, R. Drenzo, S. V. Shmelkov, F. Zhang, E. J. Feldman, P. Bohlen, Z. Zhu, H. Sun, P. Kussie, S. Rafii, *Leukemia*, **2006**; 20, 979-986.
- [40] S. Faham, R. E. Hileman, J. R. Fromm, R. J. Linhardt, and D. C. Rees, *Science*, **1996**, 271(5252), 1116–1120.

- [41] V. Eswarakumar, I. Lax, J. Schlessinger, *Cytokine Growth Factor Rev.*, **2005**; 16, 139-149.
- [42] M. Korc, R. E. Friesel, *Curr. Cancer Drug Targets.* **2009**; 9(5), 639-651.
- [43] A. Bikfalvi, S. Klein, G. Pintucci, D. B. Rifkin, *Endocr Rev*, **1997**, 18(1), 26–45.
- [44] A. Beenken, M. Mohammadi, *Nat Rev Drug Discov*, **2009**, 8(3), 235–253.
- [45] G. Seghezzi, S. Patel, C. J. Ren, A. Gualandris, G. Pintucci, E. S. Robbins, R. L. Shapiro, A. C. Galloway, D. B. Rifkin, P. Mignatti, *J Cell Biol.*, **1998**, 141(7), 1659–1673.
- [46] D. Ribatti, A. Vacca, M. Presta, *Gen Pharmacol.*, **2000**, 35(5), 227–231.
- [47] P. Carmeliet, R. K. Jain, *Nature*, **2000**, 407(6801), 249–257.
- [48] R. M. Akl, P. Nagpal, N. M. Ayoub, B. Tai, S. A Prabhu, C. M. Capac, M. Gliksman, A. Goy, K. S. Suh, *Oncotarget*, **2016**, 7(28), 44735-44762.
- [49] P. Mignatti, T. Morimoto, D. B. Rifkin, *J Cell Physiol*, **1992**, 151(1), 81–93.
- [50] G. La Venuta, M. Zeitler, J. P. Steringer, H.-M. Müller, W. Nickel, *J Biol Chem*, **2015**, 290(45), 27015–27020.
- [51] C. Legrand, R. Saleppico, J. Sticht, F. Lolicato, H.-M. Müller, S. Wegehingel, E. Dimou, J. P. Steringer, E. Ewers, I. Vattulainen, C. Freund, W. Nickel, *Commun Biol*, **2020**, 3, art n° 141.
- [52] K. Temmerman, A. D. Ebert, H.-M. Müller, I. Sinning, I. Tews, W. Nickel, *Traffic*, **2008**, 9(7), 1204-1217.
- [53] J. P. Steringer, S. Bleicken, H. Andreas, S. Zacherl, M. Laussmann, K. Temmerman, F. X. Contreras, T. A. M. Bharat, J. Lechner, H.-M. Müller, J. A. G. Briggs, A. J. Garcia-Saez, and W. Nickel, *J Biol Chem*, **2012**, 287(33), 27659–27669.
- [54] A. D. Ebert, M. Laussmann, S. Wegehingel, L. Kaderali, H. Erfle, J. Reichert, J. Lechner, H.-D. Beer, R. Pepperkok, and W. Nickel, *Traffic*, 2010, 11(6), 813–826.
- [55] H.-M. Müller, J. P. Steringer, S. Wegehingel, S. Bleicken, M. Munster, E. Dimou, S. Unger, G. Weidmann, H. Andreas, A. J. Garcia-Saez, K. Wild, I. Sinning, W. Nickel, *J Biol Chem*, **2015**, 290(14), 8925–8937.
- [56] W. Nickel, *J Cell Sci*, **2007**, 120(Pt 14), 2295–2299.
- [57] R. Z. Florkiewicz, J. Anchin, A. Baird, *J Biol Chem*, **1998**, 273(1), 544–551.
- [58] D. Brough, P. Pelegrin, W. Nickel, *J Cell Sci*, **2017**, 130, 3197-3202.

- [59] C. Powers, S. McLiskey, A. Wellstein, *Endocr. Relat. Cancer*, **2000** □□□□□□□□□□□□□□□□
- [60] I. Ahmad, T. Iwata, H. Y. Leung, *Biochim Biophys Acta*, **2012**, *4*, 850-860.
- [61] C. Thussbas, J. Nahrig, S. Streit, J. Bange, M. Kriner, R. Kates, K. Ulm, M. Kiechle, H. Hoefler, A. Ullrich, N. Harbeck, *J Clin Oncol.* **2006**; *24*, 3747-3755.
- [62] J. H. Jang, K. H. Shin, J. G. Park, *Cancer Res.*, **2001**; *61*, 3541-3543.
- [63] G. Yan, Y. Fukabori, G. McBride, S. Nikolaropolous, W.L. McKeegan, *Mol. Cell. Biol.*, **1993**, *13*, 4513-4522.
- [64] P. Savagner, A.M. Valles, J. Jouanneau, K.M. Yamada, J.P. Thiery, *Mol. Biol. Cell*, **1994**, *5*, 851–862.
- [65] C. L. Chaffer, J. P. Brennan, J. L. Slavin, T. Blick, E. W. Thompson, E.D. Williams, *Cancer Res.*, **2006**, *66*, 11271-11278.
- [66] M. Presta, L. Tiberio, M. Rusnati, P. Dell’Era, G. Ragnotti, *Cell Regul.* **1991**, *2*, 719-726.
- [67] P. Lu, K. Takai, V. M. Weaver, Z. Werb, *Cold Spring Harb Perspect Biol.*, **2011**, *3*(12), a005058.
- [68] D. Ribatti, A. Vacca, M. Rusnati, M. Presta, *Cytokine Growth Factor Rev.*, **2007**; *18*(3-4), 327-334.
- [69] B. Dobrzycka, B. Mackowiak-Matejczyk, M. Kinalski, S. J. Terlikowski, *Gynecol Oncol.*, **2013**, *128*, 454-460.
- [70] M: Relf, S. LeJeune, P. A. Scott, S. Fox, K. Smith, R. Leek, A. Moghaddam, *Cancer Res.*, **1997**, *57*, 963-969.
- [71] D. Visscher, F. DeMattia, S. Ottosen, F. Sarkar, J. Crissman, *Mod Pathol.*, **1995**; *8*, 665-670.
- [72] R. Kurimoto, S. Iwasawa, T. Ebata, T. Ishiwata, I. Sekine, Y. Tada, K. Tatsumi, S. Koide, A. Iwama, Y. Takiguchi, *Int J Oncol*, **2016**, *48*, 1825-1836.
- [73] K. Ichikawa*, S. W. Miyano, Y. Minoshima, J. Matsui, Y. Fun, *Sci Rep*, **2020**, *10*, art n°2939.
- [74] G. Yan, Y. Fukabori, G. McBride, S. Nikolaropolous, W. L. McKeegan, *Mol. Cell. Biol.*, **1993**, *13*, 4513-4522.
- [75] K. H. Noh, S.-H. Kim *et al.*, *Cancer Res.* **2016**, *76*(22), 6471–6482.
- [76] E. M. J. van Brummelen, E. Levchenko, M. Dómine, D. A Fennell, H. L. Kindler, S. Viteri, S. Gadgeel, P. G. López, V. Kostorov, D. Morgensztern, S. Orlov, M. G. Zauderer, J. F. Vansteenkiste, K. Baker-Neblett, J. Vasquez, X. Wang, D. I.

- Bellovin, J. H. M. Schellens, L. Yan, I. Mitrica, M. P. DeYoung, J. Trigo, *Invest New Drugs*, **2020**, 38(2), 457-467.
- [77] T. C. Harding, L. Long, S. Palencia, H. Zhang, A. Sadra, K. Hestir, N. Patil, A. Levin, A. W. Hsu, D. Charych, T. Brennan, J. Zanghi, R. Halenbeck, S. A. Marshall, M. Qin, S. K. Doberstein, *Sci Transl Med.*, **2013**, 5, 3005414.
- [78] G. Colombo, B. Margosio, L. Ragona, M. Neves, S. Bonifacio, D. S. Annis, M. Stravalaci, S. Tomaselli, R. Giavazzi, M. Rusnati, M. Presta, L. Zetta, D. F. Mosher, D. Ribatti, M. Gobbi, G. Taraboletti, *J Biol Chem.*, **2010**; 285, 8733-8742.
- [79] A. Tayel, K. H. Abd El Galil, M. A. Ebrahim, A. S. Ibrahim, A. M. El-Gayar, M. M. Al-Gayyar MM, *Eur J Pharmacol.*, **2014**, 72, 151-160.
- [80] J. A. Smith, T. Madden, M. Vijjeswarapu, R. A. Newman, *Biochem Pharmacol.*, **2001**, 62, 469-472.
- [81] J. W. Slaton, P. Perrotte, K. Inoue, C. P. Dinney, I. J. Fidler, *Clin Cancer Res.*, **1999**, 5, 2726-2734.
- [82] S. Zhou, F. Wang, T. C. Hsieh, J. M. Wu, E. Wu, *Curr Med Chem.*, **2013**, 20, 4102-4108.
- [83] T. D. Stephens, C. J. Bunde, B. J. Fillmore, *Biochem Pharmacol.*, **2000**, 59(12), 1489–1499.
- [84] C. Pottier, M. Fresnais, M. Gilon, G. Jerusalem, R. Longuespee, N. E. Sounni, *Cancers*, **2020**, 12, 731-748.
- [85] C. Lieu, J. Heymach, M. Overman, H. Tran, S. Kopetz, *Clin Cancer Res.*, **2011**, 17, 6130-6139.
- [86] V. K. Jain, N. C. Turner, *Breast Cancer Res.*, **2012**, 14, 208-217.
- [87] J. Matsui, Y. Funahashi, T. Uenaka, T. Watanabe, A. Tsuruoka, M. Asada, *Clin Cancer Res.*, **2008**; 14, 5459-5465.
- [88] S. Popat, A Mellempgaard, K. Fahrbach, A. Martin, M. Rizzo, R. Kaiser, I. Griebisch, M. Reck, *Future Oncol.*, **2015**, 11, 409-420.
- [89] M. Shibuya, *Genes Cancer.*, **2011**, 2(12), 1097-1105.
- [90] C. Gialeli, D. Nikitovic, D. Kletsas, A. D. Theocharis, G. N. Tzanakakis, N. K. Karamanos, *Curr. Pharm. Des.*, **2014**, 20(17), 2843-8.
- [91] Y. Nakanishi, N. Akiyama, T. Tsukaguchi, T. Fujii, K. Sakata, H. Sase, T. Isobe, K. Morikami, H. Shindoh, T. Mio, *Mol Cancer Ther.*, **2014**, 13, 2547-2558.

- [92] P. R. Gavine, L. Mooney, E. Kilgour, A.P. Thomas, K. Al-Kadhimi, S. Beck, C. Rooney, T. Coleman, D. Baker, M. J. Mellor, A. N. Brooks, T. Klinowska, *Cancer Res.*, **2012**, 72(8), 2045-56.
- [93] H. Ochiwa, H. Fujita, K. Itoh, H. Sootome, A. Hashimoto, Y. Fujioka, Y. Nakatsuru, N. Oda, K. Yonekura, H. Hirai, *Mol Cancer Ther.*, **2013**, 12, A270-A270.
- [94] J. Qing, X. Du, Y. Chen, P. Chan, H. Li, P. Wu, S. Marsters, S. Stawicki, J. Tien, K. Totpal, *J Clinical Invest.*, **2009**, 119, 1216.
- [95] U. Stelzl, U. Worm, M. Lalowski, C. Haenig, F. H. Brembeck, H. Goehler, M. Stroedicke, M. Zenkner, A. Schoenherr, S. Koeppen, J. Timm, S. Mintzlaff, C. Abraham, N. Bock, S. Kietzmann, A. Goedde, E. Toksöz, A. Droege, S. Krobitsch, B. Korn, W. Birchmeier, H. Lehrach, E. E. Wanker, *Cell*, **2005**, 122, 957–968.
- [96] G. C. Koh, P. Porras, B. Aranda, H. Hermjakob, S. E. Orchard, *J. Proteome Res.*, **2012**, 11, 2014-2031.
- [97] D. E. Scott, A. R. Bayly, C. Abell, J. Skidmore, *Nat. Rev. Drug Discov.*, **2016**, 15, 533–550.
- [98] B. I. Diaz-Eufracio, J. J. Naveja, J. L. Medina-Franco, *Adv. Protein Chem. Struct. Biol.*, **2018**, 110, 65–84.
- [99] P. Buchwald, *IUBMB Life*, **2010**, 62, 724–731.
- [100] M. C. Smith, J. E. Gestwicki, *Expert Rev. Mol. Med.*, **2012**, 14, e16.
- [101] A. C. Cheng et al. *Nat. BioTEChnol.*, **2007**, 25, 71–75.
- [102] A. A. Ivanov, F. R. Khuri, H. Fu, *Trends Pharmacol. Sci.*, **2013**, 34, 393–400.
- [103] A. G. Coyne, D. E. Scott, C. Abell, *Curr. Opin. Chem. Biol.*, **2010**, 14, 299–307.
- [104] I. S. Moreira, P. A. Fernandes, M. J. Ramos, *Proteins*, **2007**, 68, 803-812.
- [105] J. A. Wells, C. L. McClendon, *Nature*, **2007**, 450, 1001–1009.
- [106] P. J. Hajduk, J. A. Greer, *Nat. Rev. Drug Discov*, **2007**, 6, 211–219.
- [107] H. Lu, Q. Zhou, J. He, Z. Jiang, C. Peng, R. Tong, J. Shi, *Sig Transduct Target Ther.*, **2020**, 5, 213.
- [108] P. Dorr et al. *Antimicrob. Agents Chemother* **2005**, 49, 4721–4732.
- [109] D. Bailey et al., *J. Am. Coll. Cardiol.*, **2010**, 55, 2580-2589.
- [110] L. M. Tsujikawa, L. Fu, S. Das et al., *Clin Epigenet*, **2019**, 11, art n°102.
- [111] H. Mano, *Cytokine Growth Factor Rev.*, **1999**, 10(3-4), 267–280.
- [112] J. M. Bradshaw, *Cell Signal*, **2010**, 22(8), 1175–84.

- [113] L. E. Marengere, T. Pawson, *J Cell Sci. Suppl*, **1994**, 18, 97–104.
- [114] P. Liu, H. Cheng, T. M. Roberts, J. J. Zhao, *Nat. Rev. Drug Discov.*, **2009**, 8, 627–644.
- [115] G. La Venuta, S. Wegehingel, P. Sehr, H.-M. Müller, E. Dimou, J. P. Steringer, M. Grotwinkel, N. Hentze, M. Mayer, D. W. Will, U. Uhrig, J. D. Lewis, W. Nickel, *J. Biol. Chem.*, **2016**, 291(34), 17787-17803.
- [116] L. Yu, O. E. Simonson, A. J. Mohamed, C. I. Smith, *FEBS J.*, **2009**, 276, 6714–6724.
- [117] T. Vanova, Z. Konecna, Z. Zbonakova, G. La Venuta, K. Zoufalova, S. Jelinkova, M. Varecha, V. Rotrekl, P. Krejci, W. Nickel *et al.*, *Stem Cells*, **2017**, 35, 2050–2059.
- [118] E. Traer, J. Martinez, N. Javidi-Sharifi, A. Agarwal, J. Dunlap, I. English, T. Kovacsovics, J. W. Tyner, M. Wong, B. J. Druker, *Cancer Res.*, **2016**, 76(22), 6471-6482.
- [119] Perkin Elmer, May 2016, “*User’s Guide To Alpha Assays: Protein:Protein Interactions*”
https://www.perkinelmer.com/lab-solutions/resources/docs/009625A_01_GDE.pdf; (15.01.2020).
- [120] P. L. Ferrarini, C. Mori, O. Livi, G. Biagi, A. M. Marini, *J. Heterocyclic Chem.*, **1983**, 20, 1053-1057.
- [121] C. M. Shiner, T. D. Lash, *Tetrahedron*, **2005**, 61, 11628-11640.
- [122] S. N. Basahel, N. S. Ahmed, K. Narasimharao, M. Mokhtar, *RSC Adv.*, **2016**, 6, 11921-11932.
- [123] V. K. Krieble, C. I. Noll, *J. Am. Chem. Soc.*, **1939**, 61, 560-563.
- [124] M. Mößer, “Synthesis of Tec-Kinase Inhibitors as a novel class of anti-angiogenic drugs for cancer therapy“, **2015**, Bachelor thesis, Universität Heidelberg.
- [125] Unpublished data; reactions conducted by M. Mößer.
- [126] S. R. Chemler, D. Trauner, S. J. Danishefsky, *Angewandte Chem. Intl. Ed.*, **2001**, 40(24), 4544-4568.
- [127] N. Miyaura, A. Suzuki, *Chem. Rev.*, **1995**, 95(7), 2457-2483.
- [128] S. s. Gujral, S. Kathri, P. Riyal, *Indo Global J. Pharm. Sci.*, **2012**, 2(4), 351-367.

- [129] S. W. Wright, D. L. Hageman, L. D. McClure, *J. Org. Chem.*, **1994**, 59(20), 6095-6097.
- [130] G. C. Fu, *Acc. Chem. Res.*, **2008**, 41(11), 1555-1564.
- [131] H. Doucet, *Eur. J. Org. Chem.*, **2008**, 12, 2023-2030.
- [132] A. Molnár, A. Kapros, L. Párkányi, Z. Mucsi, G. Vlád, I. Hermeecz, *Org. Biomol. Chem.*, **2011**, 9, 6559-6565.
- [133] I. Ferrara, "Synthesis of small molecule inhibitors targeting the interaction of Teckinase and Fibroblast Growth Factor 2 (FGF2) in order to develop new anti-angiogenic drugs", **2018**, Universität Heidelberg.
- [134] P. Fitton, E. A. Rick, *J. Organomet. Chem.*, **1971**, 28(2), 287-291.
- [135] L. Jedinák, R. Zátoková, H. Zemánková, A. Šustková, P. Cankař, *J. Org. Chem.*, **2017**, 82(1), 157-169.
- [136] Y. Kabri, M. D. Crozet, N. Primas, P. Vanelle, *Eur. J. Org. Chem.*, **2012**, 2012(28), 5595-5604.
- [137] N. Henry, E. Thiery, J. Petriguet, H. Halouchi, J. Thibonnet, M. Abarbri, *Eur. J. Org. Chem.*, **2012**, 2012 (31), 6212-6217.
- [138] H. Mitsudera, K. Otaka, J. Fujiwara, World Intellectual Property Organization, WO2005068432 A1, 2005-07-28.
- [139] Y. Oikawa, K. Sugano, O. Yonemitsu, *J. Org. Chem.*, **1978**, 43, 2087-2088.
- [140] G. Giacomelli, A. Porcheddu, M. Salaris, M. Taddei, *Eur. J. Org. Chem.*, **2003**, 3, 537-541.
- [141] J.B. Paine, D. Dolphin, *J. Org. Chem.*, **1988**, 53, 2787-2795.
- [142] J. W. Harbuck, H. Rapoport, *J. Org. Chem.*, **1971**, 36(6), 853-855.
- [143] F. Micheli, R. Di Fabio, P. Cavanni, J. M. Rimland, A. M. Capelli, C. Chiamulera, M. Corsi, C. Conrti, D. Donati, A. Feriani, F. Ferraguti, M. Maffeis, A. Missio, E. Ratti, A. Paio, R. Pachera, M. Quartaroli, A. Reggiani, F. M. Sabbatini, D. G. Trist, A. Ugolini, G. Vitulli, *Bioorg. Med. Chem.*, **2003**, 11, 171-183.
- [144] A. C. Zuniga, *Heterocycles*, **2004**, 63, 2071-20MS77.
- [145] experiments conducted by I. Ferrara.
- [146] J. C. Sheehan, W. A. Bolhofer, *J. Am. Chem. Soc.*, **1950**, 72 (6), 2786-2788.

- [147] R. A. Smits, M. Adami, E. P. Istyastono, O. P. Zuiderveld, C. M. E. van Dam, F. J. J. de Kanter, A. Jongejan, G Coruzzi, R. Leurs, I. J. P. de Esch, *J. Med. Chem.* **2010**, *53*, 2390–2400.
- [148] S. Montalvao, T. O. Leino, P.S. Kiuru, K.-E. Lillsunde, J. Y. Kauhaluoma, P. Tammela, *Arch. Pharm. Chem. Life Sci.*, **2016**, *349*, 137–149.
- [149] M.Hügler, X. Lucas, D. Ostrovskiy, P. Regenass, S. Gerhardt, O. Einsle, M. Hau, M. Jung, B. Breit, S. Günther, D. Wohlwend, *Angew.Chem.Int. Ed.*, **2017**, *56*, 12476 –12480.
- [150] A. Jansma, Q. Zhan, B. Li, Q. Ding, T. Uno, B. Bursulaya, Y. Liu, P. Furet, N. S. Gray, B. H. Geierstanger, *J. Med. Chem.*, **2007**, *50*, 5875-5877.
- [151] G. Wagner, A. Pardi, K. Wüthrich, *J. Am. Chem. Soc.*, **1983**, *105*, 5948-5949.
- [152] C. Zehe, A. Engling, S. Wegehingel, T. Schäfer, W. Nickel, *Proc. Natl. Acad. Sci. U.S.A.*, **2006**, *103*, 15479-15484.
- [153] H. M. Müller, J. P. Steringer, S. Wegehingel, S. Bleicken, M. Münster, E. Dimou, S. Unger, G. Weidmann, H. Andreas, A. J. García-Sáez, K. Wild, I. Sinning, W. Nickel, *J. Biol. Chem.*, **2015**, *290*, 8925– 8937.
- [154] J. P. Steringer, S. Bleicken, H. Andreas, S. Zacherl, M. Laussmann, K. Temmerman, F. X. Contreras, T. A. Bharat, J. Lechner, H. M. Müller, J. A. Briggs, A. J. García-Sáez, W. Nickel, *J. Biol. Chem.*, **2012**, *287*, 27659 –27669.
- [155] Perkin Elmer Inc: *USER'S GUIDE TO ALPHA ASSAY PROTEIN:PROTEIN INTERACTIONS*; **2016** [cited Oct 14th 2020 from: <https://www.perkinelmer.com/PDFs/downloads/GDE-Alphatech.pdf>].
- [156] Peppard, J., *et al*, *J. Biomol. Screen*, **2003**, *8*, 2, 149-156.
- [157] BMG LABTECH website [cited Oct 16th 2020]:https://www.bmglabtech.com/fileadmin/06_Support/Download_Documents/Brochures/microplate-reader-nephelostar-plus-brochure.pdf
- [158] G. R. Fulmer, A. J. M. Miller, N. H. Sherden, H. E. Gottlieb, A. Nudelman, B. M. Stoltz, J. E. Bercaw, K. I. Goldberg, *Organometallics* **2010**, *29*, 2176–2179.

2 Legends

2.1 Figures

- Fig. 1** HTS identified small molecule inhibitors and control compounds for the PPI of Tec Kinase and FGF2; green box: inhibitors; red box: inactive control compounds. 20
- Fig. 2** Overview of planned SAR for **C6**; Changes of the ring structure and substituents in both head and tail group as well as changing the linker between both. 23
- Fig. 3** UPLC-MS analysis of mixed fraction during column purification of X5; A.) UV254nm chromatogram of UPLC-MS with SP (yellow) and Prod (blue) peaks including their chemical structures and the expected protonated MW; B.) MS spectra of SP and Prod peaks with respective highlighted Mass peaks. 37
- Fig. 4** UPLC-MS measurements of **167** after **A** 2h with **167** (blue peak) its corresponding mass spectra and **B** 17h without product peak. 46
- Fig. 5** ¹H-NMR of **88** in DMSO-d₆ with the identified NH-proton peak (yellow). 48
- Fig. 6** UHPLC-MS graphs of reaction mixture of to synthesise **77** after 17h; **A**. MS spectrum (ESI⁺) with main peak (yellow box) corresponding to MW of **77** in chromatogram at 1.636min (blue in lower panel); **B** MS spectrum (ESI⁺) with main peak (yellow box) corresponding to MW of **203** in chromatogram at 1.752min (blue in lower panel). 55
- Fig. 7** UPLC chromatogram of reaction control after 16-17h showing the qualitative peak size (blue) of the **203**, **204** and **205** formed in each reaction. 55
- Fig. 8** ¹H-NMR (400MHz) of **C6** at RT in CDCl₃ and DMSO-d₆ with the NH peak highlighted (yellow). 64
- Fig. 9** IC₅₀ graphs of Alpha Assay (3 techn. replic.): **A** Comp 44 graph of machine supported assay; **B** Comp 44 graph (hand pipetted); **C** Comp 41 with inhibition of <50%; **D** Precipitation of compound visible in graph at higher concentration for Comp 114. 67
- Fig. 10** Overview IC₅₀ evaluation of **C6** analogues with different substituents on the head group scaffold giving a similar or better inhibition than **C6** (**10**). 68
- Fig. 11** Alpha assay graphs for **A** comp **74** and **B** comp **75** with a high variance of measured data between the technical replicates leading to possible incorrect IC₅₀ values; **C** Graph of comp **68** only giving an inhibition level of 30%. 72
- Fig. 12** Surface biotinylation levels of FGF2-GFP and GAPDH cell lysate quantification in CHO cells expressing FGF2Wt-GFP (mock) and FGF2C77/95A-GFP

as cell control (DM) after incubation with compounds for 16h at 37°C; **A** Western Blot of full cell lysate (cell) and surface population of FGF2 treated with no compound (mock, cell control (**DM**) and **25µM** of compounds, proteins labelled with anti-FGF2(green) and anti-GAPDH (red) antibodies; **B** average and st.dev. of surface biotinylation levels at 25µM for all PPI inhibitors identified in alpha assay with **C** their GAPDH level; all data sets were normalized to average mock set to 100%. data sets calculated from min. 4 independent replicates (three repl.: **11**; five repl.: **96**; six repl.: **66, 10(C6)**; seven repl.: **33, 40, 71**; eight repl.: **51, 90**); experiments conducted by S.Wegehingel. 78

Fig. 13 Cell confluence of CHO cells after incubation with 25µM of compounds for 40h at 37°C; **A** microscopy pictures of mock and compounds **10, 73** and **96**; **B** Graph of average ± SD of cell confluence in % calculated from min. 3 repl. (4 repl.: **33, 40, 62, 67, 73, 96**; 7 repl.: **10(C6), 51, 66, 71**); confluence was normalized to average of mock set to 100%; Pictures and data was obtained by S. Wegehingel. 79

Fig. 14 Surface biotinylated FGF2-GFP population and GAPDH cell lysate quantification in CHO cells expressing FGF2Wt-GFP (mock) after incubation with compounds at 50µM, 25µM, 10µM and 5µM for 16h at 37°C; all data sets; **A** average of surface population of FGF2Wt normalized to mock set to 100% for 50µM, 10µM and 5µM and average ± SD for 25µM; **B** average of GAPDH level in cell lysate for 50µM, 10µM and 5µM, average ± SD for 25µM of compound conc.; all data sets were normalized to the average of mock set to 100%; average for 50µM, 10µM and 5µM calculated from 2 repl.; average ± SD for 25µM calculated from 4 repl.; experiments were conducted by S.Wegehingel. 80

Fig. 15 SAR results of the alpha assay for C6..... 81

Fig. 16 Overview of biological data obtained for most promising compounds of C6 SAR; green: compounds with a better/similar inhibition of FGF2 secretion; yellow: compounds with alpha assay activity but no activity in cell-based assay; red: compounds that possibly hinder cell growth. 83

Fig. 17 Overview of additional SAR approaches for C6. 85

Fig. 18 384-well plate set up capable of testing 26 compounds (two per row of C-P one in light blue wells and one in dark blue wells); negative controle without any compound used to normalize data are in yellow marked wells; background of the single proteins and solely the beads are on the right side marked in column 24. 89

2.2 Tables

Table 1 Overview of pyridopyrimidone synthesis with different substituents.	28
Table 2 Overview of test reactions for ester linker of 41	29
Table 3 Syntheses of C6 analogues with pyridopyrimodines 124-144 in combination with pyrrole building blocks 48, 52 and 53^a	31
Table 4 Test reaction of Aryl-Aryl Suzuki coupling conditions.	35
Table 5 Suzuki reaction with pyridopyrimidones 138-141	36
Table 6 Synthesis of 157	39
Table 7 Synthesis of 158	40
Table 8 Synthesis of compounds 159 and 160	41
Table 9 Synthesis of C6 analogues containing larger alkyl substituents on the head group.	42
Table 10 Synthesis of multiply substituted pyridopyrimidones.	44
Table 11 Synthesis of C6 analogues with multiple substituents on the head group.	45
Table 12 Syntheses of imidazopyridines 171, 172 and 173	47
Table 13 Syntheses of C6 analogues missing the carbonyl group in the head group.	47
Table 14 Synthesis of β -keto ester.	50
Table 15 Synthesis of nitrosylated β -keto ester.	50
Table 16 Knorr-Pyrrole Synthesis.	51
Table 17 Benzyl ester hydrogenolysis to give pyrrole building blocks 191-202	53
Table 18 Synthesis of C6 analogues 76-87	54
Table 19 Synthesis of C6 analogues 54-60 and 64	56
Table 20 N1-Alkylation of pyrrole tail group of C6	58
Table 21 Gabriel Synthesis Step I.	60
Table 22 Overview of Gabriel synthesis step II.	60
Table 23 Synthesis of C6 analogues containing an amide linker.	62
Table 24 Overview of solubility and IC ₅₀ values of C6 derivatives with position and substituent modification on head group.	66
Table 25 Overview of solubility and IC ₅₀ values of compounds with position and substituent modification on head group and the ketone on the pyrrole tail group.	69
Table 26 Comparison of IC ₅₀ values of C6 with an ethyl ester on pyrrole ring.	70
Table 27 Ethyl ester modification of most promising C6 derivatives with position and substituent modification on head group.	70

Table 28 IC ₅₀ and solubility values of compounds with multiple substituents and bigger groups.....	72
Table 29 IC ₅₀ and solubility results of compounds with imidazopyridines head groups.	73
Table 30 IC ₅₀ data for increased alkyl substituents on the tail group.....	74
Table 31 IC ₅₀ values for N-modified tail group modifications.....	75
Table 32 IC ₅₀ values for compounds 54-60 and 64	76
Table 33 IC ₅₀ of amide linked compounds 61-63 and 124	77

2.3 Schemes

Scheme 1 Overview of conventional protein secretion from translation into the ER to the transport with secretory vehicles to the plasma membrane.	2
Scheme 2 Overview of unconventional protein secretion (UPS) mechanisms Type I-IV.	4
Scheme 3 Current model of FGF2 secretion mechanism showing the membrane recruitment through ATP1A1, FGF2 bound to PI(4,5)P ₂ being phosphorylated by Tec Kinase leading to increased oligomerisation, insertion and finally translocation to the extracellular space facilitated by HSPGs. (adapted by author from Brough et al.)	9
Scheme 4 Overview of Tec kinase family showing their structural similarities and differences.	17
Scheme 6 Retrosynthesis overview for C6	26
Scheme 7 Synthetic steps for C6 analogues.	26
Scheme 7 <i>Plausible reaction mechanism of the pyridopyrimidone synthesis of 125.29</i>	
Scheme 8 Schematic overview of the different approaches possible to introduce alkyl group via Suzuki reaction.	33
Scheme 10 <i>Alkylation of 40 via Suzuki reaction</i>	35
Scheme 10 Synthesis route for substituted pyrrole carboxylic acids.....	49
Scheme 12 Schematic overview of first reaction step in the mechanism of the Knorr synthesis forming intermediate I	52
Scheme 13 Second alkylation reaction of 77	54
Scheme 13 Synthesis route for a C6 analogue containing an amide linker; I.) functionalization of 2-(chloromethyl)-pyrimidopyrimidones with an amine using the Gabriel Synthesis; II.) amide linker formation using the peptide coupling reagent EDC.	59
Scheme 10 C6 structure with A possible intramolecular H-Bond and B intermolecular H-bond with DMSO.....	63
Scheme 1 Overview of Alpha® assay for the detection of interaction partners GST-ΔN173Tec Kinase and His-FGF2WT. GST-tagged Tec Kinase is bound through interaction with Glutathione to the donor bead and His-FGF2Wt is bound to the Ni ²⁺ coated acceptor bead. The interactions of these proteins leads to a luminescent/fluorescent signal when an excitation with a 680nm laser occurs.....	88
Scheme 2 Overview of compound dilution in the mother plate followed by the predilution into the daughter plate followed by the transfer into assay plates.	90

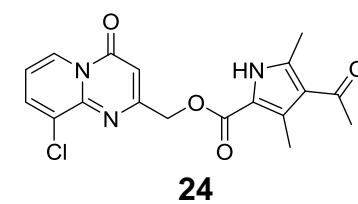
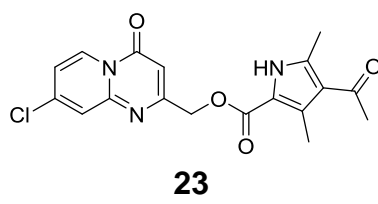
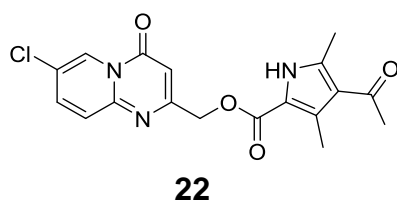
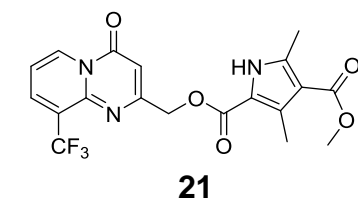
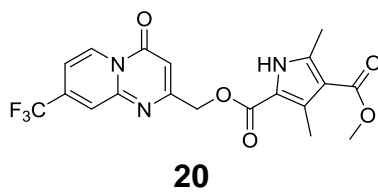
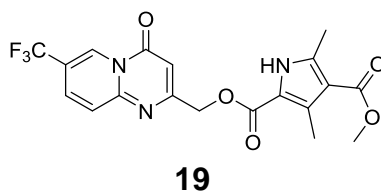
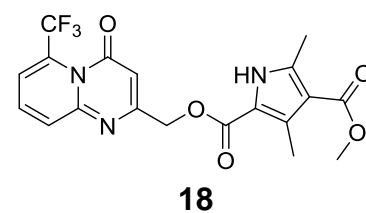
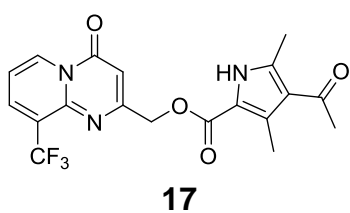
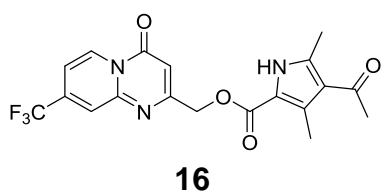
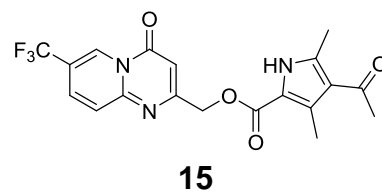
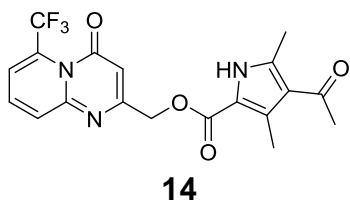
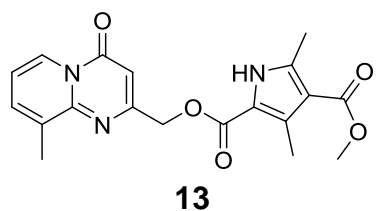
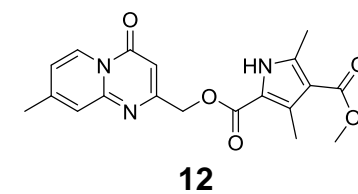
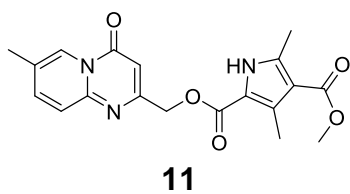
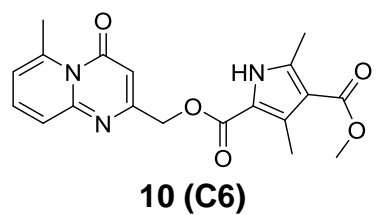
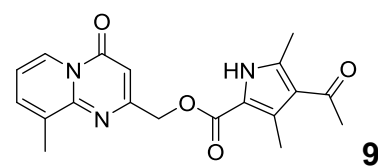
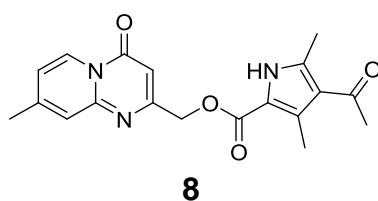
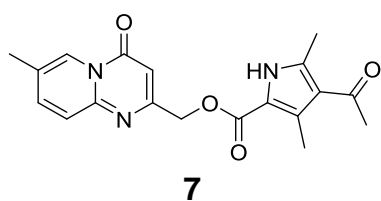
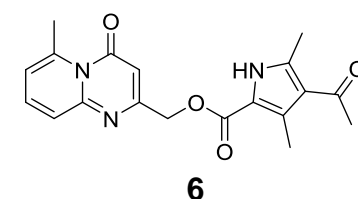
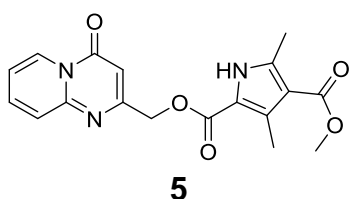
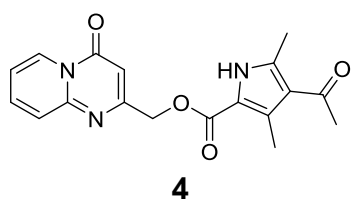
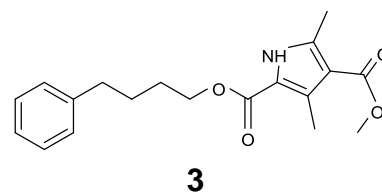
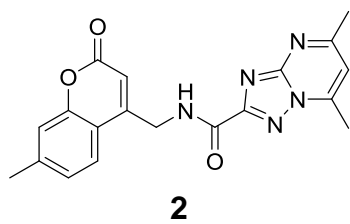
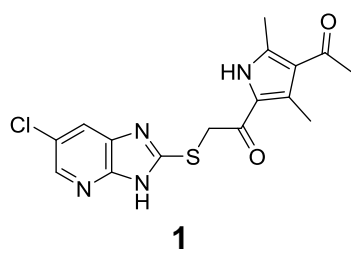
3 Abbreviation Index

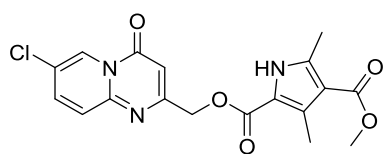
ACN	acetonitrile
AcOH	acetic acid
AKT	Protein kinase B
ATP	adenosin tr phosphate
ATP1A1	sodium/potassium-transporting ATPase subunit alpha-1
BET	Bromodomain and extra-terminal motif
BMX	cytoplasmic tyrosine-protein kinase
Bn	benzyl
BTK	Bruton's tyrosine kinase
CCR5	c-c chemokine receptor 5
CDCl ₃	deuterated chloroform
DCM	dichloromethane
DIPEA	di-isopropyle-ethyle-amine
DMAP	4-dimethylaminopyridine
DMF	dimethylformamide
DMSO	dimethylsulfoxide
DNA	desoxyribonucleic acid
DTT	dithiothreitol
ECM	extracellular matrix
EDC	1-ethyl-3-(3-dimethylaminopropyl)carbodiimide
ER	endoplasmatic reticulum
ER	Endoplasmatic reticulum
ERK	extra-cellular signal-regulated kinase
ESI	electron spray ionization
Et	ethyl
EtOAc	ethylacetate
FGF1	fibroblast growth factor 1
FGF2	fibroblast growth factor 2
FGF2	fibroblast growth factor 2
FGFR	fibroblast growth factor receptor

FLT3	Fms-like tyrosine kinase 3
Gp120	envelope glycoprotein gp120
HMW	High molecular weight
HOBt	hydroxybenzotriazole
HSPG	heparansulfate proteoglycan
HSPG	heparan sulfate proteoglycan
HSQC	heteronuclear single quantum coherence
<i>i</i> -PR	<i>iso</i> -Propyl
ITK	interleukin-2-inducible T-cell kinase
MAPK	mitogen-activated protein kinase
MCS	MedChem Standard
Me	methyl
MeOH	methanol
MW	molecular weight
NEt ₃	triethyl amine
NMR	nuclear magnetic resonance
PCR	polymerase chain reaction
PDGFR	Platelet-derived growth factor receptor
PI(3,4,5)P ₃	phosphatidylinositol-3,4,5-triphosphate
PI(4,5)P ₂	phosphatidylinositol-4,5-bisphosphate
PIP	phosphoinositide phosphate
PKC signalling	protein kinase C
PPA	polyphosphoric acid
PPI	protein-protein interaction
PPI	protein-protein interaction
PRR	proline rich region
RNA	ribonucleic acid
RT	room temperature
SM	starting material
SPR	Surface plasmon resonance
TEC	tyrosine kinase expressed in hepatocellular carcinoma

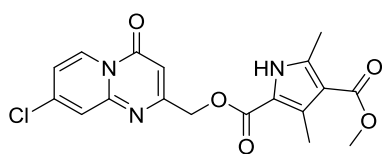
TGN	trans Golgi network
TLC	thin layer chromatography
TXK/RLK	resting lymphocyte kinase
UHPLC-MS	Ultra high pressure liquid chromatography-mass spectography
UPS	unconventional protein secretion
UPS	unconventional protein secretion
VEGF	vascular epithelial growth factor
VEGFR	vascular endothelial growth factor receptor
Zn	zinc
μ W	microwave

4 Compound Index

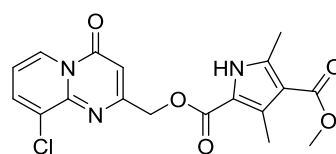




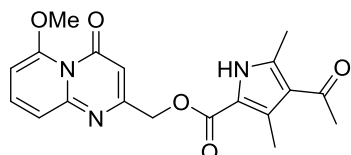
25



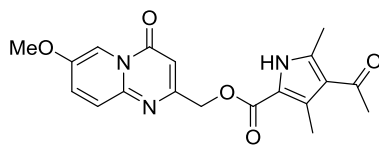
26



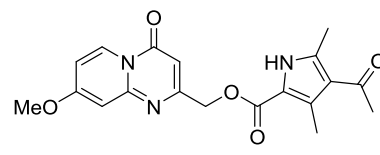
27



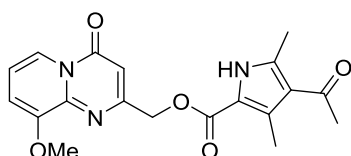
28



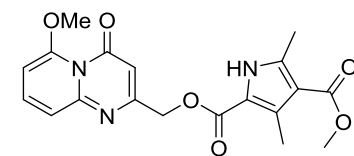
29



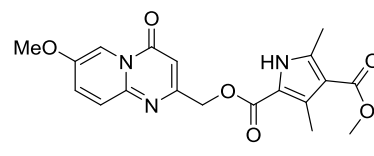
30



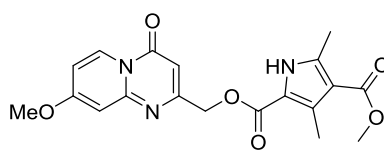
31



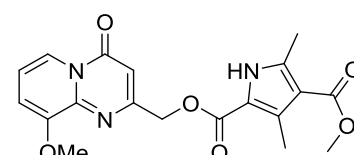
32



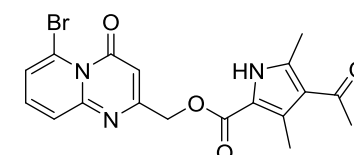
33



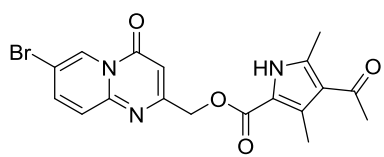
34



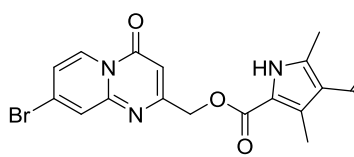
35



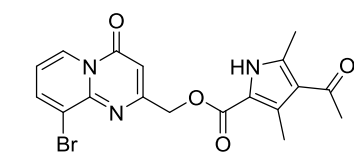
36



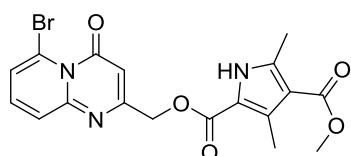
37 (14)



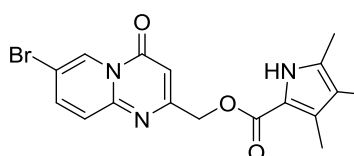
38



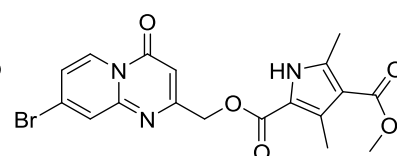
39



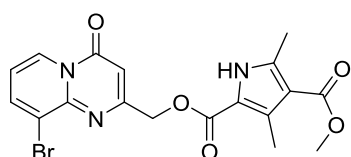
40



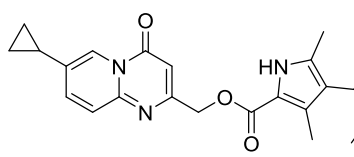
41



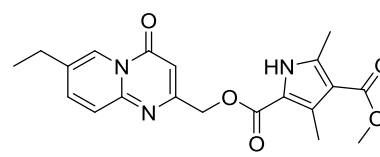
42



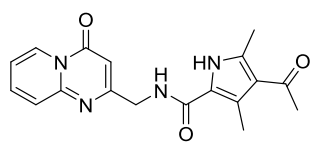
43



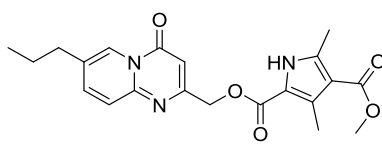
44



45



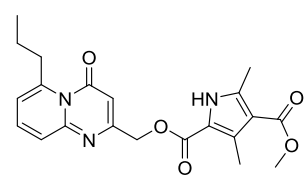
46



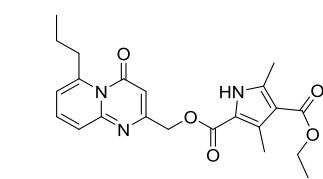
47



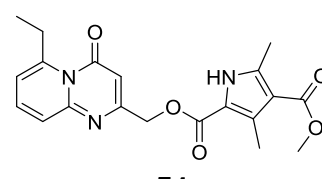
48



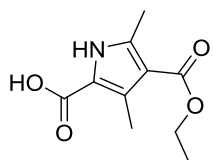
49



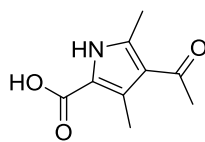
50



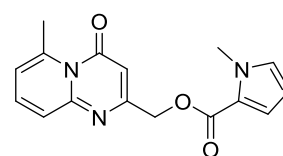
51



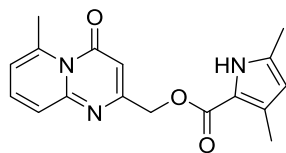
52



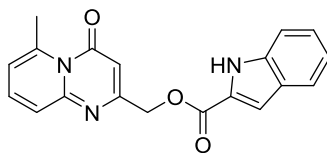
53



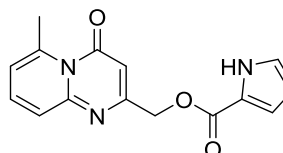
54



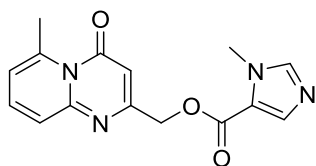
55



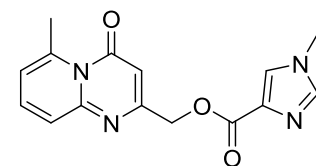
56



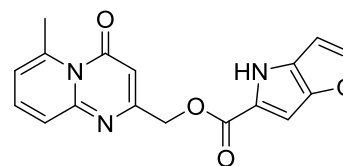
57



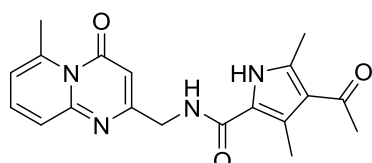
58



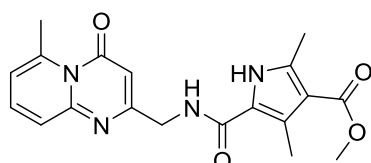
59



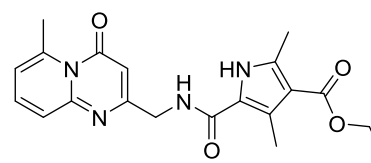
60



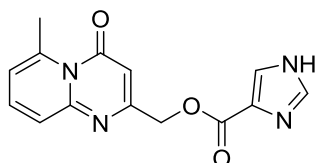
61



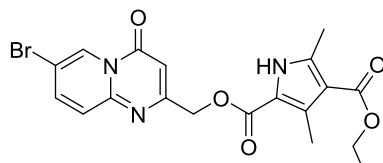
62



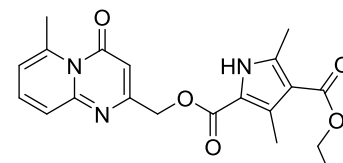
63



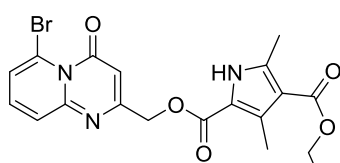
64



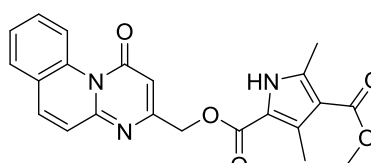
65



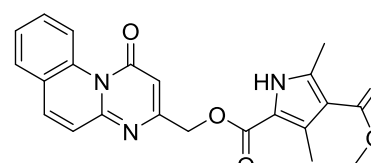
66



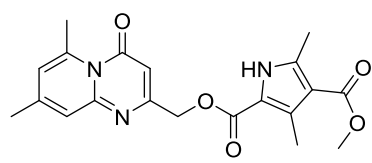
67



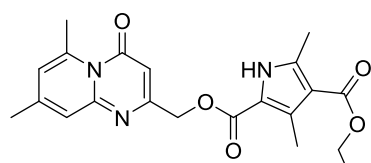
68



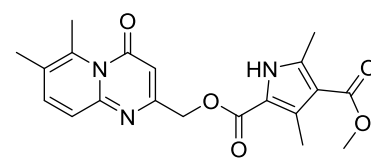
69



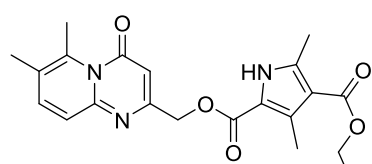
70



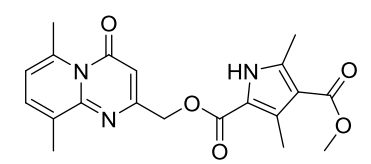
71



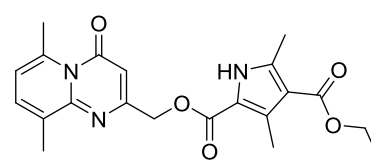
72



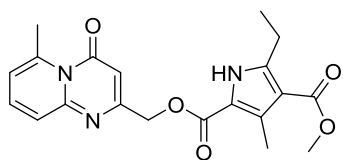
73



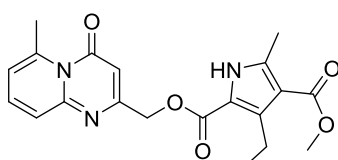
74



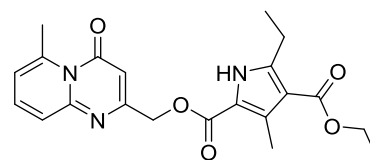
75



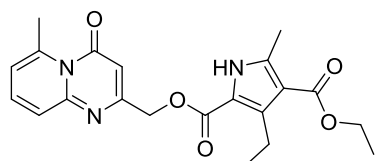
76



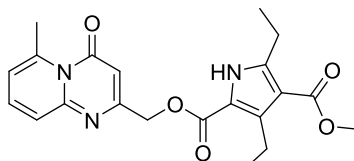
77



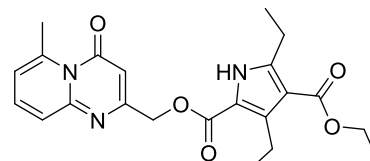
78



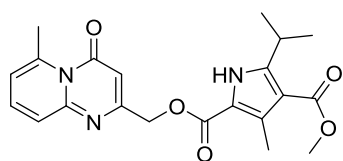
79



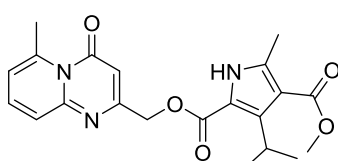
80



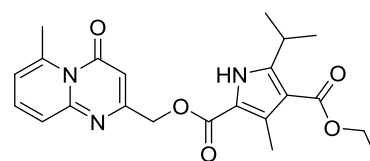
81



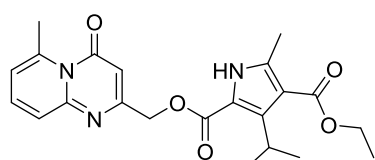
82



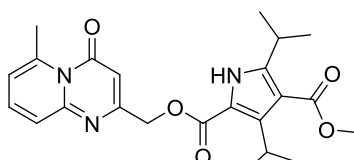
83



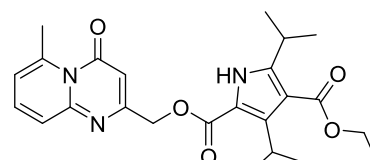
84



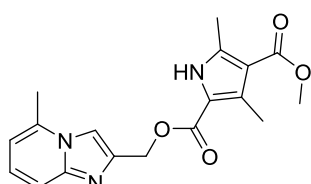
85



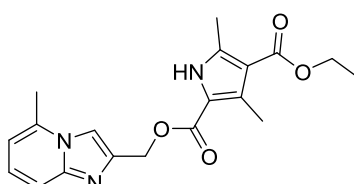
86



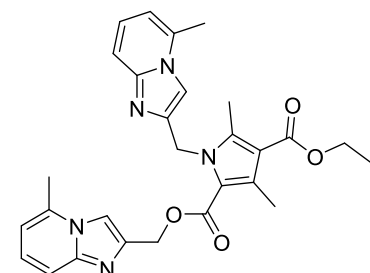
87



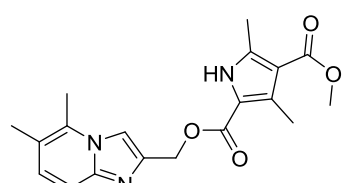
88



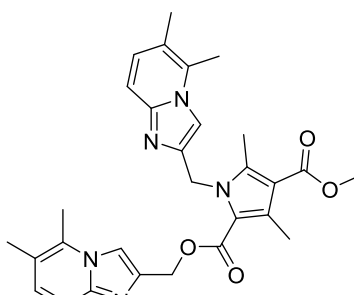
89



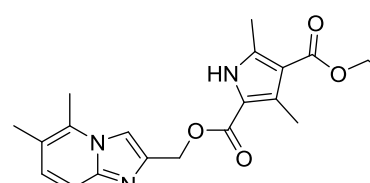
90



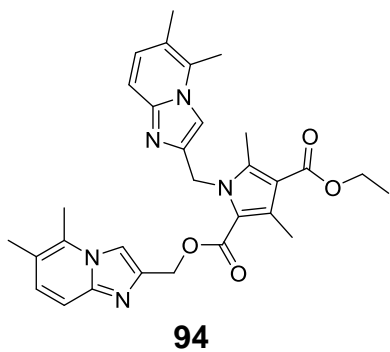
91



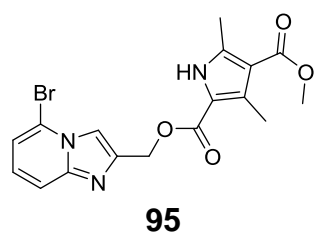
92



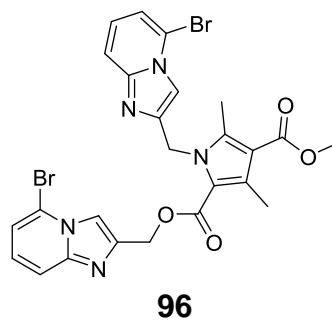
93



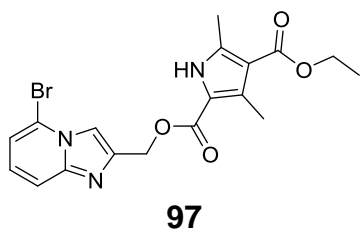
94



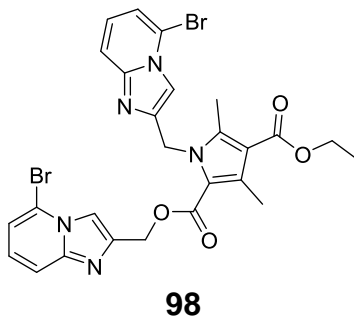
95



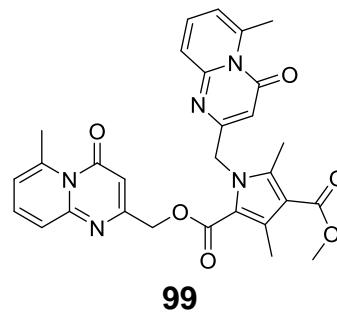
96



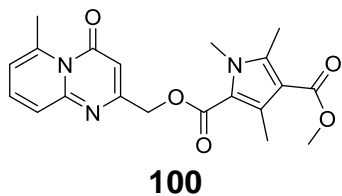
97



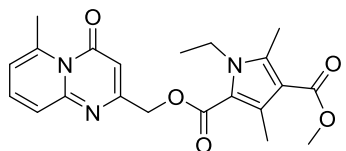
98



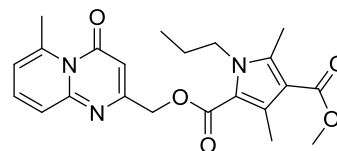
99



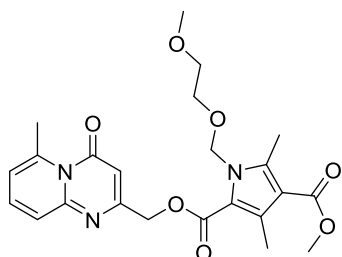
100



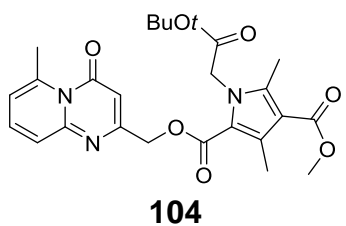
101



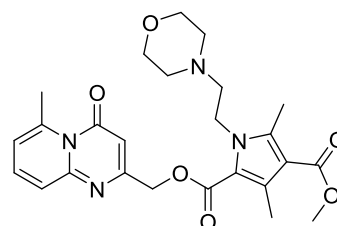
102



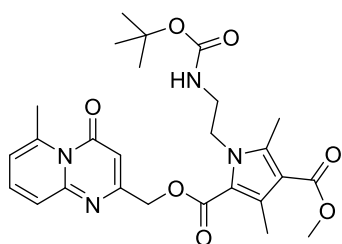
103



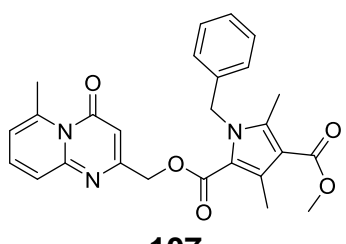
104



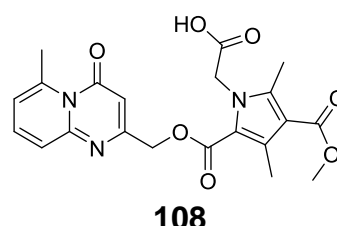
105



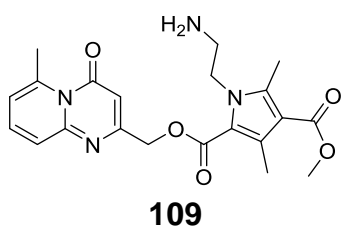
106



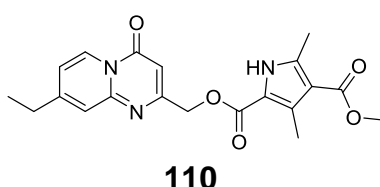
107



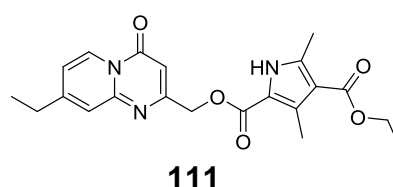
108



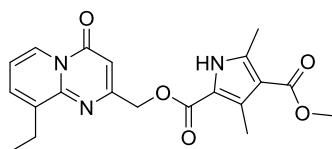
109



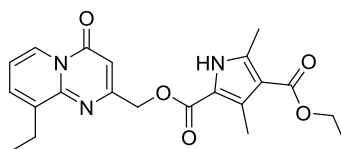
110



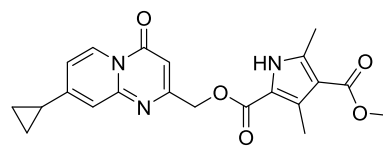
111



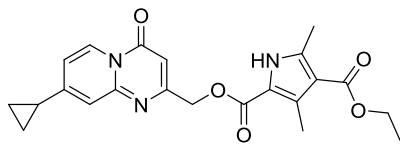
112



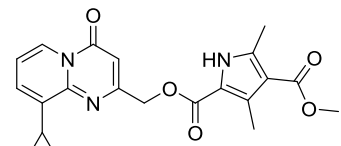
113



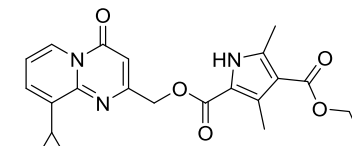
114



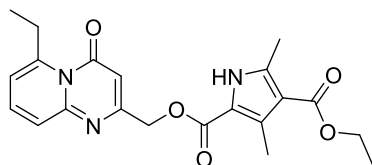
115



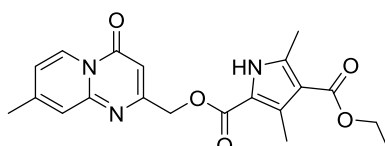
116



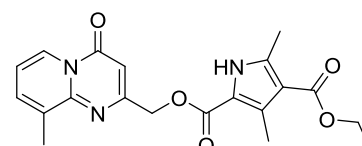
117



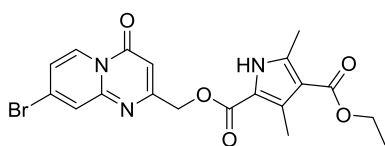
118



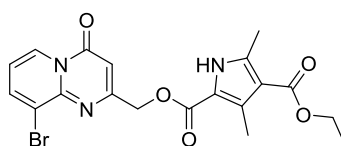
119



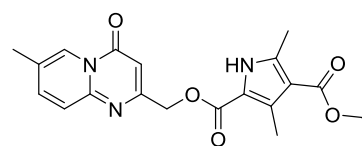
120



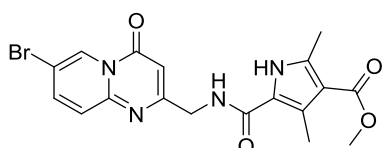
121



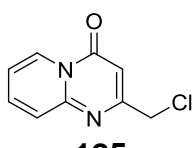
122



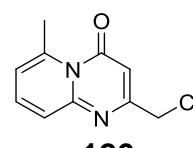
123



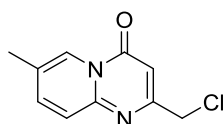
124



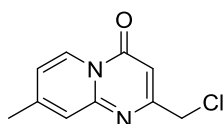
125



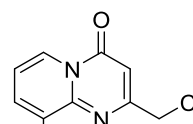
126



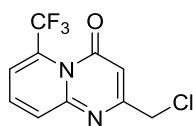
127



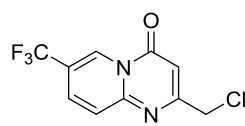
128



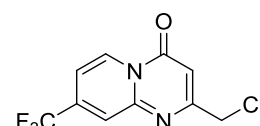
129



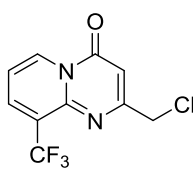
130



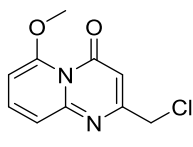
131



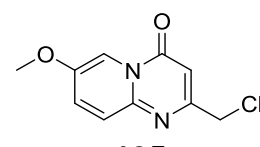
132



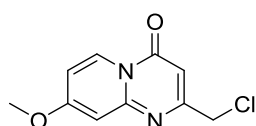
133



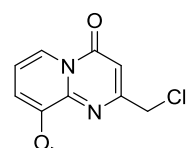
134



135



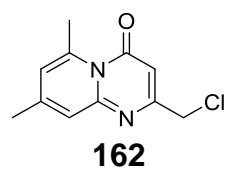
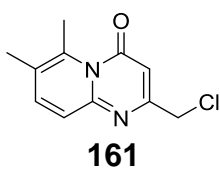
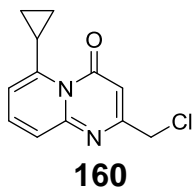
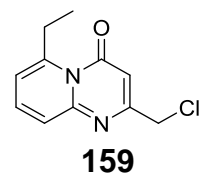
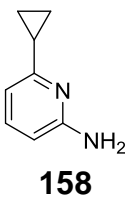
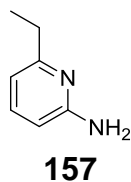
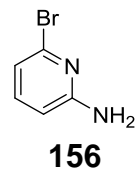
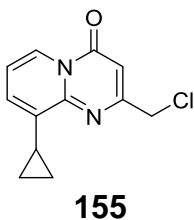
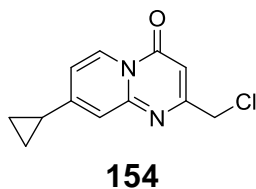
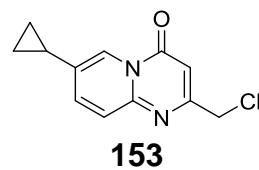
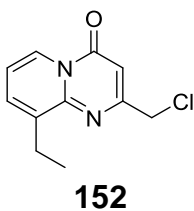
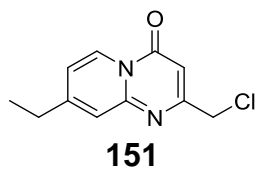
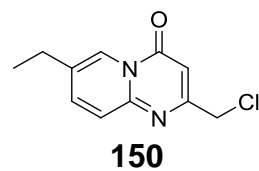
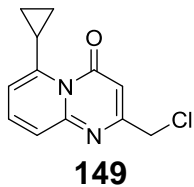
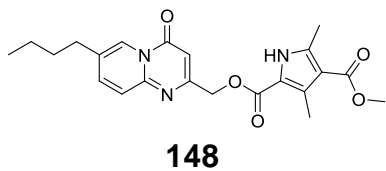
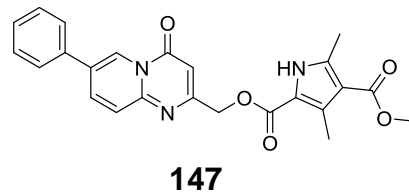
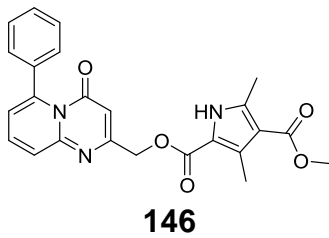
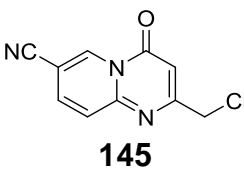
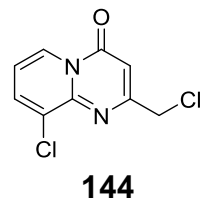
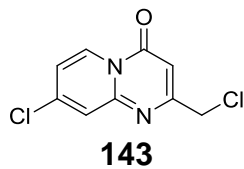
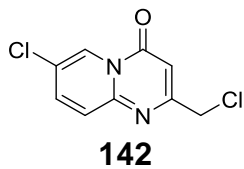
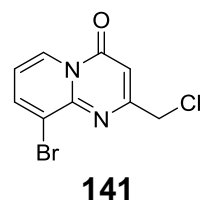
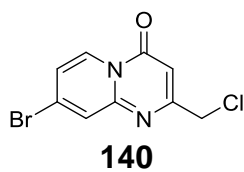
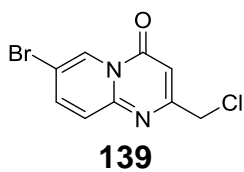
136

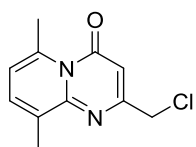


137

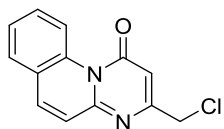


138

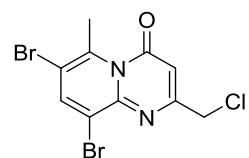




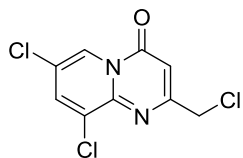
163



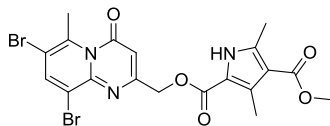
164



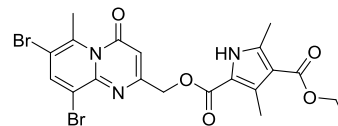
165



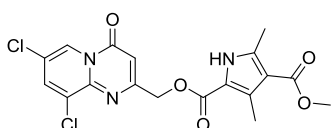
166



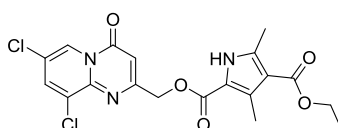
167



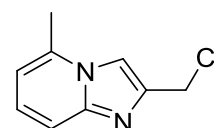
168



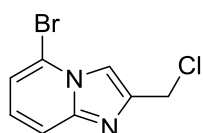
169



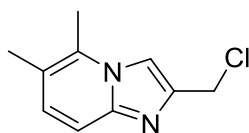
170



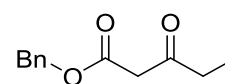
171



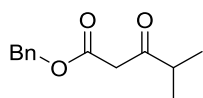
172



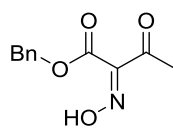
173



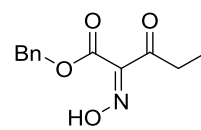
174



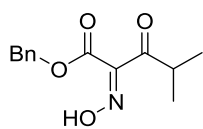
175



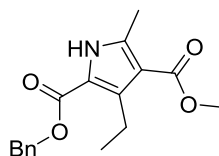
176



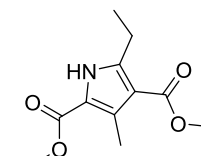
177



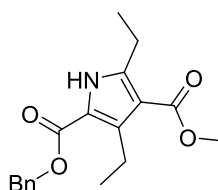
178



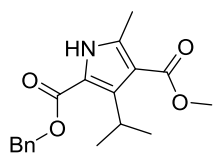
179



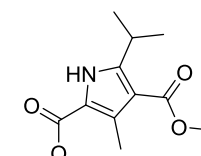
180



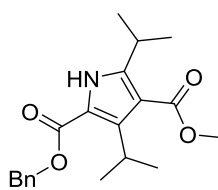
181



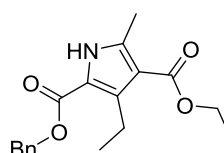
182



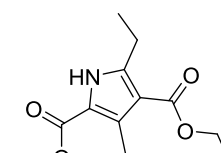
183



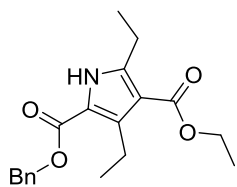
184



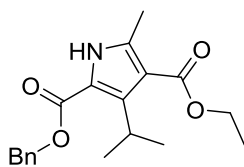
185



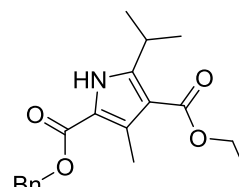
186



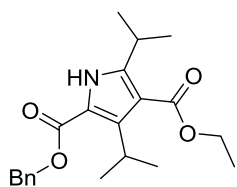
187



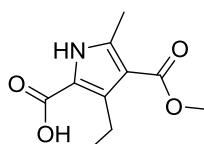
188



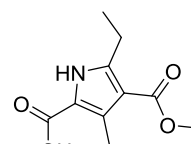
189



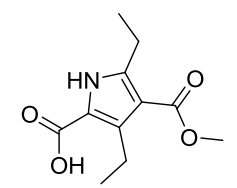
190



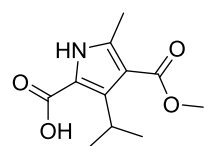
191



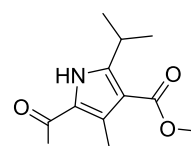
192



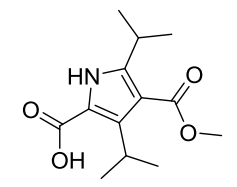
193



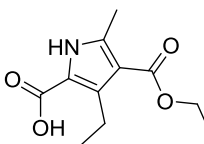
194



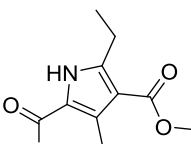
195



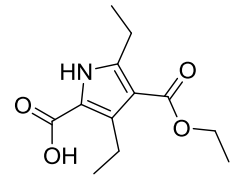
196



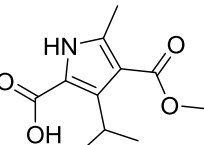
197



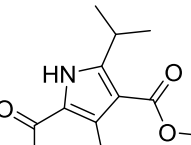
198



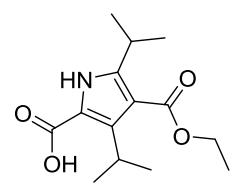
199



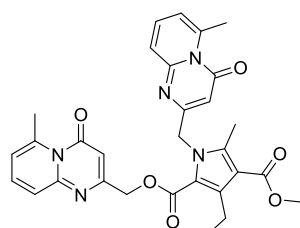
200



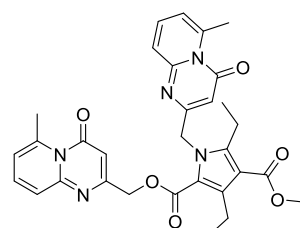
201



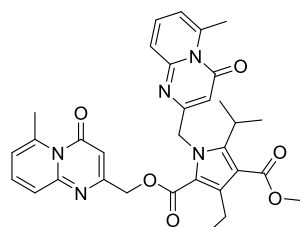
202



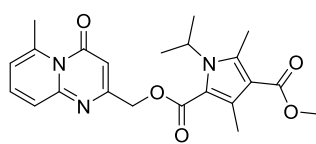
203



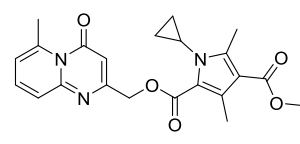
204



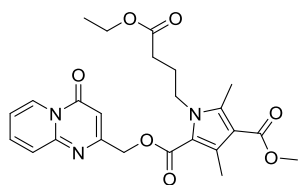
205



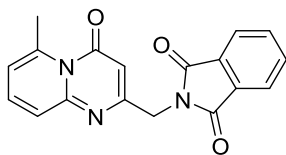
206



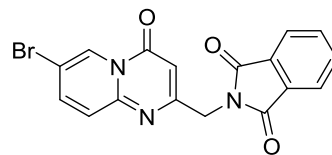
207



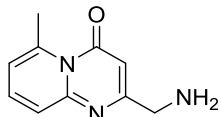
208



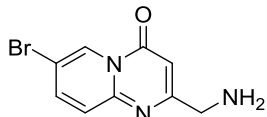
209



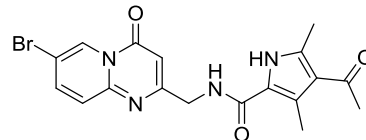
210



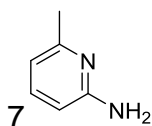
211



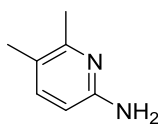
212



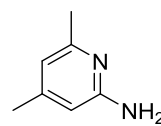
213



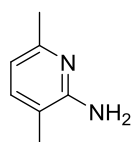
214



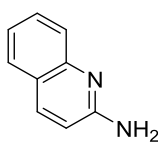
215



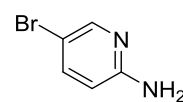
216



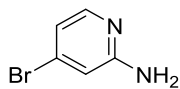
217



218



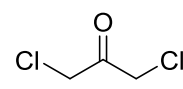
219



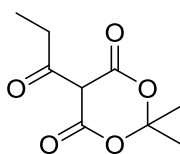
220



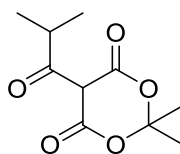
221



222



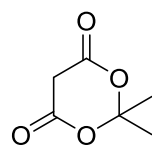
223



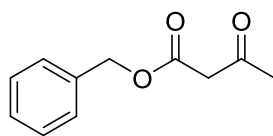
224



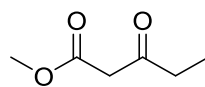
225



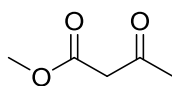
226



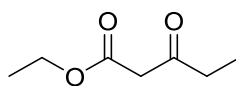
227



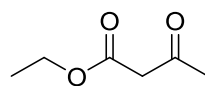
228



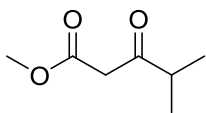
229



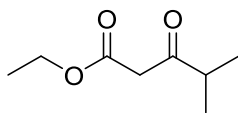
230



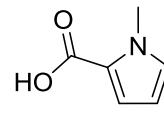
231



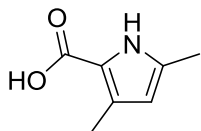
232



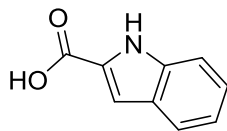
233



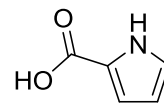
234



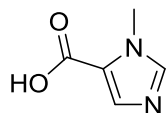
235



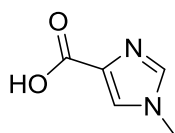
236



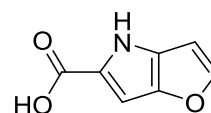
237



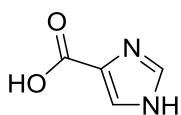
238



239



240



241

J Acknowledgment

First and foremost, I need to thank Prof. Walter Nickel for being the BEST BOSS ever. Without his constant support and trust in my abilities and skills as well as his endless knowledge in all things biology, it would have been exponentially harder to learn a whole new field of expertise. THANK YOU!!

I also want to thank Prof. Roland Krämer for agreeing to be my thesis supervisor, enabling me to pursue this project under the direct supervision of Walter Nickel.

A huge thank you also goes to David Will for teaching me the medicinal chemists mind-set of “Yield doesn’t matter, as long as you have a few milligramms to test in the end, you are fine!”, for the constant input when I was stuck, for listening to me whining and telling me to suck it up, for being the most demanding thesis corrector ever and so much more. I couldn’t have done it without you. 😊

Another thank you goes to all my interns and bachelor students who I had the pleasure to teach the joys and frustrations of research. Especially Marc Mößer who started this project and Isabella Ferrara who made a significant contribution over the 9 month she worked with me.

I also want to thank the people I managed to talk into reading and correcting this thesis. Michael, Caro and Helen thank you. Without you, this thesis would have been a bit of a mess.

Thank you also to all my amazing colleagues at the BZH. Without their constant input, productive chats over a cup of tea and a lot of patience for my endless biology questions, this time would not have been as enjoyable.

A big thank also goes to everyone in the CBCF at EMBL for hosting me all these years, for sharing their expertise in assay development and the countless thirsty Thursdays (followed by really hard early Friday mornings ;)) and beer sessions to make the transition to the weekend after a long workweek a lot of fun. It was amazing to get to work with all of you.

A very special thank you goes to all my friends, who have supported me massively over the last 5 years and without whom I would have quit a long time ago. So thank you, Helen and Annika for simply being there in the really tough moments, Cyril, Caro, Elena and Maggie for always being up for a glass of wine and loads of good food, Arnaud and the rest of the running crew for helping me to clear my head, Susanne and Emily for being very supportive room mates and the “Hühner” Laura, Kati, Stella, Anna, Isabell and Tanja without whom I would likely not be a chemist right now.

Last but not least, a HUGE thank you to my family for all their support over the years.